



HAL
open science

Selection of DNA aptamers against melanoma biomarkers

Shujaat Ali

► **To cite this version:**

Shujaat Ali. Selection of DNA aptamers against melanoma biomarkers. Human health and pathology. Université de Bordeaux, 2019. English. NNT : 2019BORD0154 . tel-03354940

HAL Id: tel-03354940

<https://theses.hal.science/tel-03354940>

Submitted on 27 Sep 2021

HAL is a multi-disciplinary open access archive for the deposit and dissemination of scientific research documents, whether they are published or not. The documents may come from teaching and research institutions in France or abroad, or from public or private research centers.

L'archive ouverte pluridisciplinaire **HAL**, est destinée au dépôt et à la diffusion de documents scientifiques de niveau recherche, publiés ou non, émanant des établissements d'enseignement et de recherche français ou étrangers, des laboratoires publics ou privés.

A thesis submitted in fulfilment of the requirements for the degree of

Doctor of Philosophy of

Université de Bordeaux

School of Life and Health Sciences

Selection of DNA Aptamers against Melanoma Biomarkers

Author: **Shujaat ALI**

Supervisor: Dr. Laurent AZÉMA

Members of the Jury:

Prof. Isabelle Berque BESTEL	(Université de Bordeaux)	Président
Dr. Frédéric DUCONGÉ	(CEA, Paris)	Rapporteur
Dr. Marcel HOLLENSTEIN	(Institut Pasteur, Paris)	Rapporteur
Dr. Frédéric SALTEL	(Université de Bordeaux)	Examineur
Prof. Jean-Jacques TOULMÉ	(Emeritus Research Director)	Invité
Dr. Laurent AZÉMA	(Université de Bordeaux)	Directeur

Date: Thursday, September 26, 2019

ACKNOWLEDGEMENT

Firstly, I would like to extend my deepest gratitude to my supervisor, Dr. Laurent Azéma for his guidance, encouragement, valuable comments and endless support during my thesis. I must acknowledge the freedom and confidence he gave me to pursue my research interest under his kind supervision. I would also like to express my sincere gratefulness to Prof. Jean-Jacques Toulmé for allowing me to work in his team and for his valuable suggestions and comments during the team meetings. I am also very grateful to Eric Dausse for all his kind advices and assistance during my thesis.

I am very thankful to all members of the Jury for agreeing to evaluate my thesis. A special thanks to Prof. Isabelle Berque Bestel for presiding the committee. I am also thankful to Dr. Frédéric Ducongé and Dr. Marcel Hollenstein for evaluating my thesis. I would like to word a real gratitude and thankfulness to Dr. Frédéric Saltel, for his distinguished scientific knowledge, support and collaboration during the years of my PhD. A special thanks to Aya Abou Hammoud for being so supportive. I am very thankful to Dr. Zeeshan Danish for his encouragement and guidance during my undergraduate studies which developed my interest in research.

I am very grateful for the guidance and encouragement of members from INSERM U1212, especially Prof. Martin Teichmann, Dr. Fabien Darfeuille, Dr. Stephan Thore, Dr Samir Amrane, Dr. Isabelle Iost, Dr. Cathy Staedel, Dr Sébastien Fribourg, Sandrine Chabas, Dr. Fanny Boisier, Dr. Nicolas Tourasse and Dr. Delphine Bronesky. In particular, I thank Dr. Lionel Minvielle-Sebastia, Dr. Helene Dumay-Odelot and Ronan Peryoutou for assisting me in performing experiments. I am also thankful to Muriel Trabado, Malika Vloeberghs and Kati Ba-Pierozzi for their help in administration. Thank you Jacques Puyol for your services in the lab. I am also grateful to our former lab members Olivier Paurelle, Emilie Daugerre and Dr. Guillaume Durand for being so supportive in the early days of my PhD thesis. I am also very appreciative for the career, research and life advice from Dr. Andrew Goldsborough.

I would like to extend a large thank you to the amazing people who have given me many entertaining memories. Dr. Arghya Sett, Dr. Sara Masachis Gelo, Finaritra Raelijaona, Lorena Zara, Dr. Emilie Rousseau and Bianca Schell, thanks to all of you for being so nice and supportive. I must say, it was a great time spent together.

As a former student of Uswa Education System, I would take this opportunity to acknowledge the efforts of Sheikh Mohsin Ali Najafi and Muhammad Ali Mehdi (late) with special gratefulness to provide a quality education in remote regions like Baltistan. I am also indebted to my school teachers especially Mr. Akbar Ali, Mr. Iftikhar Ali, Mr. Muhammad Kazim, Mr. Basharat Ali, Mr. Muhammad Iqbal and Mr. Ahmed Ali for their sincere help and support during my school life. I pay a special thanks to all of them for their services which helped us to achieve our goals in life.

I am very grateful to all many family members, friends, relatives, teachers and well-wishers. I must single out my parents: Muhammad Hadi and Safia, and my uncle Muhammad Ali. They have been an excellent role models in my life. Their love, support and encouragement throughout my life gave me the spirit to achieve my dreams in life. Finally I will dedicate this thesis to my brothers and sisters and wish them all best of luck in their future endeavours.

ABSTRACT

Melanoma is a cancer that accounts for the vast majority of morbidity and mortality caused by any skin cancer due to its involvement in metastasis. Among several reported biomarkers, Discoidin Domain Receptors (DDRs) and Matrix metalloproteinase (MMPs) are also considered as potential actors in melanoma. Recent studies demonstrate that DDRs and MMPs are overexpressed in melanoma with poor prognosis which demands the need of biomarkers specific theranostics probes. Though many advances have been made in order to reduce the risk associated with metastatic melanoma with the help of traditional monoclonal antibodies, but the drawbacks like production complexity, batch to batch variability, short shelf life, immunogenicity, cross reactivity and high cost cannot be neglected. Therefore in recent years, aptamers have gained high interests as a substitute of antibodies that can be synthesized chemically with low production cost and overcomes the limitations associated to antibodies. Aptamers are short oligonucleotides with high affinity and specificity against its target molecule, raised by a combinatorial method known as SELEX (Systematic Evolution of Ligands by Exponential Enrichment). During my thesis, I performed a SELEX against two types of DDR (DDR1 and DDR2) and Human MMP14 based on alternative supports for candidates sorting and high throughput sequencing. A group of aptamers were selected against DDR1 and the best candidate was further doped to perform more rounds of selection against DDR1. Finally an aptamer against DDR1 was selected with a K_d in low nano-molar range. This aptamer can be used as a theranostics tool in DDR1 associated melanoma studies. As aptamers have an advantage of conjugation and modifications at desired positions so we further aim to conjugate this aptamer with nanoparticles for in vivo studies.

Le mélanome est un cancer qui représente la grande majorité de la morbidité et de la mortalité causées par tout cancer de la peau en raison de son implication dans les métastases. Parmi plusieurs biomarqueurs rapportés, les récepteurs du domaine de la discoïdine (DDR) et la métalloprotéinase Matrix (MMP) sont également considérés comme des acteurs potentiels du mélanome. Des études récentes démontrent que les DDR et les MMP sont surexprimés dans les mélanomes de mauvais pronostic, ce qui nécessite le recours à des sondes thérapeutiques à biomarqueurs spécifiques. De nombreux progrès ont été réalisés pour réduire le risque associé au mélanome métastatique à l'aide d'anticorps monoclonaux traditionnels, mais les inconvénients tels que la complexité de la production, la variabilité d'un lot à l'autre, la courte durée de conservation, l'immunogénicité, la réactivité croisée et le coût élevé ne peuvent être négligés. Par conséquent, au cours des dernières années, les aptamères ont acquis un grand intérêt comme substitut d'anticorps pouvant être synthétisés chimiquement avec un faible coût de production et dépassant les limitations associées aux anticorps. Les aptamères sont de courts oligonucléotides à haute affinité et spécificité vis-à-vis de la molécule cible, développés par une méthode combinatoire appelée SELEX (Evolution systématique de ligands par enrichissement exponentiel). Au cours de ma thèse, j'ai effectué une SELEX contre deux types de DDR (DDR1 et DDR2) et de Human MMP14 sur la base de supports alternatifs pour le tri des candidats et le séquençage à haut débit. Un groupe d'aptamères a été sélectionné contre DDR1 et le meilleur candidat a ensuite été dopé pour effectuer davantage de tours de sélection contre DDR1. Finalement, un aptamère contre DDR1 a été sélectionné avec un K_d dans la gamme nanomolaire basse. Cet aptamère peut être utilisé comme outil thérapeutique dans les études sur le mélanome associé à DDR1. Comme les aptamères présentent un avantage en termes de conjugaison et de modifications aux positions désirées, nous visons en outre à conjuguer cet aptamère avec des nanoparticules pour des études *in vivo*.

Table of Contents

Acknowledgement.....	i
Abstract	iii
List of Tables.....	xii
List of Figures.....	xiii
List of Abbreviation.....	xv
Chapter 1: Aptamers and Melanoma: A brief overview.....	1
1.1 Melanoma.....	2
1.1.1 Biomarkers in melanoma.....	2
1.1.2 Discoidin Domain Receptors (DDRs).....	4
1.1.2.1 Introduction to Receptor Tyrosine Kinases (RTKs).....	4
1.1.2.2 Introduction to Discoidin Domain Receptors.....	5
1.1.2.3 Structures of Discoidin Domain Receptors.....	6
1.1.2.4 Discoidin Domain Receptor 1 Structure and Isoform.....	6
1.1.2.5 Discoidin Domain Receptor 2 Structure.....	7
1.1.2.6 Amino Acid Sequences of DDRs (Extracellular Region).....	9
1.1.2.7 Crystallographic structure of DDRs DS domain.....	10
1.1.2.8 DDRs activation by Collagen.....	11
1.1.2.9 DDR activation and signalling.....	12
1.1.2.9.1 Dimerization.....	12
1.1.2.9.2 Phosphorylation.....	12
1.1.2.9.3 DDRs initiated signaling.....	13
1.1.2.10 Role of DDRs in Cancer.....	15
1.1.2.11 Role of DDRs in Melanoma.....	15
1.1.2.12 Targeting DDRs in cancer for diagnostic or inhibitory purposes.....	16
1.1.3 Matrix Metalloproteinases (MMPs).....	17

1.1.3.1 Classification and Structure of MMPs.....	19
1.1.3.2 Activation of proMMPs.....	22
1.1.3.3 Membrane type matrix metalloproteinase (MT1-MMP).....	22
1.1.3.3.1 Expression and Regulation of MT1-MMP.....	22
1.1.3.3.2 Role of MT1-MMP in tumor.....	23
1.1.3.3.3 MT1-MMP associated metastatic melanoma.....	23
1.1.3.3.4 MT1-MMP as a target in Melanoma.....	25
1.2 Aptamers.....	26
1.2.1 Aptamers vs. Antibodies.....	26
1.2.2 Structure of Aptamer.....	27
1.2.3 Aptamer interaction with protein.....	28
1.3 SELEX (Systematic Evolution of Ligands by Exponential Enrichment).....	29
1.3.1 Principle of SELEX.....	29
1.3.2 Types of SELEX.....	31
1.3.2.1 Magnetic Beads Based SELEX.....	31
1.3.2.2 Nitrocellulose Membrane Filtration-Based SELEX.....	32
1.3.2.3 Cell SELEX.....	32
1.3.2.4 In vivo SELEX.....	33
1.3.2.5 Capillary Electrophoresis SELEX (CE-SELEX).....	34
1.3.2.6 Microfluidic SELEX.....	35
1.3.2.7 Capture SELEX.....	36
1.3.2.8 Functional SELEX.....	36
1.3.2.9 SELEX with modified nucleic acid libraries.....	37
1.3.2.10 High Throughput Sequencing in SELEX (HTS-SELEX).....	38
1.4 Application of Aptamers.....	39
1.4.1 Aptamers in Therapeutics.....	39
1.4.2 Aptamers in Diagnostics.....	41

1.4.2.1 Aptamer in Biomarker detection.....	41
1.4.2.2 Slow Off-Rate Modified Aptamers (SOMAmers).....	42
1.4.2.3 Aptamers in In vivo Imaging.....	43
1.5 Thesis aims and objectives.....	45
Chapter 2: Materials and methods.....	46
2.1 Chemicals and Reagents.....	47
2.2 Synthesis of Library.....	48
2.3 Buffer.....	50
2.4 SELEX.....	51
2.4.1 Magnetic beads based SELEX.....	52
2.4.1.1 Ni-Beads Binding capacity analysis by SDS-PAGE.....	52
2.4.1.2 Preparation of ssDNA Library in Magnetic beads based SELEX.....	53
2.4.1.3 Immobilization of histidine tagged Proteins on Ni-NTA beads.....	53
2.4.1.4 Counter Selection Step in Magnetic beads based SELEX.....	54
2.4.1.5 Selection Step in Magnetic beads based SELEX.....	54
2.4.1.6 Washing Step in Magnetic beads based SELEX.....	54
2.4.1.7 Elution Step in Magnetic beads based SELEX.....	54
2.4.2 Nitrocellulose membrane based filtration SELEX.....	55
2.4.2.1 Activation of Nitrocellulose membrane.....	56
2.4.2.2 Preparation of ssDNA Library in Filtration SELEX.....	56
2.4.2.3 Counter Selection Step in Filtration SELEX.....	56
2.4.2.4 Selection Step in Filtration SELEX.....	56
2.4.2.5 Washing Step in Filtration SELEX.....	57
2.4.2.6 Extraction of ssDNA sequences in Filtration SELEX.....	58
2.4.3 Cell SELEX.....	58
2.4.3.1 Cell Culture for Cell SELEX against DDR2.....	59
2.4.3.2 Preparation of ssDNA library in Cell SELEX.....	59

2.4.3.3 Selection step in Cell SELEX.....	59
2.4.3.4 Extraction of bound ssDNA sequences from Cells.....	59
2.4.4 Click-SELEX.....	60
2.4.4.1 Synthesis of Click Library.....	60
2.4.4.2 Deprotection of oligonucleotides.....	61
2.4.4.3 Synthesis of 3- (2-azidoethyl) -1H-indole7.....	61
2.4.4.4 Click-Reaction.....	62
2.5 Polymerase Chain Reaction Amplification.....	63
2.5.1 Optimization of PCR amplification of the SELEX Library.....	63
2.5.2 PCR amplification of the SELEX Rounds.....	66
2.6 Preparation of ssDNA strands.....	66
2.6.1 Purification by PAGE 12%.....	66
2.6.2 Exo-nuclease Digestion of antisense strand.....	67
2.7 Passive Elution of Oligonucleotides.....	69
2.8 Electro elution of oligonucleotides.....	69
2.9 Desaltation of oligonucleotides.....	70
2.10 UV Spectrophotometry.....	71
2.11 Gel electrophoresis.....	72
2.11.1 Agarose Gel Electrophoresis.....	72
2.11.2 Denaturant Polyacrylamide Gel Electrophoresis.....	72
2.11.3 Native Polyacrylamide Gel Electrophoresis.....	73
2.11.4 Sodium dodecyl sulphate polyacrylamide gel electrophoresis.....	74
2.11.4.1 Silver Staining of protein in SDS-PAGE gel.....	75
2.12 In vitro Fluorescence Assay	76
2.12.1 In vitro Fluorescence Assay for the selected candidates from DDR1 SELEX1.....	77

2.12.2 In Vitro Fluorescence Assay of Aptamer C25.....	78
2.13 Real time PCR for Quantitative Analysis.....	78
2.13.1 qPCR analysis of C25 aptamer.....	80
2.14 High throughput Sequencing.....	80
2.14.1 DNA Pool generation for Illumina High-throughput Sequencing.....	80
2.14.2 Bioinformatics analysis of ssDNA sequences.....	82
2.14.2.1 Trimming 3'.....	83
2.14.2.2 Trimming 5'.....	83
2.14.2.3 Optimization of Random Window Length.....	83
2.14.2.4 Counting of sequences.....	83
2.14.2.5 Clustering of Sequences.....	83
2.15 Structural analysis of DNA Sequences by mfold.....	84
2.16 Fluorescence Microscopy.....	84
2.17 Dot-Blot Assay by using NC membrane.....	85
2.18 In vitro Fluorescence Assay by FluMag.....	86
2.19 Surface Plasmon Resonance.....	86
Chapter 3: In vitro selection of DNA aptamers against Discoidin Domain Receptor-1 (DDR-1).....	88
3.1 Selection of DNA aptamer against DDR1 with naïve ssDNA library.....	89
3.1.1 SELEX Library.....	89
3.1.2 SELEX.....	90
3.1.3 High throughput sequence (HTS) analysis.....	91
3.1.4 Structural prediction of selected candidates by mfold.....	92
3.1.5 In vitro fluorescence assay of selected Sequences.....	94
3.1.6 In vitro fluorescence assay of aptamer C25.....	95
3.1.7 qPCR analysis of Aptamer C25.....	96
3.1.8 Aptamer C25 truncation based on mfold predicted structure.....	98

3.1.9 Surface Plasmon Resonance (SPR) of C25 and truncations.....	100
3.1.10 Discussion.....	101
3.2 Selection of DNA aptamer against DDR1 by Doped SELEX.....	102
3.2.1 SELEX.....	103
3.2.1 High throughput Sequencing of Doped SELEX.....	104
3.2.2 Evaluation of Selected candidates by Dot blot assay.....	108
3.2.3 Structural Studies of Aptamer DS_3.1.....	108
3.2.4 Determination of Kd of DS_3.1 aptamer by Blot Assay.....	110
3.2.5 Fluorescence Imaging by Confocal Microscopy.....	111
3.3 Conclusion.....	113
Chapter 4: In vitro selection of DNA aptamers against Human Matrix Metalloproteinase-14 (HMMP-14)	114
4.1 SELEX against HMMP14 with natural DNA library.....	115
4.1.1 SELEX Library.....	115
4.1.2 SELEX.....	115
4.1.3 High Throughput Sequencing analysis.....	116
4.2 EVOLUTION OF PARASITE SEQUENCES.....	118
4.2.1 mfold structural analysis of parasite sequences.....	119
4.2.2 In vitro Fluorescence Assay of m14-0.....	120
4.2.3 Application of Histidine aptamer m14-0.....	120
4.2.3.1 Protein purification.....	121
4.2.3.2 Enzyme-Linked ImmunoSorbent Assay.....	121
4.2.3.3 Surface Plasmon Resonance.....	121
4.2.4 Overcoming issues related to evolution of parasite sequences in SELEX.....	121
4.2.5 Improvement in magnetic beads SELEX.....	122
4.3 Conclusion.....	122
Chapter 5: In vitro selection of DNA aptamers against Discoidin Domain Receptor-2 (DDR-2)	123

5.1 Cross-over SELEX against Discoidin Domain Receptor 2.....	124
5.1.1 SELEX ssDNA Library.....	124
5.1.2 SELEX	125
5.1.3 High Throughput Sequencing analysis.....	127
5.1.4 Slot Blot Assay of DDR2 candidates.....	130
5.2 Conclusion.....	130
Chapter 6: Thesis Prospects and Summary.....	131
6.1 Research Perspectives of aptamer selected against DDR1.....	132
6.1.1 Biophysical characterization of DS_3.1 and DS_3.1t1 by Surface Plasmon Resonance (SPR).....	132
6.1.2 Determination of Kd of DS_3.1 and DS_3.1t1 by Isothermal Titration Calorimetry (ITC).....	133
6.1.3 In vivo imaging of melanoma cells using nanoparticles conjugated DS_3.1.....	133
6.2 Research perspectives for selection of DNA aptamers against DDR2.....	134
6.2.1 Doped SELEX against extracellular domain of DDR2.....	134
6.2.1.1 Doped Library.....	134
6.2.2 Aptabeacon approach as a Functional SELEX against DDR2.....	135
6.2.2.1 Aptabeacon library.....	136
6.2.2.2 SELEX procedure.....	137
6.3 Click-SELEX against HMMP14	140
6.3.1 SELEX libraries.....	140
6.3.2 Comparison of Click and Non-Click SELEX Libraries by HTS Sequencing.....	141
6.3.3 SELEX with Click Library.....	143
6.3.4 SELEX with Non-Click Library.....	144
6.3.5 HTS Sequencing of Click-SELEX and Non-Click SELEX.....	144
6.4 Summary.....	146
References.....	148

List of Tables

Table 1.1: The Matrix Metalloproteinase (MMPs) family.....	18
Table 1.2: Aptamer vs. Antibodies.....	27
Table 2.1: List of oligonucleotides.....	49
Table 2.2: List of buffer and reagent solutions.....	51
Table 2.3: Polyacrylamide gel percentages for PAGE purification.....	73
Table 2.4: Running and Stacking reagents and percentage for SDS-PAGE.....	74
Table 2.5: List of reagent solutions used for silver staining.....	75
Table 2.6: Reagent composition of PCR for High Throughput Sequencing.....	81
Table 3.1: Selection conditions applied for SELEX against DDR1.....	91
Table 3.2: NGS analysis of SELEX against DDR1.....	92
Table 3.3: Selection conditions applied for doped SELEX against DDR1.....	104
Table 3.4: No. of clusters and clusters sequences in each round of doped SELEX.....	105
Table 3.5: NGS analysis of Doped SELEX against DDR1.....	107
Table 4.1: Selection conditions applied for SELEX against HMMP14.....	116
Table 4.2: NGS result analysis for SELEX against HMMP14.....	118
Table 5.1: Selection conditions applied for Cross-over SELEX against DDR2.....	126
Table 5.2: Diversity of rounds in SELEX against DDR2.....	128
Table 5.3: NGS analysis of SELEX against DDR2.....	129
Table 6.1: Selection conditions applied conventional-SELEX rounds against DDR2.....	137
Table 6.2: Selection conditions applied for Click SELEX against HMMP14.....	143
Table 6.3: Selection conditions applied for Non-Click SELEX against HMMP14.....	144

List of Figures

Figure 1.1: Structures of Receptor Tyrosine Kinases (RTKs).....	5
Figure 1.2: Structure and Isoforms of Discoidin Domain Receptor-1 (DDR-1).....	7
Figure 1.3: Structure of Discoidin Domain Receptor-2 (DDR-2).....	8
Figure 1.4: DS domain of DDR-1 and DDR2.....	11
Figure 1.5: DDRs initiated signalling pathways.....	14
Figure 1.6: DDRs contribution in Cancer Hallmark.....	16
Figure 1.7: Structure of Matrix Metalloproteinases (MMPs).....	21
Figure 1.8: Activation of MMP-2 by MT1-MMP.....	24
Figure 1.9: Nucleotides with Purine and Pyrimidine bases.....	28
Figure 1.10: Schematic diagram of aptamer binding to its target.....	28
Figure 1.11: The SELEX process.....	30
Figure 1.12: Structure of mirror-image nucleic acid aptamer.....	40
Figure 2.1: SDS-PAGE gel.....	53
Figure 2.2: Magnetic Beads based SELEX.....	55
Figure 2.3: Filtration based SELEX.....	57
Figure 2.4: Western Blot analysis of DDR1 and DDR2 expression.....	58
Figure 2.5: Cell SELEX.....	60
Figure 2.6: NMR spectroscopy of ¹³ C.....	62
Figure 2.7: PCR amplification of SELEX libraryA with Taq polymerase.....	64
Figure 2.8: PCR amplification of SELEX libraryA with Phusion polymerase.....	65
Figure 2.9: Electrophoretic mobility shift assay (EMSA) gel image.....	68
Figure 2.10: Electro-elution of oligonucleotides.....	70
Figure 2.11: In vitro fluorescence assay scheme.....	77
Figure 2.12: Amplification plot of C25 aptamer.....	79
Figure 2.13: PCR amplification for High Throughput Sequencing.....	81
Figure 3.1: Alignment of selected sequences from DDR1 SELEX1.....	92
Figure 3.2: mfold predicted secondary structures of SELEX-DDR1 candidates.....	94

Figure 3.3: Binding percentage of selected candidates against DDR1.....	95
Figure 3.4: In vitro fluorescence assay of aptamer C25 against different proteins.....	96
Figure 3.5: qPCR analysis of C25 aptamer.....	98
Figure 3.6: mfold predicted structures of C25	99
Figure 3.7: SPR analysis of C25 full length aptamer and truncations.....	100
Figure 3.8: NGS analysis of base composition in the doped SELEX library.....	103
Figure 3.9: NGS data based comparison of rounds of Doped SELEX against DDR1.....	106
Figure 3.10: Alignment of selected sequences from DDR1 Doped SELEX.....	108
Figure 3.11: mfold predicted structures of aptamer DS_3.1.....	109
Figure 3.12: mfold predicted structure of DS_3.1t1.....	110
Figure 3.13: Kd determination of Aptamer DS_3.1.....	111
Figure 3.14: Confocal Microscopy for Cell Imaging.....	112
Figure 4.1: Graphical representation of enrichment of candidates in SELEX against HMMP14.....	117
Figure 4.2: Alignment of selected sequences from HMMP14 SELEX1.....	118
Figure 4.3: mfold based structure analysis of parasite sequences.....	119
Figure 4.4: Binding analysis of m14-0.....	120
Figure 5.1: Alignment of selected sequences from DDR2 SELEX1.....	129
Figure 6.1: mfold predicted structure of D2.2 and D2.3 random window.....	135
Figure 6.2: Functional SELEX against DDR2 with Aptabeacon approach.....	136
Figure 6.3: Agarose gel images of amplified rounds in conventional SELEX against DDR2.....	138
Figure 6.4: Scheme of Aptabeacon selection by particle display method.....	139
Figure 6.5: CuAAC functionalization of EdU-containing DNA molecules with Indole azide.....	141
Figure 6.6: Analysis of base compositions in Click and Non-Click SELEX libraries by NGS.....	142

List of Abbreviations

AA: Amino acid

AEgis: Artificially expanded genetic information system

ALISA: Aptamer-linked immobilized sorbent assay

AMD: Age related macular degeneration

AP: Aptamer particle

APS: Ammonium persulfate

BSA: Bovine serum albumin

CE: Capillary electrophoresis

CSPG4: Chondroitin sulfate proteoglycan

CuAAC: Copper (I)-catalyzed alkyne–azide cycloaddition

Cy5: Cyanine 5

DDRs: Discoidin domain receptors

DNA: Deoxyribonucleic acid

DOTA: 1, 4, 7, 10-tetraazacyclododecane-1, 4, 7, 10-tetraacetic acid

DS: Discoidin

EDTA: Ethylenediaminetetraacetic acid

EdU: 5-ethynyl-2'-deoxyuridine triphosphate

EGF: Epidermal growth factor

ELISA: Enzyme-linked immunosorbent assay

ELONA: Enzyme-linked oligonucleotide assay

EMSA: Electrophoretic mobility shift assay

EXJM: Extracellular juxtamembrane region

FACS: Fluorescence activated cell sorting

FAM: 6-carboxyfluorescein

IL: Interleukin

IXJM: Intracellular juxtamembrane region

HTS: High throughput sequencing

HUVEC: Human umbilical vein endothelial cells

KD: Kinase domain

LNA: Locked nucleic acid

MALDI-TOF: Matrix assisted laser desorption ionization - Time of flight
MMPs: Matrix metalloproteinases
MRI: Magnetic resonance imaging
MT-MMP: Membrane type matrix metalloproteinases
NC: Nitrocellulose
NECEEM: Non-equilibrium capillary electrophoresis of equilibrium mixtures
NGS: Next generation sequencing
Ni: Nickel
NMR: Nuclear magnetic resonance
NP: Nanoparticles
NSCLCs: Non-small cell lung carcinomas
NTA: Nitrilotriacetate
PAGE: Polyacrylamide gel electrophoresis
PBS: Phosphate-buffered saline
PCR: Polymerase chain reaction
PD: Particle display
PEG: Polyethylene glycol
PET: Positron emission tomography
RNA: Ribonucleic acid
ROX: Rhodamine X
RT: Room temperature
RTKs: Receptor tyrosine kinases
SDS: Sodium dodecyl sulfate
SELEX: Systematic evolution of ligands by exponential enrichment
SOMAmers: Slow off-rate modified aptamers
SPECT: Single photon emission computed tomography
SPR: Surface Plasmon Resonance
TAMRA: Tetramethylrhodamine
TBE: Tris borate ethylenediamine tetraacetic acid
TEMED: N, N, N', N'-Tetramethylethylenediamine
TENAcl: Tris ethylenediamine tetraacetic acid NaCl
THPTA: Tris (3-hydroxypropyltriazolylmethyl) amine
TIMP: Tissue inhibitor of metalloproteinases
TM: Transmembrane

TNF: Tissue necrosis factor

TRITC: Tetramethyl rhodamine iso thio cyanate

UV: Ultraviolet

VEGF: Vascular endothelial growth factor

μ FFE: Micro free flow electrophoresis

CHAPTER-1: APTAMERS AND MELANOMA: A BRIEF OVERVIEW

Melanoma

Melanoma, also known as malignant melanoma, is a cancer that arises from the normal pigment producing cells in the skin known as melanocytes. Melanocytes are derived from neural crest cells, which are a temporary group of cells arise from embryonic ectoderm cell layer that develop to melanocytes ¹. Though melanoma is mostly found in skin, it is also rarely occurring in other human anatomical areas like mouth, intestine and eye. Melanoma is a major health issue worldwide and is mostly increasing in Europe and US. Melanoma is mostly caused by the ultraviolet rays of the sun. In France, according to a report published in 2015, an estimation of around 10,000 melanoma cases diagnosed in adults were attributed to solar ultra violet radiation exposure which corresponds to 83% of all melanomas and 3% of all cancer cases in that year in France ². Although melanoma counts for only 5-10 percent of all skin cancer, it accounts for the vast majority of morbidity and mortality caused by any skin cancer due to its involvement in metastasis ³. It has been observed that metastasis can even occur from a thin primary tumor in the early disease progression ⁴. The process of metastasis consists of several phases including vessel formation, evasion of immune surveillance, embolism, capillary adhesion, extravasation and organ-specific colonization as described by Nguyen and Massague ⁵.

Biomarkers in Melanoma

Biological marker (Biomarker) is defined as "a characteristic that is objectively measured and evaluated as an indicator of normal biological processes, pathogenic processes or pharmacological responses to a therapeutic intervention" ⁶. Although the terminology is new, biomarkers like cells, proteins and genes are being used in preclinical studies and diagnostics for a long time by studying the genetic variation and metabolic expressional changes in proteins. Changes in the expression or state of protein indicated by a biomarkers can correlate with the progression of the diseases or the susceptibility of the diseases in response to a given treatment. Such studies have been done by generations of physicians, epidemiologist and scientist in order to investigate the disease caused to human. In clinical practice, biological markers include tools and technologies that helps in understanding the early prediction, causes, diagnosis, progression, regression, or management of any disease. Perera and Weinstein have classified biomarkers based on the sequences of event from exposure to the risk factors to the development of the particular disease ⁷. Besides using as a tool for epidemiological

investigations, biomarkers are extensively been investigated to understand the history and prognosis of the diseases as scientist believe that these biological markers have the potential to identify the earliest events in the natural history of the disease describing mechanisms related to the its pathogenesis and accounting for the variability and effect modification of risk prediction.

Some of the potentials described by Schulte ⁸ are following:

- 1) Explanation of events from exposure to the risk factor until disease development.
- 2) Early events identification in the natural history.
- 3) Dose-response establishment.
- 4) Identification of mechanism to relate exposure and disease.
- 5) Establishment of variability and effect modification.
- 6) Individual and group risk assessment.

In cancer research, biomarkers are being extensively studied for diagnosis, progression evaluation, recurrence prediction and to evaluate the therapeutic treatment efficacy of the disease in response to a drug. Several omics studies, including proteomic, transcriptomic and genomic analysis of biomarkers with the advent technologies like DNA array, Protein array, Tissue microarray, MALDI-TOF and high throughput sequence analysis have made biomarkers discovery and analysis more easy and efficient in terms of disease prediction and treatment ⁹. Proteomics approach has a huge potential in understanding the complex human physiology and the state of disease associated. Techniques like Immunohistochemistry, Western blot, ELISA and mass spectrometry have an immense potential to discover biomarkers, especially that of new diagnostic and predictive biomarkers ^{10 11}. Realizing the clinical potential of human genome containing approx. 30,000 genes, new technologies like deep and high throughput sequencing has provided an exciting opportunity for novel application in biomarker identification and disease treatment based on genome-scale information ¹². In addition to genomics and proteomics platforms based biomarker assay techniques, metabolomics, glycomics, lipidomics and secretomics are also commonly known techniques used for the identification of biomarkers.

In melanoma, a series of biomarker candidates have been studied successfully in serum and tumour specimens. Lactate dehydrogenase, Tyrosine Kinase, Vascular endothelial growth

factor, Osteopontin, YKL-40, Melanoma-inhibitory activity protein, S100 and Interleukin-8 as Serum biomarkers while Cyclooxygenase-2, Galectine-3, Matrix metalloproteinase and Chondroitin sulfate proteoglycan 4 (CSPG4) as tissue-specific biomarkers of melanoma have been identified^{13 14}.

Discoidin Domain Receptors (DDR)

Introduction to Receptor Tyrosine Kinases (RTKs):

Receptor tyrosine kinases are essential components of signal transduction pathways that mediate communication between cells determining key roles in diverse biological processes such as cellular growth, differentiation, metabolism and motility in response to internal and external stimuli¹⁵. The RTK family has around 20 subgroups, which in total include 58 different receptors which are similar in structure and mechanism of activation¹⁶. The RTKs has two main domains i.e. an extracellular binding domain at its N terminal, connected to the cytoplasmic region with single α -helix hydrophobic transmembrane region while the intracellular domain contains a juxtamembrane domain linked with a tyrosine kinase domain at its C terminal¹⁷ as shown in Figure 1.1. The extracellular domain differs among the sub groups of RTKs. The α -helix hydrophobic transmembrane domain provides stabilisation support to the receptor while the intracellular kinase domain is responsible for receptor activation and signal transduction by phosphorylation.

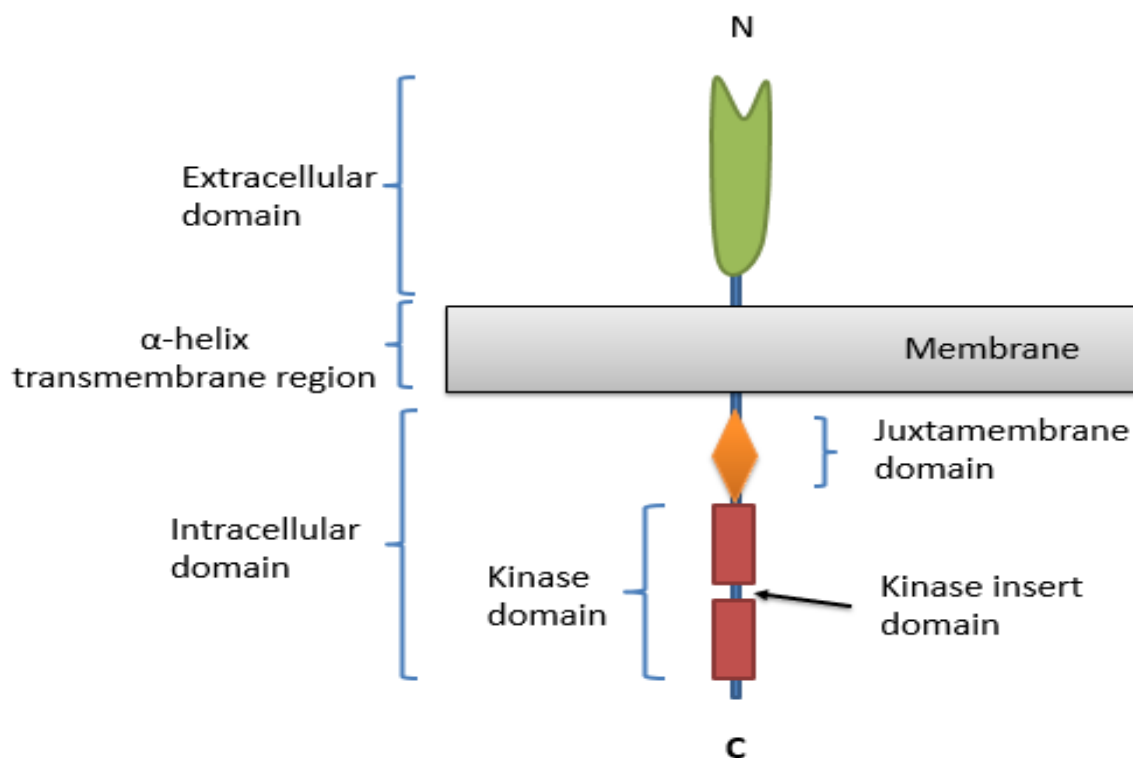


Figure 1.1 Structure of Receptor Tyrosine Kinases (RTKs). RTKs composed of an N-terminal selective ligand-binding extracellular domain that varies amongst different RTK subfamilies; a single α -helix transmembrane domain that provides stability to the receptor; and an intracellular C-terminal domain that composed of a juxtamembrane and kinase domains. The kinase domain is composed of 2 subdomains connected by one kinase insert domain and C-terminal tail. The intracellular domain is directly responsible for receptor activation and downstream signal transduction by phosphorylation of tyrosine kinase domains.

Introduction to Discoidin Domain Receptors (DDR):

Discoidin domain receptors 1 and 2 (DDR1 and DDR2) belong to the family of receptors Tyrosine Kinases (RTKs) as a sub group. These discoidin receptors were discovered initially in early 1990s by homology cloning of their kinase domains¹⁸. DDRs were considered as an orphan receptors until 1997 when two independent groups discovered that they are activated by several types of collagen^{19 20}. The function of DDRs are typical to those of RTKs and includes regulation of proliferation, cell adhesion and differentiation. They are activated through binding to collagen. It's the Discoidin (DS) domain of DDRs which distinguishes them from other types of RTKs. This DS domain is named due to its homology with the Discoidin I protein secreted by the slime mould *Dictyostelium discoideum*²¹.

Structures of Discoidin Domain Receptors:

The Discoidin domain receptors are differentiated as DDR1 and DDR2 based on the intracellular conserved kinase domain^{22 23}. DDRs are structurally characterized by 4 domains. The extracellular region composed of Discoidin domain at its N-terminal and Discoidin like domain (DS) which binds to the collagen. The Juxtamembrane domain (JX) composed of an extracellular juxtamembrane region (EJXM) constituted of about 50 AA in case of DDR1 and 30 AA residues in case of DDR2 and intracellular juxtamembrane region (IJXM) constituted of about 171 AA in case of DDR1 (depending on isoforms) and 142 AA in case of DDR2²⁴. The fourth domain is the catalytic kinase domain (KD) which constitute of about 300 AA in the intracellular region which ends at C-terminal with 8 AA for DDR1 and 6 AA for DDR2²⁵.

Discoidin Domain Receptor 1 Structure and Isoform:

The human DDR1 gene is composed of 17 exons, located in chromosome 6 (6p21.3)²⁵. Exon 1-8 encode the transmembrane domain, Exon 9 encodes the transmembrane domain, and Exon 10-12 encode the cytosolic juxtamembrane domain while other exons encodes the Kinase domain. DDRs can be spliced in 5 isoforms i.e. DDR1a, DDR1b, DDR1c, DDR1d and DDR1e. DDR1a and DDR1b are the most abundant isoforms of DDR1. DDR1a, DDR1b and DDR1c are functional receptors and DDR1d and DDR1e are considered as non-functional receptors (Figure 1.2).

DDR1a consist of 876 AA with a MW of 97 kDa, DDR1b consist of 913 AA with a MW of 101 kDa, DDR1c contains 919 AA and MW of 102 kDa, DDR1d contains 508 AA and MW of 56 kDa and DDR1e contains 767 AA and MW of 86 kDa. DDR1 has two regions i.e. extracellular region and intracellular region. The extracellular domain has Discoidin domain (DS) consist of 29-187 AA, Discoidin like domain (DS-like) 188-367 AA and Extracellular juxtamembrane region (EJXM) 368-417 AA connected to the intracellular domain with a transmembrane domain (TM) consist of 418-438 AA, while the intracellular domain contains Intracellular juxtamembrane region (IJXM) and a kinase domain (KD) at its C-terminal. Isoforms of DDR1 consist of same number of amino acid residues in extracellular domain and transmembrane domain while for the intracellular domain the number of AA differs for different isoforms i.e. for DDR1a the Intracellular juxtamembrane region (IJXM) consists of 134 AA residues ranging from AA 439-572, while for DDR1b and DDR1c there is an addition

of 37AA in this regions resulting in total number of 171AA ranging from 439-609 AA. The kinase domain consist of 285 AA residues ranging from AA 573-868 for DDR1a, AA 610-905 for DDR1b while DDR1c further contains +6 amino acids residues as compare to DDR1b ranging from AA 610-911 AA. DDR1a, DDR1b and DDR1c are functional receptors as they have the kinase domain which is active while DDR1d and DDR1e are non-functional receptors since they are kinase deficient or lack of ATP binding site because of frame shift and truncations.

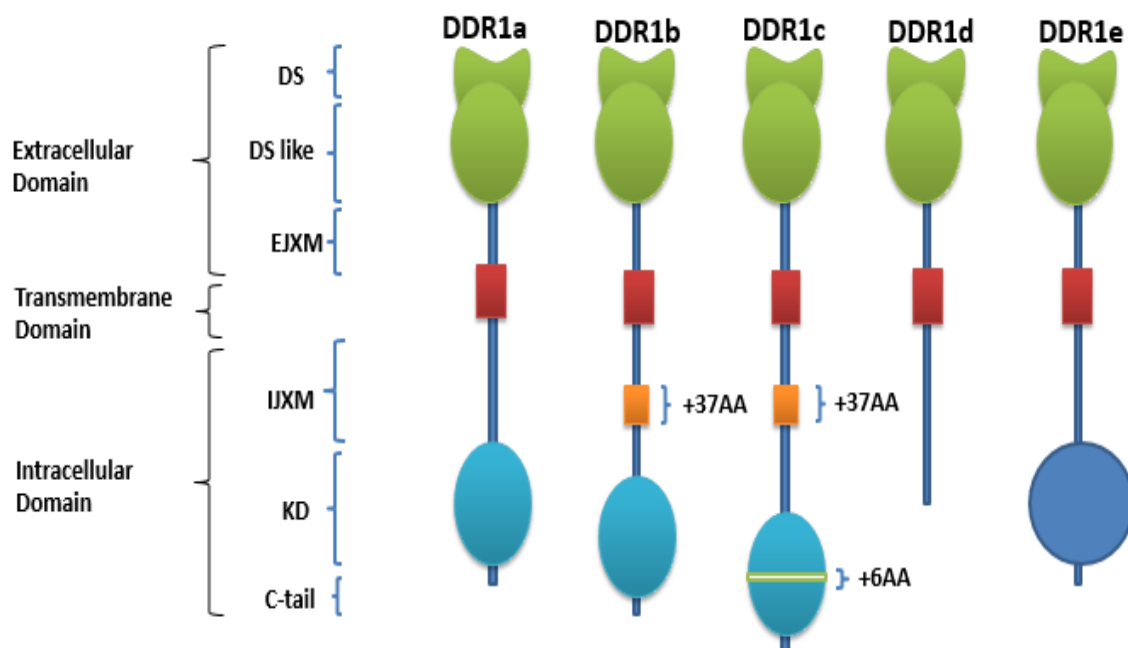


Figure 1.2: Structure and Isoforms of Discoidin Domain Receptor 1 (DDR1). DDR1 has 5 isoforms. DDR1a, DDR1b and DDR1c are enzymatically functional isoforms, whereas DDR1d and DDR1e do not present functional activity. The extracellular part of the DDR1 receptor is the same for all isoforms and differ in intracellular domain which determines the functionality of the receptor.

Discoidin Domain Receptor 2 Structure:

The human DDR2 gene is composed of 18 exons, with 3-18 as coding exons and maps to chromosome 1 (1q23.3). Since there is no alternative spliced isoforms has been described, DDR2 structure is composed of total 855 AA with a MW of 116 kDa. DDR2 also has the same protein architecture with 4 domains. Like DDR1, the Discoidin domain (DS) is composed of amino acids ranging from 29-187 AA and Discoidin like domain (DS-like) ranging from 188-367 AA while the Extracellular juxtamembrane region (EJXM) is 18 amino acids shorter as

compared to DDR1 and is composed of 32 AA ranging from 368-399 AA. The extracellular region is linked with Intracellular region with a transmembrane domain of 21 amino acids ranging from 400-420 AA. While in the intracellular region the Intracellular juxtamembrane region (IJXM) composed of amino acids ranging from 421-562 AA, the Kinase domain (KD) ranges from 563-849 AA which is further linked to the C-terminal with 6 amino acids (850-855 AA) (Figure 1.3).

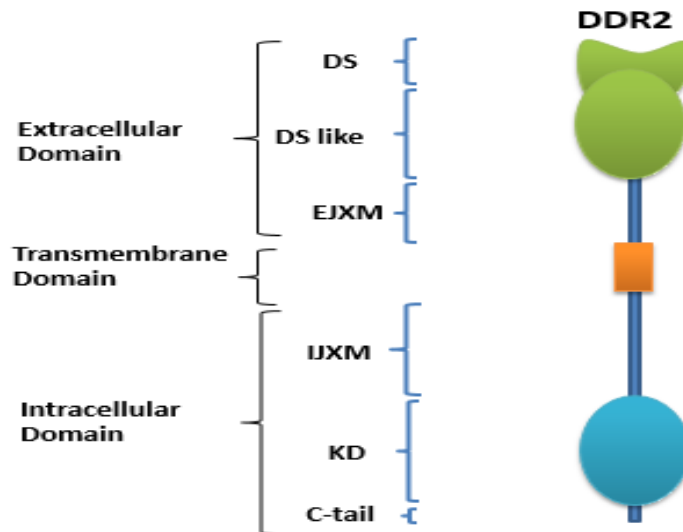


Figure 1.3: Structure of Discoidin Domain Receptor 2 (DDR2). DDR2 is composed of an N-terminal selective ligand binding extracellular domain which is connected to the intracellular domain by a transmembrane domain responsible for stabilisation of the receptor. The intracellular domain contains the kinase domain responsible for receptor activation and downstream signal transduction by phosphorylation. Unlike DDR1, there is no alternative splicing of Isoforms in DDR2.

Amino Acid Sequences of DDR1 and DDR2 (Extracellular region):

As mentioned earlier 5 isoforms of DDR1 have been described in literature which resulted from alternative splicing. All these DDR1 isoforms share same extracellular and transmembrane region while there is a difference in intracellular region. DDR1c is the longest isoform which contains 6 additional AA in its kinase domain as compare to DDR1a and DDR1b²⁶. DDR2 on the other hand has almost similar extracellular domain with a smaller extracellular juxtamembrane domain as compare to DDR1.

The DS and DS-like domain in DDRs make them unique among the RTKs family. These domains are responsible for DDR functioning as DS domain contains a collagen binding site which is responsible for mediating DDR specificity for fibrillar and non-fibrillar collagen²⁷. The function of DS-like domain of DDRs is not yet fully understood, but recent studies suggest that it contributes to collagen-induced receptor activation²⁸.

DDR1 and DDR2 share high degree of sequence homology in DS and DS- like domains with 59 and 51% of similarity, respectively²⁹.

The amino acid sequences of DDR1 extracellular domain

Met 1 – Thr 416 AA

MGPEALSSLLLLLLVASGDADMKGHFDPKCRYALGMQDR TIPDS DISASSS WSDST
AARHSRLESSDGDGAWCPAGSVFPKEEEYLQVDLQRLHLVALVGTQGRHAGGLGKE
FSRSYRLRYSRDGRRWMGWKDRWGQEVISGNEDPEGVVLKDLGPPMVARLVRFYP
RADRVMSVCLRVELYGCLWRDGLLSYTAPVGQTMYLSEAVYLNDSTYDGHTVGGL
QYGGLGQLADGVVGLDDFRKSQELRVWPGYDYVGWSNHSFSSGYVEMEFDFRLR
AFQAMQVHCNNMHTLGARLPGGVECFRRGPAMAWEGEPMRHNLGGNLGDPRAR
AVSVPLGGRVARFLQCRFLFAGPWLLFSEISFISDVVNNSSPALGGTFPPAPWWPPGPP
PTNFSSLELEPRGQQPVAKAEGSPT

The amino acid sequences of DDR2 extracellular domain

Met 1 – Arg 399 AA

MILIPRMLLVLFLLLPILSSAKAQVNPAICRYPLGMSGGQIPDEDITASSQWSESTAAK
YGRLDSEEGDGAWCPEIPVEPDDLKEFLQIDLHTLHFITLVGTQGRHAGGGHGIEFAPM
YKINYSRDGTRWISWRNRHGKQVLDGNSNPYDIFLKDLEPPIVARFVRFIPVTDHSMN
VCMRVELYGCVWLDGLVSYNAPAGQQFVLPGGSIIYLNDSVYDGAVGYSMTEGLG
QLTDGVSGLDLDDFTQTHEYHVWPGYDYVVGWRNESATNGYIEIMFEFDRIRNFTTMKV
HCNNMFAKGVKIFKEVQCYFRSEASEWEPNAISFPLVLDDVNPSARFVTVPLHHRMA
SAIKCQYHFADTWMMFSEITFQSDAAMYNNSEALPTSPMAPTTYDPMLKVDDSNTR

A sequence alignment between DS domain of DDR1 and DDR2 has been shown in Figure 1.4(A).

Crystallographic structure of DDRs DS domain.

The crystallographic studies of extracellular region of DDR1 and DDR2 shows that DDRs have two globular domains in the extracellular region i.e. the DS domain at N-terminus linked with the DS-like domain.

DDR1 and DDR2 have very high structural similarity in their DS and DS-like domains. Both domains adopt a β -barrel structure with eight strands arranged in two antiparallel β -sheets while the DS-like domain contains an additional 5 strands^{28 29}. NMR crystallographic analysis reveals the binding pocket in the DS domain for the identified DDR binding motif GVMGFO that is contained in fibrillar collagen³⁰. These strands encompass additional glycosylation sites and calcium binding site that currently has unknown significance. The GVMGFO motif present in fibrillar collagens I-III activates the DDR receptors by inducing an autophosphorylation besides lacking the capability of assembling into higher molecular structures which describes that there is no need of large molecular assemblies to induce activation. The extracellular juxtamembrane are predicted to be in unstructured form.

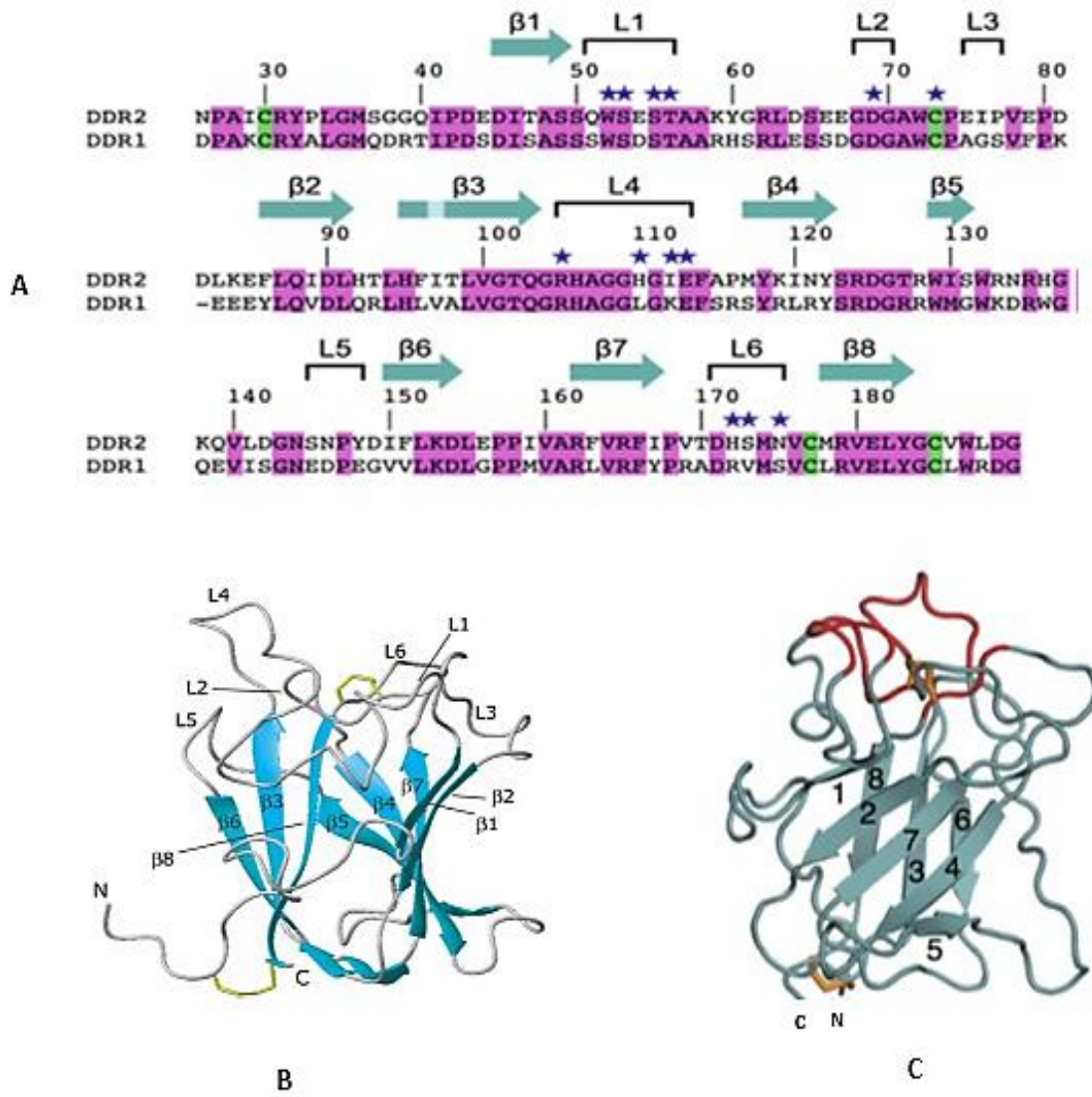


Figure 1.4: DS domain of DDR1 and DDR2. (A) Sequence Alignment of DS domain of the Human DDR1 and DDR2³¹. The sequence numbering and secondary structure elements of the DDR2 DS domain are indicated above the alignment. Conserved residues and cysteines are highlighted in magenta and green, respectively. (B) NMR structure of DDR2 DS domain²⁹. (C) NMR structure of DDR1 DS domain²⁸. Both DDR1 and DDR2 have β -barrel structure with eight strands.

DDRs activation by Collagen:

Collagen are the key constituents of extracellular matrices (ECM) that provides physical structural support to the connecting tissues³². With the interaction of matrix receptors, collagens also control cellular functions including cell differentiation, growth and morphogenesis. The interaction of collagen with cells is either directly through cell surface receptors or through an intermediary molecule that is recognized by the cell surface receptors. This interaction of collagen with cell is involved in the regulation of several physiological

processes like morphogenesis and wound healing, haemostasis and thrombosis and in regulation of immune system. But under pathophysiological conditions, these normal regulations are hijacked which leads to several diseases including metastatic tumors ³³.

DDR1 and DDR2 both bind to and are activated by collagen in its native triple helix form. DDR1 is activated by fibrillar collagen I, II, III, V and basement membrane collagen IV ¹⁹, while the denatured collagens are not able to induce receptor activation ³⁴. Basement membrane collagens are a composite of several large glycoproteins and form an organized scaffold to provide structural support to the tissue and also offer functional input to modulate cellular function. DDR2 is activated by fibrillar collagen I, II, III, V and non-fibrillar collagen X ³⁵. Vogel and co-workers described that the activation of the receptor is characterised by slow kinetics which resulted in increased maximal activity for several hours after treatment with collagen. Leitinger further described that unlike the paradigm of ligand induced dimerization of RTKs, DDRs recognize collagen only as a dimeric and not as a monomeric construct, indicating a requirement for receptor dimerization in the DDR-collagen interaction ³⁶. DDRs are already present on cell surface in dimeric form, so upon binding to collagen they are activated by dimeric conformational changes.

DDR activation and signalling:

1) Dimerisation:

DDRs form stable ligand-independent dimers on the cell surface unlike other RTKs where the receptors are thought to be monomeric and it needs a ligand to dimerize and further activate ³⁰. Xu and his co-workers demonstrated that DDRs are observed in dimeric form on the cell membrane and in the biosynthetic pathway ³⁷. No single DDR subdomain was found to be solely responsible for DDR dimerization, but it has been observed that the transmembrane domains of DDRs encode self-association in a bacterial reporter system ³⁸. The actual mechanism behind activation of kinase domain of DDR1 by collagen binding to the DS domain is not understood yet but one recent study describes collagen induce structural clusters of DDR1 which possibly lead to the activation of receptor ³⁹ but for DDR2 so far no studies have been described yet.

2) Phosphorylation:

Like other RTKs, DDRs also undergo autophosphorylation when they bind with ligand (collagen). However, the autophosphorylation induced by collagen is very slow and sustained compared to other RTKs. It can be extend up to 18 hours while autophosphorylation is usually

inhibited by phosphatases in few minutes for other RTKS¹⁹. The activation kinetics are dependable on the cell types. For example, DDR1 in embryonic kidney cells is phosphorylated at a peak after collagen stimulation of 60-90 minutes, whereas it takes several hours for a strong phosphorylation signal to appear in certain cancer cell lines^{20 40}. Studies have shown that maximal phosphorylation of DDR1 and DDR2 are dependent on the tyrosine kinase Src but the actual cellular and biochemical mechanism behind slow activation kinetics for both DDRs are still unknown^{41 42 43}.

3) DDRs initiated signalling:

Recent studies have shown that DDR1 promoted Th17 migration by activating the RhoA/ROCK and MAPK/ERK signaling pathways⁴⁴. In breast and colon carcinoma cancer cell lines, DDR1 activation triggers the regulation of Ras/Raf/ERK and P13k/Akt pathways⁴⁵. DDR2 initiated signalling is not well described so far but it is hypothesized that due to high similarity between DDR1 and DDR2, they employ similar mechanism of signalling. Studies have shown that DDR2 regulates the expression of MMPs in metastatic melanoma cells via ERK1/2 and NF- κ B signalling pathways to suppress the metastasis in response to collagen⁴⁶. Xu and co-workers have described that DDR2 promotes integrins α 1 β 1- and α 2 β 1- cell adhesion by enhancing integrin activation⁴⁷. Iwai and co-workers further described that cross talk signalling with Insulin enhances DDR2 phosphorylation⁴⁸. Valiathan and co-workers have beautifully explained the pathways associated to DDRs in cancer in the figure 1.5 published in their review paper which summarizes the downstream events regulated by DDRs.

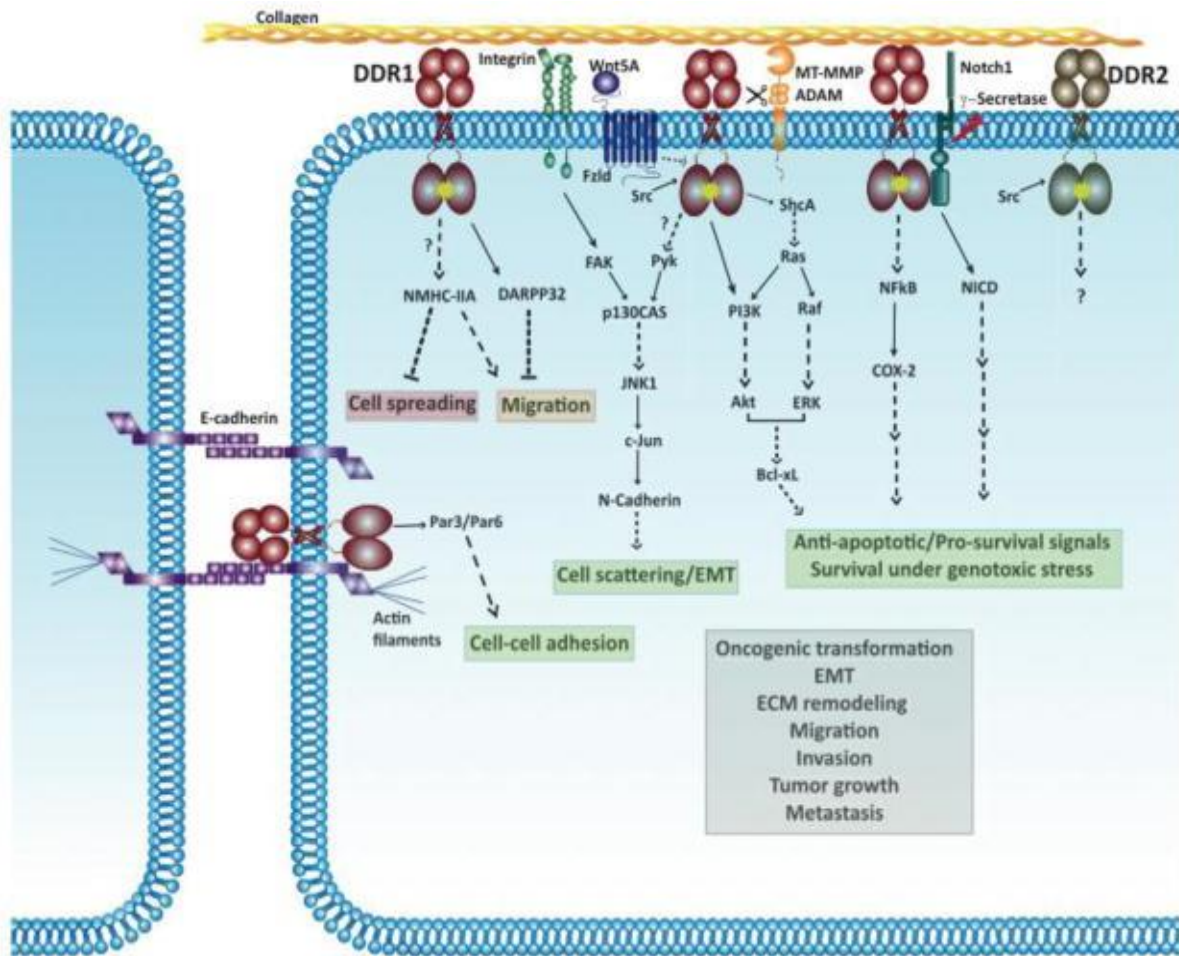


Figure 1.5: DDRs initiated signalling pathways⁴⁹. DDRs initiated signalling pathways described by Valiathan et al. In this figure they have shown signalling pathways with direct interaction of DDRs (solid lines), in-direct interactions mediated through one or more intermediate steps (dashed lines), activation of DDRs by Src (arrow pointing towards DDRs) and pathways triggered by DDR activation (arrows pointing away from DDRs). Here the DDRs with green stars are the activated DDRs. Regarding functioning of DDRs, red box indicates processes that are suppressed by DDRs, green box indicates processes that are promoted by DDRs and orange box indicates that processes suppressed or promoted by DDRs while the grey box indicates that these functions are processed due to DDRs but their signalling pathways mechanism is not understood yet. DDR1 activation triggers pro-survival Ras/Raf/ERK and PI3K/Akt pathways in human breast and colon carcinoma cell lines, resulting in upregulation of anti-apoptotic Bcl-xL and survival under conditions of genotoxic stress⁴⁵. In human breast cancer cells, DDR1 activation also increases NFkB DNA binding activity and cyclooxygenase (COX)-2 expression resulting in increased chemoresistance⁵⁰. In colon cancer cell, DDR1 activation triggers Notch1 cleavage by γ -secretase and forms Notch 1 Intracellular Domain (NICD), which translocates to the nucleus and upregulates pro-survival genes such as Hes1 and Hey2⁵¹. DDR1 activation, in conjunction with integrin β 1, triggers a p130CAS/JNK pathway in pancreatic cancer cells that results in upregulation of N-cadherin and epithelial to mesenchymal transition (EMT)-like cell scattering⁵². DDR2 signaling pathways in cancer are unknown practically.

Role of DDRs in Cancer

All human cancers almost display one of more RTKs dysregulated expression in the cells. Until today, the actual mechanism behind RTKs dysregulation in cancers is not well understood but it is quite evident that DDRs as collagen sensors are highly involved in degrading the extracellular matrices of the cells which leads to the cell migration and invasion in cancer ⁵³. Several tumors cells hijack DDRs resulting in disruption of normal cell-matrix communication and initiate metastasis. Some studies suggest that mutation in DDRs are also a common features of most cancers which play key roles in diseases development and progression ⁴⁹. It has been demonstrated that DDRs dysregulation plays a major role in many tumors including Non-small cell lung carcinomas (NSCLCs) associated with DDR2 expression ⁵⁴, while breast carcinoma ¹⁸, brain tumors glioma ⁵⁵, ovarian cancer ⁵⁶, hepatocellular carcinoma ⁵⁷ and lymphoma and leukaemia ⁵⁸ associated with the expression of DDR1 has been described so far.

Role of DDRs in Melanoma:

Melanoma also displays all the hallmarks of cancer like other solid tissue malignancies ⁵⁹. Frederic Saltel and his team has recently demonstrated the hallmarks of cancer associated with DDRs expressed in A375 melanoma cells ⁶⁰ (Figure 1.6). DDR1 is involved in the formation of invasive structures called linear invadosomes through the Cdc42-Tuba pathway which results in the overexpression of matrix metalloproteinase that leads to the cell migration and invasion by the degradation of extracellular matrix ⁶¹.

Recent studies have demonstrated the role and expression of DDRs in normal and melanoma cells. DDR1 mediates the adhesion of melanocytes to Collagen IV in the basement membrane with E-cadherin and this complex prevents the phosphorylation of DDR1 and cell spreading. This study suggest that E-cadherin localizes DDR1 to cell junction and prevents its binding with collagen which results in the elimination of DDR1 activity and DDR1-suppressed cell spreading ⁶².

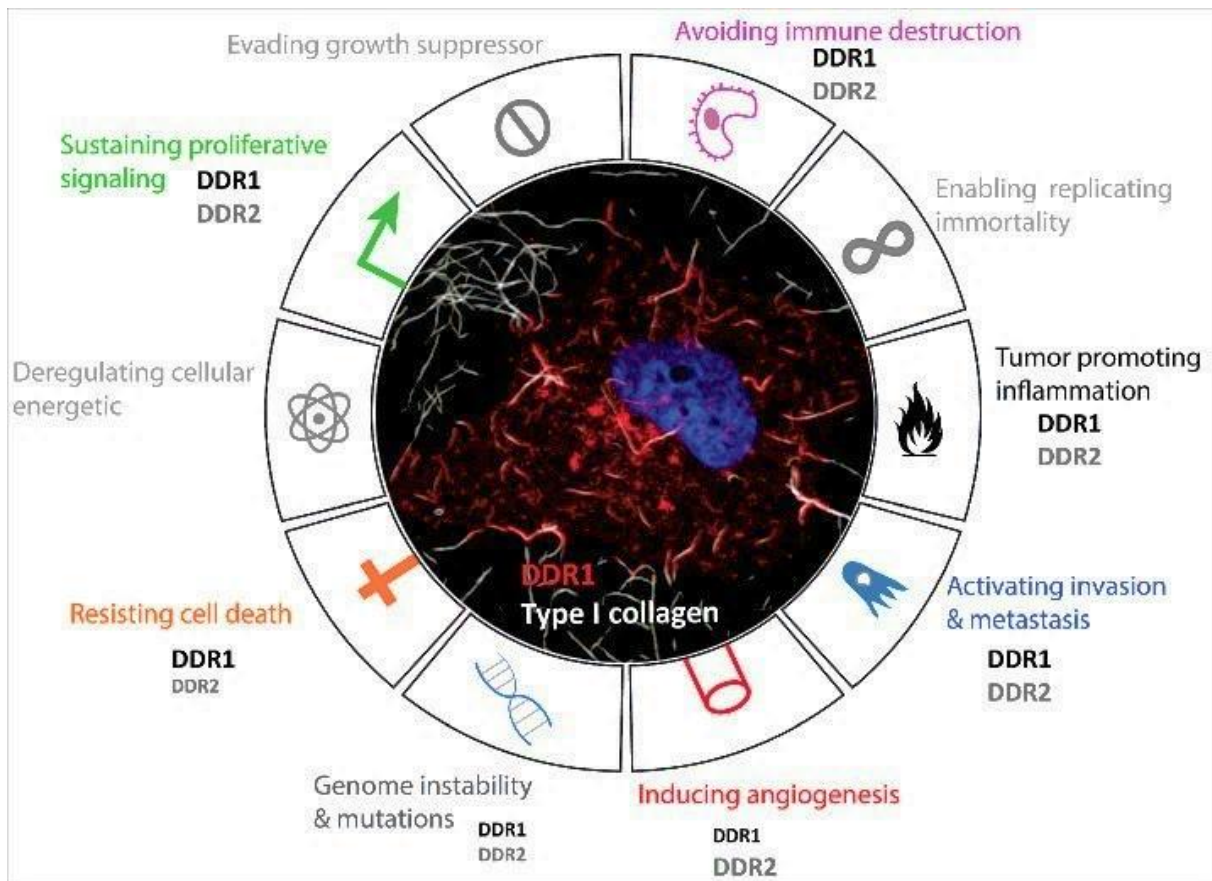


Figure 1.6: DDRs contribution in Cancer Hallmark.⁶⁰ A representative confocal image of A375 melanoma cells have been shown in the centre. The cells with fluorescent nucleus (blue) expresses DDR1 (red) co-localized on the collagen fibrils (Grey). The font size indicates the reported involvement of one of the DDRs more than other as described in literature.

Targeting DDRs in cancer for diagnostic or inhibitory purposes:

DDR1 and DDR2 are biomarkers for large number of cancers including melanoma. The contribution of DDRs in tumor progression clearly indicates that inhibition of these kinase receptors might represent a promising strategy for therapeutics. Several drugs have been reported inhibiting DDRs interaction with collagen but some of them are either not efficient due to bad affinity⁶³ or they target other RTKs as well due to non-specificity. FDA approved potent small-molecule like Dasatinib, imatinib, nilotinib and ponatinib were identified as inhibitors of DDR1 and DDR2^{64 65}, but they also inhibit other tyrosine kinases which puts a limitation on their usage. However in recent years, small molecules specifically targeting DDRs could potentially help developing drugs for treating cancers but it could also be interesting to target DDR1 or DDR2 specifically with an aptamer^{66 67}.

Matrix Metalloproteinases (MMPs):

Extracellular matrix (ECM) is a complex structure composed largely of collagens, glycoproteins and proteoglycans which provides structural support to the cell ⁶⁸. Apart of the structural support, ECM is also involved in cell signalling ⁶⁹. Cell surface receptors transduce signals into cells from ECM, which regulates diverse cellular functions, such as cell growth, cell survival, cell proliferation, cell migration, cell differentiation and cell homeostasis. ECM is secreted by fibroblasts and chondroblasts and is decomposed by many proteolytic enzymes ⁷⁰.

Matrix metalloproteinases (MMPs) are zinc endopeptidases and are implicated in the extracellular matrix (ECM) degradation under both physiological and pathological conditions ⁷¹. The first collagenase activity, in vertebrates, was shown by Gross and Lapse in 1962, during the study of the maturation of a tadpole tail. Since then, within different species, commonly called the (zinc and calcium) family of enzymes were identified as MMPs because of their catalytic activity dependent on metal ions and their ability to degrade all components of the ECM ⁷². Today, there are more than twenty MMPs as described by Egebald and Werb, listed in table 1.1 ⁶⁹.

Physiologically, MMPs are implicated at the level of consequent remodelling in the morphogenesis of branched structures of the body (such as angiogenesis), in healing, ossification, menstrual cycle and involution of post-lactation mammary glands ⁷³. In addition, the activity of MMPs allows the cell migration physically and modifies the signalling inherent to the extracellular matrix. This degradation of the ECM implies the modulation of different growth factors and growth inhibitors linked to the ECM by involving in direct cleavage, by breaking the links to the ECM or by the modulation of the activity of the antagonists of these molecules ⁶⁹.

MMP	Structural Class	Common Name
MMP-1	Simple hemopexin domain	Collagenase-1, interstitial collagenase, fibroblast collagenase,
MMP-2	Gelatin-binding Gelatinase A	72-kDa gelatinase, 72-kDa type IV collagenase,
MMP-3	Simple hemopexin domain	Stromelysin-1, transin-1, proteoglycanase, procollagenaseactivating
MMP-7	Minimal domain	Matrilysin, matrin, PUMP1, small uterine metalloproteinase
MMP-8	Simple hemopexin domain	Collagenase-2, neutrophil collagenase, PMN collagenase,
MMP-9	Gelatin-binding	Gelatinase B, 92-kDa gelatinase, 92-kDa type IV collagenase
MMP-10	Simple hemopexin domain	Stromelysin-2, transin-2
MMP-11	Furin-activated and secreted	Stromelysin-3
MMP-12	Simple hemopexin domain	Metalloelastase, macrophage elastase, macrophage
MMP-13	Simple hemopexin domain	Collagenase-3
MMP-14	Transmembrane	MT1-MMP, MT-MMP1
MMP-15	Transmembrane	MT2-MMP, MT-MMP2
MMP-16	Transmembrane	MT3-MMP, MT-MMP3
MMP-17	GPI-linked	MT4-MMP, MT-MMP4
MMP-18	Simple hemopexin domain	Collagenase-4 (Xenopus; no human homologue known)
MMP-19	Simple hemopexin domain	RASI-1, MMP-18
MMP-20	Simple hemopexin domain	Enamelysin
MMP-21	Vitronectin-like insert	Homologue of Xenopus XMMP
MMP-22	Simple hemopexin domain	CMMP (chicken; no human homologue known)
MMP-23	Type II transmembrane	Cysteine array MMP (CA-MMP), femalysin, MIFR
MMP-24	Transmembrane	MT5-MMP, MT-MMP5
MMP-25	GPI-linked	MT6-MMP, MT-MMP6, leukolysin
MMP-26	Minimal domain	Endometase, matrilysin-2
MMP-27	Simple hemopexin domain	
MMP-28	Furin-activated and secreted	Epilysin

Table 1.1: The Matrix Metalloproteinase (MMPs) family.

Classification and Structure of MMPs:

As their name suggests, MMPs represent a large family of enzymes proteolytics that require the presence of a metal ion (zinc and calcium) for their enzymatic activity. MMPs can be classified into 6 subfamilies according to their structural differences ⁷⁴:

- a. The Interstitial Collagenases: Interstitial collagenases (MMP-1, MMP-8 and MMP13) form a group of MMPs that mediates the breakdown of fibrillar collagen, including collagens type I, II, III and VII. Proteolytic cleavage of fibrillar collagen by these enzymes leads to the formation of denatured collagen (gelatin) which can then be degraded by gelatinases.
- b. The Gelatinases: MMP-2 and 9 are known as gelatinases and are involved in the degradation of several types of collagen and the 3 replicates of fibronectin type II confer a capacity to degrade the denatured collagen, gelatin.
- c. The Stromelysins: MMP-3 (stromelysin-1) and MMP-10 (stromelysin-2) are two similar proteins known as stromelysins with extended proteolytic spectrum that includes many glycoproteins and proteoglycans. They are produced by normal epithelial cells and some carcinomas. MMP-3 is considered to have a great catalytic power as compared to MMP-10. Recently MMP-11 (stromelysin-3), has been also added to this group which are expressed by mesenchymal cells, and is involved in the cleavage of serine protease inhibitors and appears to play a minor role in the degradation of the extracellular matrix.
- d. The Matrilysins: MMP-7 (matrilysin-1) and MMP-26 (matrilysin2) constitute the class of matrilysins. These are structurally simpler MMPs because they do not contain a homologous domain of hemopexin. These proteases are specifically expressed by cancer cells of epithelial origin.
- e. The Transmembrane MMPs: The transmembrane metalloproteases (MMP-14, -15, -16, -17, -24, -25 also called MT1-MMP to MT6-MMP) are the only insoluble MMPs. They are anchored to the cell surface either via a hydrophobic transmembrane site present in their homologous domain of hemopexin, or by an inositol phosphate bridge. They are

subdivided according to their cytoplasmic extension, some are of type 1 (MMP-14, 15, 16 and 24) and the others are proteins anchored with a glycosyl phosphatidylinositol (MMP-17 and 25). The role of Transmembrane MMPs particularly MTI-MMP will be discussed later in detail.

- f. The others: Several MMPs (MMP-12, MMP-18, MMP-19, MMP20, MMP-21, MMP-22, MMP-23A/B, MMP-27 and MMP-28) are newly discovered MMPs and their functions are still unclear. The involvement of these latest MMPs in cancer remains to be determined.

MMPs structures possess sequences that have certain homologies preserved between them. Conventionally, at the N-terminus is the predomain, which corresponds to the signal peptide and directs the protein to the endoplasmic reticulum (ER) ⁷⁵. This predomain is followed by a pro-domain responsible for maintaining MMPs in an inactive form. The prodomain located downstream of the predominant is usually composed of 80 hydrophobic residues which maintains the enzymatic activity in its latent form. Secreted by the cells in the form of zymogen (inactive), the MMPs comprise in this prodomain a conserved peptide sequence, Pro-Arg-Cys-Gly-X-Pro-Asp. The cysteine residue assures the "cysteine switch" by interacting via its thiol group (SH) with the zinc atom located in the catalytic site. Like the prodomain, the catalytic domain has a conserved His-Glu-X-Gly-His-XX-Gly-XX-His zinc binding motif which corresponds to the active site but also to a binding site for Ca⁺² ions. The prodomain is characterized by a sequence that contains three residues of histidines which chelate the zinc atom of the active site ⁷⁶. With the exception of MMP-7 and MMP-26 (matrilysin-1 and -2), most MMPs have a fourth C-terminal domain, hemopexin-like, which exhibits structural similarity with hemopexin and vitronectin ⁷⁷. This domain is responsible for the binding of MMPs to their substrates, as well as tissue inhibitors of MMPs (TIMPs) ⁷⁸. It has been shown that proMMP-2 activation is done via the interaction of its C-terminal domain with the MTI-MMP, as well as its interaction with TIMP-1 and TIMP-2 ⁷⁷. The hemopexin-like domain is connected to the catalytic domain via a hinge region. All MMPs are secreted in the extracellular medium, except the transmembrane MMPs which are located in the plasma membrane through a transmembrane domain at their C-terminus followed by a short cytosolic domain that serves for the intracellular signal transduction ⁷⁹.

The structural classification of MMPs given by Egeblad and Werb is given in Figure 1.7.

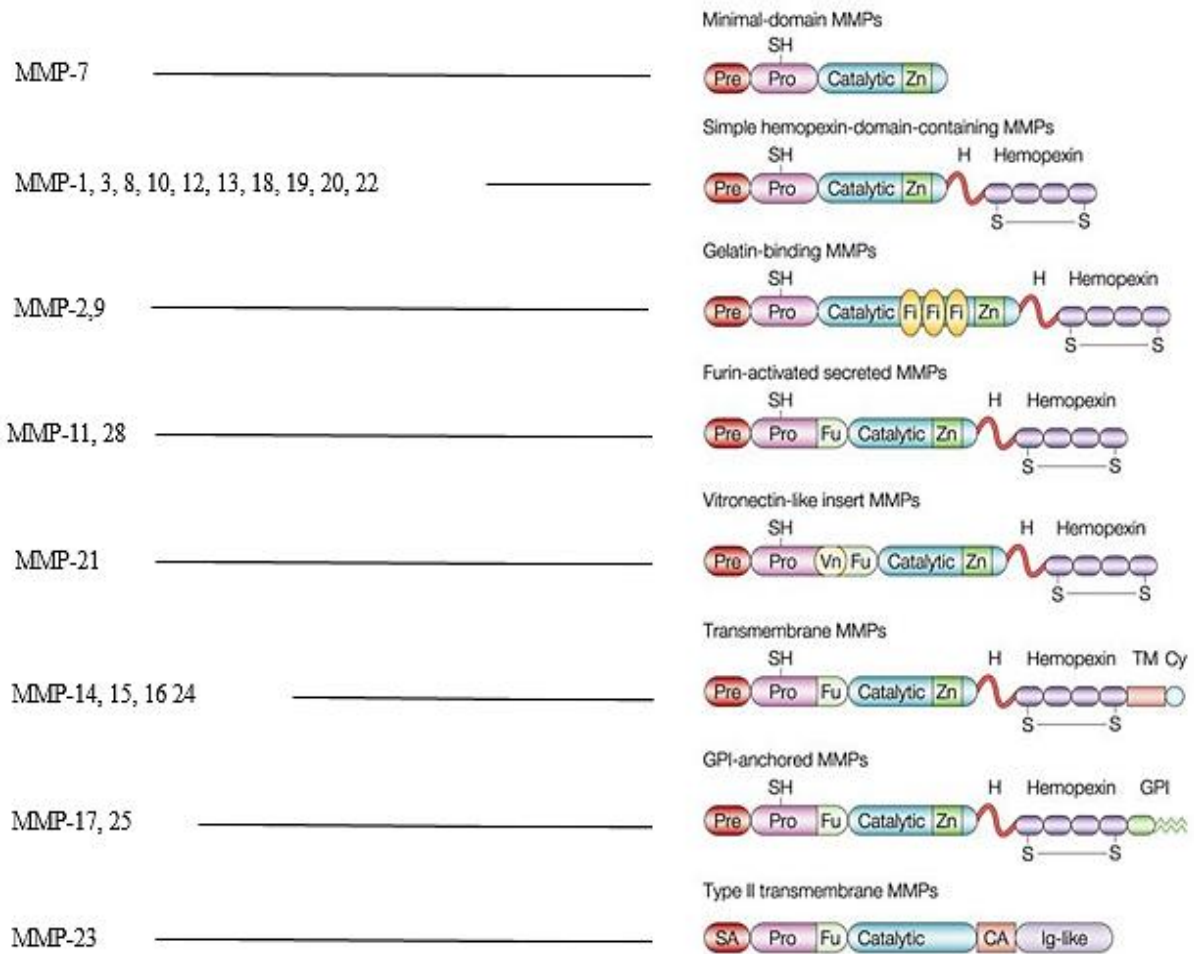


Figure 1.7: Structure of Matrix Metalloproteinases (MMPs)⁶⁹. At the amino-terminus is the predomain (Pre), the signal of excretion, which directs the MMP to the endoplasmic reticulum. Next, the prodomain (pro) is responsible for maintaining the latency state of the zymogen with a cysteine (SH) that interacts with the catalytic site. The catalytic site comprises a zinc binding site. The gelatinases have 3 fibronectin II type inserts binding the collagen (Fi). The hemopexin-like domain provides interaction with endogenous TIMPs inhibitors, cell surface localized molecules, and substrate recognition. It is connected to the catalytic domain via a hinge region (H) rich in proline and comprises a disulphide bridge (S-S). The MT-MMPs comprise at their carboxy-terminal end a transmembrane region (TM) and a short cytoplasmic domain (Cy) or a membrane anchoring domain glycoposphatidylinositol (GPI). MMP-23 has a particular anchoring system rich in cysteine and proline (CA), a region homologous to the interleukin 1 receptor and a region homologous to immunoglobulin G. Some MMPs contain a furine recognition pattern (Fu) for intracellular serine proteases allowing the activation of MMPs and a vitronectine (Vn) motif.

Activation of ProMMPs:

Most MMPs are secreted as latent zymogens, achieving catalytic properties in the ECM milieu. Some of these MMPs are intracellularly processed while few of them are processed at the cell membrane, into fully active enzymes. Non-proteolytic compounds such as 4-aminophenylmercuric acetate (APMA), denaturants (SDS) and commercial perturbants (detergents) or proteases open the cysteine to zinc switch in order to trigger the proMMP activation⁸⁰. The prodomain of MMP is removed in an autocatalytic manner or by proteases where the cysteine is replaced by water molecule to allow enzyme catalysis to proceed⁸¹. MT-MMPs contain a furin-like enzyme recognition conserved motif (RXRXXR) between their pro- and catalytic domains, and are activated intracellularly in the Golgi network^{82 83}.

Membrane type matrix metalloproteinase (MT1-MMP):

MT1-MMP which is also known as MMP14 is the first membrane type MMP to be discovered. Since these MMPs are anchored in the membrane, they play a unique role compared to secreted MMPs in the localized degradation of the ECM.

Expression and Regulation of MT1-MMP:

Matrix metalloproteinases are usually expressed at very low levels in healthy cells, however the level of expression of MMPs can be induced in physio pathological circumstances that require remodelling of the ECM. The expression of the majority of MMP genes is induced by growth factors such as epidermal growth factor (EGF), pro-inflammatory cytokines like TNF- α interleukin 1 β (IL-1 β), and phorbol esters⁸⁴. These mediators lead to the activation of I κ B kinase and MAP kinase (intracellular signaling pathways) resulting in the nuclear recruitment of different transcription factors such as NF- κ B⁸⁵ which will upregulate transcription of MMPs. It has been demonstrated that TNF- α stimulates activation of pro-MMP2 in human dermal fibroblasts through NF- κ B mediated induction of MT1-MMP⁸⁶.

Furthermore, Lafleur and colleagues demonstrated that an overexpression of MT1-MMP in endothelial cells stimulated by pro angiogenic factors such as VEGF and TNF- α confirms its role in angiogenesis and tumor growth⁸⁷. Until now, MT1-MMP is the only MMP that is rigorously co-expressed with MMP-2 and TIMP2 mainly at the stromal cell level⁸⁸. This co-expression is consistent with the activation of proMMP-2, which suggests an essential role for MT I-MMP in the tumor invasion and the metastases⁸⁹.

Role of MT1-MMP in tumor:

The involvement of MMPs in tumor progression has been demonstrated from animal models in which the expression of certain MMPs in cancer cells has been shown detrimental ⁹⁰. However, these proteins can play a protective role for the organism ⁶⁹ such as:

- release of TGF-B which inhibits plasminogen tumor growth
- collagen XVIII
- modulation of apoptotic signals of integrins
- activation of chemokine CXL12 (pro-metastatic molecule)
- Promotion of cell differentiation (by an unknown mechanism).

Nevertheless, most of the effects of MMPs are pro-tumor. They play a key role in tumor progression by degrading the ECM. They intervene in tumor growth, the promotion of cell survival, angiogenesis, invasion, epithelial / mesenchymal transition and the decrease of the immune response. Indeed, MT1-MMP is involved in tumor invasion process and in the formation of metastases ⁹¹. MT1-MMP degrades Collagen type I, II and III, Fibrinectin, Laminin I and V, Vitronectin, Fibrin and aggrecan ^{92 93}.

MT1-MMP associated metastatic melanoma:

MMPs are the primary agents responsible for the degradation of ECM degradation and their expression has been linked to the progression of many cancers including melanoma ⁹⁰. MT1-MMP have been implicated as pro-tumorigenic and pro-metastatic factor along with MMP2, in a wide variety of cancers including melanoma ⁸⁶.

The most reported mechanism of involvement of MT1-MMP in metastatic melanoma tumor is through the activation of pro-MMP2 to active MMP2 at the plasma membrane of the cells. The activation process is based on the formation of a trimolecular complex between MT1-MMP, TIMP-2 and proMMP-2 that forms on the surface cells (Figure1.8). At first, MT1-MMP binds via its catalytic domain to the N-terminal domain of TIMP-2. In fact, the interaction between these two molecules is accomplished via the C-terminal domain of TIMP-2 and the hemopexin domain of proMMP-2. Once the MT1-MMP / TIMP-2 / proMMP-2 complex is formed, a second neighbouring active and free MT1-MMP molecule, cleave proMMP-2 at site Asn³⁷ _Leu³⁸ of the prodomain. In a second step, the Asn⁸⁰-Tyr⁸¹ of the prodomain of MMP-2 is cleaved either by self-cleavage or by the action of plasmin or other active MMPs (MMP-1, -2 and -7), to generate the active form of MMP-2 ⁹⁴. In this mechanism, TIMP-2 acts as an activator and not

an inhibitor by acting as an adapter molecule. Indeed, the pericellular concentration of TIMP-2 seems decisive for the activation of proMMP-2 by MTI-MMP, since the activation of proMMP-2 is only possible at low concentrations of TIMP-2, sufficient for formation of the trimolecular complex MTI-MMP / TIMP-2 / proMMP-2, while an excess of TIMP-2 can saturate all the MTI-MMP required for the proteolysis of proMMP-2.

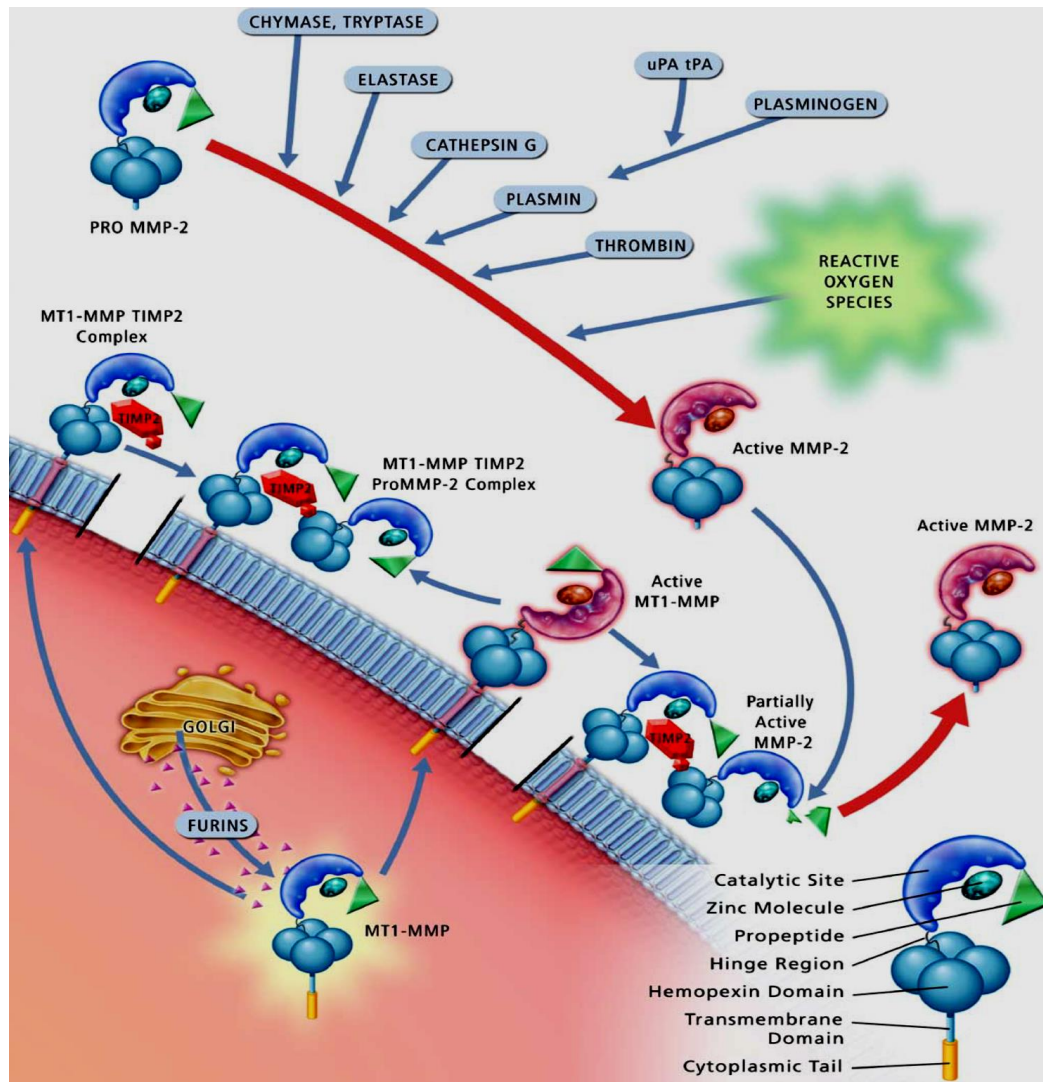


Figure 1.8: Activation of MMP-2 by MT1-MMP⁹⁵. MMP-2 activation depends on its interaction with complexes of MT1-MMP (MMP-14) and TIMP2. MT1-MMP is activated by furins in the Golgi and translocates to the cell membrane where it is inhibited by TIMP-2 forming a complex. ProMMP-2 then binds to TIMP-2 via its hemopexin domain (as shown in the MMP structure at bottom right). This leaves the proMMP-2 molecule vulnerable to cleavage by adjacent active molecules of MT1-MMP, which partially activates MMP-2. Other active MMP-2 molecules accomplish the final cleavage of the propeptide. Other mechanisms that involve serine proteinases or reactive oxygen species can also activate MMP-2 (as shown in the upper figure). Red arrows show steps which produce active MMP-2 while blue arrows indicate steps in the pathway.

MT1-MMP as a target in Melanoma:

The important role of MMPs in tumor progression has made it a target of anti-cancer therapy. Several synthetic inhibitors of MMPs have been developed in recent years to control the formation of metastases and tumor angiogenesis. Most of these inhibitors have the characteristic of carrying an acid hydroxamic, a carboxamic acid, phosphoramidate, thiol or other groups functional that chelate Zn^{2+} the catalytic site of the MMPs, which leads to their inhibition. The crucial roles that MT1-MMP exerts at different levels of tumor progression, as well as its involvement in resistance to chemotherapy and radiotherapy demands more attention. However, some inhibitors such as batimastat (BB94) and Marimastat (BB2516), hydroxamate inhibitors, have been developed to target a broad spectrum of MMPs and their results are highly encouraging but the major side effect of most of these drugs in humans, such as musculoskeletal pain in joints caused by inflammation and fibrosis has been observed in advance cancer cases.

Aptamers:

Aptamers are single stranded structured oligonucleotides (either DNA or RNA, this thesis will focus on DNA aptamers) capable of binding to their selected target with high affinity and specificity^{96 97}. The term “Aptamer” was coined by Ellington referring to the Latin word “aptus” meaning to fit, and the Greek word “meros” meaning part. Aptamers are considered as nucleic acid based chemical antibodies which can be selected against variety of targets i.e proteins^{98 99}, viruses^{100 101}, bacteria^{102 103 104}, small metabolites^{105 106}, cells^{107 108} and now a days even in tissues¹⁰⁹. Aptamers are generated by a combinatorial method known as SELEX (Systematic Evolution of Ligands by Exponential Enrichment) with a starting library contains 10^{14} – 10^{15} different sequences that fold into different structures depending on their particular sequence^{110 111}. Aptamer binds to its target based on three dimensional conformational changes. This 3D structure is the result of a combination of Hydrogen bonding, Electrostatic and Vander Walls interactions and stacking of aromatic rings¹¹².

Aptamers vs. Antibodies:

Even though antibodies have been known for a long time in the diagnostics and treatment of diseases, antibody based treatments suffer from various drawbacks as they are highly immunogenic, laborious and expensive to produce and with high batch to batch variation. Aptamers thus show inherent advantages that merit their application in biomedical and analytical sciences, as well as in basic molecular biology. Aptamers can be prepared by a simple automated chemical reaction while antibodies preparation needs tedious procedures involving cells for production. Unlike antibodies, aptamers are considered to be chemically robust with high stable structure i.e. it regains its activity once it comes to its natural environment after heat exposure and denaturation. This property makes aptamers highly a molecule of interest for many analytical applications. Being a chemical antibody, aptamers have a high shelf life as compare to antibodies (Table 1.2).

	Antibodies	Aptamers
Method of Production	Biological	Chemical
Size Range	10^4 – 10^5 Da	10^4 Da
Shelf life	Limited	Long (lyophilized/frozen)
Activity	Variable with batch	Uniform
Modifications	Random	Controlled
Affinity	nM– μ M	pM–nM

Table 1.2: Aptamers vs. Antibodies

With all these advantages, aptamers have some limitations but these limitations can be easily overcome by PEGylation or conjugation. As aptamers are small in size, they show higher clearance rate in vivo as compared to antibodies^{113 114}. It can also be an advantage for imaging of tumor cells with radio-elements. Beside this, the nuclease degradation of aptamers in plasma can easily be overcome with a controlled modification at its desired position^{115 116}. The modifications on aptamers will be discussed later in this chapter with detail.

Structure of Aptamer:

Nucleic acids are polymers of elementary blocks called nucleotides. Each nucleotide consists of three parts: a nitrogen base, a sugar and a phosphate group (Figure 1.9). DNA and RNA are differentiated by the nature of sugar i.e. 2-deoxyribose for DNA and ribose for RNA. Adenine (A), cytosine (C) and guanine (G) are present in both DNA and RNA, whereas thymine (T) is specific for DNA and uracil (U) for RNA.

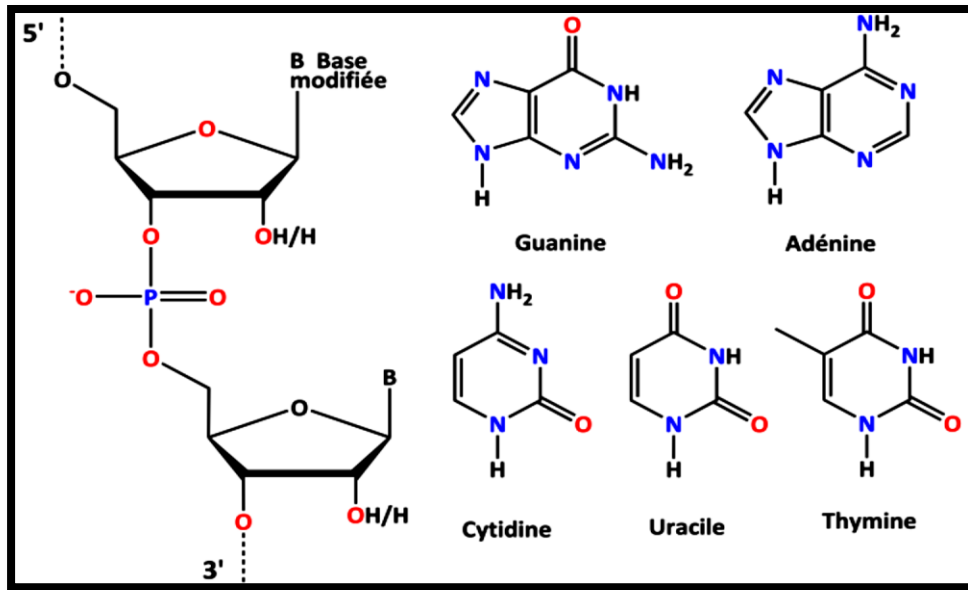


Figure 1.9: Nucleotides with Purine and pyrimidine bases

Aptamer interaction with protein:

The interaction of aptamer against its target is analogous to the interaction of antibodies with the epitope of the protein. Aptamer goes under structural conformational changes while binding to its target ^{117 118}. Aptamers bind to its target protein with a three dimensional structure formation which fits on the binding site of the protein called aptatope as shown in Figure 1.10 ¹¹⁹.

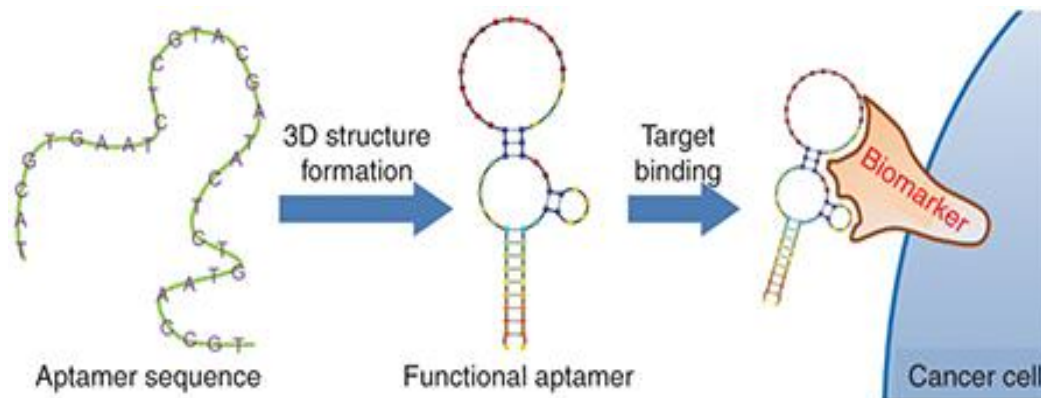


Figure 1.10: Schematic diagram of aptamer binding to its target.

This compact folding of aptamer enhances the “trapping” of aptamer in the protein pocket which makes the binding stronger ¹²⁰.

SELEX (Systematic Evolution of Ligands by Exponential Enrichment):

The process by which aptamers are selected against its target molecule is known as SELEX (Systematic Evolution of Ligands by Exponential Enrichment). SELEX was initially introduced in 1990 by two groups working independently^{110 97}.

Principle of SELEX:

Generally SELEX is an in vitro evolution method based on combinatorial chemistry. The term SELEX was first used by Larry Gold and Tuerk to describe a set of experiments performed to isolate single stranded RNA ligands to T4 DNA polymerase⁹⁶. Basically the principle of SELEX is similar to that of natural selection in evolution proposed by Charles Darwin over 150 years ago. In SELEX, aptamers are selected through the model “Survival of the fittest” as it is based on molecular evolution theory. Aptamers are selected as an evolved molecule after performing iterative rounds of selection with PCR amplification which results in the enrichment and existence of the evolved molecule (aptamer) after stringent conditions (Figure 1.11). The selection of ligands beyond natural systems emanates from a chemically synthesized nucleic acid library with a huge diversity of variant sequences. The diversity of the library depends on the length of the variable region of the variant sequences. Sequences with a variable region of 30 oligonucleotides approximately have $4^{30}(\cong 10^{18})$ random oligonucleotide sequences.

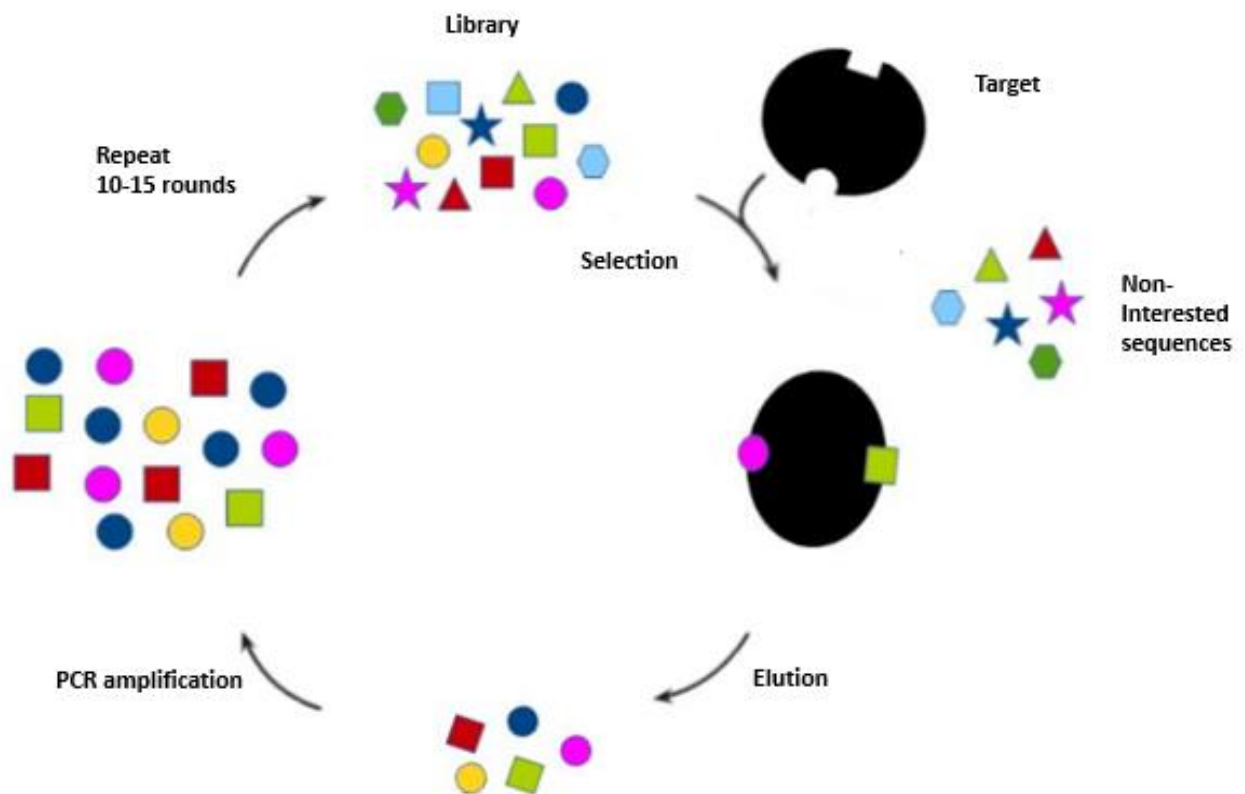


Figure 1.11: The SELEX process. The library containing DNA or RNA molecules (10^{15} sequences) is incubated with the protein target of interest. The bound sequences of interests are then recovered by elution or extraction method and amplified by Polymerase Chain Reaction (PCR), and this process is repeated until the library is enriched with the potential aptamer sequences.

For the selection of DNA aptamer, the library is used as a starting library while in case of RNA aptamer selection, a transcription of the library is required⁹⁷. The oligonucleotide sequence library is then optionally incubated with any negative target to discard all the non-specific sequences. The recovered library is then incubated with the target molecule where all sequences bound to the target molecule are extracted/eluted and amplified by PCR (for DNA library) or RT-PCR and transcription (for RNA library). After PCR, the sense strand is then separated and used as a library for next round. During SELEX, an iterative rounds of SELEX is normally required depending on the method used for selection¹¹². The SELEX process is carried out under same conditions for which the aptamer is being developed. Once the SELEX step is

finished, rounds of SELEX are sequenced by Sanger Sequencing after cloning ¹²¹ or High Throughput Sequencing (HTS) ¹²².

Types of SELEX:

The conventional SELEX method mainly consists of the following three steps i.e. selection, partitioning and amplification for enrichment. Based on the nature of target molecule and the SELEX library, different types of SELEXs are performed to select an aptamer with high affinity and specificity. Although there are many types of SELEX reported in literature but in this chapter we will focus only on the common methods along with recently reported SELEX methods.

1) Magnetic Beads Based SELEX:

Magnetic Beads based SELEX is one of the methods extensively used in the selection of aptamers. It employs magnetic beads for the immobilization of the target molecule. Bruno and colleagues first introduced a SELEX based on magnetic beads to select a DNA aptamer against chloroaromatics using magnetic microbead-based affinity separation ¹²³. In this method, the target protein is first immobilized on magnetic beads followed by an incubation with an oligonucleotide library which results in a target–aptamer complex formation that was separated from unbound oligonucleotides by a magnetic separator. Given the wide utility of the (Histidine)₆-Ni²⁺-nitrilotriacetate (Ni-NTA) system in molecular biology and biotechnology for affinity chromatography-based protein purification, this system has also been exploited to select an aptamer against the histidine tagged protein fixed on Ni-NTA magnetic beads ¹²⁴. Another vast technique, used in Magnetic beads based SELEX is the streptavidin-coated magnetic beads for the immobilization of the biotinylated molecule ¹²⁵.

A more convenient and relatively effortless method, FluMag-SELEX was described by Stoltenburg and colleagues in 2005 which made the magnetic beads SELEX more interesting ¹²⁵. The principle of FluMag SELEX is based on immobilizing the target on magnetic beads, where after the first round of selection, the selected ssDNA library is amplified with a fluorescence labeled primer to generate fluorescent labeled library which will be used to evaluate the SELEX rounds by fluorescence measurement of the library ¹²⁶.

Research of magnet use in SELEX has led to the development of new SELEX methods like

microfluidics based SELEX Technology (M-SELEX). These advent technologies have been successfully described with the selection of high affinity aptamers. M-SELEX method exploits a number of unique phenomena occurring at microscale that implements a design enabling it to manipulate small numbers of beads precisely and isolate high-affinity aptamers (Kd in low nanomolar range) rapidly ¹²⁷. Magnetic beads based SELEX will be discussed later in detail.

2) Nitrocellulose Membrane Filtration-Based SELEX:

Nitrocellulose membrane is highly used in western blot and Atomic force microscopy (AFM) for the immobilization of protein due to its non-specific binding to amino acids. Nitrocellulose membrane was first used by Kramlova's group in 1968, for the micro chromatographic separation of proteins from RNA molecules ¹²⁸. Since then, nitrocellulose membrane has been extensively used for the separation of proteins from other molecules. This method was then applied for the selection of aptamers against protein targets as Filtration SELEX. In Filtration SELEX, the sequences of interest and non-interest are separated by using nitrocellulose filter membranes ^{129 130 98}. In fact the first SELEX performed by Larry Gold and his colleagues was based on nitrocellulose membrane filtration-based SELEX, where an aptamer against the T4 DNA polymerase was selected using nitrocellulose membrane ⁹⁶. Nitrocellulose membrane filtration based SELEX is limited to SELEX performed against protein targets, since the nitrocellulose membrane has no affinity against small molecules and peptides. Detailed discussion of nitrocellulose membrane based filtration SELEX will be given later.

3) Cell SELEX:

In vitro selection targeting recombinant purified proteins has been succeeded so far with high ratio of selecting an aptamer against the purified protein target. However in some cases, the selected aptamers are not able to bind its target receptor present on cells in its natural environment. This problem can be countered by selecting an aptamer directly against the cell expressing the target receptor on its surface. The difference between Cell SELEX and other SELEXs is that, in Cell SELEX the knowledge of the target is not necessary as it will target whole cell ¹³¹.

This makes Cell-SELEX more advantageous than other SELEXs, as the targets are present in their native conformation which provides a natural environment for the oligonucleotide library to recognize its target molecule. Furthermore, the partition step of Cell-SELEX is

relatively simple as compare to other SELEXs, because the unbound sequences can be easily removed by centrifuge or wash (for adherent cells). Blank et al. first reported Cell-SELEX in 2001, employing rat endothelial cells (YPEN-1) and mouse microglial cells (N9) for positive and negative selection steps respectively ¹³². Since then Cell SELEX has been widely used worldwide for the selection of aptamer especially against cancer cells ^{133 134 135}.

In the last decade, there has been an improvement in Cell SELEX Strategy. Hicke and colleagues developed a hybrid of Cell SELEX and Protein SELEX known as Cross-Over SELEX in which an aptamer was selected against the purified tenascin-C and tenascin-C expressing glioblastoma-derived cell line, U251 ¹⁰⁷. Since protein receptors are present in their natural conformation in cells, while aptamer selection against the recombinant purified protein is more specific. These advantages of both SELEX can be helpful in selecting an aptamer which recognizes its target in native conformation with high affinity and specificity. In 2012, Giangrande's group reported another distinctive cell SELEX based method which is a combination of cell-internalization SELEX and high throughput screening ¹³⁶. A vascular smooth muscle cell specific internalizing RNA aptamer was selected through this method. The RNA library was incubated with the cells for 90 minutes (predetermined time for cell internalization), then all internalized RNA was isolated, extracted and amplified by PCR. Concentrated solution salts were used for the removal of unbound or non-internalized RNA. The selected aptamers were then analysed by high throughput screening.

Mayer in collaboration with Famulok described another improved version of Cell SELEX known as FACS-SELEX. In FACS SELEX, the selection process during whole Cell-SELEX could be monitored and sorted by flow cytometry where fluorescently labeled nucleic acid library is incubated, and bound to targets ¹³⁷. FACS-SELEX overcomes the limitations of the basic Cell-SELEX i.e. the perfect separation of bound from unbound or nonspecifically bound oligonucleotides. Even live cells can be easily distinguished from dead cells by using FACS. Mayer later also described that aptamers selected by whole-cell SELEX using FACS are more sensitive and specific to bacteria as compared to antibodies, suggesting that aptamers can be a promising alternative of antibodies in biosensor ¹³⁸. Cell SELEX against DDR2 expressing cells will be discussed later in detail.

In vivo SELEX:

In vivo SELEX is a technique by which aptamers are selected using living organisms. The first in vivo SELEX was reported by Berkhout and colleagues in 1993 for the in vivo selection

of randomly mutated viral genomes with multiple rounds of viral replication in CD4+ cells ¹³⁹. Another in vivo SELEX targeting the 5' untranslated leader region of the (HIV-1) RNA genome (containing motif for viral replication) was recently reported ¹⁴⁰.

During last few years, In vivo SELEX methodology has been extensively used for selection of aptamers against tumors cells. In 2010, Sullenger's group firstly reported a selection of RNA aptamer in mice with intrahepatic colorectal metastases ¹⁴¹. For this purpose, the library with 2'-fluoropyrimidine-modified RNA sequences were injected into mice with intrahepatic colorectal metastases. The liver of the mice was then isolated and RNA aptamers were extracted and amplified. In this SELEX, total 14 rounds of selection were performed. In each round the library was injected into a new mice with metastasized liver. In vivo SELEX is similar to in vitro SELEX in methodology but in vivo SELEX is performed inside living organism. In vivo SELEX has been used to select aptamer against human colorectal cancer ¹⁴² and prostate cancer bone metastasis ¹⁴³. As discussed earlier that aptamers face limitations due to fast renal clearance which makes the in vivo selection very difficult. Overcoming these limitations, two independent groups have successfully reported an in vivo SELEX using PEGylated DNA library ¹⁰⁹ and 2'-fluoropyrimidine-modified PEGylated RNA library ¹⁴⁴ in xenograft mice models. Cheng and colleagues have also reported a selection of brain penetrating aptamer through in vivo SELEX ¹⁴⁵.

4) Capillary Electrophoresis SELEX (CE-SELEX):

Capillary Electrophoresis SELEX (CE-SELEX) is one of the most frequently used SELEX method. Unlike conventional SELEXs which require around 15 rounds of selection, CE-SELEX is fast with the enrichment of SELEX library in only few rounds of selection. It was first reported in 2004 by Mendosa and Bowser by selecting aptamer against IgE with a Kd of 27nM ¹⁴⁶. CE-SELEX differs from other conventional methods as the separation of interested and non-interested sequences is based on their electrophoretic mobility ¹⁴⁷. In CE-SELEX, oligonucleotide library is incubated with its target in vitro, and this mixture is then injected into a capillary. The aptamer-protein complex has lower mobility as compared to the free oligonucleotide which results in the separation of the bound and unbound library while running through capillary with constant pressure. A collection window is already determined for the complex which can easily be recovered. The collection strategy depends on the coated or uncoated capillaries as discussed by Demsovski and Bowser ¹⁴⁸. The recovered sequences are then amplified to generate enough pool for proceeding rounds. CE-SELEX is highly

advantageous as compared to other conventional SELEX methods, as in CE-SELEX the concentration of the target can be decreased until 1pM and the volume to 5uL for incubation. In comparison with affinity column methods, CE-SELEX selection occurs in free solution, eliminating the unfavourable kinetics associated with elution of high-affinity sequences ^{149 150}.

CE-SELEX has been modified further to accelerate the selection procedure and to minimize the PCR biasness amplification. In 2006, Berezovski's group reported a new method known as Non-SELEX, which selects aptamer without amplification ¹⁵¹. In Non-SELEX, the repetitive step of partitioning required for the separation of aptamer-target complex from free oligonucleotides is performed based on Non-Equilibrium Capillary Electrophoresis of Equilibrium Mixtures (NECEEM) ¹⁵². Since there is no amplification step in Non-SELEX, it shortens the selection time to hours in contrast to weeks or months required for other SELEX methods. The major limitation of CE-SELEX is the limited number of sequences (10^{12} sequences) due to low volume injection ¹⁴⁶. This limitation is overcome by micro Free Flow Electrophoresis (μ FFE) ¹⁵³, which is a modified form of CE-SELEX where the starting library can be 10^{14} sequences (almost 300 fold improvement in library size over CE-SELEX).

5) Microfluidic SELEX

Microfluidics SELEX (M-SELEX), an emerging type of SELEX is basically a combination of conventional SELEX method with microfluidics system developed by Hybarger et al. in 2006 ¹⁵⁴. An RNA aptamer against lysozyme was successfully selected by using the microfluidics SELEX prototype which contains reagent-loaded micro-lines, a pressurized reagent reservoir manifold, a PCR thermocycler and actuatable valves for selection and sample routing. Later in 2009, an upgraded version of this system was reported by Tom Soh, which integrates magnetic beads-based SELEX with microfluidics technology and a continuous-flow magnetic activated chip-based separation device ¹²⁷. This method was considered very efficient and rapid, as an aptamer was selected against recombinant Botulinum neurotoxin type A (with low-nanomolar dissociation constant) after a single round of selection. However, this system had a limitation due to the aggregation of magnetic beads in the microchannel resulting in low aptamer purity and recovery. Tom Soh and colleagues further improved this system by fabricating the microchannel with ferromagnetic materials, which overcomes all the disadvantages. By this method, an aptamer against streptavidin was selected with high affinity in few rounds of selection. Ryckelnyck and colleagues described another approach by using droplet-based microfluidics to improve the catalytic properties of RNA (selection and

optimization of RNA fluoregenic aptamers) ¹⁵⁵. Fluorogenic RNA mango aptamer with Kd around 1nM was selected by using this method ^{156 157}.

6) Capture SELEX:

In vitro selection of aptamers against small molecules is highly challenging due to difficulty in immobilization of small molecules on solid support for SELEX. This limitation is overcome by Capture-SELEX method reported by Li and Colleagues in 2005 ¹⁵⁸. Capture-SELEX utilizes a special DNA library with a fixed domain in the center flanked by two random domains, each of which is further flanked by primer-binding sequences. The fixed domain in the centre is designed to be a complementary sequence for an antisense oligonucleotide biotinylated at its 3' or 5' prime end. This biotinylated antisense is required for the library to immobilize on the streptavidin beads by hybridization. It is then incubated with the small molecule targets, where the bound sequences change their conformation on recognizing the target resulting in separation from the antisense and release in the supernatant which can be easily recovered and amplify.

Capture SELEX has been successfully used for the selection of both DNA and RNA aptamer. DNA aptamer against aminoglycoside antibiotics ¹⁵⁹, Penicillin G ¹⁶⁰ and tobramycin ¹⁶¹ has been reported. Selection of RNA aptamers against small molecules has also been reported ¹⁶². Recently Sues's group has reported a successful selection of several synthetic riboswtiches with the improvement in the original Capture-SELEX protocol ¹⁶³. Synthetic riboswitches against paramomycin ¹⁶⁴ has been selected successfully by Capture-SELEX.

7) Functional SELEX:

In functional SELEX, each sequence in the library is sorted by high throughput functional screening during each SELEX round. The SOH lab at Harvard recently reported a new method named as particle display SELEX inspired by a technique used for virus and bacterial surface display in protein engineering ¹⁶⁵. This method transforms libraries of solution-phase aptamer into single aptamer particles, each displaying many copies of a single sequence on its surface. The affinity of every aptamer candidate sequence in a library is quantitatively measured by Fluorescent Activated Cell Sorting (FACS) analysis individually sort by high-throughput manner ¹⁶⁶.

An aptamer library up to 100 million (10^8) sequences can be sorted out by the FACS where the affinity of each aptamer as aptamer particles (APs) is measured individually ¹⁶⁷ and aptamers with higher affinity can be separated easily. The aptamer particles are synthesized by

emulsion PCR (ePCR) where each magnetic bead contains single DNA molecule with thousands of copies¹⁶⁸. After PCR, the emulsion is broken down and the pool is incubated with protein which will be sorted out by FACS. These sorted aptamer particles are amplified by PCR to generate enough library for next round or sequencing¹⁶⁶. High number of functional aptamers with high affinity Kd have been selected through Particle display method¹⁶⁹.

8) SELEX with modified nucleic acid libraries:

Although SELEX with natural nucleic acid has been successful due to the huge library and structural conformations, but the unreported and unsuccessful SELEX stories are also the fact. This result in failure of the SELEX is suspected due to the limited chemical diversity of natural nucleic acid bases. Larry Gold and his group explored that various functional group at the 5-position of uracil drive the SELEX successfully by selecting high affinity ligands with very low dissociation rate constants called SOMAmers (Slow off-rate modified aptamers) with a Kd around 30nM¹⁷⁰. Ichiro Hirao and colleagues described a SELEX with the introduction of an unnatural nucleotide with the hydrophobic base 7-(2-thienyl) imidazo [4,5-b]pyridine (Ds) in the random DNA sequence library¹⁷¹. Up to three Ds nucleotides were incorporated in a random sequence library which are expected to increase the chemical and structural diversity of the DNA molecules. Aptamers selected by this method have 100 fold better Kd (0.65 pM against VEGF)-165 and 38 pM against interferon- γ) than aptamers generated by natural nucleic acid libraries.

Recent developments in SELEX technology has implemented amino acid-like residues into nucleic acid scaffolds (e.g., Indole, benzyl, or alkyne moieties) which are expected to increase the diversity of the SELEX library and they are easily compatible with the polymerases regarding amplification¹⁷². Based on this ideology, Mayer's group has recently reported a Click-SELEX with the selection of an aptamer with high affinity (Kd= 18.4 nM) against Cycle 3 GFP using 5-ethynyl-2'-deoxyuridine triphosphate (EdU) in the SELEX library instead of thymine (dT)¹⁷³. The dUTP in the library was further derivatized with the addition of Indole by click chemistry¹⁷⁴. Recently a boronic acid-modified aptamer has been generated first time against epinephrine by applying Click-SELEX in particle display screening¹⁷⁵. All these results shows that SELEX with modified DNA libraries can make it more versatile and flexible to generate high affinity aptamers. Click SELEX will be discussed with detail in later chapter.

Benner and coworkers have introduced AEGIS-SELEX (artificially expanded genetic

information system - SELEX) with a library composed of the four naturally occurring nucleotides and two artificial nucleotides, 2-amino-8-(10- β -D-2-deoxyribofuranosyl)-imidazo[1,2-a]-1,3,5-triazin-4(8H)-one (P) and 6-amino-5-nitro-3-(10- β -D-2-deoxyribofuranosyl)-2(1H)-pyridone (Z) ¹⁷⁶. An aptamer with 30nM Kd was selected against breast cancer cells using the AEGIS library through Cell SELEX. Moreover, they have demonstrated that the artificial “P” and “Z” are required for the aptamer to function; removing them either decrease or eliminates the binding affinity. Hollenstein and colleagues successfully selected a catalytic DNazymes using heavily functionalized DNA libraries ¹⁷⁷. They have reported that selection of DNazyme 12-91 (Dz12-91), a nucleic acid catalyst modified with amines, guanidines and imidazole cleaves a target containing a lone ribocytosine unit with even greater efficiency as compared to DNazyme Dz9-86, that was selected from the same library to cleave a target containing a single ribonucleotide ¹⁷⁷. This cleavage of RNA targets is independent of divalent metal cations (M^{2+}) ¹⁷⁸.

High Throughput Sequencing in SELEX (HTS-SELEX)

High-throughput sequencing or Next Generation Sequencing is a method which has replaced the traditional methods for sequencing based on the clonal sequencing methods. Since its introduction, HTS has brought a revolution into selection of aptamers which makes us able to solve the mysteries in black box of SELEX providing significant information about SELEX pools by sequencing millions of sequences within no time. The most predominant characteristics of HTS-SELEX is that it allows us to sequence the earlier rounds including the starting library. Thus, enriched sequences are visible at a much earlier round, which made SELEX more time efficient. Tom SOH and colleagues reported selection of an aptamer by Microfluidics SELEX through HTS analysis with the successful selection of an aptamer in 3 rounds of selection. This aptamer binds to its target PDGF-BB protein with 3nM Kd ¹⁷⁹. Later in 2012, Berezhnoy and colleagues reported a selection of murine interleukin-10 receptor blocking oligonucleotide aptamer after 5 rounds of selection by HTS analysis ¹⁸⁰. Duconge and colleagues have demonstrated that HTS can provide time-lapse imaging of the evolutionary pathway that is taken by a macromolecule during in vitro selection to evolve by successive mutations through better fitness ¹²². In addition, Duconge and colleagues demonstrated that global analysis of large sequence datasets by robust bioinformatics tools (eg PATTERNITY seq program developed by Duconge’s team) can further facilitate comprehensive characterization of aptamers, including binding affinity and/or specificity, structure prediction, abundance quantification and aptamer-target interactions ^{181 182}. Nowadays, HTS analysis has

been extensively used in selection of aptamers with deep sequence analysis ¹⁸³. HTS analysis will be discussed with detail in next chapters.

Application of Aptamers:

1) Aptamers in Therapeutics

Since 1990, aptamers have been studied on a large scale making them an interesting tool from selection to theranostics. The unique characteristics of aptamers provide vast potential for therapeutic application as compared to antibodies ¹⁸⁴. For in vivo applications, aptamers are usually modified during SELEX or post-SELEX to avoid nucleases degradation and fast renal clearance. Chemical modifications like 2'-fluoro, 2'-O-methyl or 2'-amino-substitutions, introduction of locked nucleic acid (LNA) or phosphorothioate linkages (PS-linkages) and 3'-end capping with inverted thymidine or other blocking molecules are introduced ¹¹⁵. Carrier molecules such as polyethylene glycol (PEG) or cholesterol are added at the end of aptamers which increases their half-life to several hours required for pharmacological effect ¹¹⁵.

To date, 11 aptamers have been successfully entered in clinical trial as therapeutic agents in macular degeneration, cancer, diabetes, inflammation and blood coagulation ¹⁸⁵. Pegaptanib (27 nucleotide PEGylated RNA aptamer with fluoro-modified sugar) is the first therapeutic aptamer described to treat wet age related macular degeneration (AMD) which inhibits the vascular endothelial growth factor (VEGF) in patients ¹⁸⁶. Likewise E10030, a 29 nucleotide PEGylated DNA aptamer selected against platelet-derived growth factor (PDGF) has been reported to block the PDGF activity in angiogenesis, thereby preventing ocular vascular diseases ^{187 188}. ARC1905, a 38 nucleotide PEGylated RNA aptamer has been reported as a therapeutic agent in both wet and dry AMD. ARC1905 specifically binds and inhibits the expression of the C5 component of human complement and prevents the formation of other complementary proteins and the membrane attack complex (MAC) responsible for retinal cell lysis ¹⁸⁹.

NOX-E36, a 40 nucleotide PEGylated L-RNA Spiegelmer aptamer has been reported to treat diabetic nephropathy ¹⁹⁰. Spiegelmer is the trade name of L-aptamers, and are initially selected as D-aptamers against the enantiomer of the target ligand ^{191 192}. These L-RNA or L-DNA aptamers are highly resistant to nuclease degradation as they are not recognized by the ubiquitous plasma nucleases due to their structure (figure 1.12). This makes them highly suitable for therapeutic purposes ¹⁹³. NOX-E36 strongly binds and blocks the activity of Human

C-C chemokines Ligand 2 (CCL2), which overexpression is associated to many inflammatory diseases ¹⁹⁴. Similarly NOX-H94, a 44 nucleotide L-RNA aptamer has been reported to enter in clinical trial as a third Spiegelmer. NOX-H94 blocks hepcidin-regulated ferroportin degradation and reversed hyperferremia activity, thus can be used as a potential therapeutic agent for the treatment of Anaemia of Chronic Inflammation (ACI) ¹⁹⁵.

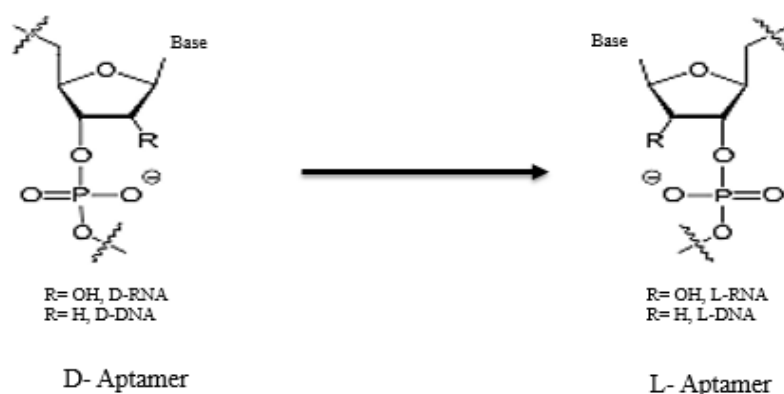


Figure 1.12: Structure of mirror-image nucleic acid aptamer. Aptamers are first selected as D-aptamers against the enantiomer of the target by SELEX. After the selection, L-aptamer is synthesized which recognizes the target molecule.

AS1411 and NOX-A12 has been reported as therapeutic agents in cancer. AS1411 is basically a highly stable G-quadruplex (26 bases oligonucleotide) with an unmodified DNA backbone, reported to be the first aptamer in clinical trials to treat cancer in human ¹⁹⁶. Nucleolin protein (NCL) is highly expressed on the surface of tumor cells which is involved in blood vessel formation during tumorigenesis. AS1411 thus binds to the NCL and internalize resulting in the destabilization of B-Cell Lymphocytes 2 (BCL2) mRNA, leading to the reduction in synthesis of BCL2 protein and probably induce apoptosis ¹⁹⁶. NOX-A12, a 45 nucleotide PEGylated L-RNA aptamer is the second Spiegelmer reported to enter in clinical trial in general, and the first Spiegelmer so far as a cancer therapeutic agent. It has been reported to inhibit the activity of C-X-C Chemokine Ligand 2 (CXCL2) which is responsible for tumor proliferation leading to metastasis ¹⁹⁷.

So far, aptamers as therapeutic agent in blood coagulation (thrombosis and vascular diseases) have been mostly reported to enter in clinical trials. Thrombin is a serine proteases which plays an important role in blood coagulation pathway. An essential step in thrombus formation is the conversion of prothrombin to thrombin. NU172 is the optimized form of the first DNA aptamer selected against thrombin ¹⁹⁸. Unlike other therapeutic aptamers with

modifications, it is 26 nucleotide unmodified DNA aptamer reported to bind and inhibit the exocite 1 on thrombin ¹⁹⁹. Currently NU172 aptamer is in the second stage of clinical trial. Platelet adhesion occurs when platelet glycoprotein Ib/IX binds to von Willebrand factor (VWF) that has been exposed on vessel surface in atherosclerosis due to endothelial injury. VWF plays a key role in platelet adhesion, activation and promotion of thrombosis. As a DNA aptamer, ARC1772 has been reported to bind the GPIb (also known as the A-1) domain of VWF and blocks the VWF-mediated activation pathway resulting in potential inhibition of platelet activation and pathological thrombosis ²⁰⁰.

Factor IXa (FIXa) plays a key role in thrombin formation and therefore represents a promising target for therapeutic development. A 31 nucleotide RNA aptamer RB006 has been selected against FIXa from a library with 2-fluorpyrimidine modification. RB006 has been reported to bind and impede the activity of FIXa in a dose dependant manner, thus preventing thrombin formation. Interestingly, a 15 nucleotide modified RNA aptamer (RB007) that functions as an antidote reverse the activity of aptamer RB006. RB006 conjugating with cholesterol moiety 5'- end was tested in vivo with the antidote RB007. The aptamer RB006 increased the activated partial thromboplastin time reliably in a porcine model anticoagulation while the antidote RB007 reversed the activity rapidly ²⁰¹. This RB006/RB007 is currently in clinical trial ²⁰².

2) Aptamers in Diagnostics

A few years ago, antibodies were considered the only molecules that were appropriate for accurate target detection or quantification, because of the specific interaction between an antibody and an antigen. However, the development of SELEX has enabled the discovery of new molecules whose major characteristic is based on the specificity of the target's recognition. As true rival of antibodies, aptamers have developed a wide field of application in the field of diagnosis due to their inherent properties of high specificity and stability as compared to antibodies ^{203 204}.

Aptamer in Biomarker detection:

As discussed earlier that aptamers are highly stable and binds to its target receptor with high specificity. Due to these properties aptamers are in competition with antibodies as standard diagnostics for the detection of proteins in biological fluids. In 1996, after few years of aptamer discovery; NeXstar introduced an ELISA-like test called ELONA (Enzyme-Linked

OligoNucleotide Assay) ²⁰⁵. VEGF was immobilized with an antibody and detected via a fluorescein-bearing aptamer at the 5' end. This fluorescein was then recognized by a secondary antibody leading to a chemoluminescent reaction. The results obtained by ELONA were reproducible and similar to those obtained by ELISA. It is important to note that the actual detection in this study was provided by an enzyme conjugated to the anti-fluorescein antibody responsible for chemoluminescence. Later in 2006, Kiel's group introduced another detection assay known as Aptamer-Linked Immobilized Sorbent Assay (ALISA). They demonstrated the feasibility of ALISA detection method via a comparative study with ELISA ²⁰⁶. Both these detection methods led to an idea of using aptamer as aptasensors (aptamer biosensor) which is one of the major application of aptamers in diagnostics ^{207 208}. These aptasensors can be constructed through a variety of methodologies, including electrochemical aptasensors ²⁰⁹, fluorescence based optical aptasensors ²¹⁰, colorimetric-based optical aptasensor ²¹¹ and nano aptasensors ²¹².

Slow Off-Rate Modified Aptamers (SOMAmers)

Aptamers are negatively charged molecules and isolating an aptamer to a negatively charged protein is highly difficult. To overcome such challenges, Larry Gold and his colleagues developed slow off-rate modified aptamers (SOMAmers) ²¹³. SOMAmers consist of a short single-stranded DNA sequence that incorporates a series of modifications that give the SOMAmer "protein-like" appendages. To generate SOMAmers, 5-position of uracil is functionalized with different protein-like moieties (e.g., benzyl, 2-naphthyl or 3-indolyl-carboxamide). These features expand the chemical diversity of standard aptamers and enhance the specificity and affinity of protein-nucleic acid interactions. Importantly, SOMAmers engage their protein targets with surfaces that have significantly more hydrophobic character compared with conventional aptamers, thereby increasing the range of epitopes that are available for binding. Gold et al. has demonstrated that SOMAmers with modified library isolated high affinity aptamers in comparison to the non-modified library ¹⁷⁰. During selection of SOMAmers, the main pharmacological parameters optimized was the off rate (dissociation rate more than 30 mins) to minimize the non-specific binding. This led a revolution in aptamer based multiplex proteomic technology in biomarker discovery ²¹⁴. Somalogic founded by Larry GOLD, recently developed SOMAmers based biomarker discovery platform known as SOMAscan which has the ability to detect and quantify more than 1,300 proteins (aiming for 5000 proteins detection in future) simultaneously from a small volume (50 μ L) of clinical sample ²¹⁵. Moreover, it can easily detect a protein signature down to 40 fM concentration ²¹⁶. SOMAscan has been used to

discover trace biomarkers for variety of diseases including Alzheimer's disease²¹⁷, tuberculosis²¹⁸, cardiovascular disease²¹⁹, inflammatory bowel disease²²⁰ and non- small cell lung cancer²²¹.

Aptamers in In vivo Imaging:

The molecular weight of aptamers, between 8 and 14 kDa, much lower than that of antibodies (150 kDa), is a serious advantage in terms of tissue penetration and rapid elimination. These two parameters are essential when it is desired to use a molecule in imaging. Due to ease modification on aptamers, they can easily be conjugated with number of detector molecules for in vivo Imaging. These include: luminescent nanocrystals²²², fluorescently functionalised quantum dots²²³ and radiolabelling of the aptamer^{98 224}. Several aptamers have been tested so far as molecular probes in different imaging methods, including magnetic resonance imaging (MRI), positron emission tomography (PET), single photon emission computed tomography (SPECT), X-ray computed tomography (X-ray CT), and fluorescence imaging. Here in this section, we will discuss about few aptamers which were validated by above mentioned in vivo imaging methods.

The DNA aptamer NX21909 selected against human neutrophil elastase was the first aptamer used in biomedical in vivo Imaging²²⁵. This molecule was isolated from a random DNA library, on which a small reversible inhibitor of elastase was conjugated. In an in vivo imaging study of inflammation in rats, this aptamer showed inhibitory properties in reducing inflammatory lesions in rats²²⁶ and was radiolabeled with technetium 99 (^{99m}Tc)²²⁷. In parallel, an anti-elastase anti-body, immunoglobulin G (IgG), usually used to visualize inflammatory sites in vivo, served as a control. The aptamer and the antibody were delivered by intravenous injection 4h after the onset of inflammation in the forelimb. Encouraging results from this experiment demonstrated that aptamers appear to offer significant advantages over antibodies in terms of signal to noise due to faster clearance reducing the signals corresponding to the background noise.

Many aptamers have been successfully used for the imaging of tumor cells. An RNA aptamer F3B selected against matrix metalloproteinase 9 (MMP-9) successfully demonstrated high tumor uptake than a control oligonucleotide in SPECT imaging⁶⁶. For this purpose, F3B aptamer was fully modified with 2'OMe-Purine/2'F-Pyrimidine and the biodistribution was evaluated by radiolabelling either with ^{99m}Tc-MAG or ¹¹¹InDOTA after 30, 60 and 120 minutes post injection. Significant tumor targeting was observed with both labels but it was interesting

to see that there was a difference in the biodistribution which demonstrated that labelling of specific radiotracers highly influenced the biodistribution of aptamers. In vivo fluorescent imaging was also performed with F3B in melanoma cancer ⁶⁶. For this purpose F3B aptamer and control sequence were labeled with Cyanine 5 (Cy5) fluorophore. Dorsal images were acquired 1h after i.v. injection of 100 μ L of Cy5-F3B-aptamer or Cy5-control-sequence (1 to 5 nmole) into mice bearing human melanoma tumor. Mice were sacrificed at 1h post injection and tissues of interest (kidneys, liver, brain, spleen, heart, lungs bone, skin muscle, digestive tract and tumor) were imaged. Fluorescence imaging of the tumor tissues revealed a moderate signal in the tumor for F3B-Cy5 as compare to Control-Cy5 sequence.

Similarly Jacobson and colleagues evaluated a DNA aptamer selected against tenascin-C by PET imaging in mice bearing a subcutaneous tumor xenograft. For this purpose, the aptamers was labeled with ¹⁸F or ⁶⁴Cu radiotracer ²²⁸. A scramble sequence was used as a negative control. In this study they have demonstrated that the tenascin-C aptamer provided clear visualization of tenascin-C-positive but not tenascin-C-negative tumors. Furthermore, in tenascin-C positive tumors, the uptake of tenascin-C aptamer was significantly higher than that of control aptamer.

Imaging of cancer cells by aptamers are also being studied by Magnetic Resonance Imaging technology (MRI). Currently MRI is one of the most powerful imaging methods for living organisms with high spatial resolution and non-invasion. It uses strong magnetic fields, electric field gradients, and radio waves to generate images. In MRI, contrast agents for accurate diagnosis i.e. T1-positive paramagnetic agents and T2-negative super paramagnetic nanoparticles have been developed as contrast agents. Yang et al. evaluated aptamer AS411 conjugated Mn₃O₄@SiO₂ core-shell nanoprobles (NPs) in human cervical carcinoma tumor-bearing mice by MRI ²²⁹. In this work they have demonstrated that AS1411 aptamer-conjugated Mn₃O₄@SiO₂ core-shell NPs successfully target accumulation in tumour sites ²²⁹. They have further reported that NPs doesn't show any in vivo toxicity which advocates their usage safely for long term body tracking.

Thesis Aims and Objectives:

Aptamers have been selected successfully by a process called SELEX since three decades. These ligands have a unique property that lies in their ability to adopt a three-dimensional conformation specific to the targeted molecule. One of the features of the SELEX method is the wide variety of targets against which this strategy can be applied. Indeed, a starting library is composed of millions of unique sequences that adopt different structures, so it is considered that within this library at least one structured molecule adapted to the shape of any target is represented. So far, aptamers have been selected against bacteria, viruses, small metabolites, proteins, peptides, cells and even in tissues of living organism. Aptamers with modified bases have also been selected against different targets as highly versatile molecules. During my thesis, I mostly focus on the selection of DNA aptamers against various targets as a biomarker in metastatic melanoma.

The basic aim of the thesis are following:

- 1) Selection and characterization of DNA aptamer against Discoidin Domain Receptor 1 (DDR1).
- 2) Selection and characterization of DNA aptamer against Discoidin Domain Receptor 2 (DDR2).
- 3) Selection and characterization of DNA aptamer against Human Matrix Metalloproteinase 14 (HMMP14).

The basic objective of this thesis is to select specific aptamers as theranostics agents. Moreover, given the interest that imaging aptamers can bring, their use as a molecular probe in imaging has been considered for a moment. For this purpose we aim to perform an MRI with DDR1 selected aptamers conjugated with Silica nanoparticles in the near future.

Chapter-2: Materials and Methods

Chemicals and Reagents:

Mostly DNA libraries and aptamers were synthesized by Eurofins at a scale up to 200 nmoles while some of them were synthesized in our lab at 1 μ mole scale. For PCR amplification, Go-Taq Polymerases (Promega), Gold Taq, Phusion Polymerases and DMSO (Thermo fisher Scientific), Hot-Star Polymerases for NGS (Qiagen), Primers (Eurofins) and dNTPs (Eurogentec) were purchased. Lo-Bind tubes used for experiments were purchased from Eppendorf. The lambda Exonuclease reagents were purchased from New England Bio labs. The chemicals Agarose, Tris, Tris-HCl, Sodium Hydrogen Phosphate, Sodium Chloride, Sodium Bicarbonate, Sodium Acetate, Sodium Sulphate, EDTA, THPTA, Sodium Ascorbate, Ethyl Acetate, Potassium Chloride, Potassium Hydrogen Phosphate, Sodium Chloride, APS, Bromophenol Blue and Xylene Cyanol FF in solid form and Reagents PBS, Chloroform: Isoamyl alcohol (24:1), Phenol pH 8, Acrylamide 30%, DMF, Ammonium Hydroxide, Formamide 99.5% and 2-propanolol in solution form were purchased from Sigma. Reagent solutions SDS 20%, Glycerol 100%, TBE 10X, TG-SDS 10X, TEMED and Ethidium Bromide were purchased from Euromedex. Reagents MgCl₂, Glucose, Potassium Sulphate, Potassium Hydroxide were purchased from Fluka while Urea in solid form and Acrylamide/ Bis-Acrylamide 40% (19:1, 37.5:1 and 75:1) solutions were purchased from Biosolve Chimie. EtOH Absolute from VWR International, Tween 20 from Amresco and DPBS 1X from Gibco were purchased as well. The nuclease-free water and competitors tRNA, BSA (Sigma) and Herring Sperm DNA (Promega) used during SELEX were purchased from Sigma Aldrich.

The Recombinant Histidine tagged extracellular Domain of DDR1 and DDR2 were purchased from Elabsciences and Creative BioMart as a solution in sterile PBS pH 7.4 containing 5% Trehalose, 5% mannitol, and 0.01% Tween-80. These proteins were dissolved in water upon delivery. Recombinant GST, HMMP2 and HMMP14 proteins were purchased from Abcam and Prospec as a solution in sterile PBS pH 7.4 containing 10% Glycerol solution. All proteins were aliquoted and stored at -80°C upon delivery. The Ni-NTA Agarose Magnetic beads were purchased from Qiagen while the Dynabeads M-280 Streptavidin Beads were purchased from Invitrogen. The Nitrocellulose membrane filters of 0.2 μ m and 0.45 μ m pore sizes were purchased from Millipore.

Synthesis of Library

Different libraries were used to perform SELEXs against different receptors. The libraries were either purchased from Eurofin at the synthesis scale up to 0.2 μ mole or synthesized in our lab at 1 μ mole scale. Libraries purchased from Eurofin were purified by HPLC while those libraries synthesized in our lab were purified using polyacrylamide 10% gel as discussed below in this chapter. All the libraries were synthesized with forward and reverse primers for amplification purpose. The detail about libraries are given in Table 2.1.

Name	Sequence 5'-3'
SELEX Library A	GCC TGT TGT GAG CCT CCT GTC GAA – N30 - TT GAG CGT TTA TTC TTG TCT CCC
Forward Primer (P5)	GCC TGT TGT GAG CCT CCT GTC GAA
Reverse Primer 5'-Phosphate (P3 5'-P)	[PHOS] GGG AGA CAA GAA TAA ACG CTC AA
Reverse Primer Heavy (P3A1C12)	ACT GAC TGA CTG ACT GAC TA - C12 - GGG AGA CAA GAA TAA ACG CTC AA
SELEX Library B	GCC TGT TGT GAG CCT CCT GTC GAA – N40 - TT GAG CGT TTA TTC TTG TCT CCC
Click-SELEX Library	CAC GAC GCA AGG GAC CAC AGG – N42 – CAG CAC GAC ACC GCA GAG GCA N= dA:dG:dC:EdU = 1:1:1:1
Forward Primer (P1)	CAC GAC GCA AGG GAC CAC AGG
Reverse Primer (P2)	[PHOS] TGC CTC TGC GGT GTC GTG CTG
Reverse Primer Heavy (P2A1C12)	ATA TAT ATA TAT ATA TAT AT-C12- TGC CTC TGC GGT GTC GTG CTG
AptaBeacon Library (1-30)	GAC GCA CGG ACG GAC TGA GCA- T VV VVV VVV VVV VVV VVV VVV VVV VVV VVV – GAC CGG AGC GAG GCA GGC AGG Random region contains 1T and 29 V (V=A, G, C). Whereby T is sitting in each position once for each library
AptaBeacon Forward Primer	GAC GCA CGG ACG GAC TGA GCA
AptaBeacon Reverse Primer	[PHOS] CCT GCC TGC CTC GCT CCG GTC
AptaBeacon Reverse Heavy Primer	ATA TAT ATA TAT ATA TAT AT-C12- CCT GCC TGC CTC GCT CCG GTC

SELEX DDR1 Doped Library (C25)	<p>gcc tgt tgt gag cct cct gtc gaa – TAG AGT GGG TGT ACA TTA TCT GTA CTA CT –ttg agc gtt tat tct tgt ctc cc</p> <p>A: 76% A, 8% T, 8% C, 8% G</p> <p>T: 76% T, 8% A, 8% C, 8% G</p> <p>C: 76% C, 8% A, 8% T, 8% G</p> <p>G: 76% G, 8% A, 8% T, 8% C</p>
SELEX DDR2 Doped Library (C2.2)	<p>gcc tgt tgt gag cct cct gtc gaa – GCC ATC CCG TCA GTC TCA GTC ACC TCA TTG GTG TCG TCG–ttg agc gtt tat tct tgt ctc cc</p> <p>A: 85% A, 5% T, 5% C, 5% G</p> <p>T: 85% T, 5% A, 5% C, 5% G</p> <p>C: 85% C, 5% A, 5% T, 5% G</p> <p>G: 85% G, 5% A, 5% T, 5% C</p>
SELEX DDR2 Doped Library (C2.3)	<p>gcc tgt tgt gag cct cct gtc gaa – TAT CAC CCC GTC AAG TCA GTC AAG GTT AGTT GTG TCG TGC G– ttg agc gtt tat tct tgt ctc cc</p> <p>A: 85% A, 5% T, 5% C, 5% G</p> <p>T: 85% T, 5% A, 5% C, 5% G</p> <p>C: 85% C, 5% A, 5% T, 5% G</p> <p>G: 85% G, 5% A, 5% T, 5% C</p>

Table 2.1: List of oligonucleotides.

Buffer:

Buffer	Composition	Storage
Cell-SELEX Binding Buffer 1X	1 liter of DPBS contains 4.5 g glucose, 100 mg tRNA, 1 g BSA and 1 M MgCl ₂	4°C
Cell-SELEX Washing Buffer 1X	1 liter of DPBS contains 4.5 g glucose and 1 M MgCl ₂	4°C
Phosphate Buffer Saline (PBS) 1X	137 mM NaCl, 2.7 mM KCl, 10 mM Na ₂ HPO ₄ , 1.76 mM KH ₂ PO ₄	4°C
Protein-SELEX Binding Buffer	PBS 1X (137 mM NaCl, 2.7 mM KCl, 10 mM Na ₂ HPO ₄ , 1.76 mM KH ₂ PO ₄) + MgCl ₂ 1 mM, Herring Sperm 10 µg/mL and BSA 1 µg/mL.	4°C
Protein-SELEX Washing Buffer	PBS 1X (137 mM NaCl, 2.7 mM KCl, 10 mM Na ₂ HPO ₄ , 1.76 mM KH ₂ PO ₄) + MgCl ₂ 1 mM.	4°C
PBS- Tween 20 Buffer 1X (PBS-T)	137 mM NaCl, 2.7 mM KCl, 10 mM Na ₂ HPO ₄ , 1.76 mM KH ₂ PO ₄ and 0.005 % Tween 20	4°C
TBE Buffer (10X)	890 mM Tris, 890 mM Boric acid, 20 mM EDTA. pH 8.0	25°C
TB-Mg Buffer (10X)	890 mM Tris, 890 mM Boric acid, 10 mM MgCl ₂ . pH 8.0	4°C
TG-SDS Buffer (10X)	250 mM Tris, 1.92 M Glycine and 1% SDS	25°C
Agarose Loading Buffer (5X)	1 mL Agarose Loading Buffer 5X contains 500 µL Glycerol 100%, 250 µL TBE 10X, 150 µL H ₂ O and 100 µL Bromophenol Blue 0.1%.	4°C

Formamide Loading Buffer FLB (5X)	10 mL of FLB contains 9.8 mL Conc. Formamide (99.8%), 200 μ L EDTA 0.5 M pH 8.3, 0.25 mg Xylene Cyanol and 0.25 mg Bromophenol Blue.	4°C
Native PAGE Loading Buffer (5X)	1 mL Native Loading Buffer 5X contains 500 μ L Glycerol 100%, 250 μ L TB 10X, 150 μ L H ₂ O and 100 μ L Bromophenol Blue 0.1%.	4°C
Laemmli Buffer (5X) SDS-PAGE	300 mM Tris-HCl pH 6.8, SDS 10%, Glycerol 50%, β -mercaptoethanol 25% and 0.04% Bromophenol Blue	-20°C
Extraction Buffer TENaCl 1X	100 mL TENaCl buffer 1X contains 1 mL Tris-HCl 1M pH 7.5, 500 μ L NaCl 5M, 200 μ L EDTA 0.5 M and H ₂ O qs. 100 mL	4°C
Lambda Exonuclease Reaction Buffer (1X)	67 mM Glycine-KOH, 2.5 mM MgCl ₂ , 50 μ g/m BSA, pH 9.4	-20°C
Staining Solution	0.005% (w/v) Stains-All 0.1% stock, 10% (v/v) Formamide, 25% (v/v) isopropanol, 15 mM Trizma - HCl, pH 8.8 and 65% (v/v) H ₂ O	4°C

Table 2.2: List of Buffers and Reagent Solutions

Systematic Evolution of Ligands by Exponential Enrichment (SELEX):

Systematic Evolution of Ligands by Exponential enrichment is a combinatorial method used to select an aptamer against the target molecule with high affinity and specificity¹¹⁰. SELEX and its types have been discussed in chapter 1 with detail. Here in this chapter we will discuss about the SELEX methods used to select aptamer against different receptors during the thesis.

Magnetic Beads Based SELEX

Ni-NTA Magnetic Agarose beads from Qiagen were used to immobilize the histidine tagged proteins for selection and counter selection steps in SELEX to generate aptamers targeting the protein biomarker. These Ni magnetic beads were 20 μm in size. First the binding capacity of the Ni-NTA Magnetic Agarose beads were determined against the histidine tagged proteins through SDS-PAGE ²³⁰.

Ni-Beads Protein binding capacity analysis by SDS PAGE

SDS-PAGE analysis was performed to analyze the Ni-NTA agarose beads binding capacity for histidine tagged DDR1. For each analysis, 3 tubes (protein lo-bind 1.5 mL eppendorf) were prepared with 10 μL of Ni-NTA beads having binding capacity up to 2 mg/ml suspension (5%) in each tube. The beads were washed 3 times with 10 μL of PBS 1X Buffer. To the tubes, Histidine tagged DDR1 (5 pmoles, 15 pmoles and 45 pmoles) in buffer PBS 1X were added respectively for immobilization. The mixture was then incubated for 1 hour at 5rpm in the rotor at RT. After the incubation, the supernatant was transferred to new tubes respectively named as supernatant (S1 for 5 pmoles, S2 for 15 pmoles and S3 for 45 pmoles respectively) by applying magnet. For elution of protein, 20 μL of Imidazole 500mM (maximum conc.) into PBS 1X was added to the tubes. The mixture was then incubated for just 30 seconds at RT followed by immediate recovery of the supernatant by applying magnet. These eluted samples were transferred to new tubes named as E1, E2 and E3 respectively. 5 μL of Laemmli Buffer 5X was then added to each tube and loaded in the SDS-PAGE gel for electrophoresis. A protein marker of 0.5 μg was also loaded in one well of the gel to validate the size of proteins. An SDS-PAGE analysis performed to determine the Ni-NTA Agarose beads binding capacity for histidine tagged DDR1 is given in Figure 2.1. This experiment demonstrated that 5 pmoles of histidine tagged DDR1 was fully loaded on 10 μL of Ni-NTA beads as there is no trace of protein left unbound in the supernatant (S1). While with 15 pmoles of DDR1, 10 μL of Ni-NTA Agarose beads are highly saturated and a part of the histidine tagged DDR1 left unbound to the beads in the supernatant (S2). So based on this experiment, we decided to load 10 pmoles of histidine tagged DDR1 on 10 μL of Ni-NTA Agarose beads during SELEXs. The SDS-PAGE protocol is described later in detail in paragraph (2.11.4). Similarly, the loading capacity of Ni-NTA agarose beads for histidine tagged DDR2, HMMP2, HMMP14 and GST were also analysed by SDS-PAGE. The determined loading capacity against 10 μL of Ni-NTA Agarose

beads is 10 pmoles for DDR2, 15 pmoles for HMMP2, 15 pmoles for HMMP14 and 50 pmoles for GST respectively.

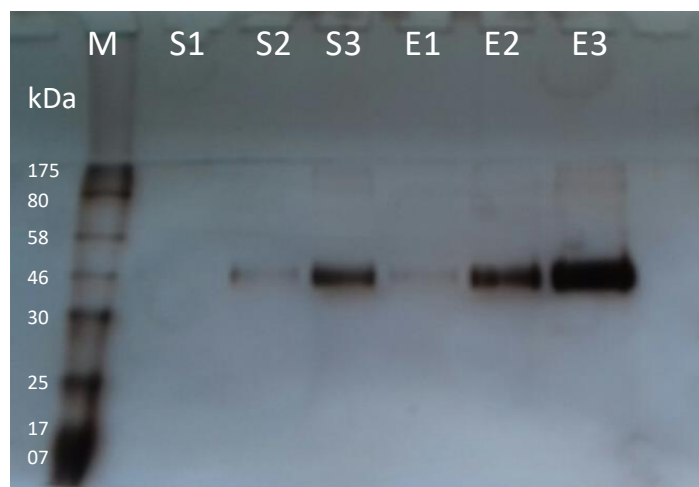


Figure 2.1: SDS-PAGE gel. SDS-PAGE result of protein binding capacity of Ni-NTA Agarose beads. In this image, M corresponds to protein marker while S1, S2 and S3 correspond to the supernatant and E1, E2 and E3 correspond to the eluted sample of 5 pmoles, 15 pmoles and 45 pmoles DDR1-H respectively.

Preparation of ssDNA Library in Magnetic beads based SELEX:

In Magnetic-Beads based SELEX as shown in Figure 2.2, we started the SELEX with an ssDNA pool having a number of 10^{15} sequences. The starting amount of the library was used different for each target as discussed in their respective chapters. In order to ensure correct folding of the candidates, the ssDNA library was firstly denatured at 75°C for 5 minutes followed by immediate cooling for 10 minutes on ice (4°C). After folding, the Protein SELEX binding buffer (1X final conc.) was introduced to the pool to make the folding stable and to perform the SELEX.

Immobilization of histidine tagged Proteins on Ni-NTA beads:

To immobilize the histidine tagged proteins on Ni-Beads, 10 μ L of beads were washed three times with 20 μ L PBS-T 1X. Each time the supernatant was removed. Once the beads were washed, we incubated the required amount of protein with the beads for 1 hour at 5 rpm on the rotor at RT to immobilize the protein on beads for SELEX. After immobilization, the supernatant was removed and the beads were washed with 20 μ L PBS 1X buffer to remove every trace of unbound protein. The amount of Ni-beads was determined according to their

binding capacity to specific proteins, thus the washing and immobilization volume can vary depending on the amount of beads.

Counter Selection Step in Magnetic beads based SELEX:

During SELEX, for the counter selection step, the prepared ssDNA pool was introduced with the protein of non-interest immobilized on Ni magnetic beads and incubated at RT on the rotor at 5 rpm. Once the incubation was done, the non-binding sequences present in the supernatant were recovered by applying the magnet while bound sequences were discarded. With this recovered supernatant containing sequences of interest, we further performed another counter selection or selection.

Selection Step in Magnetic beads based SELEX:

During the selection step to select an aptamer against the target protein, the required amount of target protein was first immobilized on Ni-Beads for 1 hr at RT on the rotor at 5 rpm. After the immobilization, the beads were washed once with 20 μ L PBS 1X to remove every trace of unbound target protein (if any). The supernatant recovered from the counter selection part was introduced with the target protein immobilized on the Ni Beads. The mixture was incubated for specified time at RT at 5 rpm on the rotor. After incubation the supernatant containing non-interested sequences were discarded while interested sequences bound to the target protein were recovered as described later.

Washing Step in Magnetic beads based SELEX:

After selection step, the Ligand-protein complex was washed in order to remove the non-specific and the low binding candidates (Candidates with bad Kd) to select candidates with only better Kd. The washing was performed by PBS-Mg 1X. The number and time of washing was increased as the rounds proceeded in SELEX.

Elution Step in Magnetic beads based SELEX:

During selection step, the sequences of interest bound to the protein resulted in complex formation. In order to break the complex and to recover the interested candidates, an elution step was introduced. For this purpose, 100 μ L of DNase free water was added to the tube followed by heating at 75°C for 1 minute. The complex was broken and the candidates were

released in the supernatant due to heat shock. These candidates were recovered and amplified by PCR (described later in this chapter) to get enough library for next round or analysis.

The Magnetic Beads based SELEX is well described in Figure 2.2.

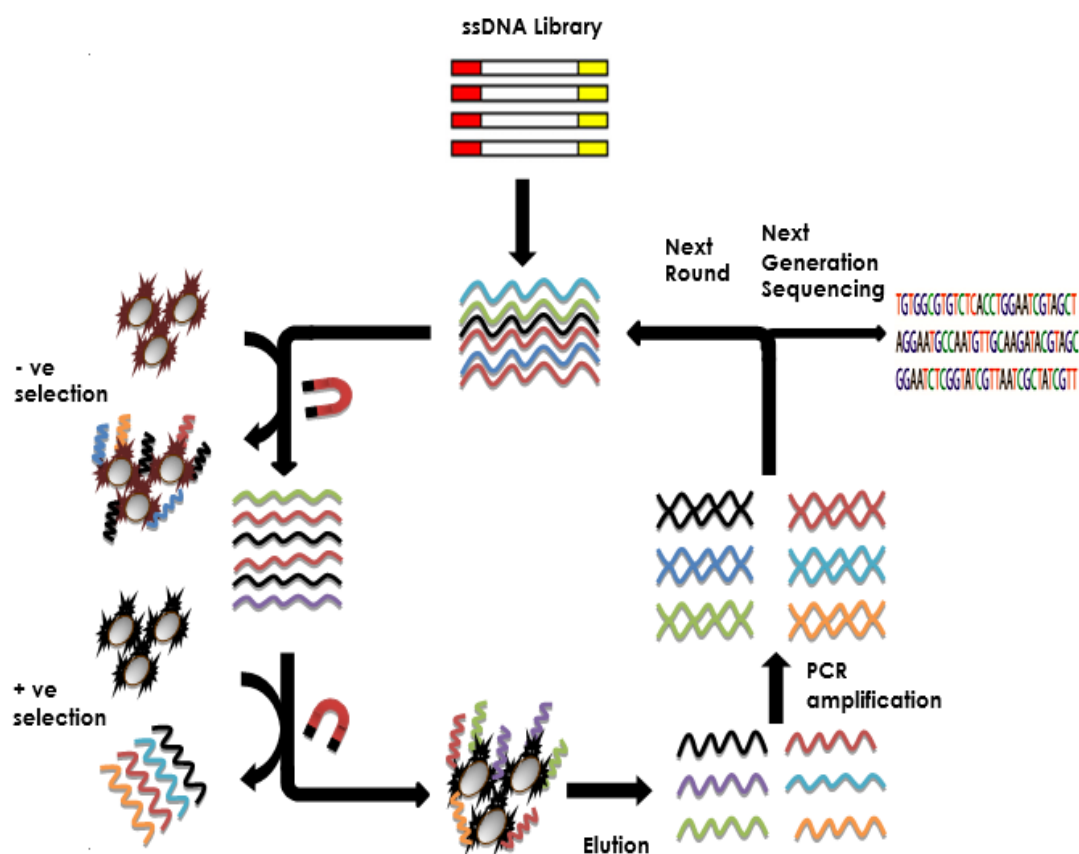


Figure 2.2: Magnetic Beads Based SELEX. An ssDNA library is first incubated with the negative protein for counter selection. The recovered sequences are then incubated with the target proteins. After washing, the bound ssDNA sequences are eluted by heating. The eluted ssDNA sequences are then amplified by PCR. The PCR products are separated into ssDNA for the next round of selection. Finally the enriched library with aptamer sequences are analysed by High throughput sequencing to select aptamer candidates.

Nitrocellulose membrane based Filtration SELEX:

Unlike other SELEXs performed earlier, the bound and non-binding sequences were separated by filter membranes in filtration SELEX¹²⁹. For this purpose we used nitrocellulose membrane filters (HAWP, Millipore) which compose of a mixture of acetate and nitrocellulose having a pore size of 0.45 μm ¹²⁹. As this membrane retains the protein and the molecules associated to it, we can use it to separate the binders and non-binders.

Activation of Nitrocellulose membrane:

In order to avoid non-specific retention of oligonucleotides, nitrocellulose membranes were treated in alkali solution²³¹. The NC membrane was first activated in KOH 0.5M at 25°C for 20 minutes followed by 3 times washing with distilled H₂O. Membranes were then washed once with 100mM Tris-HCl, pH 7.5 and stored in the same buffer at least for 45 minutes at 4°C before using it. The ssDNA is not retained while protein-DNA complex is efficiently retained by alkali washed filters.

Preparation of ssDNA Library in Filtration SELEX:

The amount of the ssDNA library was varied based on the SELEX against different targets. The library was denatured at 75°C for 5 minutes followed by immediate cooling for 10 minutes on ice (4°C). After folding, the Protein SELEX binding buffer (1X final conc.) was introduced to the pool to make the folding stable and to perform the SELEX.

Counter Selection step in Filtration SELEX:

The first step consists of washing the NC membrane by 1 mL PBS-Mg 1X to remove the traces of Tris-HCl (storage buffer for NC membranes). For counter selection, the required amount of negative protein in PBS-Mg 1X was first put on the NC membrane and the buffer was sucked by applying vacuum. This resulted in retaining the protein on the NC membrane. This NC membrane containing the fixed negative protein on its surface was then cut into small pieces. NC membrane pieces were then incubated in 1.5 mL effendrof DNA Lo-Bind tubes with the ssDNA library for 20 minutes at RT. The unbound sequences in the supernatant were then recovered for selection.

Selection Step in Filtration SELEX:

The selection step is based on incubation in solution for selection. For this purpose, the ssDNA library was incubated with the target protein in solution at RT for 30 minutes. This mixture was then passed through the activated NC membrane by applying vacuum. Since the NC membrane has a property of protein retention, the complex were retained on the membrane while the non-binders were passed through the NC membrane. Before performing selection step, the NC membrane was first washed with 1 mL PBS-Mg 1X.

Washing step in Filtration SELEX:

In order to get rid of the low binding molecules, the washing step with PBS-Mg 1X was introduced. For each washing, a suction vacuum was applied to suck the buffer. The volume and time of washing varied from round to round in each SELEX process and is described in their respective chapters. Once the washing was done, the filter was recovered and cut into very small pieces. It was then transferred to 1.5 mL DNA Lo-Bind tubes for extraction.

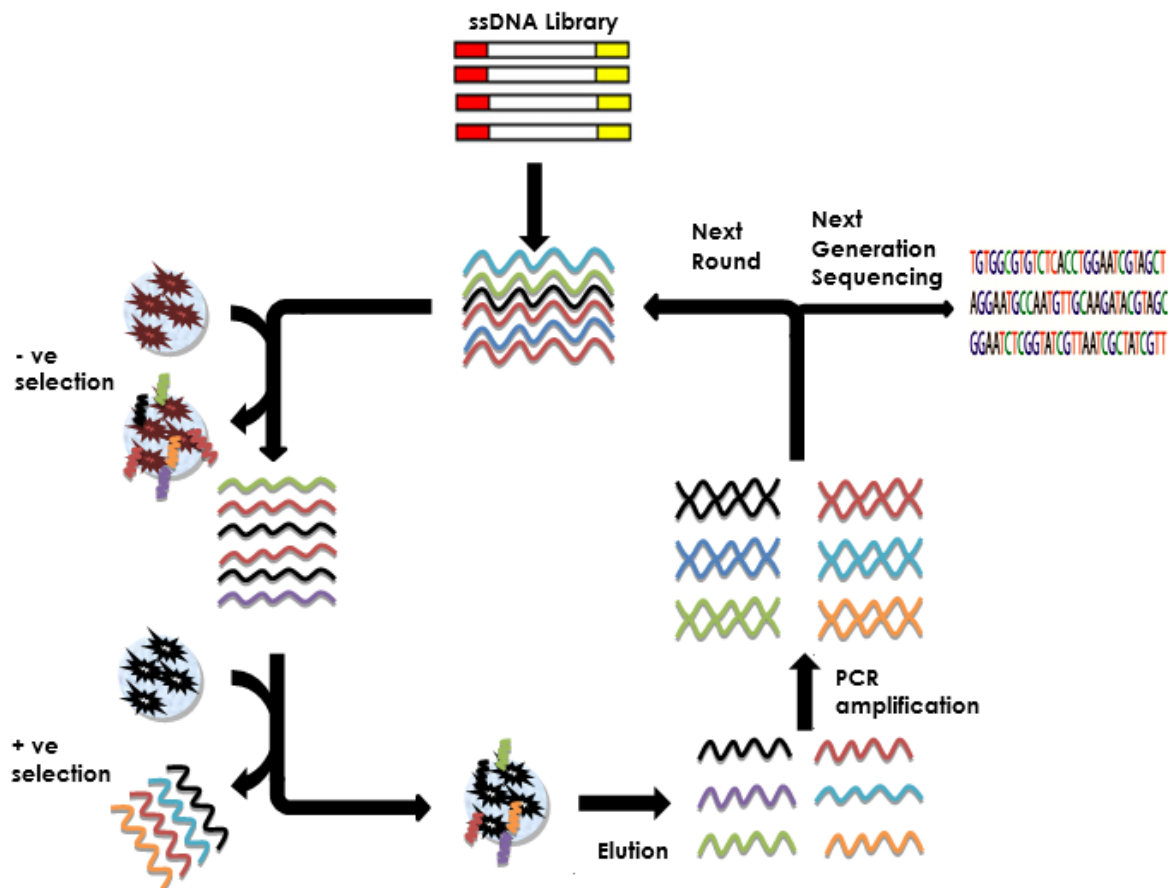


Figure 2.3: Filtration based SELEX. An ssDNA library is first incubated with the negative protein fixed on NC membrane for counter selection. The recovered sequences are then incubated with the target protein and interested and non-interested sequences are separated by using NC membranes. The bound ssDNA sequences which are retained on the NC membrane along with target protein are extracted by Phenol: Chloroform. The extracted ssDNA sequences are then amplified by PCR. The PCR products are separated into ssDNA for the next round of selection. Finally the enriched library with aptamer sequences are analysed by High throughput sequencing to select aptamer candidates.

Extraction of ssDNA sequences in Filtration SELEX:

The ssDNA sequences were extracted by Phenol: Chloroform extraction method ²³². For extraction of interested ssDNA sequences from the NC membrane, 500 μ L mixture of phenol pH 8/Urea 7 M (1/1, V/V) was added to the pieces of NC membrane and heated at 65°C for 20 minutes by shaking at 13000 rpm using thermomixer. The mixture was then centrifuged at 13400 rpm for 1 minute at RT. After centrifugation, the supernatant (500 μ L) was recovered and treated with a 500 μ L mixture of Chloroform: Iso-Amyl alcohol (24:1). It resulted in the separation of membrane debris in the organic phase (down) leaving the isolated sequences in the aqueous phase (up) ²³³. The aqueous phase containing the sequences was then recovered and transferred in a new tube. It was then precipitated by Ethanol (details is mentioned later in this chapter) and later dissolved in 100 μ L H₂O.

This matrix was amplified by PCR to prepare a library for next round as mentioned later in this chapter. A detailed overview of the Filtration SELEX is given in Figure 2.3.

Cell SELEX:

Cell SELEX was performed against DDR2 expressing HUVEC Cells ²³⁴ to select aptamers targeting DDR2. Total two rounds of Cell SELEX were performed in the Cross-Over SELEX against DDR2. The 1st round of Cell SELEX was performed with 2.5 million cells while the 2nd round was performed with 1 million cells. A western blot assay was performed by our collaborators to demonstrate the expression of DDR2 specifically by HUVEC cells (Figure 2.4).

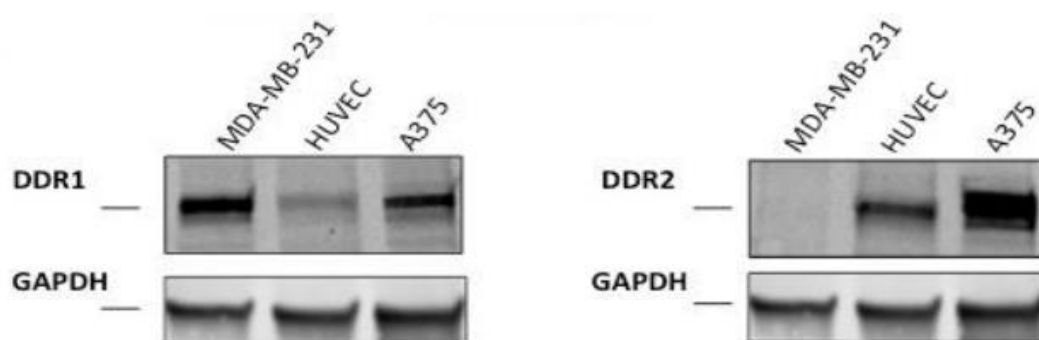


Figure 2.4: Western Blot analysis of DDR1 and DDR2 expression. Western blot results provided by Saltel's group demonstrates that both DDR1 and DDR2 are highly expressed in A375 melanoma cells while MDA-MB-231 breast adenocarcinoma cells expresses DDR1 and HUVEC cells expresses DDR2 specifically.

Cell Culture for Cell SELEX against DDR2:

For cell SELEX, the cells were prepared and provided by Saltel's group. HUVEC cells were maintained in Endothelial Cell Growth medium 2 with supplement Mix (Promo Cell, C22011). These HUVEC cells were generated with stable overexpression of DDR2. For this purpose, these cells were infected twice in 2 days with lentiviral particles expressing DDR2 at a multiplicity of infection (MOI) of 5.

Preparation of ssDNA library in Cell SELEX:

The total volume of the ssDNA library used during selection was 1 mL as described by a method paper published by Tan group¹⁰⁸. For this purpose the required ssDNA library was first prepared in 360 μ L Cell SELEX Binding Buffer 1X. It was then denatured by heating at 95°C for 5 minutes followed by immediate cooling at 4°C for 5 minutes. Then 640 μ L of Cell SELEX binding buffer 1X was added to make the volume 1 mL.

Selection step in Cell SELEX:

The selection step of cell SELEX was performed against HUVEC cells expressing DDR2 receptors. For this purpose the cells were prepared in petri dish. The confluence was above 90%. Before the selection step, the cells were washed with 2 mL of Cell SELEX washing buffer. For Selection, the library in 1 mL of selection buffer was incubated with the cells for 30 minutes at RT. After incubation, the supernatant containing non-interested sequences was discarded. The cells were then washed with washing buffer with 2 minutes of washing time in each washing step. The number and volume of washing was varied in 1st and 2nd round of cell SELEX against DDR2 as described in Chapter 4.

Extraction of bound ssDNA sequences from Cells:

After washing the cells, 500 μ L of DNase-free water was added to the cells. The surface of the petri dish was scrapped to collect the cells containing bound sequences. These scrapped cells were transferred to 1.5 mL DNA LoBind tubes followed by heat shock at 95°C for 5 minutes which resulted in the dissociation of the complex. The supernatant containing the candidates were recovered after centrifugation for 5 minutes at 14000 rpm. This eluted matrix was concentrated by decreasing the volume up to 100 μ L and later amplified by PCR to get enough ssDNA pool for next round. The overview of Cell SELEX is given in Figure 2.5.

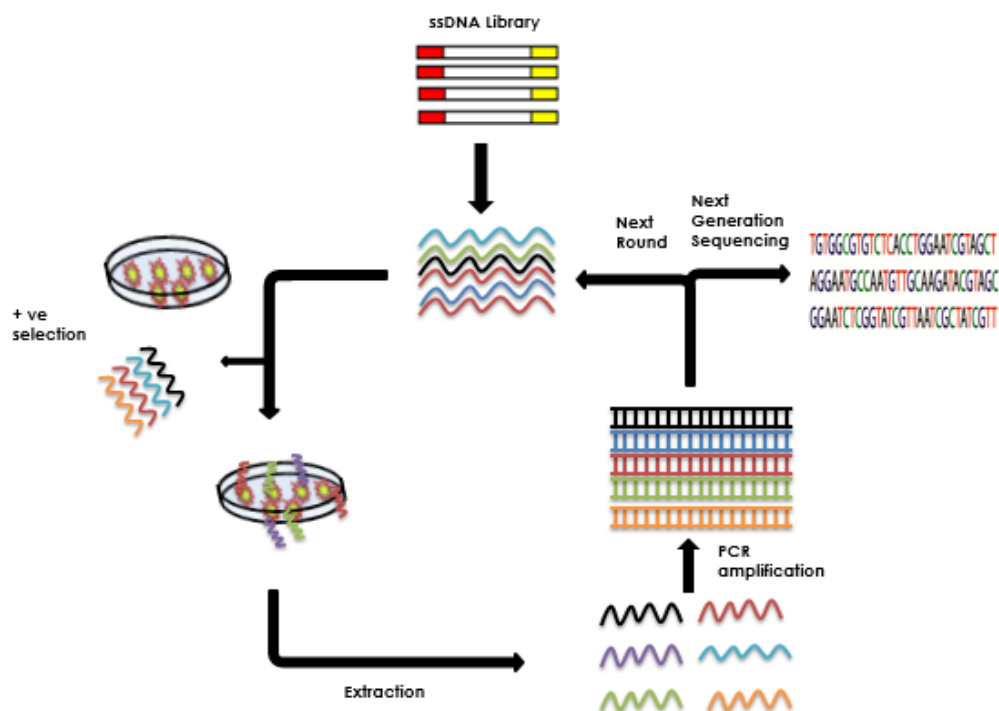


Figure 2.5: Cell SELEX. An ssDNA library is incubated with target cell. After washing, the bound ssDNA are extracted by heat shock at 95°C. After centrifugation, the supernatant containing the eluted ssDNA is collected and amplified by PCR. The PCR products are separated into ssDNA for the next round of selection. Finally the enriched library with interested sequences is analysed by High throughput sequencing to obtain aptamer candidates.

Click-SELEX

For a SELEX against HMMP14 target, a Click-SELEX²³⁵ was performed. For this purpose a library of 42 nucleotide random window flanked by 21 nucleotide primers was used (Table 2.1). The Thymidine (dT) in the random window was replaced with 5-ethynyl-2'-deoxyuridine triphosphate (EdU) bearing alkyne function at position C5 of the pyrimidine. This EdU bearing synthetic library was further modified by azide bearing Indole through CuAAC reaction. The library was then used for Click SELEX. A detailed discussion about Click SELEX is given in Chapter 6, but in this Chapter we will just discuss the methods we used during Click-SELEX.

Synthesis of the Click library

For Click-SELEX, the 42N window library with primers was synthesized at 1 μ mole scale in our lab by using the EdU phosphoramidite instead of regular thymidine in the mix of 4

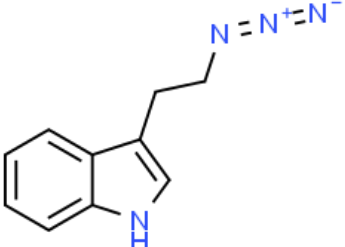
nucleotides for the random window synthesis. This library was deprotected by heating in NH_4OH solution as described later in this chapter. The size and synthesis purity was analysed by 20% Polyacrylamide Gel Stains-All. The library was then purified by polyacrylamide 6% denaturant PAGE and extracted by electro-eluter Biorad followed by desaltation using G10 sephadex column). The samples were then precipitated by EtOH and recovered in DNase-free water. Finally the purity of library was analysed by 20% Polyacrylamide Gel Stains-All.

Deprotection of Oligonucleotides

The synthesis of oligonucleotides in our lab was based on a solid support synthesis by the phosphoramidite method on DNA synthesizer²³⁶. Thus the oligonucleotides were synthesized in 3' to 5' direction on CPG support by using phosphoramidite monomers protected with 4-tert-butyl phenoxy acetyl. After synthesis the supports were transferred to 1.5 mL eppendorf tube and 1 ml of 37% NH_4OH solution was added for deprotection. The suspension was then heated at 55 ° C for 5 hours in the thermo mixer by mixing it at 1000 rpm.

After deprotection, the sample solution was mixed well by vortexing it followed by a centrifugation at 13400 rpm for 1 minute. The supernatant containing oligonucleotides was transferred to a new 1.5 mL tube. The CPG pores were rinsed thrice with 150 μL DNase-free water followed by centrifugation at 13400 rpm for 30 seconds. After each rinsing, the supernatant was transferred to the new tube of oligonucleotide. The solution was then evaporated in speed vac evaporator overnight at RT. The oligonucleotides were then dissolved in DNase-free water and the concentration was measured by using UV spectrophotometry.

Synthesis of 3-(2-azidoethyl)-1H-indole

<p>$\text{C}_{10}\text{H}_{10}\text{N}_4$ MW = 186,218 g.mol⁻¹ Rf : 0,3 (Pentane/(CH₂Cl₂/AcOEt 1/1) = 9,5/0,5 v/v)</p>	
--	--

1 g of 3- (2-bromoethyl) -1H-indole (4.46 mmol) and 0.32 g of sodium azide (4.9 mmol) are dissolved in 10 mL of anhydrous DMF and stirred under argon at 80 °C. The progress of the reaction is monitored by thin layer chromatography. The reaction mixture is subjected to liquid-liquid extraction with ethyl acetate and saturated NaCl water. The solvent is evaporated under vacuum and the crude reaction product is purified on a silica column (eluent 95% pentane / 5% dichloromethane / Ethyl acetate 1/1). After evaporation of the solvent, the compound is obtained in the form of a yellow oil (m = 0.56 g, ρ = 67%) (75MHz, CDCl₃) δ (ppm) : 136,42 ; 127,33 ; 122,71 ; 122,37 ; 119,74 ; 118,79 ; 112,25 ; 111,67 ; 51,81 ; 25,20 (Figure 2.6).

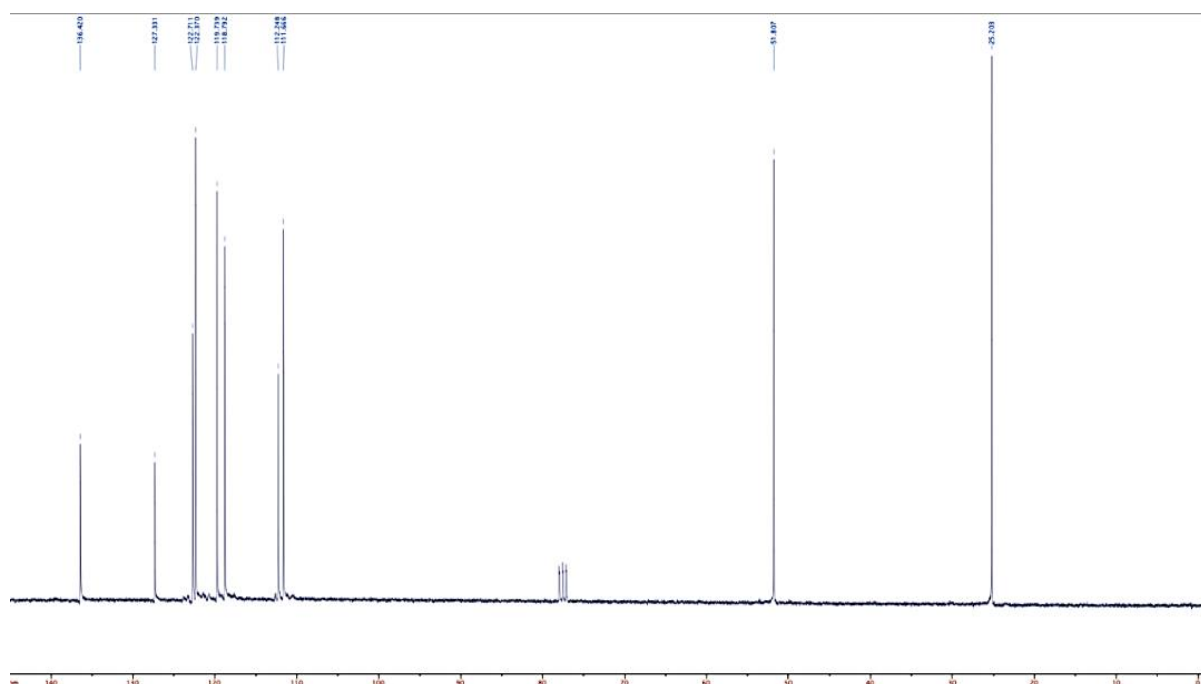


Figure 2.6: NMR spectroscopy of ¹³C.

CLICK reaction

The Huisgen reaction was performed to modify the EdU with addition of azido Indole through Copper Assisted Azide/Alkyne Coupling following described protocol in literature²³⁵. For this purpose, 100 μ L of Cu (I) catalyst solution was first prepared by addition of 70 μ L DNase-free water, 4 μ L THPTA (100 mM), 1 μ L copper sulphate (100 mM) and 25 μ L of Sodium Ascorbate (100 mM). The three solutions were freshly prepared for each reaction. This mixture was then put for 10 minutes at room temperature to allow the reduction of copper. During this time, 90 μ L reaction mixture was made by adding 10 μ L of azide solution (10 mM

in DMSO), 10 μL of phosphate buffer (100 mM, pH 7) and 70 μL of DNA (500 pmoles) containing EdU (thymidine analog). The click reaction was performed in 100 μL total volume i.e. (10 μL of catalyst solution + 90 μL of reaction mixture) with an incubation of 1 hour at 37 $^{\circ}\text{C}$, 800 rpm.

The medium was then desalted on the G25 column (Sephadex®), in which 100 μL of the reaction is stamped on 900 μL of the resin before centrifuging for few minutes at 4000 rpm. The column is rinsed by addition of 100 μL of water and centrifugation. The filtrates are recovered and passed on a Nanosep 10K column. The oligonucleotide is recovered on the membrane by adding 50 μL of water and its concentration is determined by UV spectrometry.

Polymerase Chain Reaction Amplification

Optimization of PCR amplification of the SELEX Library:

In SELEX, the sequences of interest are amplified by PCR to obtain a library for next round of selection. Since PCR is one of the main and critical steps in SELEX, it must be optimized for the progress in SELEX through the enrichment of interested sequences. The number of cycles in PCR needs to be optimized in order to avoid any by product formation during PCR, which will highly influence the evolution in SELEX ²³⁷. Before performing SELEX, we amplified the library to optimize the number of cycles of PCR required during SELEX. We performed the PCR amplification of the SELEX libraryA (table 2.1) with Taq and Phusion Polymerases. Initially 1 pmole of library was amplified in total 100 μL of PCR Volume.

After PCR amplification, 4 μL of the amplified pool mixed with 1 μL of agarose loading dye 5X were loaded in 3% agarose gel. The gels were visualized under UV. The results show that with the above mentioned PCR protocols, 20 cycles of PCR were enough to amplify the sequence in case of both high fidelity (Phusion) and low fidelity (Taq) polymerases, as the gel image in Figure 2.7 B and 2.8 B demonstrate that there was no formation of any dimers/by products.

Following protocol was adapted to perform PCR with the polymerases respectively

PCR amplification with Taq Polymerases:

Reagent	Volume (1000 μ L)
PCR Buffer 10X	10 μ L
MgCl ₂ 25 mM	8 μ L
DMSO 100%	5 μ L
dNTPs 20 mM	1 μ L
Forward Primer 100 μ M	1 μ L
Reverse Primer 100 μ M	1 μ L
DNA pool 1 μ M	1 μ L
Taq polymerase 5 U/ μ L	2 μ L
H ₂ O q.s	100 μ L

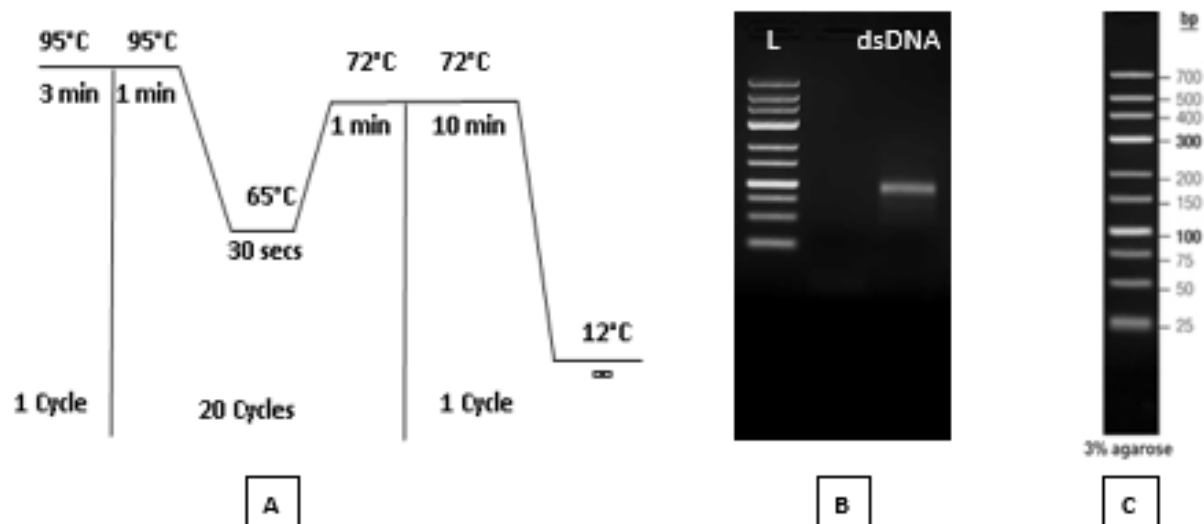


Figure 2.7: PCR amplification of SELEX libraryA with Taq Polymerase. **A**= The PCR was performed by Taq polymerases where initial denaturation was 3 mints at 95°C followed by 20 cycles of PCR (denaturation 1 mint at 95°C, annealing 30 secs at 65°C and extension 1 mint at 72°C). The final extension was performed for 10 minutes at 72°C and cooled down at 12°C. **B**= Agarose 3% gel analysis of the PCR product of SELEX libraryA with 0.5 ug of DNA ladder (L). **C**= picture of Gene Ruler ultra-low range DNA ladder taken from thermo fisher website.

PCR amplification with Phusion Polymerases:

Reagent	Volume (100 μ L)
PCR Buffer 5X containing 7.5 mM MgCl ₂	20 μ L
DMSO 100%	5 μ L
dNTPs 20 mM	1 μ L
Forward Primer 100 μ M	1 μ L
Reverse Primer 100 μ M	1 μ L
DNA pool 1 μ M	1 μ L
Phusion polymerase 2 U/ μ L	1 μ L
H ₂ O q.s	100 μ L

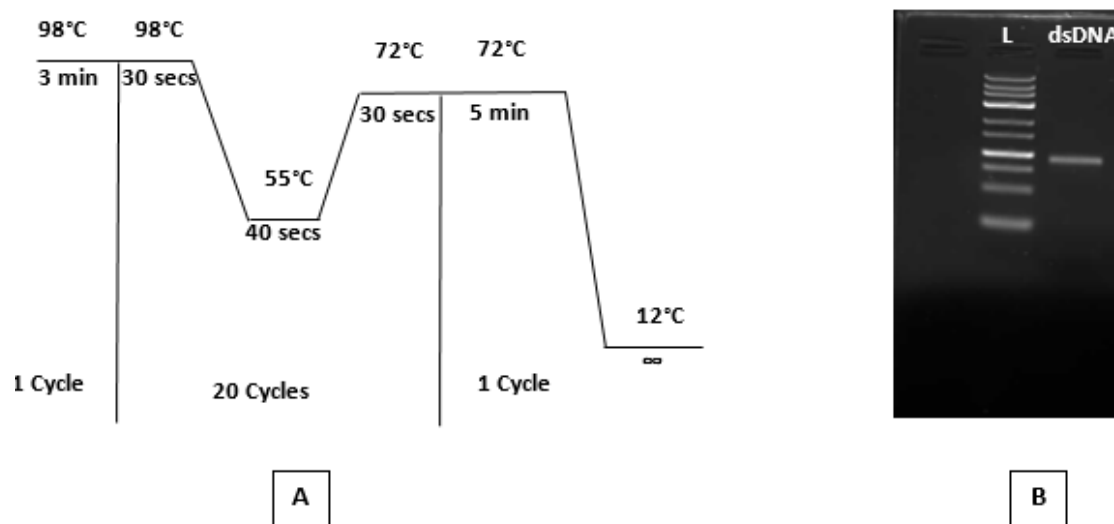


Figure 2.8: PCR amplification of SELEX library A with Phusion Polymerase A= The PCR was performed by Phusion polymerases where initial denaturation was 3 mints at 98°C followed by various no of cycles of PCR (denaturation 30 secs at 98°C, annealing 40 secs at 55°C and extension 30 secs at 72°C). The final extension was performed for 5 minutes at 72°C and cooled down at 12°C. **B**= Agarose 3% gel analysis of the PCR product of SELEX library A.

PCR amplification of SELEX rounds:

During SELEX, the initial rounds were mostly amplified by low fidelity Taq polymerases while the last rounds were mostly amplified by High fidelity Phusion Polymerase. As the eluted volume was 100 μL for all SELEX methods, we performed a PCR in accordance to 100 μL PCR volume for each 10 μL of eluted matrix. Since in the first round of SELEX, the bound sequences have a single copy so we decided to amplify the full eluted volume i.e. 100 μL . For this purpose, PCR was performed in 1000 μL total volume. While for the proceeding rounds we amplified only 90% of the eluted volume in 900 μL total volume of PCR. The other 10% of the eluted pool was stored to evaluate the SELEX rounds by In vitro Fluorescence Assays.

Preparation of ssDNA strands

In SELEX, PCR is one of the main steps in order to get more copies of evolved candidates. Since the PCR products are double stranded DNA so we needed to separate the sense strand from the antisense to use it as a library for next round of selection in SELEX. There are many types of strand separation methods available in the literature ²³⁸ depending on the type of PCR performed.

Purification by PAGE 12%

Separating the strands of PCR products by using PAGE gel is one of the well-known methods used during SELEX ²³⁹. Since the migration is based on the number of phosphate groups present in the compound, we needed different number of bases in sense and antisense strand. For this purpose, we used a large reverse primer i.e. 5'-ACT GAC TGA CTG ACT GAC TA-C12-reverse primer-3' while performing the PCR. This antisense strand had 20 bases extended with a C12 linker attached to the normal antisense strand. Since the PAGE gel is a denaturing gel, the strands were separated resulting in faster mobility of the sense strand as compared to the large antisense strand during electrophoresis. The sense strand was then recovered from the gel.

Exonuclease Digestion of antisense strand:

Production of single-stranded DNA templates by exonuclease digestion following the polymerase chain reaction has upgraded SELEX technology²⁴⁰. Lambda Exonuclease selectively digests the 5'-phosphorylated strand of dsDNA in 5' → 3' direction²⁴¹. For this purpose, phosphate was added to the 5' position of the antisense strand into the dsDNA by using the 5'-phosphorylated reverse primer during PCR.

For Exonuclease digestion, Native-PAGE was first performed to optimize the time and quantity of Lambda Exonuclease needed to digest specific amount of the antisense strand completely (Figure 2.9). The dsDNA PCR product of SELEX libraryA was first treated by Nanosep 10K column for the removal of dNTPs. For this purpose, the membrane of Nanosep 10K was first activated by adding 500 μ L DNase free H₂O (maximum limit) following a centrifugation at 5000 g for 10 minutes. The filtrate was discarded and 500 μ L of dsDNA was then added to the tube and centrifuged again at 5000 g for 30 minutes. Once the centrifugation was done, the dsDNA retained on the membrane of Nanosep 10K was recovered by dissolving it into 100 μ L of H₂O and the concentration was measured by UV Spectrophotometry.

50 pmoles of dsDNA amplified pool were then incubated with 5U of Exonuclease enzyme for digestion in 100 μ L total volume which contains dsDNA 50 pmoles, 10 μ L of Exonuclease buffer 10X, 1 μ L Exonuclease enzyme 5U/ μ L and H₂O q.s 100 μ L. These mixtures were then separately incubated at 37°C for 10, 15 and 20 minutes followed by an immediate heat shock at 80°C for 10 minutes to denature the enzyme. These sample were then again treated with nanosep 3K to remove the enzyme and buffer salts by centrifugating at 13400 rpm for 30 minutes. The candidates were recovered in total 20 μ L volume each sample. For native PAGE analysis, 5 μ L of native loading dye was added to all samples and loaded in native PAGE as discussed in paragraph 2.11.3. 25pmoles of 77bp ssDNA (SELEX libraryA) and 50 pmoles of amplified dsDNA of SELEX libraryA without exonuclease lambda treated were loaded separately.

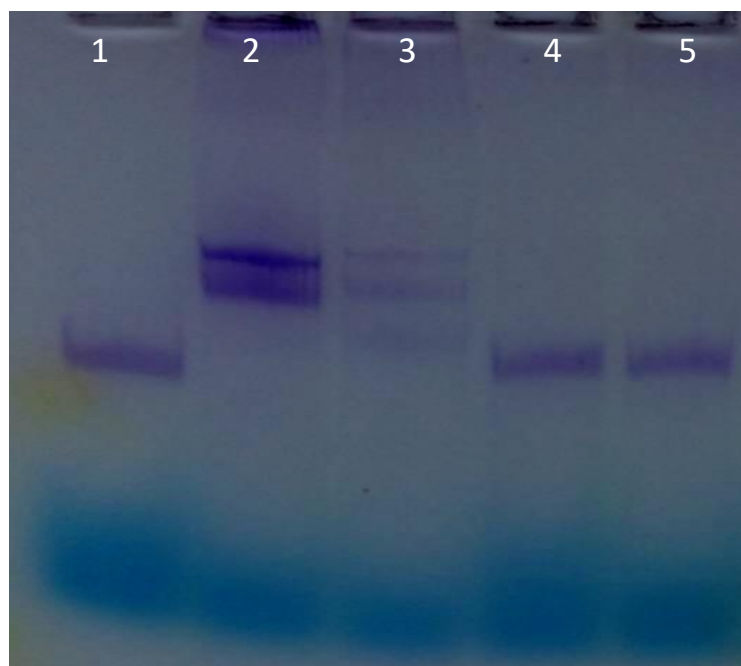


Figure 2.9: Electrophoretic Mobility Shift Assay (EMSA) gel Image: EMSA with 15% Polyacrylamide gel to analyse the digestion capacity of Lambda Exonuclease. The following samples were loaded in the gel. Lane 1= 25pmoles of ssDNA SELEX libraryA, Lane 2= 50 pmoles of dsDNA of SELEX libraryA without Exonuclease digestion, Lane 3=50 pmoles of dsDNA of SELEX libraryA treated with Exonuclease for 1 . Lane 4=50 pmoles of dsDNA of SELEX libraryA treated with Exonuclease for 10 minute. Lane 5=50 pmoles of dsDNA of SELEX libraryA treated with exonuclease for 20 minutes.

As shown in the Figure 2.9, the antisense strand of 50 pmoles of dsDNA was partially digested by 5U of exonuclease lambda in 10 minutes, while in 15 minutes it was fully digested. It is also demonstrated that there is no observed effect of exonuclease lambda on the sense strand upon incubation for 20 minutes at 37°C.

Based on the above demonstration, during SELEX the strand separation by lambda exonuclease enzyme was performed in 200 µL total volume for 20 minutes at 37°C. For this purpose, the amplified pool was first concentrated by using 10K nanosep column as mentioned earlier. Another reason to use the 10K nanosep column was to remove all dNTPs presented in the amplified pool. Later the dsDNA pool was recovered in 100 µL total volume and concentration was determined by UV spectrophotometry. The dsDNA pool was then incubated with exonuclease enzyme for digestion in 200 µL total volume containing 100 µL of dsDNA solution, 20 µL of exonuclease buffer 10X, volume of exonuclease enzyme 5U/µL required to digest at 1U/10 pmoles of dsDNA and H₂O q.s up to 200 µL. The incubation was done at 37°C for 20 minutes followed by an immediate heat shock at 80°C for 10 minutes to denature the

enzyme. This sample was then again treated with nanosep 3K to remove the enzyme and buffer salts by centrifugating at 13400 rpm for 30 minutes. The ssDNA retained on the membrane of the nanosep tube was then recovered into 50 μ L water and sample concentration was measured by UV spectrophotometer and analyzed by agarose gel 3%.

Passive Elution of Oligonucleotides

After purification of PCR amplified SELEX libraries by denaturing PAGE, we extracted them from the polyacrylamide gel through passive elution²⁴². For this purpose, we cut the interested band in the gel into small pieces and put in 1.5 mL DNA-Lo bind eppendorf tube along with 1 mL of TENaCl Extraction buffer and heated it at 65°C for 90 minutes. The extracted ssDNA sequences were then separated from the gel by using Spin-X centrifuge tube with a cellulose acetate membrane of 0.45 μ m pore size. For this purpose the gel containing buffer was transferred to the Spin-X tubes followed by centrifugation at 13400 rpm for 15 minutes. The filtrate containing the ssDNA sequences was collected. This filtrate was then precipitated by adding 3X volume cold EtOH 100% and 1/10th volume of NaOAc 3 M followed by an incubation at -20°C ON. The solution was then centrifuged at 14000 rpm for 30 minutes at -4°C. As a result of this centrifugation, the oligonucleotides form a pellet. The supernatant is then discarded and the pellets were further washed with 200 μ L of 70% EtOH following a centrifugation at 14000 rpm for 10 minutes. The supernatant was discarded and the oligonucleotides were dissolved into 100 μ L H₂O and sample concentration was measured by UV spectrophotometry and analyzed by agarose gel 3%.

Electro Elution of Oligonucleotides

For oligonucleotides synthesized in our lab at μ mole scale, we performed an electro elution method to extract the oligonucleotides from the polyacrylamide gel. This experiment was performed by using an electro eluter from Bio-Rad which was electrically connected to the Apelex electrophoresis for power supply and VWR magnetic stirrer used for electro elution. For electro elution, initially the electro-eluter membrane green cap with a cut off of 3K was activated.

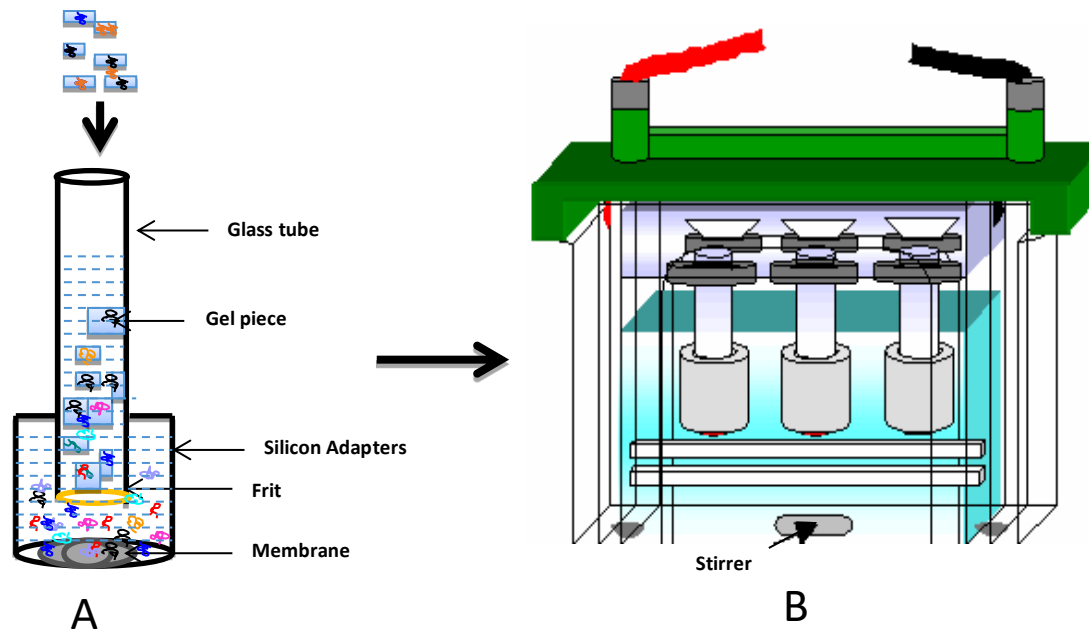


Figure 2.10: Electro-elution of oligonucleotides. **A**= A glass tube fixed with Silicon adapter with an activated membrane cap at its lower end. The gels pieces are in the glass tube with Buffer TBE 0.5X. **B**= an image taken from Bio-Rad website which shows that the glass tubes containing gel pieces are fixed on the Bio-Rad electro eluter with 0.5X TBE filled in both upper and lower part. During electro elution, the oligonucleotides are extracted from the gel and move downwards towards the positive electrode. It passes the frit and gets trapped in the silicon adopter. It is then recovered from the silicon adapter.

For this purpose, the membrane was put into 15 mL falcon tube containing TBE 1X buffer and heated at 65°C for 90 minutes in the thermo-mixer. The apparatus was assembled in a way that a glass tube of 10 mm size was blocked at its lower end by Bio-Rad electro-eluter Frits Model 422. This glass tube was fixed in a silicon adapter with lower end fixed by the activated green membrane cap. The gel pieces were then transferred to this glass tube and fixed on the Bio-Rad electro-eluter as shown in Figure 2.10. The upper and lower part of the Bio-Rad electro-eluter was filled with TBE 0.5X and the experiment was run for 30 minutes at 10 mA current with constant stirring by magnet at 260 rpm which is required to force the oligonucleotides to cross the frit and trap inside the silicon adapter. Polarity was reversed for 30 secs. The solution inside the silicon adapter containing the trap oligonucleotides was then recovered and concentrated by vacuum for desalination.

Desalination of ssDNA Oligonucleotides

After passive elution, the oligonucleotides were desalted by using Nanosep tubes by PALL which have pore size of 10K as described earlier. The oligonucleotides were recovered in 100 μ L DNase free water which were then precipitated by adding 3X volume cold EtOH 100% and 1/10th volume of NaOAc 3 M followed by an incubation at -20°C ON. The solution was then

centrifuged at 14000 rpm for 30 minutes at -4°C. As a result of this centrifugation, the oligonucleotides formed a pellet. The supernatant was then discarded and the pellets were further washed with 200 µL of 70% EtOH following a centrifugation at 14000 rpm for 10 minutes. The supernatant was discarded and the oligonucleotides were dissolved into 100 µL H₂O and sample concentration was measured by UV spectrophotometer and analyzed by agarose gel 3%.

After electro elution, the oligonucleotides were first concentrated in 100 µL and desalted by using gel filtration resin G10 Sephadex. For this purpose G10 solution of 20% (w/v) in milliQ water was prepared and stored ON at 4°C. 1 mL of G10 solution was then added to a 2 mL Syringe having a piece of fiber glass cotton at its lower end to retain the solution in the syringe. The syringe was then centrifuge at 4000 rpm for 2 minutes which resulted in the condensation of G10 sephadex inside the syringe while the water was filtered out of the syringe. The oligonucleotides solution was added to the syringe and centrifuged at 4000 rpm for 20 minutes. The filtrate containing the oligonucleotides was recovered and the concentration was measured by UV spectrophotometer.

UV Spectrophotometry

The concentration of DNA was measured by UV spectrophotometer (Denovix®, DS-11). The instrument was first calibrated with water and blanked according to the protocol suggested by the provider. The absorption of light was measured ranging from 220 nm to 340 nm wavelength for DNA samples. The concentration was then measured by Beer-Lambert Law

$$\mathbf{A = \epsilon bc}$$

Where,

A is absorbance (no unit), ϵ is the molar absorptivity ($\text{L mol}^{-1} \text{cm}^{-1}$), b is the path length of the sample (cm) and c is the concentration of the sample (mol L^{-1})

If b= 1cm

$$\mathbf{C = A_{260}/\epsilon_{260}}$$

Here A_{260} is the absorbance of DNA sample at 260 nm absorption wavelength and ϵ_{260} is the molar absorptivity of the DNA bases calculated as

$$\mathbf{\epsilon = (15400 * A + 11700 * G + 7500 * C + 9200 * T) * 0.88.}$$

Gel Electrophoresis:

Agarose Gel Electrophoresis

Agarose gel electrophoresis is extensively used in separating DNA by size for visualization. Agarose gel electrophoresis uses an electrical field to move the negatively charged oligonucleotides through an agarose gel matrix towards a positive electrode. Shorter oligonucleotides migrate through the gel more quickly than longer ones. Thus, we determine the approximate length of a DNA fragment by running it on an agarose gel alongside a DNA ladder. Furthermore, the ethidium bromide present in the gel binds to the DNA and gives fluorescence for visualization.

We used 3% (w/v) agarose gels to analyze the DNA molecules especially for the PCR validation. For this purpose 3 g of agarose was mixed in 100 mL of TBE 0.5X. This mixture was heated in microwave at 500W until the agarose particles dissolved and then cooled down at RT for few minutes. 0.5 ug/mL of ethidium bromide was then added to the suspension. It was then poured in a cassette with a comb and solidified at RT for 30 minutes. The comb was then removed and gels were stored in TBE 0.5X until used.

For electrophoresis, DNA samples were mixed with Agarose loading buffer (1X final) and loaded into the gel with DNA ladder as a control. The gel was run into 0.5X TBE buffer with a voltage of 100 V. The running time depends on the length of the sample. Once the electrophoresis was done, the gels were analyzed under UV of 100 milli secs in G-BOX syngene as the gel was supplemented by ethidium bromide, which binds to DNA and gives fluorescence with an excitation at 525 nm wavelength.

Denaturant Polyacrylamide Gel Electrophoresis:

Denaturant PAGE is used to purify the oligonucleotides. Polyacrylamide gels of 6%, 8% and 10% and 12% were used based on the nucleotide length of the samples (PCR products/Synthesized oligonucleotides) for their purification (Table 2.3). For this purpose, required percentage of gel was prepared by mixing a solution of 20 % of Polyacrylamide solution containing 7 M Urea and a solution of 0 % of Polyacrylamide solution containing 7 M Urea in TBE 0.5X. APS 0.01% and TEMED 0.001 % were also added before casting the gel. The gels were made in 100 mL falcon and then poured on the glass plate of 35 cm length. A comb of required size was fixed inside the gel and let it polymerized. After polymerization, the

gel along with glass plates was fixed on gel electrophoresis chamber and both upper and lower parts were filled with TBE 0.5X. The gel was preheated for 20 minutes with 12W power. Samples were then loaded with formamide loading buffer (FLB) 1X final. Electrophoresis was performed at 20W power for a specific time based on oligonucleotide length. The FLB contained DNA trekker blue dyes which is needed to track the DNA migration. After enough migration, the current was stopped and the gel was analyzed under UV 280nm wavelength with a silica plates. The interested band was marked and cut into pieces for elution.

PAGE 70 mL	6%	8%	10%	12%
Acrylamide 20%, 7M Urea	21 mL	28 mL	35 mL	42 mL
Acrylamide 0%, 7M Urea	48.23 mL	46.23 mL	34.23 mL	32.23 mL
APS 10%	700 µL	700 µL	700 µL	700 µL
TEMED	70 µL	70 µL	70 µL	70 µL

Table 2.3: Polyacrylamide Gel Percentages for PAGE purification.

In our lab we also used denaturant PAGE 20% to analyze the DNA samples as sometimes highly structured oligonucleotides show irregular migration in agarose gel electrophoresis. For this purpose we used 20 mL of Polyacrylamide 20% solution in TBE 0.5X containing 7 M Urea. 0.01% APS and 0.001 % TEMED were also added before polymerization. For polymerization, the gel of 1mm was casted in glass plates of 15 cm length. A comb was also fixed in the gel to make wells of equal size for loading. 1 µg of oligonucleotide samples were loaded with 10 µL of FLB loading dye along with a reference oligonucleotide. Experiments were run at 12W power. After migration the gel was shifted to staining tray where it was stained with stain-all solution at RT until the bands were visualized with naked eyes.

Native Polyacrylamide Gel Electrophoresis

Native PAGE electrophoresis was performed to evaluate the digestion capacity of oligonucleotides by lambda exonuclease. For this purpose, 15% polyacrylamide gel was prepared in 50 mL (50 mL of Polyacrylamide Solution contained 37.5 mL Polyacrylamide 20% in TBE 0.5X, 11.95 mL of TBE 0.5X, 500 µL of APS 10% and 50 µL of TEMED). The gel was

polymerized in glass plates of 15 cm length for 1 hour at RT. A comb was also fixed in the gel to make wells of equal size for loading. The gel was preheated for 20 minutes at 300 volt. 20 μ L of samples were loaded with 5 μ L of Native Loading dye 5X in the specific lanes of the gel with the continuation of current. The gel was run for 2 hours at 300 volt. After enough migration, the gel was transferred to the staining tray and stained by Stains-all solution. After staining the bands were visual with naked eye.

Sodium dodecyl sulphate polyacrylamide gel electrophoresis (SDS-PAGE):

The SDS-PAGE was performed using Protein Electrophoresis Equipment by BIO-RAD to evaluate the binding capacity of the Ni-NTA agarose magnetic beads with His-tagged proteins. For this purpose 1 mm glass castes were used for the gel thickness. The SDS PAGE gel in a single electrophoresis run had two parts i.e. Stacking gel and Running gel. The percentage of gels and the concentration of reagents in the gels are given in table 2.4. The running gel of 10% was first prepared into a 15 mL falcon tube and poured into the glass castes fixed on the stand for polymerization. 1 mL propanol was added immediately into the glass castes soon after pouring the gel to label the gel before it polymerized. Stacking gel was poured on the running gel once it was solidified and then a comb of 1.0 mm thickness was fixed inside the stacking part of gel and let it solidify.

Gel Running	Percentage 10%	Gel Stacking	Percentage 5%
H ₂ O	1.983 mL	H ₂ O	2.1 mL
Acrylamide 30%	1.667 mL	Acrylamide 30%	500 μ l
Tris 1.5M, pH 8.8	1.25 mL	Tris 1M, pH 6.8	380 μ L
SDS 10%	50 μ L	SDS 10%	30 μ L
APS 10%	50 μ L	APS 10%	30 μ L
TEMED	2 μ L	TEMED	3 μ L

Table 2.4: Running and Stacking Gel reagents and percentage for SDS-PAGE.

To all protein samples of 20 μ L, Laemmli 5X buffer 5 μ L was added. The samples were first denatured at 95°C for 2 minutes and loaded into the gel. 0.2 μ g of protein marker was also added in the side well of the gel as a control. The electrophoresis was run at 100 Volt for 2 hours in TG-SDS buffer 1X.

Silver Staining of protein in SDS PAGE gel:

After electrophoresis, the gel was stained by silver staining according to the protocol suggested by GE Health Care. Reagent solutions i.e. Fixing Solution, Sensitizing Solution, Silver Solution, Developing Solution and Stop Solution were made by using the chemicals provided in the Staining Kit (Table 2.5). First, the proteins in the gel were fixed by adding 80 mL of fixing solution to the gel with an incubation of 10 minutes at RT. The gel was then incubated with 80 mL of Sensitizing solution for 10 minutes at RT. It was then washed 4 times with 80 mL of H₂O with 4 minutes each washing. Then it was treated by 80 mL of Silver Solution for 10 minutes at RT in dark followed by 2 immediate washings with 80 mL of H₂O for 1 minute each washing. After the washing, the developing solution was introduced to visualize the protein bands for 1-5 minutes (until the bands were exposed well). Once the bands were exposed, the bands development was stopped by putting stop solution.

Reagent Solutions	Composition per 80 mL
Fixing Solution	24 mL EtOH absolute + 8 mL Glacial acetic acid + 48 mL H ₂ O
Sensitizing Solution	24 mL EtOH absolute + 3.2 mL Sodium thiosulphate (5% w/v) + 5.44 g of Sodium Acetate + add 0.4 mL glutardialdehyde (25% w/v) before use.
Silver Solution	8 mL Silver nitrate solution 2.5% w/v + 72 mL H ₂ O
Developing Solution	2 g of Sodium carbonate + 80 mL H ₂ O + add 0.05 mL formaldehyde 37% w/v before use
Stop Solution	1.168 g of EDTA-Na ₂ .2 H ₂ O into 80 mL H ₂ O

Table 2.5: List of Reagent Solutions used in Silver Staining

In vitro Fluorescence Assay

An in vitro fluorescence assay was performed for the analysis of aptamers. For this purpose the aptamer candidates were purchased from Eurofins with fluorescence attached at the 5' prime end. The experiments were performed in 1.5 mL DNA Lo-bind tubes. For this assay 1 nM final concentration of fluorescent labeled candidates were incubated with recombinant protein of desired concentration in buffer PBS-Mg 1X with 50 μ L total volume. The candidates were firstly denatured at 75°C for 5 minutes followed by immediate cooling for 10 minutes on ice (4°C). A binding buffer PBS-Mg 1X final conc. was then added to the candidates and incubated with the desired concentration of proteins for 30 minutes at RT. After incubation the fraction of bound and unbound sequences were separated by using NC membrane of 0.45 μ m pore size. For this purpose the NC membrane was first activated with KOH as described earlier. This resulted in retaining the protein on the membrane with sequences bound to the protein while the unbound sequences passed through the membrane into the filtrate as shown in Figure 2.11. The filtrate containing the unbound portion of the candidates was recovered and transferred to Quartz Cuvette of 3 mm Lightpath window to measure the fluorescence spectrum by Horiba Fluoromax 3rd generation spectrofluorometer. For this purpose the excitation of the fluorescent labeled candidates was adjusted at respective excitation wavelength and the emission spectrum was measured in the range of 50 nm wavelength window. The bandwidth for both excitation and emission spectrum measurement was adjusted at 5nm. The fluorescence intensity (a.u) at high emission wavelength was taken into account and calculated against the control fluorescein concentrations without protein which were also passed through the NC membrane in the same way. The difference was then calculated as Binding percentage with the formula $B\% = (1 - (F/F_0)) * 100$ where “F” stands for the fluorescence intensity of the filtrate of candidates (unbound portion) incubated with protein while “F₀” is the fluorescence intensity of the candidates without incubation with protein. Further detail about in vitro fluorescence assay is discussed in Chapter 3 with an example of fluorescein labeled candidates.

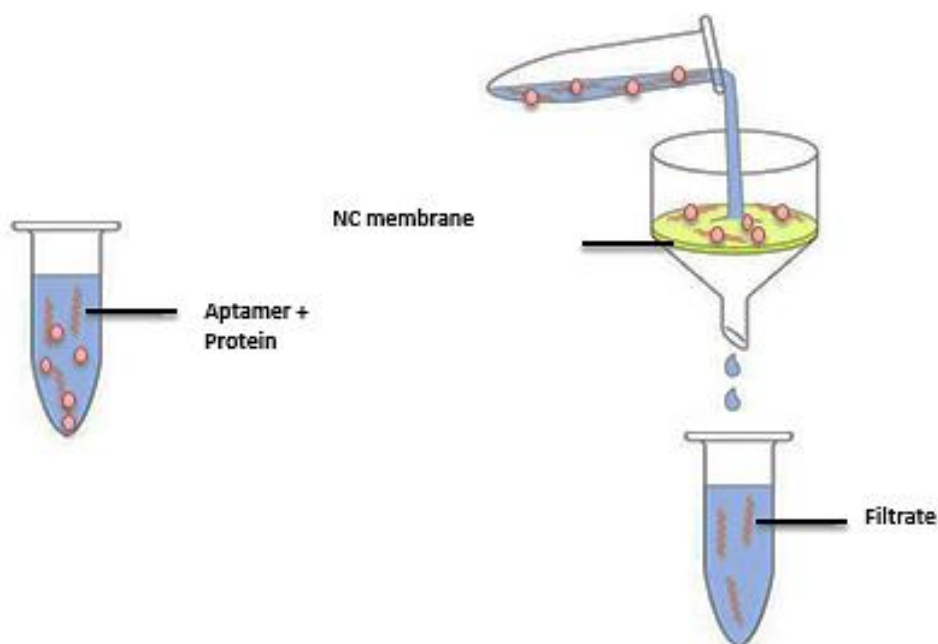


Figure 2.11: In vitro Fluorescence Assay scheme. The fluorescence labeled candidates (spring shaped) were initially incubated with the protein (pink dots) in 1.5 mL lobind tube. After incubation the solution was then passed through the NC membrane (yellow). The complex was retained on the NC membrane while the unbound sequences were passed in the filtrate. The filtrate was then recovered to measure the fluorescence intensity by Fluoromax spectrofluorometer. The figure was taken from Creative-Biomart website and modified.

a) In vitro Fluorescence Assay for the selected candidates from DDR1 SELEX1:

The selected candidates from DDR1 SELEX1 were first analyzed by in vitro fluorescence assay. Fluorescein (FAM) was attached on the 5' prime end of the candidates to measure the fluorescence intensity. The in vitro fluorescence assay was performed with 1 nM of the FAM labelled candidates against 50 nM of DDR1 as described in Figure 2.11. As the candidates are labelled with FAM at 5' prime, the excitation spectrum was fixed at 490 nm wavelength while the emission spectrum was scanned from 500 nm to 550 nm wavelength. The bandwidth for both excitation and emission was fixed at 5 nm. FAM labelled candidates with 1 nM conc. passed through the NC membrane were used as a control for fluorescence intensity. All the experiments were performed in triplicate. After the experiment, the data was converted in MS Excel format and the fluorescence intensity at 515 nm λ was considered to calculate the binding percentage of candidates against DDR1 protein.

b) In vitro Fluorescence Assay of Aptamer C25

In order to validate the specificity of C25 aptamer, an in vitro fluorescence assay was performed with 1 nM of FAM labeled C25 against 50 nM of DDR1 as target protein while DDR2 and GST as negative proteins. The reason to use DDR2 as a negative target was to make sure that Aptamer C25 binds specifically with DDR1 and not with DDR2 since there is a sequence homology of almost 60% between these two targets as described earlier in Chapter 1. As a control, 1 nM of FAM labeled C25 aptamer into 50 μ L passed through NC membrane was used. The experiment was performed as described in figure 2.11. As mentioned earlier, the emission spectrum of fluorescein at 515 nm λ was taken into consideration for evaluation. All the experiments were performed in triplicate.

Real time PCR for Quantitative Analysis

qPCR was monitored with the increase in fluorescence intensity of green dye SYBR, which intercalates with the dsDNA (amplicon) and fluoresces. The increase in fluorescence intensity of SYBR is proportional to the increase in amplicon concentration corresponding to each amplification cycle. The graphical plot of fluorescence vs. cycle number is displayed with the background (control) or baseline (ΔR_n). Then a threshold of fluorescence is set manually within the linear of amplification for all plots but above the baseline. The cycle number at which the amplification plot crosses this level of threshold fluorescence is called threshold cycle (C_t) (Figure 2.12). C_t is correlated to the initial concentration in the starting amplicon concentration i.e. the more concentrated samples have earlier C_t value than the lower concentrated samples.

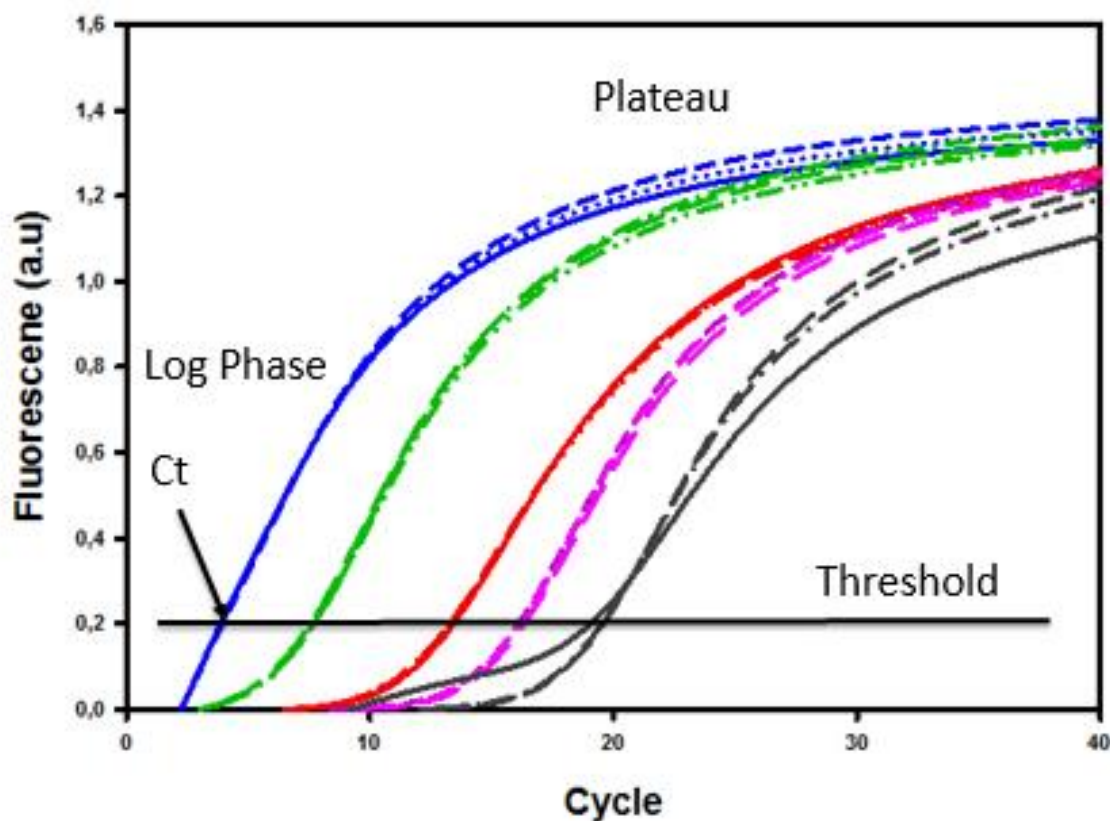


Figure 2.12: Amplification plot of C25 aptamer. Amplification plot of five serial dilutions i.e. 10⁶(black), 10⁷(pink), 10⁸(red), 10⁹(green) and 10¹⁰(blue) sequences of C25 Aptamer. All experiments were performed in triplicate.

The qPCR experiments were performed by Rotor-Gene Qiagen real-time PCR machine with Rotor-Gene Q Software analysis and monitoring. The final volume of all qPCR samples for calibration curve was 12 μL which contains 6 μL of Go Taq Master Mix 2X (final 1X), 1.66 μL of Aptamer solution, Forward and Reverse Primer each 0.12 μL of 100 μM (final 1 μM) and 4.1 μL of nuclease free water. The qPCR parameters were as follows: initial denaturation for 10 minutes at 95°C, cycling for 30 seconds at 95°C, 15 seconds at 65°C and 20 seconds at 72°C by repeating 40 times followed by the final step at 72°C for 5 minutes. The melting curve analysis was performed from 72°C to 95°C with a rising of 1 degree Celsius in each step. The waiting time for pre melt condition was 90 seconds in the first step and 5 seconds in each proceeding steps. A standard calibration curve was also performed using C25 full length aptamer with a series of dilution starting from 1.66e10⁻¹⁸ moles (1e10⁶ sequences) to 1.66e10⁻¹⁴ moles (1e10¹⁰ sequences) (Figure 2.12). The calibration curve generated will be discussed in chapter 3.

qPCR analysis of C25 aptamer

Real time PCR or qPCR has been used in the selection and characterization of aptamers ¹⁶⁷. Real time PCR was performed to validate the binding specificity of C25 against its target DDR1. In this experiment DDR2 was used as a negative target. For this purpose C25 aptamer was first denatured by heating at 75°C for 5 minutes followed by immediate chilling at 4°C for 10 minutes. After preparation of the C25 pool, 50 pM of C25 aptamer was incubated with 50 nM of DDR1 or DDR2 in total 50 µL volume with a buffer PBS-Mg 1X. The binding and non-binding fraction was separated by using NC membrane as discussed in Figure 2.11. The filtrate containing the non-binding fraction was recovered and 3.32 µL of 10X dilution from each filtrate was used for qPCR analysis of C25 aptamer. 10X dilution of 50 pM C25 aptamer without incubating with protein passed through the NC membrane was used as a control. The final volume of all qPCR samples was 12 µL which contains 6 µL of Go Taq Master Mix 2X (final 1X), 3.32 µL of filtrate solution recovered after the experiment, Forward and Reverse Primer each 0.12 µL of 100 µM (final 1 µM) and 2.44 µL of nuclease free water. The qPCR parameters were same as described earlier.

High-throughput Sequencing

High-throughput sequencing or Next Generation Sequencing is a method which has replaced the traditional methods for sequencing based on the clonal sequencing methods. Since its introduction, HTS has brought a revolution into selection of aptamers, providing significant information about SELEX pools by sequencing millions of sequences within no time ¹⁸¹.

DNA Pool generation for Illumina High-throughput Sequencing

HTS was performed on Illumina instrument available at CEA, Saclay France or ICM (Pitié-Salpêtrière, Paris). For HTS, the ssDNA products from specific rounds of SELEX were amplified by PCR using forward and reverse primers containing adapters suggested by the platform performing HTS. In addition each reverse primer contains different 6 base sequences index which is required to differentiate the samples for analysis. The PCR was performed in 200 µL for all samples by using Hot-Star Taq polymerase by Qiagen (Table 2.6). All PCR reactions were performed in Sensoquest labcycler PCR machine following the programme mentioned in Figure 2.13.

Composition	Volume (μL)
Hot Star Buffer containing dNTPs 5X	40
Forward Primer 100 μM	2
Hot Star Taq Polymerase (2,5 U/ μl)	2
Reverse Primer (Index) 100 μM	2
ssDNA (1 μM)	2
H ₂ O	152
Total	200

Table 2.6: Reagent composition of PCR for High Throughput Sequencing.

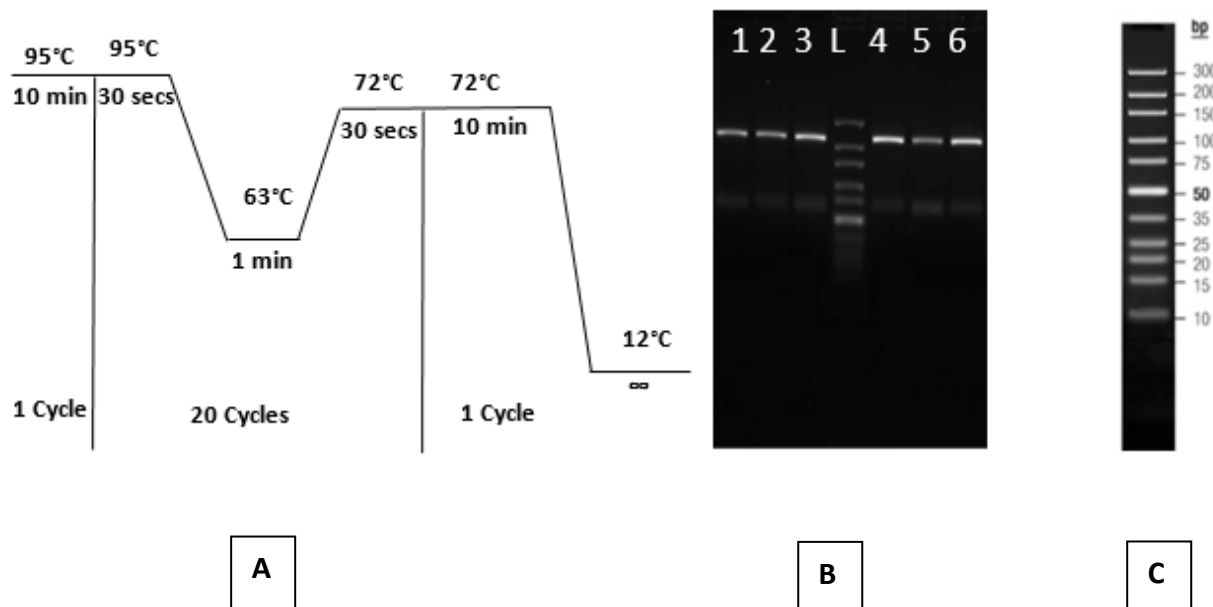


Figure 2.13: PCR amplification for High Throughput Sequencing. A= The PCR performed by Hot star polymerases for NGS where initial denaturation was 10 mints at 95°C followed by 20 cycles of PCR (denaturation 30 secs at 95°C, annealing 1 mint at 63°C and extension 30 secs at 72°C). The final extension was performed for 10 minutes

at 72°C and cooled down at 12°C. **B**= Agarose 3% gel analysis of the NGS PCR product with 0.5ug of DNA ladder. **C**= Gene Ruler ultra-low range DNA ladder.

After PCR, the size and quantity of the amplified products were validated by 3% agarose gel. For this purpose we used 4 µL of amplified product, along with 4 µL of water and 2 µL of Agarose loading buffer 5X. The samples were loaded into the gel along 0.5 µg of the DNA ladder as a reference. The gel was run for 40 minutes at 100V in TBE 0.5X. The bands were then analyzed in G-BOX Syngene under UV (Figure 2.13B). The samples were then sent to the platform where it was purified by 3% agarose gel and recovered by passive elution in TE-NaCl buffer 1X. All eluted samples were then precipitated by ethanol and dissolved in water. The samples were then sequenced by Illumina.

Bioinformatics analysis of DNA Sequences:

For the SELEX against HMMP14 with naïve DNA library, HTS analysis was performed by the platform. For this purpose after illumina sequencing, the HTS data was de-multiplexed and recovered in FASTQ format by bcl2fastq conversion software suggested by Illumina. In order to analyze the sequences, the FASTQ files were processed by a special software PATTERNITY-SEQ¹²² developed by MIRCen at Francois Jacob Institute of Biology, Paris France(<http://jacob.cea.fr/drf/francoisjacob/english/Pages/Departments/MIRCen/Platforms.aspx?TypeChapitre&numero=6>). The adapter sequences and primers were removed from each sequence in order to analyze the only variable regions. Then, sequences that contained at least one base with a quality score (Q) below 30 were removed before being saved in a FASTA format. This quality score can be converted to a probability of error (P) using the formula $P = 10^{(-Q/10)}$. Thus, the recovered sequences contain bases with a potential probability of error below 0.001 (1 in 1000). For clustering, first the frequency of each sequence in different libraries was calculated. The threshold of frequency was adjusted to 0.001%. This means that sequences which has a threshold frequency above 0.001% was recovered for analysis. These sequences were then clustered into families using the Levenstein edit distance of 6.

For other described SELEXs, the HTS analysis was performed in our lab. For this purpose after sequencing by Illumina, the HTS data was demultiplexed and provided in FastQ files for further analysis. The analysis was performed with following procedure.

D) Trimming 3'

Cutadapt software was used for the trimming of the adapters and primers used for sequencing²⁴³.

All the sequence bases after the random window at 3' were truncated by cutadapt 1.11 with python 2.7.10.

2) Trimming 5'

All the sequence bases before the random window at 5' were truncated by cutadapt 1.11 with python 2.7.10.

3) Optimization of Random Window length

The random window was further optimized by removing all the sequences that were either shorter or longer than the original window length by cutadapt 1.11 with python 2.7.10. For this purpose, In the analysis of SELEX libraries with 30 nucleotide random window, all sequences with random window less than 27 or more than 32 were removed. While for SELEX libraries with 40 nucleotide random window, sequences shorter than 37 and longer than 42 nucleotides were removed. Similarly for SELEX libraries with 42 nucleotide random window, sequences shorter than 39 and longer than 45 nucleotides were removed.

4) Counting of Sequences:

The sequences were counted by FASTAptamer software. FASTAptamer toolkit is an open source collection of scripts developed by "The Burke lab" at Missouri US. FASTAptamer seamlessly performs many of the first-stage, sequence-level tasks that are common to all SELEX methods independent of the SELEX technology. It processes FASTQ formatted sequencing data, counts sequence frequency, ranks and sorts by abundance, clusters sequences based on a user-defined Levenstein edit distance and calculates fold-enrichment (change in genotypic frequency across populations)¹⁸². In our case we performed Sequence counting and clustering by using FASTAptamer. The sequences were evaluated on the basis of their presence in the pool as reads per million (RPM).

5) Clustering of Sequences:

Sequence clustering was performed to make a non-redundant set of representative sequences. These sequences were then sequentially clustered in families using FASTAptamer with a Levenshtein distance of 7 (i.e. sequences with no more than 7

substitutions, insertions or deletions). In order to analyse only evolved and enriched sequences, the data was filtered by removing all those sequences which had less than specific reads per million in the clusters (in discussion part). This task was performed by using a software BMap, which is a splice-aware global aligner for DNA and RNA sequencing reads.

The HTS analysis for each SELEX has been discussed in their respective chapters. After analysis, the data converted into text file. It was then exported to excel files. The clusters were ranked according to their presence in the pool. The presence of the sequences were ranked based on reads per million (RPM). Sequence with highest RPM in the cluster was considered as the representative of the cluster.

Structural analysis of DNA Sequences by mfold:

Secondary structure analysis of all selected sequences was performed online by using mfold (<http://unafold.rna.albany.edu/?q=mfold>). mfold predicts the folding and hybridization of the sequences and gives ensembles of structures based on the average minimum free energy (ΔG) which reflects the stability of each structure²⁴⁴. Based on mfold predicted structures, the selected aptamers were truncated.

Aptamer with primers (full length) and without primers (random window) were folded by mfold given the conditions of folding temperature at 20°C with 1M conc. of Na⁺ and 1mM conc. of Mg⁺⁺.

Fluorescence Microscopy:

Confocal fluorescence microscopy was performed to analyze the binding of aptamer DS_3.1t1 against DDR1 target selected by DDR1 Doped SELEX (detail is given in chapter 3). For this purpose we used MDA-MB-231 breast adenocarcinoma cells expressing DDR1⁶¹ as a target cell and Human metastatic melanoma cells 501MEL which don't express DDR1/DDR2, as a negative control cells. The cell assay with confocal microscopy was performed in collaboration with Saltel's lab. For this experiment, all cells were prepared and provided by Saltel's laboratory.

For cell assay, MDA-MB-231 cells were purchased from American Type Culture Collection and were maintained in Dulbecco's modified Eagle's medium (1X) with 4.5 g/liter glucose + Glutamax-I (gibco) supplemented with 10% fetal calf serum and 100 U/mL penicillin–streptomycin (Invitrogen). Saltel's lab generated MDA cells with stable

overexpression of DDR1. For that these cells were infected with lentivirus particles expressing DDR1-GFP at a multiplicity of infection (MOI) of 2.5 and were selected using puromycin antibiotic at a concentration of 1 $\mu\text{g}/\text{mL}$. While as negative control 501Mel (Melanoma cell line) were maintained in RPMI medium 1640 (1X) + Glutamax-I (gibco) supplemented with 10% fetal calf serum and 100 U/mL penicillin–streptomycin (Invitrogen). The Cells were seeded in small borosilicate cover glasses. Total 60 thousand cells were seeded and stored at 37°C in the incubator until use. Before performing the cell assay, the living cells and confluency was confirmed using Zoe Fluorescence cell imager Bio-Rad.

For the confocal microscopy, DS_3.1t1 was labelled with TRITC fluorophore at its 5' prime end. The scramble sequence of DS_3.1t1 with TRITC labelled was used as a control. The experiment was performed with 100 nM of the TRITC labelled aptamers. For cell assay the aptamers were first denatured at 75°C for 5 minutes followed by immediate cooling at 4°C for 10 minutes. A buffer PBS-Mg (Final 1X) was then added to the aptamers to make a final volume of 1 mL for each sample. Initially the cells were washed thrice with 2 mL of PBS-Mg 1X. 100 nM TRITC labelled candidates was then incubated with the cells in 1 mL PBS-Mg 1X buffer at 37°C for 30 minutes. After incubation, the cells were washed thrice with 2 mL PBS-Mg 1X to remove the unbound aptamers. Finally 1 mL of PBS-Mg 1X buffer was added to the cells and it was analysed with Leica Confocal Microscope.

Dot-Blot Assay by using NC membrane:

For the evaluation of selected candidates from doped SELEX DDR1, an in vitro fluorescence assay was performed by a dot blot technique (slot format). This technique is based on a filter retention method. The candidates used for this experiment were synthesized by Eurofins with a ROX fluorophore attached at the 5' prime end. The experiment was performed in 50 μL final volume. The candidates were first denatured at 75°C for 5 minutes followed by immediate cooling at 4°C for 10 minutes. Buffer PBS-Mg 1X final was then added to the candidate solution. It was incubated with 50 nM of ECD of DDR1 in binding Buffer PBS-Mg 1X for 30 minutes at RT. The mixture was then passed by activated NC membrane filters having a pore size of 0.2 μm with continuous vacuum. The membranes were then washed ten times with 10 μL of PBS-Mg 1X buffer. The DDR1 bound candidates retained at the NC membrane along with DDR1. This NC membrane was then dried and imaged in Bio-Rad ChemiDoc MP with the laser specified for Fluorophore ROX. The image was then export in tif file and

quantified by ImageJ and fluorescence intensity was measured. All the experiments were performed in triplicate.

In vitro Fluorescence Assay by FluMag:

The in vitro fluorescence assay of m14-0 was performed by Flumag method²⁴⁵. Infact this method correlates with the Magnetic Beads based SELEX method. For this purpose, the FAM labeled m14-0 full length aptamer was synthesized and purified by Eurofins. The assay was performed in 50 μ L total volume by using Ni-NTA beads where 50 nM of HMMP14 was immobilized on 10 μ L Ni-beads in PBS-Mg 1X. The beads were washed with 10 μ L of washing buffer PBS-Mg 1X thrice before and once after the immobilization. 1 μ M of FAM labeled m14-0 was then incubated with the HMMP14 containing beads for 30 minutes at RT and the supernatant was recovered. The beads were washed with 50 μ L of PBS-Mg 1X and was then eluted in 50 μ L of DNase free water. The washing and eluted samples were also recovered. The experiment was performed in triplicate and the supernatant, washing and eluted samples were analyzed by measuring the fluorescence intensity against 1 μ M of 50 μ L FAM labeled m14-0 alone as a control. We performed the same experiment against 50 nM of histidine 6X fixed on Ni beads as a control. All experiments were performed in triplicate. The binding fractional occupancy was calculated by the Formula

$$\text{Fractional occupancy} = \left(\frac{F}{F_{50}} \right) * 100$$

Here F= Fluorescence intensity of the eluted samples while F_{50} = Fluorescence intensity of the 50 nM of F_{original} (1 μ M).

Surface Plasmon Resonance:

SPR measurements were used to analyze the binding affinity of aptamer C25 and its truncations to the target protein DDR1. The experiment was performed by using BiaCore 3000 apparatus, BiaCore AB, Sweden. For this purpose we used the NTA BiaCore sensor chip. The chip was first functionalized by coating with Nickel for coupling the histidine tagged protein on the chip. As there are 4 tracks on the surface of the chip so we immobilized histidine tagged DDR1, DDR2 and GST-H on track 2, 3 and 4 respectively while Track 1 was kept as a reference channel.

25 μ g/mL of protein was solubilized in total 50 μ L of 10 mM NaOAc with pH 6 for histidine tagged DDR1 and DDR2 while pH 5.5 for histidine tagged GST based on the pI of the proteins.

As it is suggested that the pH of the buffer should be 0.5 pH value above or below than its pI for better solubility. The proteins were injected at the rate of 5 $\mu\text{L}/\text{min}$ until nearly 1000 RU generated for each track. The immobilisation of proteins were assessed for their stability by regenerating with 20 mM NaOH at the injection rate of 5 $\mu\text{L}/\text{min}$ for 1 minute followed by washing of the track with running buffer PBS-Mg 1X for 1 minute at 5 $\mu\text{L}/\text{min}$ flow rate .

The aptamer candidates in a running buffer were injected for 1 minute at the flow rate of 5 $\mu\text{L}/\text{min}$ in all 4 tracks. Followed by every aptamer injection, 20 mM NaOH and PBS-Mg 1X (Binding Buffer) were injected at the flow rate of 5 $\mu\text{L}/\text{min}$ for 1 minute each to regenerate and wash the surface of the chip. The RU for each track was then calculated after subtracting the RU in track 1 for the evaluation of data. The resultant sensorgrams were analysed using BIAevaluation software (BIAcore AB Inc., GE Healthcare, Buckinghamshire, UK).

**Chapter-3: In vitro selection of DNA
aptamers against Discoidin Domain
Receptor-1 (DDR-1)**

Discoidin domain receptors 1 (DDR1) belongs to the family of receptors Tyrosine Kinases (RTKs) ¹⁸. The functions of DDR1 are typical to those of RTKs and includes regulation of proliferation, cell adhesion and differentiation while the activation mechanism of DDRs are different than other RTKs where DDR1 as a collagen sensor needs collagen for its activation ¹⁹ ²⁴⁶. In pathophysiological conditions, DDR1 in response to collagen starts auto phosphorylation resulting in activation of the matrix metalloproteinases responsible for the degradation of extracellular matrix leading to cell invasion and migration ⁵⁵. It has been observed that DDR1 is potentially involved in metastatic melanoma ²⁴⁷ which makes it a diagnostic and therapeutic target ²⁴⁸. DDR1 and its role in cancer has been discussed in Chapter 1.

The conventional methods like chemotherapy and radiotherapy are high effective in treating cancer, but they have limitations with high risk in killing normal cells as well ²⁴⁹. For example, metastatic melanoma harbors a mutation in the BRAF gene, with V600E being the most common mutation resulting in the activation of BRAF protein which increases the proliferation of melanoma cells ²⁵⁰. Targeted therapy with BRAF inhibitors (e.g vemurafenib) is associated with significant treatment benefit in patients with BRAF V600-mutated melanoma; however half of patients show resistance after six months of treatment ²⁵¹. Early cancer detection increases cancer treatment and survival rate. Aptamers thus provide an earlier and more sensitive cancer detection due to its high specificity against the target ²⁵² ⁶⁶.

Aptamers are selected against its target by SELEX ²⁵³ ⁹⁶. In this chapter we will discuss about selection of aptamers against DRR1 through different SELEX methods. In DDR1 SELEX, two SELEXs from different ssDNA libraries will be discussed which were performed against the histidine tagged extracellular domain of DDR1 recombinant protein receptor, as this extracellular region is involved in collagen binding ³⁷. An aptamer against DDR1 extracellular domain was selected in both SELEX.

1) Selection of DNA aptamer against DDR1 with naive ssDNA library:

SELEX Library:

SELEX was performed with LibraryA containing 30 nucleotide random window flanked with primers P5 (forward) and P3 (reverse) as mentioned in table 2.1. This naïve ssDNA library has approximately 4^{30} ($\cong 10^{18}$ diversity) random oligonucleotide sequences. The reason to perform a SELEX based on ssDNA library is the stability of DNA as compared to RNA. Since

we were interested in aptamers as theranostics agent, the stability of DNA aptamer in serum is higher (30-60 minutes) as compared to RNA aptamer (few seconds) ²⁵⁴.

SELEX:

Since 1990, different SELEX methods have been described in the literature. Two SELEX methods i.e. Magnetic beads based SELEX and Filtration SELEX were performed to select an aptamer against the extracellular domain of Discoidin domain receptor (DDR1). Total 6 rounds of SELEX were performed against the extracellular domain of DDR1 with the conditions described in Table 3.1. The first 4 rounds were based on magnetic beads based SELEX while the last 2 rounds were based on filtration SELEX. Although it is a bet to prefer one SELEX method on another, we hereby focused on selecting aptamers against DDR1 immobilized on solid support (Ni beads) as well as in solution form to avoid support-effect evolution.

Counter selection in SELEX was performed to discard the sequences of non-interest by incubating the SELEX pool with negative proteins. In the SELEX performed against the extracellular domain of DDR1, we introduced a counter selection step with histidine tagged GST and DDR2 proteins. The reason to perform a counter selection with DDR2 is to select an aptamer specific to DDR1, since DDR2 has a sequence homology with DDR1 ²⁵⁵. As mentioned earlier in chapter 1 that DDR1 and DDR2 share high degree of sequence homology in their DS and DS- like domains with 59 and 51% of similarity, respectively ²⁵⁶. The DS and DS like domains are the main domains of the extracellular region which is responsible for ligand binding.

Counter selection against histidine tagged GST was also performed to discard sequences which could bind to such tags. As it is demonstrated in the literature that an aptamer can bind to such tags with an affinity in pM ²⁵⁷. Counter selection against nitrocellulose membrane was also performed during filtration SELEX rounds to discard all sequences bound to nitrocellulose membrane.

For selection, 10 pmoles of DDR1 extracellular domain was used in initial round against 300 pmoles of ssDNA candidate (diversity of 10^{14} sequences) with a ratio of 1:30. Since proteins can have more than one aptatope where each aptamer can bind through conformational changes, such ratio will create a competition between sequences to bind to the aptatope on protein. As the SELEX proceeded the ratio was increased up to 1:40 so only sequences with high affinity can bind to the target. Meanwhile the concentration of the protein and sequences

were also decreased to select candidates with better Kd. The decrease in concentration by dilution is expected to be more efficient than increasing the ratio. After selection, the number and volume of washing was also increased as the round proceeded in order to remove low affinity binders. The detail about the DDR1 SELEX performed has been given in the table 3.1.

Round	Counter Selection	Selection DDR1	Library ssDNA	Ratio DDR1: ssDNA	Washing PBS-Mg (1X)	Polymerases for PCR
1	Magnetic Beads SELEX 1*GST-H 500 nM	100 nM	3.0 μ M	1 :30	1*100 μ L	Gold Taq Pol
2	Magnetic Beads SELEX 1*GST-H 500 nM 1*DDR2-H 50 nM	100 nM	3.0 μ M	1 :30	1*100 μ L	Go Taq Pol
3	Magnetic Beads SELEX 2*GST-H 1 μ M 1*DDR2-H 50 nM	75 nM	3.0 μ M	1 :30	5*100 μ L	Go Taq Pol
4	Magnetic Beads SELEX 2*GST-H 1 μ M 1*DDR2-H 50 nM	70 nM	3.0 μ M	1 :40	10*100 μ L	Go Taq Pol
5	Filtration SELEX 1*NC Membrane 1*GST-H 1 μ M	70 nM	2.8 μ M	1 :40	1*1 mL	Phusion Pol
6	Filtration SELEX 1*NC Membrane 1*GST-H 1 μ M 1*DDR2-H 50 nM	50 nM	2.8 μ M	1 :40	5*1 mL	Phusion Pol

Table 3.1: Selection conditions applied for SELEX against DDR1.

High throughput sequence (HTS) analysis:

After performing 6 rounds of SELEX, we analyzed the SELEX by HTS analysis of starting library (R0), Round 3 (R3), Round 4 (R4), Round 5 (R5) and Round 6 (R6). An evolution was observed as the rounds of SELEX proceeded. The diversity of the pool was decreased to 90% in round 6. Sequences were distributed into clusters with the Levenstein distance of 7 base. Sequences were analyzed based on their presence in the pool as reads per million (RPM). Sequences with less than 30 rpm were discarded. Based on the exponential evolution profile, 8 sequences were selected. All these selected candidates were the representative sequence of their clusters (Figure 3.2).

Name	Sequences	Cluster No	R0	R3	R4	R5	R6
C25	TAGAGTGGGTGTACATTATCTGTACTACT	1	6.13	0	1.26	21.41	1155.03
C25.2	TTGACGTGTGTGTACATCTTTGTATCTACG	2	2.04	0	2.52	5.84	651.64
C28	CCTGTTGGTGCCTGTGGTAGTCTATAGGGC	3	8.17	1.79	3.78	21.41	500.31
C210	ACCCATCAGCAGGGACTACCCCATGGCAGG	4	2.04	0.89	11.35	16.54	280.01
C211	TAGCGTGTGACCAAGTTTTGGTTATGACTT	5	0	0	0	4.86	149.27
C212	AGCCGTTGCGTACTTGTCTTCCATGACGGA	6	0	0	1.26	0.97	132.8
C213	AACGCGGGTGTGCCTCTGTGCAACTACTT	7	0	0	0	1.95	101.91
C215	GCTGTGCGGGTTGGATACTTCCATGACT	9	0	0	0	2.92	73.09

Table 3.2: NGS analysis of SELEX against DDR1. The number of selected sequences as reads per million has shown in starting library (R0), R3, R4, R5 and R6. Sequences shown in the table are the representative sequences with higher RPM from different clusters. These 8 sequences were selected as candidates for further characterization.

All the selected sequences were 29 or 30 nucleotide long as we already discussed that the length can vary due to errors induced by the polymerase during PCR. We further aligned these sequences with reference to the sequence with highest rpm (C25), where we identified conserved motifs that occurred in every sequence in combination with each other as described in figure 3.1.

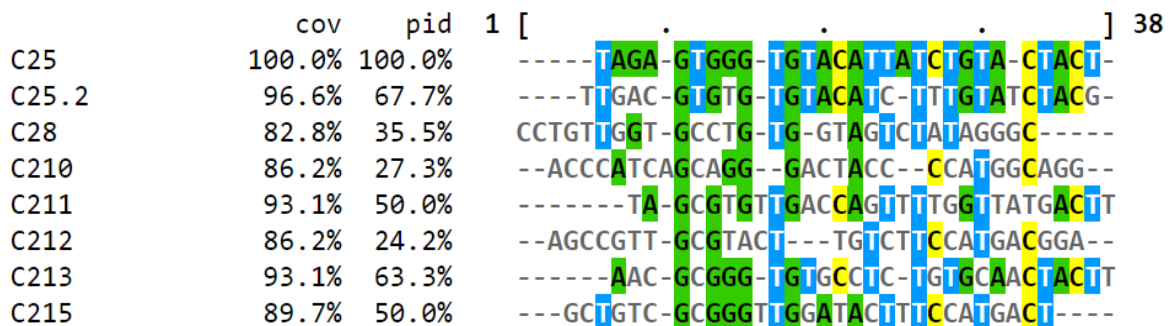
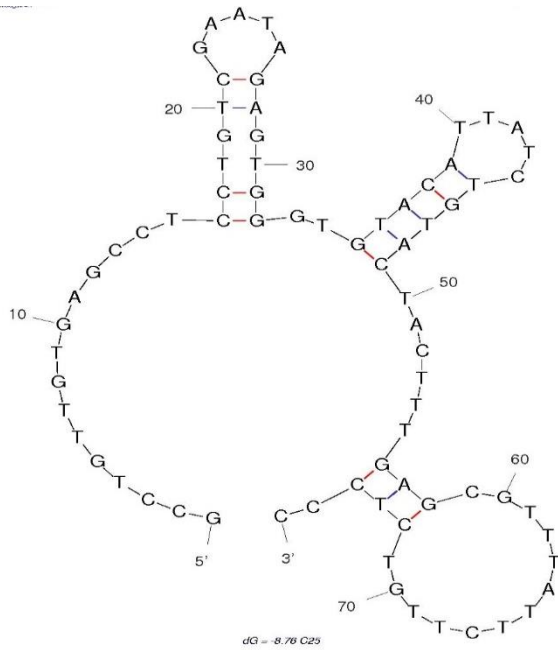


Figure 3.1: Alignment of selected sequences from DDR1 SELEX. Sequences were aligned by using ClustalW. The alignment of sequences are given with cov % (percentage of positions covered by motif) and PID (percentage identity) with reference to C25 aptamer. Different conserved motifs identified in all sequences are indicated in the background colours.

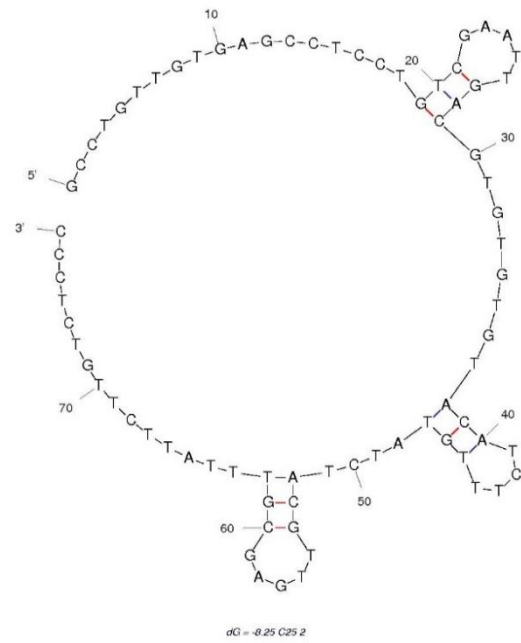
Structural prediction of selected candidates by mfold:

Structure of the selected candidates were predicted using mfold. Structures were folded by mfold given the conditions of folding temperature at 20°C with 1M conc. of Na⁺ and 1mM conc. of Mg⁺⁺ respectively which corresponded to the folding of candidates in selection buffer

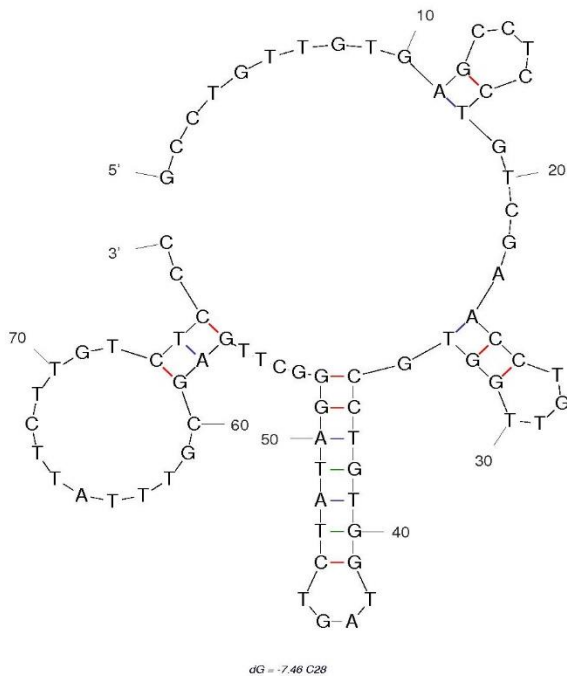
at RT while performing SELEX. mfold predicted structures reveals that primers are also highly involved in structure formation (Figure 3.2) .



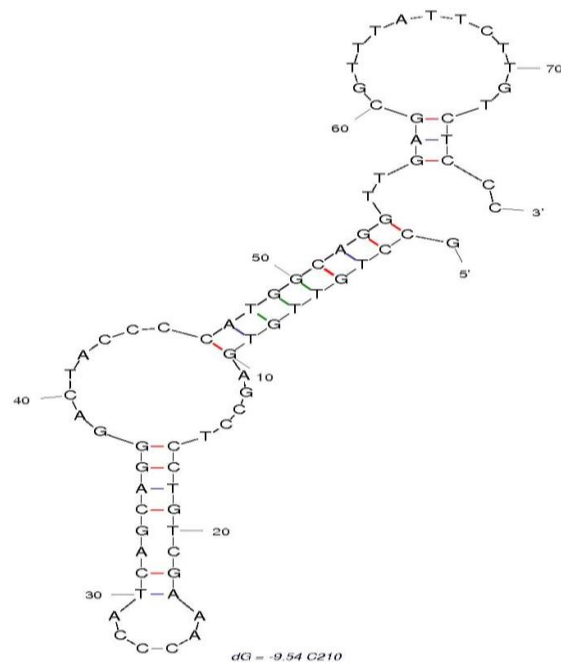
C25 $\Delta G = -8.76$



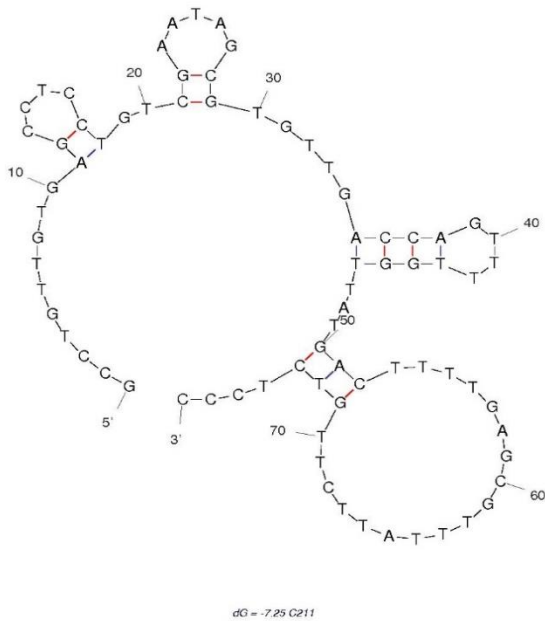
C25.2 $\Delta G = -8.25$



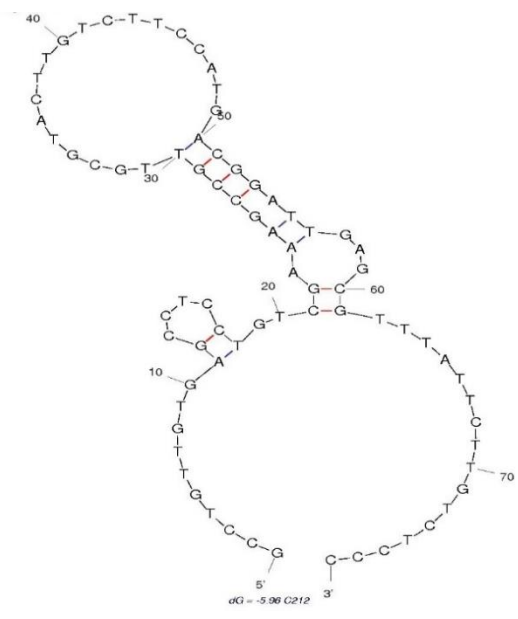
C28 $\Delta G = -7.46$



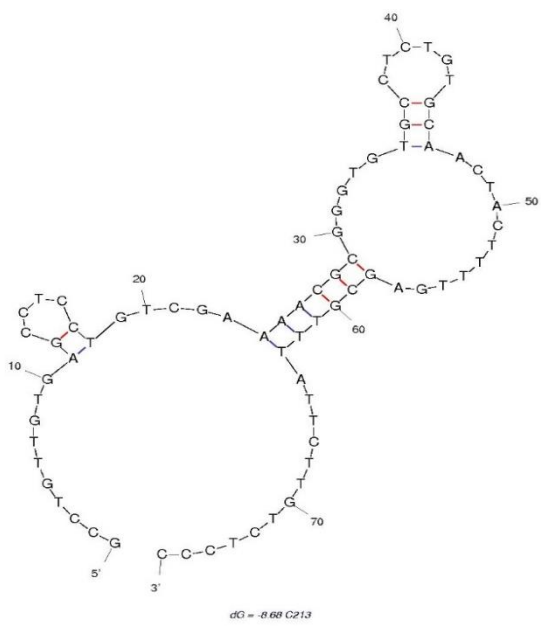
C210 $\Delta G = -9.54$



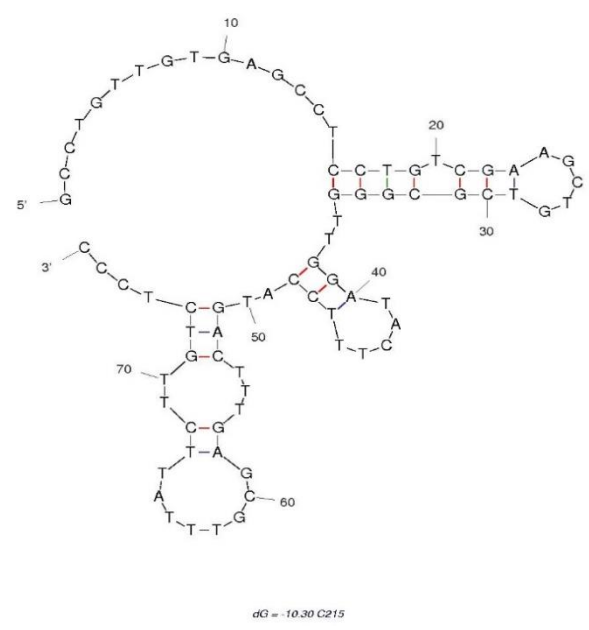
C211 $\Delta G = -7.25$



C212 $\Delta G = -5.96$



C213 $\Delta G = -8.68$



C215 $\Delta G = -10.30$

Figure 3.2: mfold predicted secondary structures of SELEX-DDR1 candidates. mfold predicted structures of selected candidates from DDR1 SELEX. The structures are shown with the forward and reverse primers.

In vitro Fluorescence Assay of Selected Sequences:

The selected candidates from DDR1 SELEX1 were further analyzed by in vitro fluorescence assay. The experimental procedure has been discussed in Chapter 2. As the candidates were

labeled with FAM at 5' prime, the fluorescence intensity at $\lambda= 515\text{nm}$ was considered to calculate the binding percentage of candidates against DDR1 protein (Figure 3.3). The experiment was performed in triplicate. This experiment reveals that candidate C25 has a higher binding percentage as compared to other candidates.

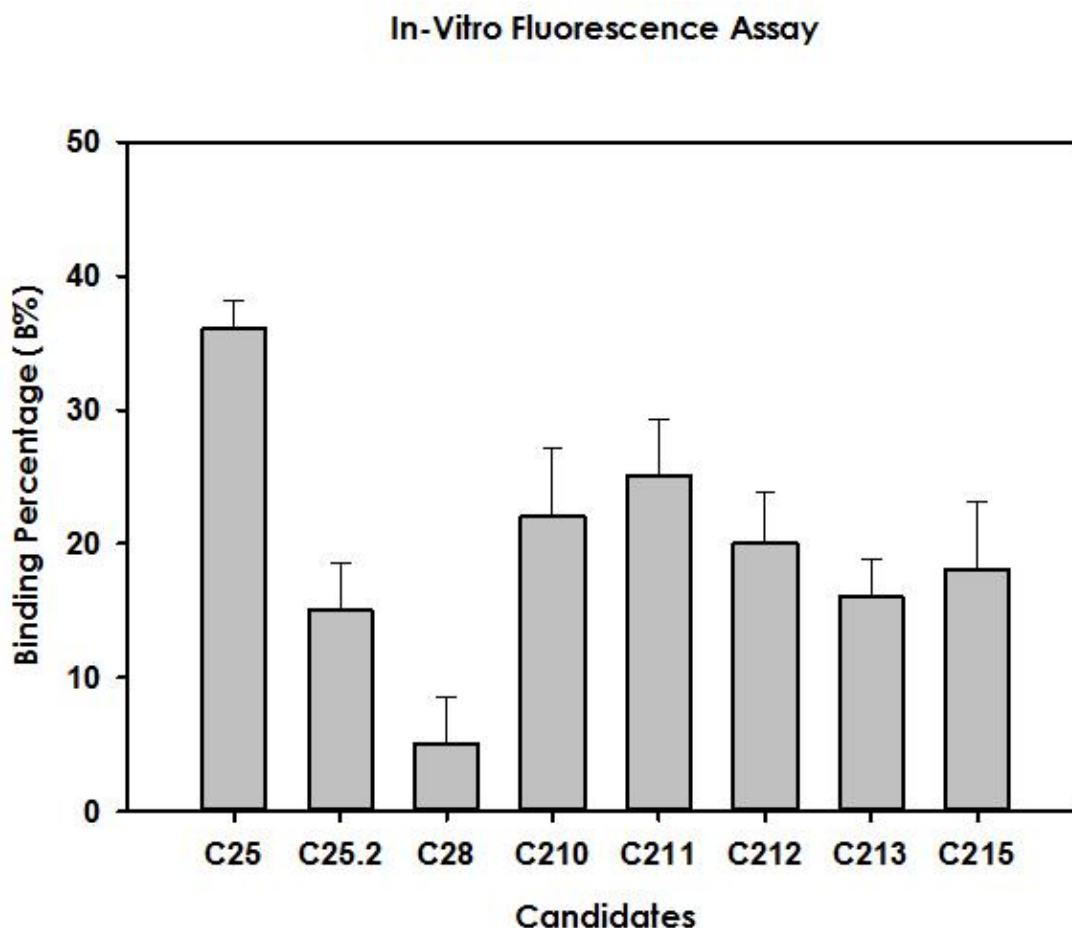


Figure 3.3: Binding percentage of selected candidates against DDR1. The binding percentage of 8 selected candidates (1nM) against DDR1 (50nM) was calculated by the formula $B\% = (1 - (F/F_0)) * 100$. “F” is the fluorescence intensity of unbound portion of candidates while “F₀” corresponds to the original fluorescence intensity of 1nM candidates. All experiments were performed in triplicate.

In vitro fluorescence Assay of Aptamer C25:

The binding specificity of C25 was analyzed with an in vitro fluorescence assay as discussed earlier. For this purpose 1 nM of FAM labelled C25 was used against 50 nM of DDR1, DDR2 and GST. All the experiments were performed in triplicate. As shown in the figure 3.4, C25 aptamer specifically binds to DDR1 while there is almost no binding with DDR2 and GST proteins.

In-Vitro Fluorescence Assay

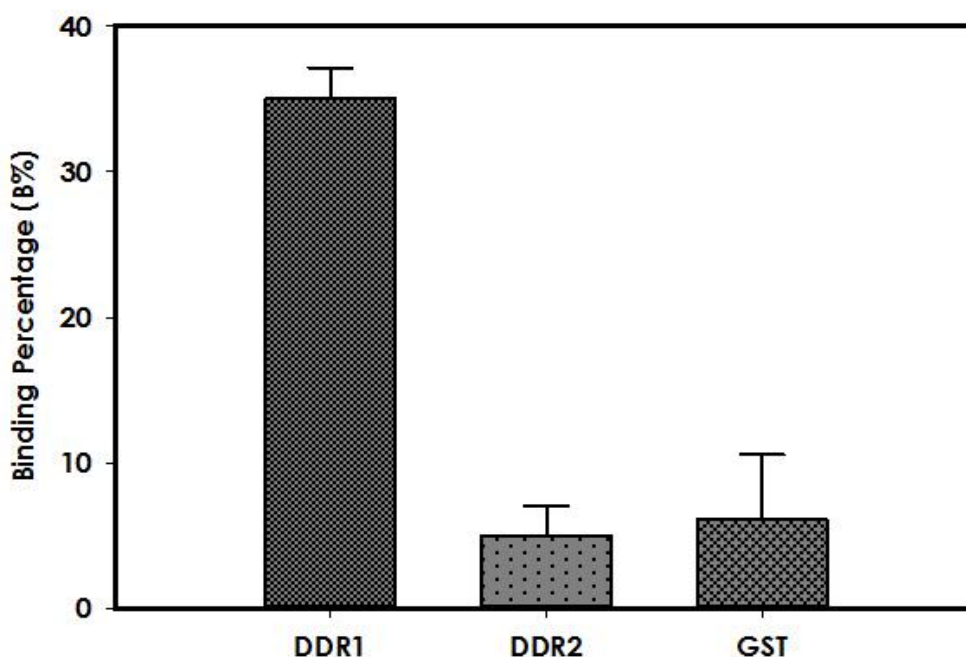


Figure 3.4: In vitro fluorescence assay of aptamer C25 against different proteins. The binding percentage of C25 (1nM) against 50nM of DDR1, DDR2 and GST was calculated by $B\% = (1 - (F/F_0)) * 100$. “F” is the fluorescence intensity of unbound portion of C25-FAM while “F₀” corresponds to the original fluorescence intensity of 1nM C25-FAM. All experiments were performed in triplicate.

As in this in vitro assay, the DDR1 had only 50 fold excess in terms of concentration as compared to C25. The detection limitation of the fluorimeter was 1nM, so we decided to perform qPCR analysis to evaluate the binding at low concentration of C25 aptamer (50 pM) against the protein 50 nM. Since proteins are usually aggregate at higher concentrations so we did not increase the concentration of protein.

qPCR Analysis of Aptamer C25:

Quantitative PCR (qPCR) has been used in the selection and characterization of aptamers^{100 258}. Real time PCR was performed to validate the binding capacity of C25 against its target. For this purpose 50 pM of C25 aptamer was incubated with 50 nM of Protein. The experimental procedure has been described in chapter 2. In parallel to the analysis of C25 binding specificity, qPCR calibration curve was constructed. As shown in Figure 3.5-A, a linear range of 5 orders of magnitudes (10^6 , 10^7 , 10^8 , 10^9 and 10^{10} sequences) was achieved for aptamer C25 with a correlation efficient “R²” of 0.9897. The minimum quantity of aptamer C25 template detected was in the attomolar range i.e. 1.66×10^{-18} moles, which describes the high efficiency of the

real time PCR. The slope of the calibration graph is 3.69 which means that decrease in 10 fold concentration of the aptamer results in increase of Ct value of 3.69. This slope is higher than the standard slope i.e 3.32. This difference in the slope may be due to the melting temperature (T_m) of the primers. As the forward primer 5'-GCC TGT TGT GAG CCT CCT GTC GAA-3' (T_m= 65-70) contains more GC in comparison to the reverse primer 5'- GGG AGA CAA GAA TAA ACG CTC AA-3' (T_m= 55-60). This problem can be solved by lowering the GC content of forward primer since primers with T_m around 55-60 are highly recommended for PCR. The melting curve analysis was performed from 72°C to 95°C with a rising of 1 degree celsius in each step. Here we observed that at higher temperature the primers started forming dimers as well. The dimerization of primers can be avoided by optimizing the temperature. Using this calibration curve, the amount of unbound fraction of C25 aptamer was quantified by interpolating the average Ct value.

The number of sequences were calculated by the polynomial linear formula

$f = y_0 + a * x$, where $y_0 = 39.4660$ and $a = -3.6970$. All the experiments were performed in triplicate and the average value of Ct was considered. According to this average Ct value, the number of sequences presented in each sample was determined with the formula given above. The binding percentage of C25 aptamer against DDR1 and DDR2 was determined according to the number of sequences presented in each sample against the total number of sequence presented in the control pool.

The binding percentage against DDR1 had increased as compared to the previous experiment (Figure 3.5-B vs. Figure 3.4). Even C25 aptamers shows some binding to DDR2. It can be assumed that in qPCR analysis the concentration of DDRs are 1000 fold excess so there might be some binding with DDR2 which shares 60 percent sequence homology with DDR1 as discussed in chapter 1.

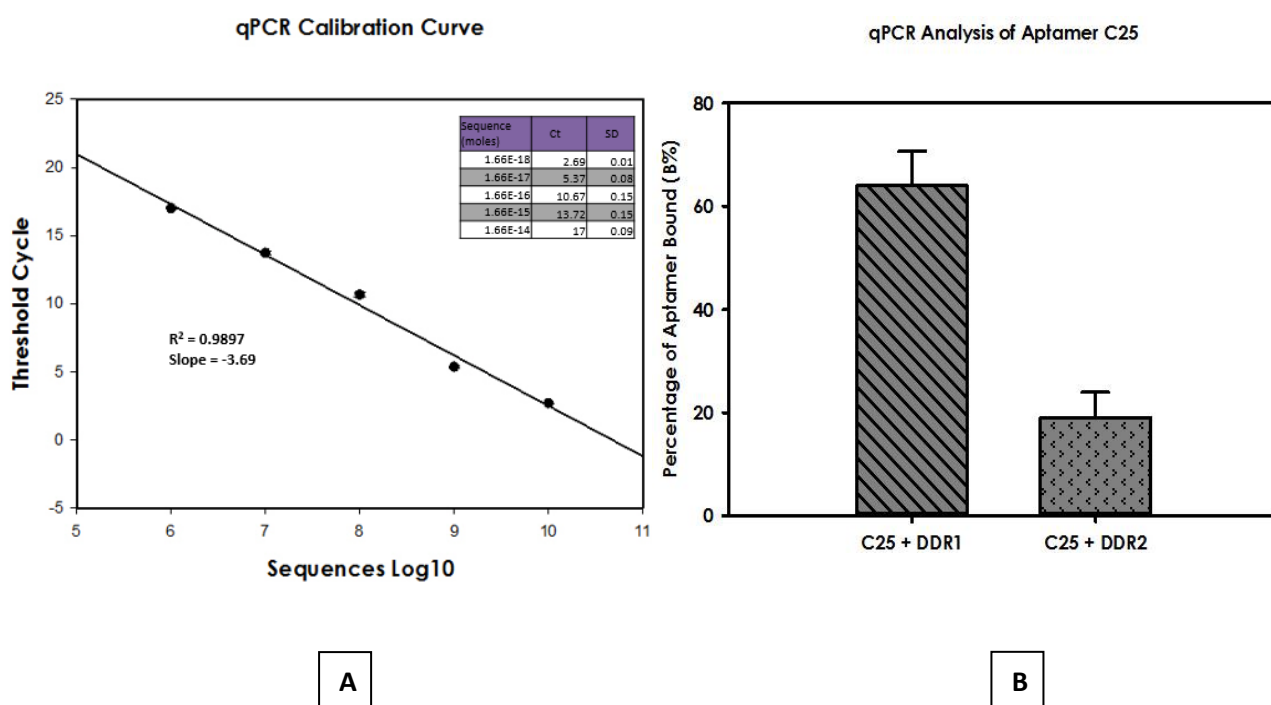


Figure 3.5: qPCR analysis of C25 aptamer. **A**= Standard qPCR calibration curve with 5 serial dilutions of 10^6 , 10^7 , 10^8 , 10^9 and 10^{10} sequences of C25 Aptamer. **B**= Binding percentage of aptamer C25 calculated against DDR1 and DDR2. The experiments were performed with 50pM of C25-FAM against 50nM of DDR1 in PBS-Mg 1X buffer as discussed in chapter 2. All experiments were performed in triplicate.

Aptamer C25 truncation based on mfold predicted structure:

Two structures C25a and C25b were predicted by mfold with ΔG of -8.76 and -8.02 respectively for full length C25. As shown in figure 3.6, the mfold structures of the full length C25 aptamer predict that a part of the primer 5' is involved in the loop formation. Therefore, we truncated this aptamer into two versions as C25_t1 and C25_t2 based on the structural prediction of C25a and C25b respectively. C25_t1 is a 36 nucleotide base long sequence which contains 10 bases of primer at its 5', while C25_t2 is a 38 nucleotide base long sequence with 12 bases of primer at its 5'.

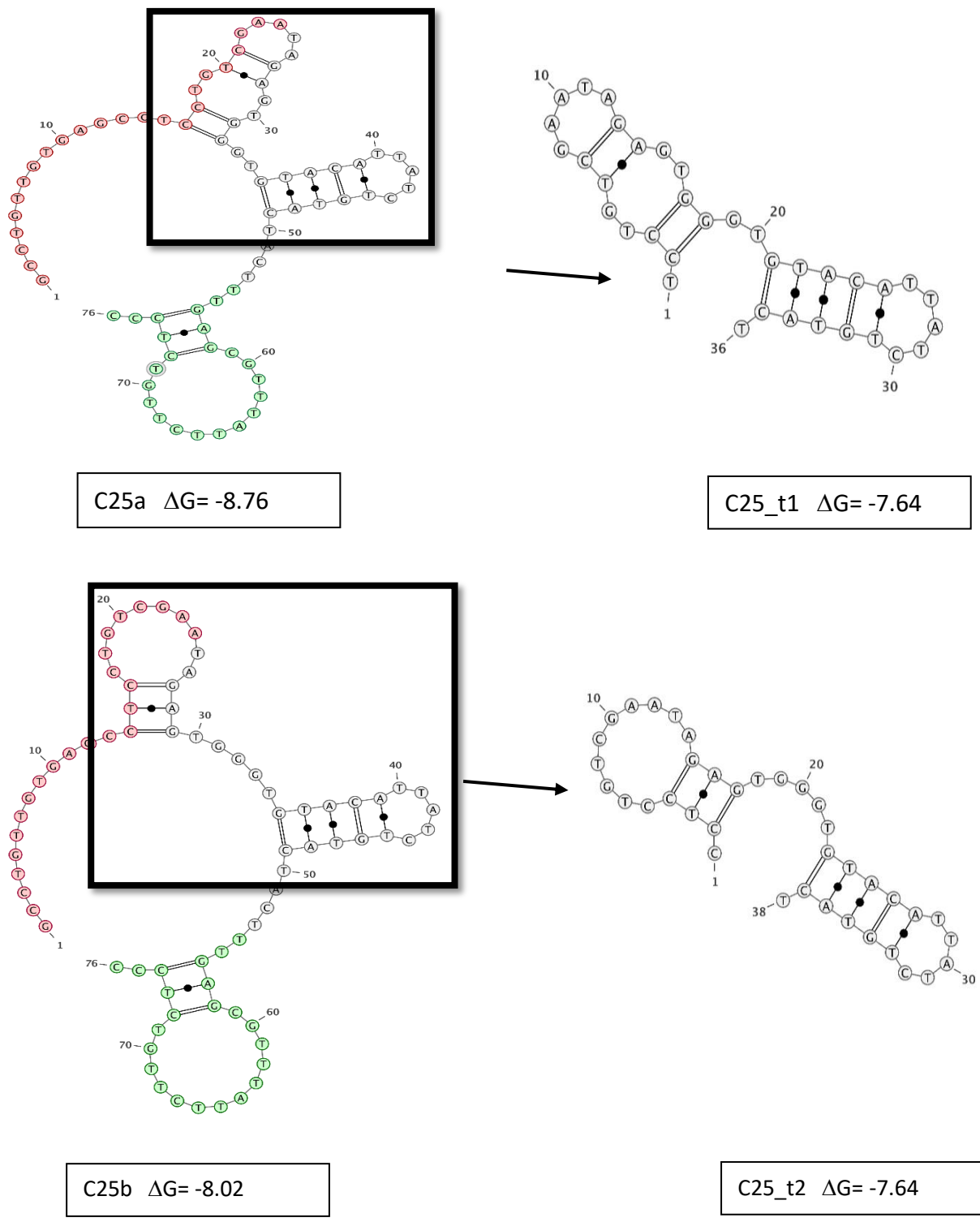


Figure 3.6: mfold predicted structures of C25. mfold predicted structures C25a and C25b of aptamer C25 are given. The full length C25 aptamer consists of random window (colourless) forward primer (light pink) and reverse primer (light green). A part of the forward primer is involved in loop formation. Based on these two structures C25 aptamer was further truncated into C25_t1 and C25_t2.

Surface Plasmon Resonance (SPR) analysis of C25 and truncations:

The specificity of Aptamer C25 and its truncations were determined against 6x-histidine tagged DDR1 target by Surface Plasmon Resonance. 6x histidine tagged DDR2 and GST were used as a negative protein. Aptamer C25 and truncations in PBS-Mg1X were injected later to flow through the chip against histidine tagged proteins immobilized on Ni coated chip as discussed in chapter 2.

Initially 1 μ M of aptamers C25, C25_t1 and C25_t2 were injected but the binding responses were not significant at 1 μ M (data not shown). Aptamers of 10 μ M conc. were then injected. Although the general response was low, but aptamer C25 (full length) and its truncated version C25_t2 showed a significant response against DDR1 target as compared to other negative proteins shown in Figure 3.7. It seems that the truncated C25_t2 is more specific to DDR1, while there was no response observed for C25_t1 (data not shown).

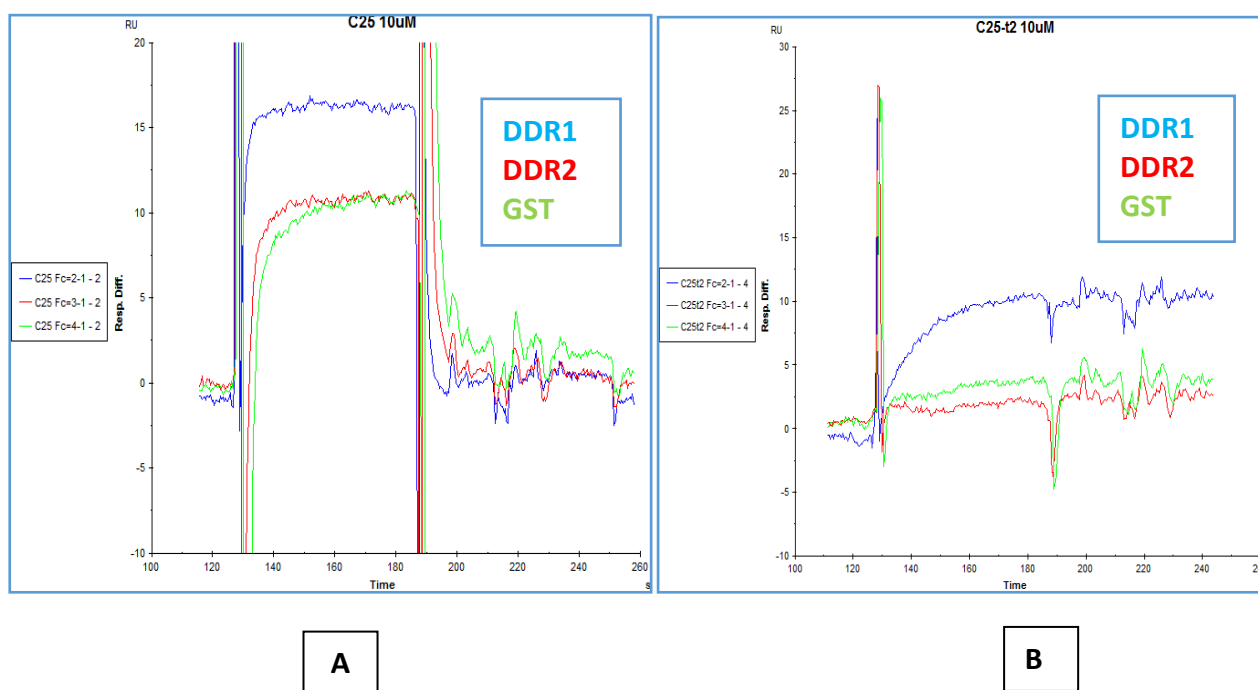


Figure 3.7: SPR analysis of C25 full length aptamer and truncations. **A**= Evaluation of Full length C25 at 10 μ M concentration **B**= Evaluation of Full length C25_t2 at 10 μ M concentration. In this analysis aptamer binding was characterized against target DDR1 (blue signal), DDR2 (RED signal) and GST (green signal). The RU was generated after deducting the signal from track 1 which was used as a reference.

In conclusion, SPR method was used to analyse the binding kinetics of Aptamer C25 and its truncations. Although this method supports the results from other in vitro experiments discussed earlier, a meaningful contribution to the analysis could not be made by the BiaCore data as the response units (RU) were not that much significant. We can hypothesize that since the target protein DDR1 protein consisted of 409 amino acids with a predicted mass of 45.7 kDa as an extracellular domain of the receptor, there may be changes in conformation of the extracellular domain of the recombinant protein after coupling on Ni coated chips. These conformational changes may not match to that of the fully expressed surface receptor extracellular domain, as DDRs are present in a dimeric form on the surface of cells.

Another assumption is that the aptatope of the DDR1 might not be available free to bind with aptamer due to fixation of protein on Ni coated chips. An alternative method for SPR is the fixation of the aptamer candidates on the sensor chip and flow of the protein through the tracks ²⁴⁵. For this purpose, aptamers biotinylated at 5' end are immobilized on the streptavidin coated sensor chip while the protein is passed through the tracks to analyse the binding.

Discussion:

The goal of this work was to select an aptamer as a theranostics agents against DDR1. For this purpose, a hybrid of Magnetic beads SELEX and Filtration SELEX was performed targeting the extracellular domain of DDR1 as a bait. The SELEX was initiated with a pool of ssDNA library having a diversity of 10^{14} sequences. In Magnetic Beads SELEX, the histidine tagged extracellular domain of DDR1 was immobilized on Ni-NTA Agarose beads providing a selection based on solid support. While filtration SELEX was based on a selection in solution form which was then passed through the nitrocellulose membrane to separate the binders from the non-binders. In order to select an aptamer against DDR1, heavy counter selection and washing steps were also introduced during the SELEX process to increase the stringency resulting in faster evolution. After 6 rounds of selection, the SELEX was evaluated by high throughput sequencing. 8 candidates were selected which showed higher evolution during the SELEX as compared to other evolved sequences. The candidates were evaluated against DDR1 by in vitro fluorescence assay. Aptamer C25 was selected among the candidates as it showed higher binding as compared to others.

Aptamer C25 was further characterized by in vitro experiments. The binding specificity of C25 was determined by in vitro fluorescence assay and real-time PCR. These experiments demonstrated that C25 binds to DDR1 more specifically. The structural characterization of C25

by mfold predicted the structural conformation of C25. It was further truncated into two versions which are 36 nucleotide C25_t1 and 38 nucleotide C25_t2. An SPR analysis was further performed in order to validate the binding capacity of C25 and its truncated versions. Although the results from SPR were not so promising but the data demonstrates that C25 and C25_t2 bind to target DDR1 as compared to negative targets DDR2 and GST.

In addition, an in vitro fluorescence assay was performed to determine the K_d of full length C25 with FAM labeled at its 5' prime. The K_d was estimated around 500nM for C25 (data not shown). Since the binding affinity of C25 and C25_t2 are not as high as expected or required for cell imaging, we decided to further proceed the SELEX with the doped library of C25.

2) Selection of DNA aptamer against DDR1 by DOPED SELEX:

Doped SELEX is usually performed post-selection using a well-characterized in vitro selected nucleic acid structure that is mutagenized as a starting pool subjected to a reselection²⁵⁹. Identification of better variant molecules using a doped library of aptamers or ribozymes after a few rounds of in vitro selection have been successfully demonstrated^{169 259 260}. For the first time, Duconge and colleagues have beautifully explained the mutational landscape from the doped SELEX by high throughput analysis based time-lapse imaging of molecular evolution¹²². The analysis was performed by using a partial doped library of an aptamer ACE4 which was previously selected against Annexin A2 using Cell SELEX²⁶¹. An additional 4 rounds of Cell SELEX was performed with the library based on ACE4 aptamer doped at a rate of 7.5% with an equal mixture of all three other bases in the random window. ACE4 represented only 1.8% of the starting doped library, whereas most of the library contained ACE4 variants with one, two, or three mutations.

For a doped SELEX against DDR1, we synthesized a partially randomized DNA library based on the sequence of the C25 random window 5'-TAG AGT GGG TGT ACA TTA TCT GTA CTA CT-3'. Each position in the random window of the doped library contained 76% of the initial base and 8 % of other three bases. The primers used were similar as C25 aptamer. The percentage of doped was enough to generate a library of 10¹⁵ diversity as this doped library contains theoretically only 0.026 percent of the original sequence.

Before performing the SELEX, NGS analysis of the doped library was performed to validate the percentage of mutations. The distribution of bases at each position was according to the theoretical value (Figure 3.8). The sample for HTS sequencing was prepared according to the protocol suggested by CEA sequencing platform as described in chapter 2.

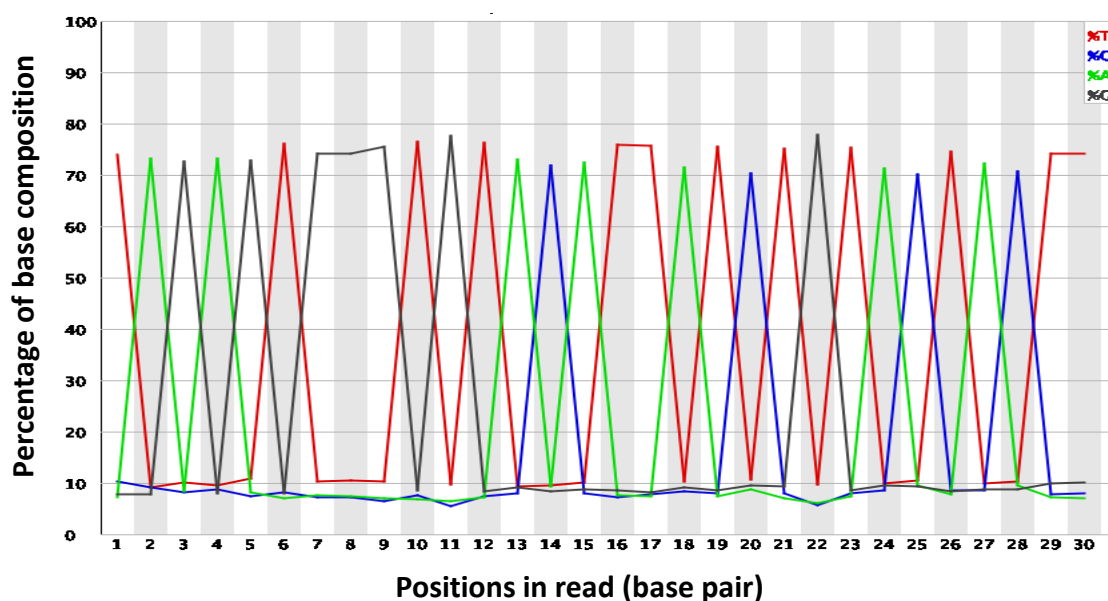


Figure 3.8: NGS analysis of base composition in the doped SELEX library. The NGS analysis confirms that in a doped library based on C25 random window 5'-TAG AGT GGG TGT ACA TTA TCT GTA CTA CT-3', the percentage of original bases are around 75% with mutations of other 3 bases at 8% each.

SELEX:

Total 5 rounds of selection was performed with the doped library against the extracellular domain of DDR1 receptor. The SELEX was started with 200 pmoles of ssDNA library against 5 pmoles of extracellular domain of DDR1 in the initial round with a ratio of 1:40. The ratio between ssDNA library and DDR1 concentration was kept similar throughout the SELEX, while the conc. was decreased in order to select aptamers with better K_d as discussed in table 3.3.

The selection was based on filtration SELEX, where nitrocellulose membrane was used for the separation of interested and non-interested sequences. In the previous SELEX against DDR1, the rate of evolution in terms of exponential enrichment seemed higher in the last two

rounds performed by filtration SELEX. As in filtration SELEX, the selection was performed in solution form which might favored the selection of aptamers against DDR1. With this assumption, we decided to proceed the SELEX with doped library by filtration SELEX method.

Round	Counter Selection	Selection DDR1	Library ssDNA	Ratio DDR1 : ssDNA	Washing PBS-Mg (1X)	Polymerases for PCR
7	1*NC Membrane 1*DDR2-H 50 nM	50 nM	2.0 μ M	1 :40	5*1 mL	Phusion Pol
8	1*GST-H 500 nM 1*DDR2-H 60 nM	25 nM	1.0 μ M	1 :40	6*1 mL	Phusion Pol
9	1*GST-H 1 μ M 1*DDR2-H 60 nM	10 nM	0.4 μ M	1 :40	7*1 mL	Phusion Pol
10	1*GST-H 1 μ M 1*DDR2-H 80 nM	7.5 nM	0.3 μ M	1 :40	8*1 mL	Phusion Pol
11	1*GST-H 1 μ M 1*DDR2-H 100 nM	5 nM	0.2 μ M	1 :40	10*1 mL	Phusion Pol

Table 3.3: Selection conditions applied for doped SELEX against DDR1.

To avoid the selection of aptamers against nitrocellulose membrane, in the first round we performed counter selection against only nitrocellulose membrane. We also performed a counter selection with DDR2 and GST proteins to discard sequences of non-interest. The concentration of negative proteins and the number of washings were also increased to make the SELEX more stringent. For amplification, high fidelity Phusion polymerase was used to avoid the incorporation of mutations, as the error rate of Phusion (4×10^{-7}) is 50X less than Taq polymerases ($1-20 \times 10^{-5}$)^{262 263}. As we were interested in selecting variants of C25 aptamer drawn by the SELEX itself, so we avoided mutations resulted from the biasness of low fidelity polymerases. The detail about this SELEX is mentioned in table 3.3.

High Throughput Sequencing of DOPED SELEX:

After performing further 5 rounds as a doped SELEX, we analysed all rounds with NGS sequencing. Sequences were distributed into clusters with the Levenstein distance of 7 base. It has been observed that within the clusters which were based on Levenstein distance of 7, usually

sequences were present with an edit distance of 1 or 2. It can be hypothesized that in the pool, the subpopulations are present with either higher distant (resulting in cluster formation) or low distant (present in same cluster). Sequences were analyzed based on their presence in the pool as reads per million (RPM). Sequences with less than 30 rpm were discarded. The sequences were evaluated on the basis of their presence in the pool as reads per million (RPM).

Rounds	No. Of Clusters	No. of Sequences to cluster
Library	2	83
R07	2	237
R08	8	40
R09	9	60
R10	233	378
R11	1046	2480

Table 3.4: No. of clusters and clusters sequences in each round of doped SELEX

More than thousand clusters were appeared in last round as compared to the library where only 2 clusters were present (Table 3.4). The high number of cluster formation describes the evolution of the pool during SELEX. The presence of the sequences were ranked based on reads per million (RPM). Sequence with highest RPM in the cluster was considered as the representative of the cluster. The data from NGS result analysis showed an evolution as the round proceeded but the diversity of the pool is not much decreased (Figure 3.9). As in conventional SELEX methods, the rate of decrease in the diversity of the library is slow.

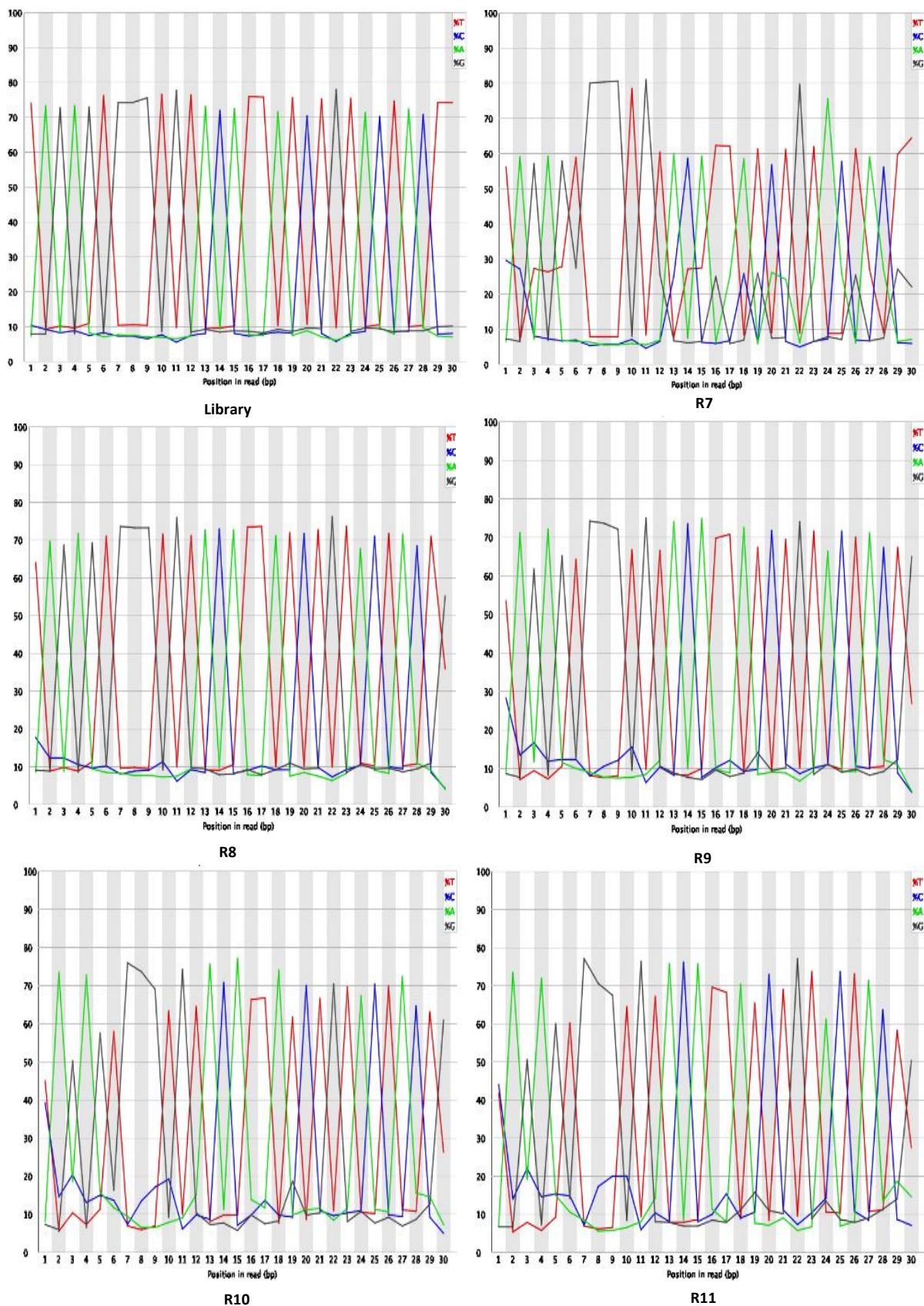


Figure 3.9: NGS data based comparison of rounds of Doped SELEX against DDR1. Sequence content across all bases Adenine (green), Guanine (brown), Thymine (red) and Cytosine (blue) in the random window of doped Library, Round 7, Round 8, Round 9, Round 10 and Round 11 of doped SELEX analysed by NGS sequencing.

Based on the exponential evolution profile, 8 sequences were selected. All these selected candidates were the representative sequence of their respective cluster (Table 3.5). Surprisingly C25, which was 0.026 percent of the initial doped library was not enriched again during the SELEX. Instead the RPM of C25 had decreased as the round proceeded. We can therefore predict that performing SELEX in more stringent selection conditions favoured the selection of high affinity binders ²⁶⁴. Ten most abundant sequences were selected for evaluation.

Candidates	Sequence	Library	R08	R09	R10	R11
DS_2.1	CCTTTGGGGTGGCTTGACGAAGAAAGTAG	681.88	1554.9	4273.7	14317	2071.9
DS_3.1	CAACCGAACAAACAGCACTGGGCTACAACAG	0	17.24	79.51	361.14	662.09
DS_6.1	CCAACGGCTGATCACTATCTGTACATCG	0	1.44	8.56	60.44	347.55
DS_7.1	TAGACCGGGCGAACATCAGGTGTACTACA	0	1.44	4.89	69.51	203.16
DS_8,2	CATACTGGCGGTAATGCATCCGTACAACA	0	1.44	3.67	46.84	190.79
DS_10.1	CATACGGCCATCGTACGTTGCCCTTCCCCG	0	1.44	7.34	10.58	190.79
DS_11.2	CAACGTGGCTGACCATTTGCTGTACTGCG	0	1.44	9.79	10.58	162.94
DS_12.1	CACGGCTATCCAACGACTCTCCACCATCCA	0	1.44	9.79	68	158.82
DS_32.1	TCAACAGCGTGTACGTTATCTGTCTATG	0	0	3.67	4.53	105.19
DS_34.1	CAAAGGCGGTGGAGACCATGCGTGTTACT	0	0	4.89	12.09	103.13
C25	TAGAGTGGGTGTACATTATCTGTACTACT	295.23	125.02	66.05	10.58	24.75

Table 3.5: NGS analysis of Doped SELEX against DDR1. Ten most abundant sequences are shown with their RPM in Doped starting Library, R8, R9, R10 and R11. The RPM of C25 aptamer has decreased as the SELEX proceeded.

All the selected sequences were 29 or 30 nucleotide long. On alignment of these sequences with reference to C25, we identified conserved motifs that occurred in combination with each other for all sequences except DS_2.1 as described in figure 3.10. Sequences DS_2.1 and DS_3.1 being highly evolved candidates share less homology to C25 as compare to other evolved candidates.

	cov	pid	1 [. . .] 36
C25	100.0%	100.0%	TAGAG-TGGGTGTACATTA--TCTGTACTACTI----
DS_2.1	93.1%	12.9%	CCTTTGGGGTGGCTTGACG----AAGAAAGTAG---
DS_3.1	93.1%	25.0%	CAACC-GAACAACA--GC ACTGGGCTACAACAG---
DS_6.1	100.0%	62.1%	CCAAC-TGGCTGATCACTA--TCTGTACATCG----
DS_7.1	100.0%	72.4%	TAGAC-CGGGCGAACATCA--GGTGTACTACA----
DS_8.2	93.1%	45.2%	CATAC-TGGCGGTAATGCATCCG--TACAACA----
DS_10.1	96.6%	29.0%	CATAC--GGCCATCGTACGTTGCCCTTCCCCG----
DS_11.1	96.6%	62.1%	-CAACGTGGCTGACCATTI--GCTGTACTGCG----
DS_12.1	89.7%	38.7%	--CAC--GGCTATCCAACG--ACTCTCCACCATCCA
DS_32.1	100.0%	69.0%	TCAAC-AGCGTGTACGTTA--TCTGTCTATG----
DS_34.1	96.6%	56.7%	CAAAGGCGG-TGGAGACCA--TGCGTGTACTI----

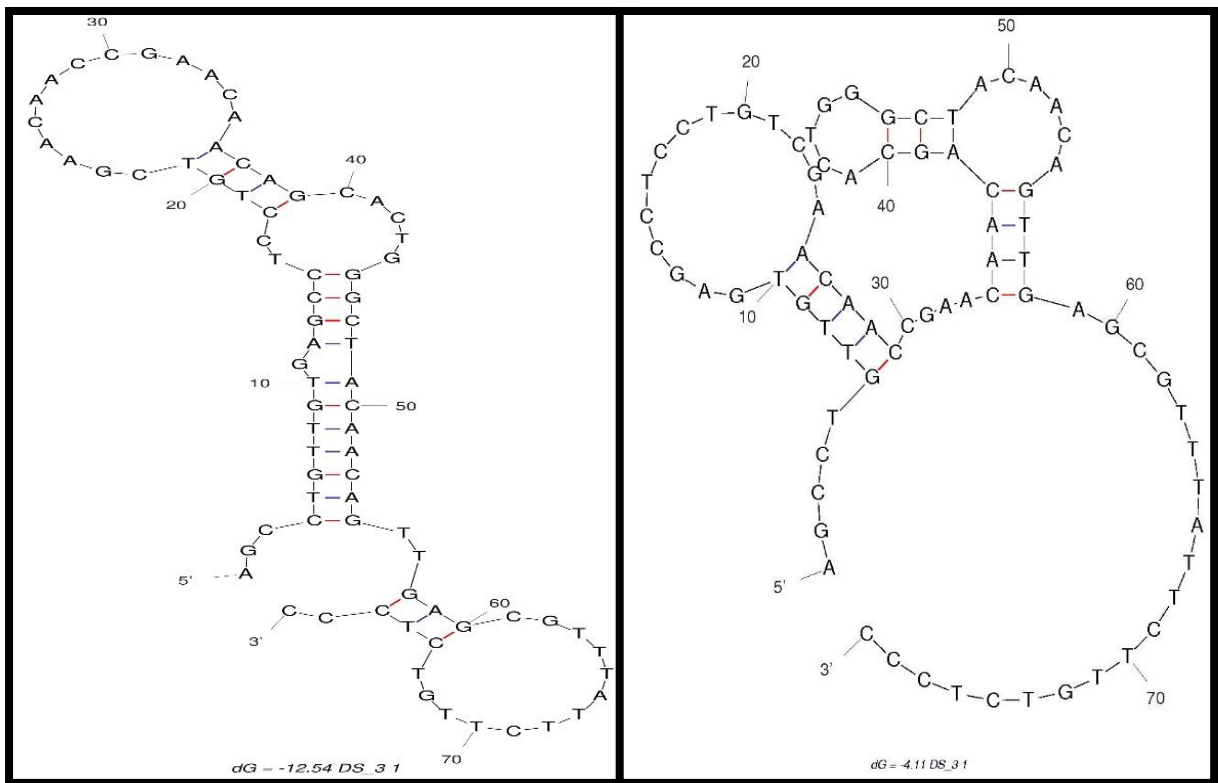
Figure 3.10: Alignment of selected sequences from DDR1 Doped SELEX. Sequences were aligned by using ClustalW. The alignment of sequences are given with cov % (percentage of positions covered by motif) and PID (percentage identity) with reference to C25 aptamer. Different conserved motifs identified in all sequences are indicated in the background colours.

Evaluation of Selected candidates by Dot-blot assay:

The candidates were evaluated by a dot-blot assay (slot format), an in vitro experiment based on nitrocellulose membrane. For this purpose the candidates were synthesized with ROX fluorophore labeled at the 5' prime end. 5 nM of ROX labeled candidates were analysed against 50 nM of extracellular domain of DDR1. The experimental procedure is described in chapter 2. Out of 10 candidates, DS_3.1 was the only candidate which showed binding to DDR1 (Data not shown). We further evaluated DS_3.1 with structural and in vitro studies as discussed below.

Structural Studies of Aptamer DS_3.1:

Aptamer DS_3.1 was further characterized and truncated based on mfold structural predictions. The mfold predicts two structures with different free energy (ΔG). The mfold predicted structure DS_3.1a with ΔG of -12.54 is highly stable as compare to DS_3.1b (ΔG - 4.11). The stability of this structure is due to the three G-C base pairs closing the stem loop of DS_3.1a as shown in figure 3.11.



DS_3.1a
 $\Delta G = -12.54$

DS_3.1b
 $\Delta G = -4.11$

Figure 3.11: mfold predicted structures of aptamer DS_3.1.

Based on the structural prediction, as highly stable aptamer DS_3.1 was truncated into one small aptamer named as DS_3.1t1 (35 nt aptamer with 13 nt of the forward primer). mfold predicts 5 different structures of the DS_3.1t1 but the structure with lowest free energy ($\Delta G = -4.11$) is highly stable as the stem loop is closed with three G-C base pairs which makes the structure very stable²⁶⁵ (Figure 3.12).

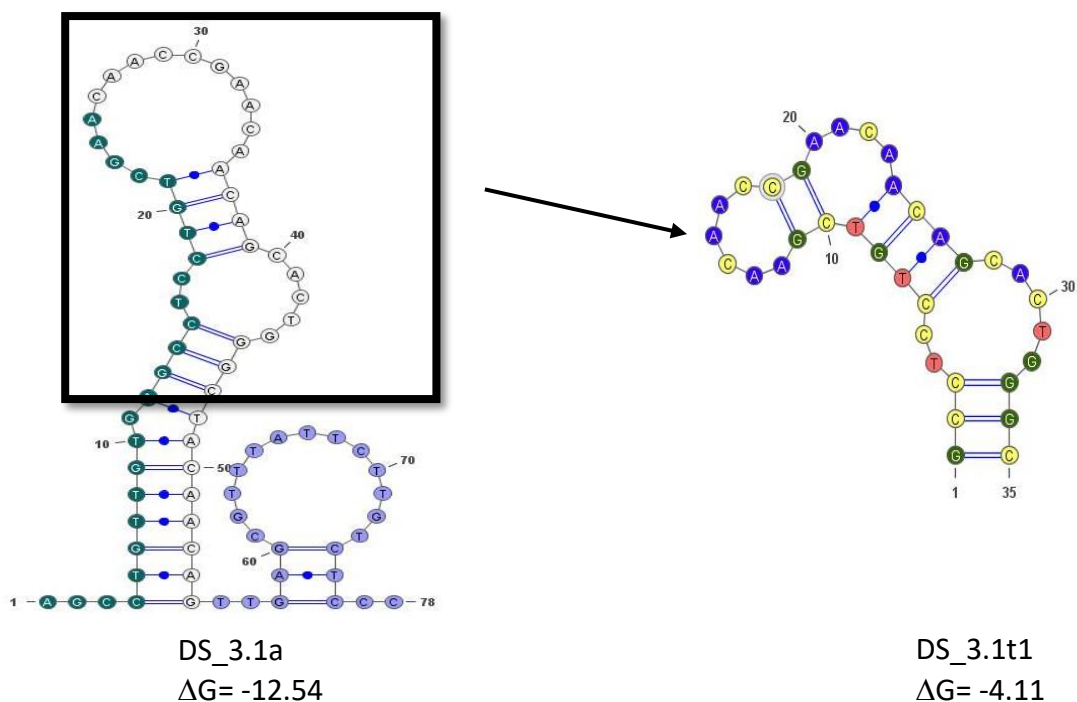


Figure 3.12: mfold predicted structure of DS-3.1t1. mfold predicted structure of full length aptamer DS_3.1 (right side) shows that the primers are involved in structure conformation. Aptamer DS_3.1 was further truncated based on the mfold predicted structure (highlighted by box).

Determination of K_d of DS_3.1 aptamer by Blot Assay:

As discussed in the earlier paragraph, DS_3.1 was selected out of ten candidates as it shows a binding to DDR1. In order to validate the binding kinetics of DS_3.1 against extracellular domain of DDR1, a Dot-Blot assay in a slot format was performed by using nitrocellulose membrane as mentioned earlier. For this purpose, we used the DS_3.1 aptamer labeled with ROX fluorophore at its 5' prime end. The concentration of aptamer was kept 5nM while DDR1 conc. was varied as 0nM, 10nM, 20nM, 35nM, 50nM, 75nM and 100nM. The image was captured and exported into tif file and analysed by ImageJ software (Figure 3.13-A). The fluorescence intensity was measured and the fluorescence enhancement for each sample was determined in terms of fold excess. The K_d of the aptamer DS_3.1 was then determined based on the values of the fold excess by plotting a graph with 4 parameters (Hillslope, min, max and EC50) logistic curve with the following formula

$$f = \text{min} + (\text{max} - \text{min}) / (1 + \frac{x}{\text{EC50}})^{-\text{Hillslope}}$$

The curve was fit with an $R^2=0.9944$ with a Hill slope value of 7.6. The Hill slope value shows a strong cooperative binding between the aptamer and its target. The K_d of DS_3.1 calculated by this method is 33.65 ± 1.23 nM (Figure 3.13-B).

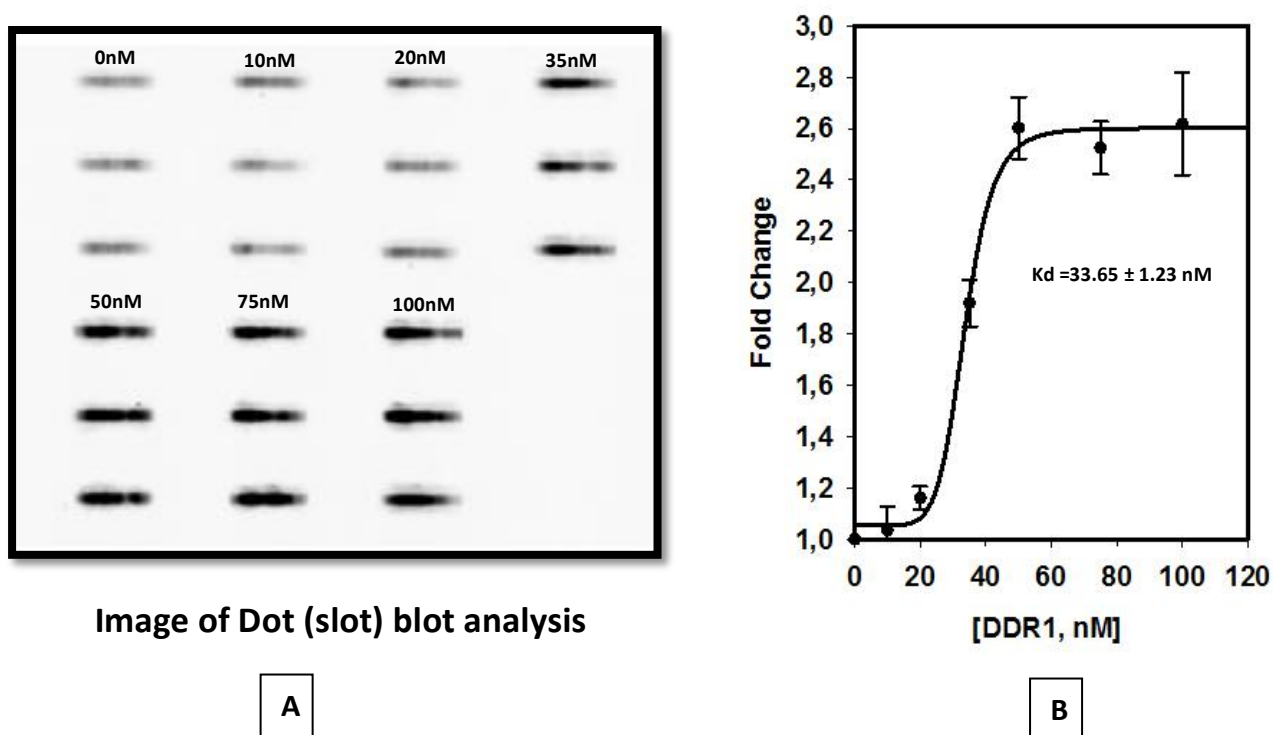


Figure 3.13: K_d determination of Aptamer DS_3.1. **A=** Image of the nitrocellulose membrane taken by ChemiDoc MP Imager used to determine the K_d of aptamer DS_3.1 by dot blot assay. The experiment was performed by increasing the concentration of DDR1 up to 100nM. The experiment was performed in triplicate. **B=** Graph of DS_3.1 K_d plotted by software Sigma.

Fluorescence Imaging by Confocal Microscopy:

The truncated aptamer DS_3.1t1 was evaluated against MDA-MB-231 breast adenocarcinoma cells overexpressing DDR1, while melanoma cell line 501Mel was used as a negative control cell which doesn't express any of the discoidin receptor. 100nM of TRITC labeled DS_3.1t1 was used for fluorescence microscopy assay. A scramble sequence of DS_3.1t1 labeled with TRITC was used as a control. The cells were analysed with Leica Confocal Microscope (Figure 3.14).

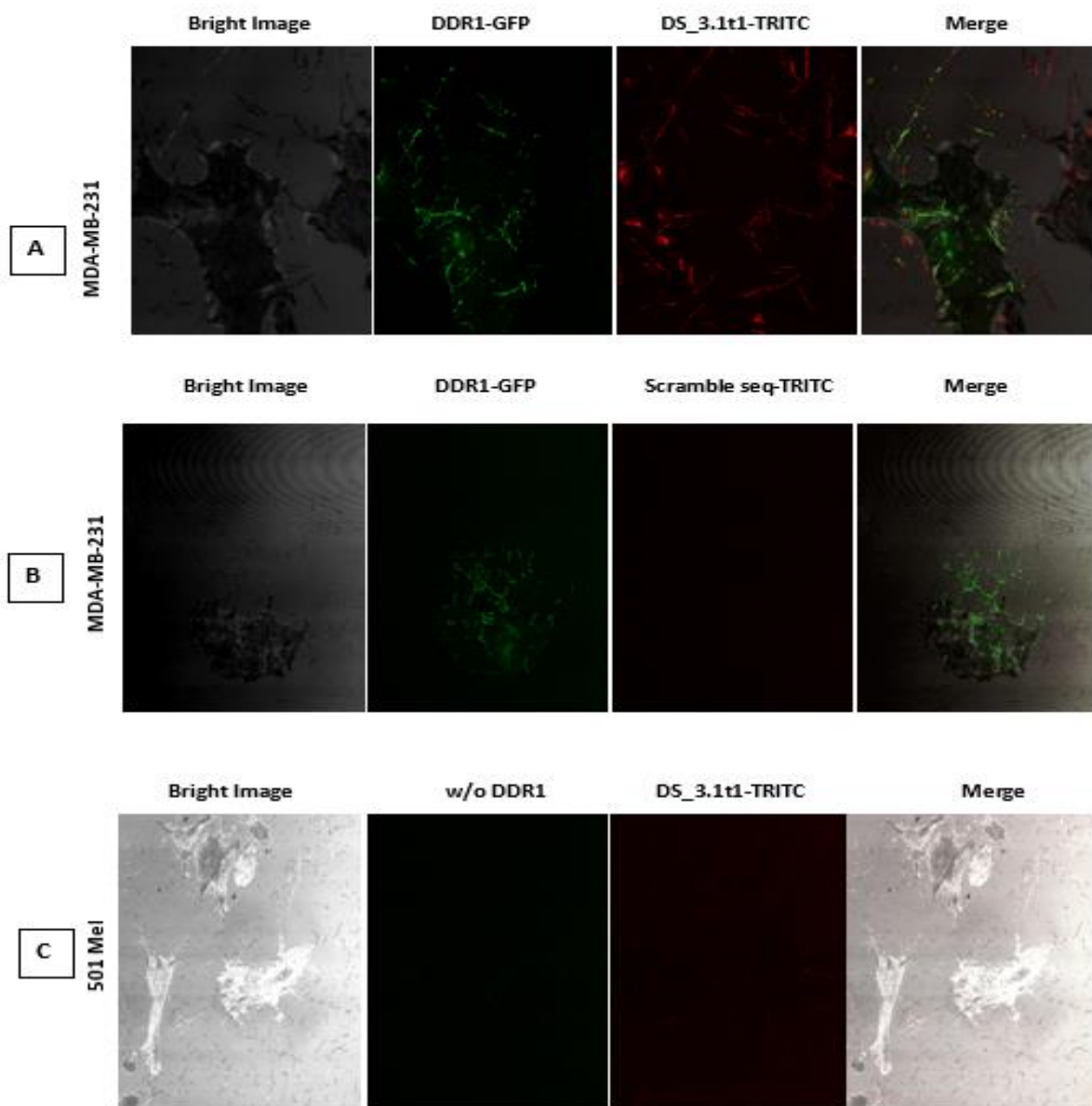


Figure 3.14: Confocal Microscopy for Cell Imaging. Confocal images at scale bar 25 μ m. **A=** Confocal images of aptamer DS_3.1 against MDA-MB-231 cells overexpressing DDR1 target receptor. **B=** Confocal images of Control Sequence against MDA-MB-231 cells overexpressing DDR1 target receptor. **C=** Confocal images of aptamer DS_3.1 against 501Mel negative Cells.

Aptamer DS_3.1t1 was able to stain the MDA-MB-231 cells with red fluorescence signal but the signal was mysteriously observed in the extracellular region along with the collagen (Figure 3.14-A). While there was almost no signal in the 501Mel cells which didn't express DDR1 on their surface (Figure 3.14-B). In order to validate the specificity of the signal in the DDR1 expressing MDA-MB-231 cells associated to DS_3.1t1, we used scramble sequence of

DS_3.1t1 as a negative control. As compared to DS_3.1t1, the signal associated to the scramble control sequence was very low which could be a background signal (Figure 3.14-C). From all these cell assays, it is assumed that aptamer DS_3.1t1 is mostly staining the collagen 1 fibrils. Since DDR1 is dependant of collagen 1 fibrils and it co-localizes along with the collagen^{266 248}, we assume that endogenous DDR1 co-localized on the collagens possibly in the cell trajectory is recognized by the aptamer. As DDR1 is labelled with GFP, this could also impair the recognition of DDR1 by blocking the aptamer binding site. Another hypothesis could be an electrostatic interaction between DNA aptamer and collagen fibres but there was no signal observed with the control sequence which doesn't support this hypothesis.

In order to further validate the binding of DS_3.1t1 aptamer in the cells expressing DDR1, we further aim to perform a cell assay where we can use DDR1 specific antibody to locate the DDR1 in the cells and target it with DS_3.1t1 aptamer.

Conclusion:

In this chapter, we have reported a successful selection of DNA aptamer by targeting the extracellular domain of DDR1 through SELEX. Initially after performing 6 rounds of selection, an aptamer C25 was selected which showed a binding against DDR1. As demonstrated by in vitro experiments, the binding affinity of C25 and its truncations was not stronger to use for in vivo imaging. We therefore decided to proceed the SELEX with C25 doped library to generate better variants of C25. After performing further 5 rounds of selection against the extracellular domain of DDR1 with the C25 doped library, the SELEX was analysed by high throughput sequencing.

In conclusion, we have selected an optimized aptamer DS_3.1 as a variant of C25 which binds specifically to its target DDR1 with a K_d 33.65 ± 1.23 nM (almost 15X better than C25). Aptamer DS_3.1 can be exploited as molecular probe in the detection of DDR1 overexpression in melanoma. Therefore, it can be used as a promising diagnostic module for non-invasive cancer diagnosis and can provide a novel cost effective alternative to conventional antibody. Nevertheless, extensive research with animal models is still required to evaluate the in vivo binding specificity of this aptamer.

**Chapter-4: In vitro selection of DNA
aptamers against Human Matrix
Metalloproteinase-14 (HMMP-14)**

Matrix metalloproteinase 14 (MMP-14) is a significant protease which plays vital roles in many biological processes. MMP14 is overexpressed in numerous types of cancer including melanoma and is associated with poor prognosis. Therefore, MMP14-specific aptamer has potential use in the diagnosis and treatment of MMP14-positive melanoma. Due to the large interest of diagnostics in this protein, there is a high demand of aptamers as an imaging probe. MMP14 and its role in melanoma has been already described in chapter 1, so here in this chapter we will discuss the selection of aptamers against HMMP14.

SELEX against HMMP14 with natural DNA library:

SELEX Library:

The ssDNA library used to select an aptamer against HMMP14 is the SELEX Library A which has a 30 nucleotide random window flanked with primers P5 and P3 respectively as shown in table 2.1.

SELEX:

The selection against HMMP14 was based on Magnetic beads SELEX and Filtration SELEX. Total 15 rounds of SELEX were performed against the recombinant HMMP14. The SELEX was initiated with 300 pmoles of ssDNA library against 10 pmoles of HMMP14 in the starting round with a competition ratio of 1:30. As the SELEX proceeded the competition was made higher up to 1:40. The concentrations of ssDNA library and HMMP14 receptor were decreased with the assumption of favouring the conditions to select high affinity aptamers. As there are many aptatopes on the target receptor, this decrease in concentration is expected to be more efficient for selection.

Unlike other SELEX protocols described in this thesis, we introduced a counter selection from round 6. Counter selection against NC membrane, GST-H and HMMP2 was performed in specific rounds. As the SELEX proceeded, the concentration of counter selected proteins and the washing volume were increased to discard all non-binders or weak binders which resulted in decreasing the diversity of the pool. The SELEX procedure has been described in Table 4.1 with detail.

Rounds	Counter Selection	Selection HMMP14	Library ssDNA	Ratio	Washing	
		pmoles	pmoles	pmoles	PBS-Mg 1X	
1	Magnetic Beads SELEX	None	10	300	1:30	1* 100 μ L
2	Magnetic Beads SELEX	None	10	300	1:30	1* 100 μ L
3	Magnetic Beads SELEX	None	8	240	1:30	2* 100 μ L
4	Magnetic Beads SELEX	None	6	180	1:30	2* 100 μ L
5	Magnetic Beads SELEX	None	5	150	1:30	2* 100 μ L
6	Magnetic Beads SELEX	1*GST-H 1 μ M 1*HMMP2-H 50nM	5	150	1:30	2* 100 μ L
7	Magnetic Beads SELEX	1*GST-H 1 μ M 1*HMMP2-H 60nM	4	120	1:30	3* 100 μ L
8	Magnetic Beads SELEX	1*GST-H 1 μ M 1*HMMP2-H 60nM	3	90	1:30	5* 100 μ L
9	Magnetic Beads SELEX	1*GST-H 1 μ M 1*HMMP2-H 60nM	2	75	1:37.5	6* 100 μ L
10	Magnetic Beads SELEX	1*HMMP2-H 70nM	2	80	1:40	6* 100 μ L
11	Filtration SELEX	1*NC membrane 1*GST-H 1 μ M	2	80	1:40	1* 1 mL
12	Filtration SELEX	1*NC membrane 1*HMMP2-H 70nM	2	80	1:40	2* 1 mL
13	Filtration SELEX	None	2	80	1:40	2* 1 mL
14	Filtration SELEX	None	1	40	1:40	5* 1 mL
15	Filtration SELEX	None	0.5	20	1:40	10* 1 mL

Table 4.1: Selection conditions applied for SELEX against HMMP14.

High throughput Sequence Analysis:

High throughput sequencing was performed for all rounds of the SELEX including the library as described in chapter 2. As discussed earlier that the HTS analysis of this SELEX was performed using PATTERNTY-SEQ software, where the sequences were recovered based on the adjusted Q score of 30. A threshold of 0.001% was put to display and calculate the data.

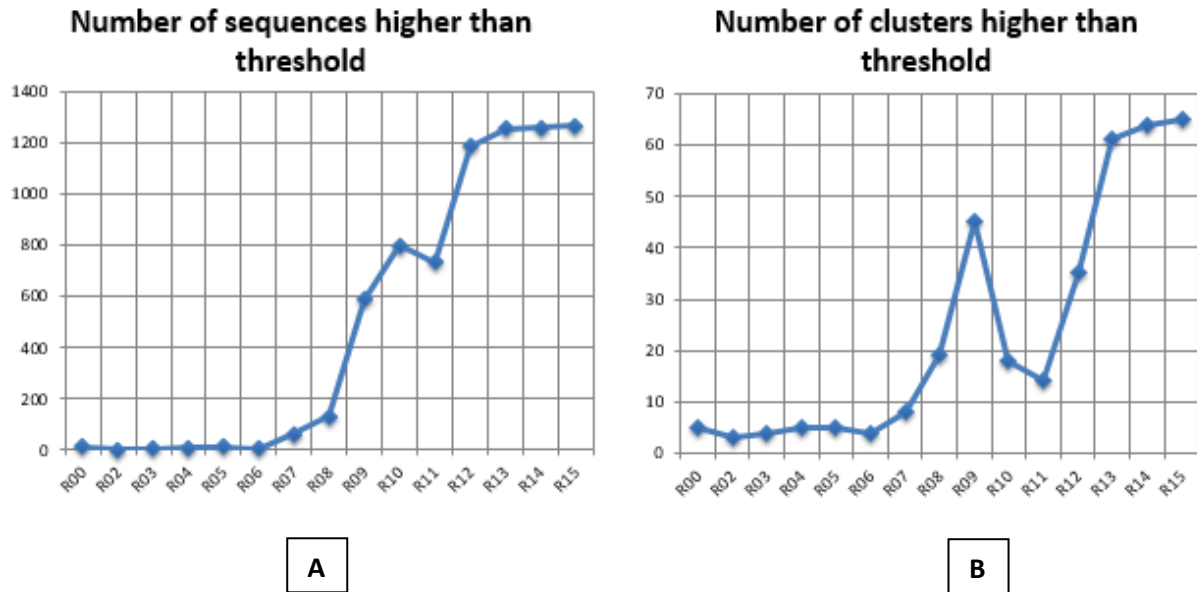


Figure 4.1: Graphical representation of enrichment of candidates in SELEX against HMMP14. A threshold of 0.001% was adjusted to display and calculate the data. **A=** Number of sequences higher than the threshold in each round of SELEX. **B=** Number of clusters higher than threshold in each round of SELEX.

Strong evolution was observed for the SELEX starting from round 9 as shown in figure 4.1. This can be explained with the increase in the competition ratio (HMMP14: ssDNA) from 1:30 (R8) to 1:37.5 (R9) which was further increased up to 1:40 in next rounds (Table 4.1). As the SELEX rounds proceeded, the number of sequences higher than the threshold 0.001% had increased, instead for R11 where the SELEX was shifted from Magnetic beads based SELEX to Filtration SELEX (Fig 4.1-A). The decrease in number of cluster during round 10 and 11 was due to enrichment of specific sequences (Figure 4.1-B). The HTS analysis shows the enrichment of the sequence (5'-ACT CCC AGA CGG AAT GCA GAC GTC CCA GTG-3') up to 50 percent of the pool in R10 and R11, which was then decreased in proceeding rounds (Figure 4.2).

The clusters were ranked according to their presence in the pool with the most abundant cluster as top. The sequences were analyzed in clusters based on the most abundant sequence as a representative of the cluster. Representative sequences of the first 4 clusters shared a same motif GAATGCAG as shown in Table 4.2.

Name	Sequences	R0	R08	R09	R10	R11	R12	R13	R14	R15
m14-0	ACTCCCAGACGGAATGCAGACGTCCCAGTG	0.003	2.708	33.34	49.97	49.08	33.19	26.41	18.81	23.52
m14-1	GGCACGCTCACGCAGGGAATGCAGACCCAG	0.002	0.236	8.092	26.86	19.2	20.51	20.15	17.87	18.43
m14-2	ATCATCCATAGAATGCAGCTGCAGGATGT	0.002	0.016	0.965	9.331	12.07	18.99	21.72	19.27	18.92
m14-3	GCCATGCAGGGGAATGCAGCCCCATGTGG	0	0.01	0.278	1.018	0.354	1.326	2.827	4.528	4.871
m14-4	TGCCCCAGGACTCCATGCGCGTCCCAGGC	0	0.003	0.075	0.229	0.106	0.547	1.541	2.748	4.012

Table 4.2: NGS result analysis for SELEX against HMMP14. Representative sequences of top 5 clusters with their individual percentage present in the SELEX rounds. The top 4 highly evolved sequences share the motif GAATGCAG and enriched up to 70 % in the pool.

All the selected sequences were 30 nucleotide long. On alignment of these sequences with reference to m14-0, we identified conserved motifs that occurred in combination with each other for all sequences as described in figure 4.2.



Figure 4.2: Alignment of selected sequences from HMMP14 SELEX1. Sequences were aligned by using ClustalW. The alignment of sequences are given with cov % (percentage of positions covered by motif) and PID (percentage identity) with reference to m14-0 aptamer. Different conserved motifs identified in all sequences are indicated in the background colours.

Evolution of Parasite sequences:

Parasite sequences are those sequences which affect the SELEX with contamination resulting in selection of an aptamer against co-receptors rather than the actual target receptor. Many SELEX fail due to enrichment of such parasitic sequences which in competition defeat the sequences of interest. The reason of parasitic sequence enrichment may be due to PCR biasness²³⁷ or enrichment of sequences against co-receptors.

In HMMP14 SELEX, we observed a high evolution of sequences sharing the same motif GAATGCAG among the top four clusters. On in vitro characterization of these sequences

(discussed later), it had been observed that in fact these were parasite sequences evolved against the His-tag rather than the HMMP14 itself, since we used the histidine tagged HMMP14 during selection. Surprisingly the introduction of negative selection with histidine tagged GST and HMMP2 from Round 6 was not able to remove the sequences. Since histidine is a small molecule as compared to HMMP14, a short sequence **GAATGCAG** evolved against it very fast. Secondly as the NGS results show in table 4.2, that the sequences containing motif **GAATGCAG** had together contaminated around 80 percent of the pool in round 10 and round 11 which was later decreased to 70 %. This decrease may be associated to switching the SELEX method from Magnetic beads to Filtration SELEX. Indeed the washing volume was also increased in the last rounds. It can be assumed that efficient counter selection and washing couldn't remove this high percentage of parasite sequence due to amplification by PCR in each round.

mfold structural analysis of parasite sequences:

The structures of the parasite sequences without primers were predicted by mfold. As we can see in figure 4.3, the motif **GAATGCAG** presented in these sequences are highly involved in the formation of the apical loop closed by different number of GC base pairs which is highly suspected in binding.

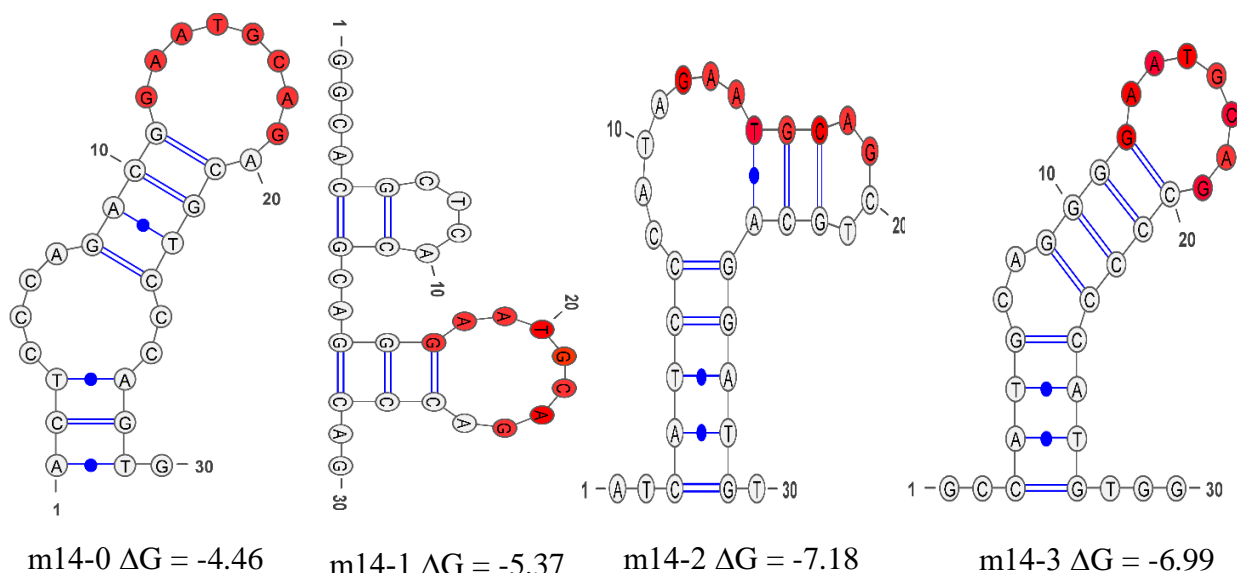


Figure 4.3: mfold based structure analysis parasite sequences. mfold prediction of parasite sequence without primers. All these sequences share the motif GAATCGAG (in red).

In vitro Fluorescence Assay of m14-0:

The aptamer m14-0 was characterized by FluMag based in vitro fluorescence assay as described in chapter 2. For this purpose, 1 μ M of FAM labeled m14-0 was analyzed against 50nM of 6X histidine tagged HMMP14. The binding of m14-0 was also analyzed against only 6X histidine as a negative target. Surprisingly m14-0 showed a similar binding affinity to both targets with a fractional occupancy of around 90 percent as shown in Figure 4.4. It is proved that m14-0 binds to the histidine with very high affinity (K_d expected to be in low nM range).

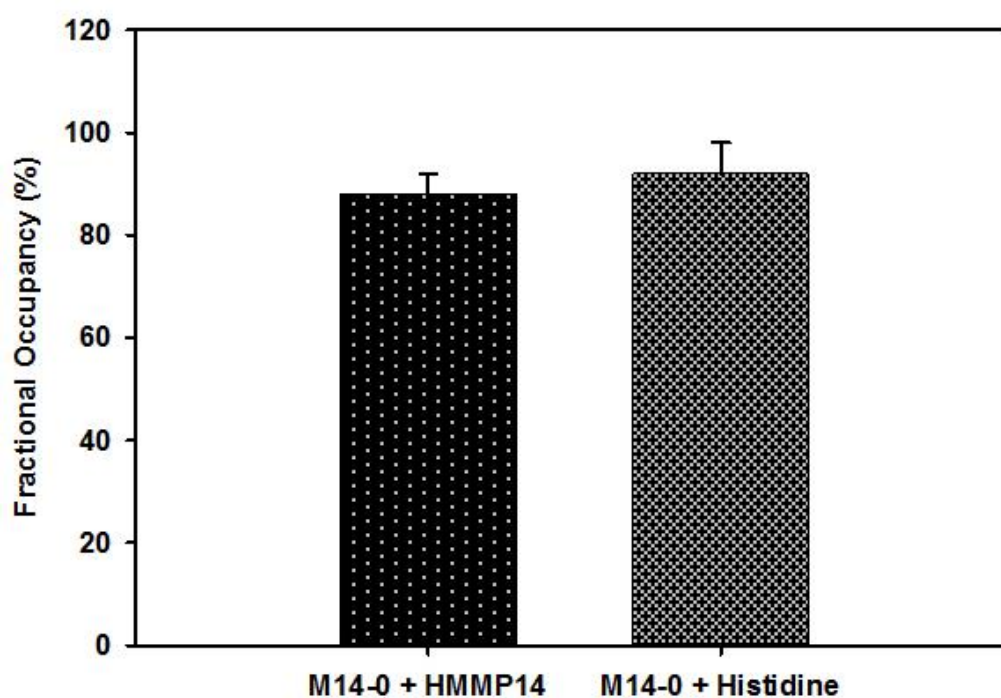


Figure 4.4: Binding analysis of m14-0. The binding affinity of aptamer m14-0 was analysed by FluMag based in vitro fluorescence assay using magnetic beads. The fractional occupancy was calculated based on the fluorescence intensity.

Applications of histidine aptamer m14-0:

Due to high purity and low cost production, aptamer can be used in many analytical or biophysical methods that has traditionally utilized antibodies. Since aptamer m14-0 is highly specific to histidine, we can use it for following applications.

i) Protein Purification:

Affinity chromatography is one of the most effective technologies used for the purification of proteins from crude or semi purified extracts. Proteins are often expressed with fusion-tags like His-tags for affinity purification and to aid solubility in commercially available plasmid vectors. Aptamer mediated affinity chromatography enables purification of proteins in a single step. Aptamer m14-0 selected against histidine can easily bind to a histidine tagged protein. Thus Protein loading, washing and elution can be easily carried out through affinity chromatography.

ii) Enzyme-Linked ImmunoSorbent Assay

Enzyme-Linked ImmunoSorbent Assay, is based on the use of monoclonal or polyclonal specific to a target for quantitative detection. ELISA is highly applicable for the detection of protein biomarkers in research, diagnostics and therapeutics. Since antibodies have limitations, we can use aptamers as Enzyme-Linked Aptamer Sorbent Assay (ELASA). Thus, anti His-tag aptamer m14-0 can be used to detect the histidine tagged proteins in ELISA.

iii) Surface Plasmon Resonance:

As discussed in previous chapters that SPR is used for the affinity analysis in ligand-target binding assays. In SPR, Nickel coated sensor chips are used which has a limited application due to electrostatic interaction. Anti his-tag aptamer provides a better method where aptamer can be conjugated to surface with streptavidin/biotin conjugation without loss of selectivity / affinity, and can be regenerated or refolded. Histidine tagged protein can thus easily bound to the aptamer resulting in the fixation at the surface for SPR experiment.

Overcoming issues related to evolution of parasite sequences in SELEX:

To overcome the problems related to the evolution of parasite sequences in general, Duconge proposed an introduction of antisense oligonucleotide in the proceeding rounds of SELEX as an antidote. This antisense oligonucleotide will lead to decrease in the parasitic sequences resulting in an enrichment of other new sequences having an affinity for the target. Indeed, this can be easily monitored by HTS analysis after every round.

Improvement in Magnetic Beads SELEX:

We have observed that there are many complications with magnetic beads SELEX which should be addressed carefully. Since magnetic beads are used for such selections to immobilize the target, these beads usually settle down during incubation resulting in aggregation (not visible by naked eyes) which can highly affect the SELEX. Such problems can be overcome by using an incubator which forces the beads to disperse after every specified time unlike spinning rotors. As these aggregates are not visible with naked eyes that can also lead to poor washing resulting in the recovery of non-interested sequences.

One of the major complications with magnetic beads is the elution of interested sequences by heating. To overcome this problem, we propose that after washing, the interested sequences can be amplified directly on the magnetic beads. This can enhance the possibility of amplifying only sequences that are bound to the target immobilized on beads.

Since in the literature, so far many SELEX processes have been reported based on the nature of the target. However, it is a fact that there is no exact criteria for SELEX. Although the SELEX is initiated with a library having a huge diversity of sequences, the selection of aptamer is highly influenced by many parameters i.e. SELEX type, SELEX library, buffer conditions, library and target concentrations, PCR amplification, washing and elution etc. It is a beauty of SELEX that evolution of candidates are highly dependent on the conditions of SELEX provided, so we suggest that more than one SELEX should be run in parallel with different parameters.

Conclusion:

In conclusion, we performed a selection against HMMP14 target receptor with natural nucleic acid library of 10^{15} diversity but this DNA naïve library drove the selection against the receptor tagged histidine (co-receptor) resulting in the enrichment of parasite sequences. We assumed that the failure of this SELEX was due to late introduction of counter selection step from the round 6 resulting in the enrichment of parasite sequence which were then not able to be removed due to PCR amplification. However the histidine specific aptamer can be used in many analytical and biophysical methods.

Chapter-5: In vitro selection of DNA aptamers against Discoidin Domain Receptor-2 (DDR-2)

Discoidin domain receptor-2 (DDR2) as a family member of receptor tyrosine kinases is involved in many biological processes such as cellular growth, differentiation, metabolism and motility in response to internal and external stimuli¹⁵. This receptor is activated by collagen in order to perform their kinase activity but in pathophysiological conditions it leads to the activation of matrix metalloproteinase which are responsible for cell invasion and migration by degrading the extracellular matrix of cells through invadosomes^{36 53}. The detail about DDR2 structure and its role in melanoma has already been discussed in Chapter 1, so in this chapter we will discuss the selection of an aptamer against the DDR2 to be used as a theranostic agent.

Cross-Over SELEX against Discoidin Domain Receptor 2:

Cross-Over SELEX is a hybrid of different SELEX methods introduced to enhance the selection efficiency and to avoid the generation of aptamers against potential co-receptors of the biomarker of interest. Cross-Over SELEX can be performed against target in both recombinant form and in cells¹⁰⁷. In order to select an aptamer against DDR2, we performed a Cross-Over SELEX as a hybrid of three different SELEXs i.e. Magnetics Beads SELEX, Filtration SELEX and Cell SELEX.

Magnetic Beads SELEX was performed by the immobilization of the 6X histidine tagged DDR2 recombinant purified protein on Ni-NTA agarose magnetic beads. Filtration SELEX was performed also by using the recombinant purified DDR2. The interested and non-interested sequences were then separated by using NC membrane. Cell SELEX was also performed to generate an aptamer which can recognize the extracellular domain of DDR2 in its native condition. For this purpose we used HUVEC cells with overexpression of DDR2 prepared by Saltel's lab at University of Bordeaux.

SELEX ssDNA Library:

The ssDNA library used in this SELEX has a 40 nucleotide random window with primers P5 (forward primer) and P3 (reverse primer) as given in table 2.1. The reason to select a library of 40 nucleotide random window was to avoid selection of aptamers which need the primers for target recognition. As in SELEX against DDR1 (chapter 3) we had observed that the primers are usually involved in structural conformation, which can be avoided with a longer library. These primer sequences cause non-specific binding by their nature, and have been reported to lead to large numbers of false-positive binding sequences, or to interfere with binding of sequences within the random regions²⁶⁷.

SELEX:

The SELEX was initiated with 2nmoles of ssDNA library (10^{15} sequences) against 10 pmoles of the extracellular domain of DDR2 with a ratio of 200:1 which was decreased as the SELEX rounds proceeded. SELEX rounds with recombinant form of EC domain of DDR2 was performed with a protein-SELEX binding buffer while SELEX rounds with HUVEC cells expressing DDR2 was performed in cell SELEX Binding buffer mentioned in Table 2.2. While the respective buffers without competitors in both SELEX were used as washing buffer.

In general we performed total 14 rounds of Selection against the EC domain of DDR2 where 7 rounds were based on Magnetic beads based SELEX, 5 rounds as Filtration SELEX and 2 rounds as Cell SELEX. The detail about SELEX procedure is given in table 5.1.

During the SELEX, we also focused on the stringency by introducing counter selection from the early rounds. We performed counter selection against Ni Beads or NC membrane (depending on the type of SELEX), as described earlier that during SELEX usually there are sequences that bind to these solid supports as a parasite sequence resulting in the wrong direction of SELEX. In order to make the selection more stringent we also performed a counter selection against GST protein from the starting round. The washing and time was increased as the SELEX rounds proceeded to discard non-binders and the weak binders.

Conditions of SELEX DDR2								
Types of SELEX		Library ssDNA pmoles	CS 1 NC/ Beads	CS 2 GST-H pmoles	CS 3 DDR1-H pmoles	Selection DDR2-H pmoles	Ratio ssDNA : DDR2	Washing PBS-Mg 1X
1	Magnetic beads SELEX	2000	None	52.5	None	10	200 : 1	2 (100 µL)
2	Magnetic beads SELEX	1000	None	105	5	10	100 : 1	5 (100 µL)
3	Filtration SELEX	300	NC	105	6	8	37.5 : 1	3 (1 mL)
4	Filtration SELEX	300	NC	105	6	8	37.5 : 1	6 (1 mL)
5	Filtration SELEX	225	None	None	6	6	37.5 : 1	6 (1 mL)
6	Cell SELEX	150	None	None	None	2500000	None	3 (1 mL) Cell SELEX WB
7	Filtration SELEX	150	None	None	6	5	30 : 1	6 (1 mL)
8	Cell SELEX	100	None	None	None	1000000	None	5 (1 mL) Cell SELEX WB
9	Filtration SELEX	30	None	None	None	0.8	37.5 : 1	6 (1 mL)
10	Magnetic beads SELEX	100	5µL Ni Beads	105	6	2.5	40 : 1	5 (100 µL) 1 minute
11	Magnetic beads SELEX	80	5µL Ni Beads	105	4	2	40 : 1	6 (100 µL) 2 minutes
12	Magnetic beads SELEX	60	5µL Ni Beads	None	3	1.5	40 : 1	8(100 µL) 2 minutes
13	Magnetic beads SELEX	40	5µL Ni beads	None	2	1	40 : 1	10 (100 µL) 2 minutes
14	Magnetic beads SELEX	30	5µL Ni beads	None	1.5	0.75	40 : 1	10 (100 µL) 5 minutes

Table 5.1: Selection conditions applied for Cross-over SELEX against DDR2. Conditions of Cross-Over SELEX performed against DDR2 receptor. Total 14 rounds of SELEX was performed with 7 rounds of magnetic beads SELEX (Green), 5 rounds of Filtration SELEX (Yellow) and 2 rounds of Cell SELEX (Orange).

The candidates were amplified into a total volume of 1 mL according to the procedure described in chapter 2. In this SELEX, we switched the polymerase after every round with Go Taq, Gold Taq, Diamond Taq and Phusion. The reason of switching of the polymerases was to avoid the biased amplification if any. As it has been demonstrated that polymerases sometimes shows biasness during incorporation, or not able to incorporate all bases correctly resulting in production of short sequences ²⁶⁸. Before performing the amplification, we optimized the amplification with each polymerases in order to avoid any by-product formation ²³⁷ as described in chapter 2. Another reason to use Taq polymerases and Phusion polymerase is their “processivity”, as Taq Pols have 5 times while Phusion has 10 times more processivity than Pfu polymerase. Processivity is the ability of DNA polymerase to carry out continuous DNA synthesis on a template DNA without frequent dissociation which can be measured by the average number of nucleotides incorporated on a single association/disassociation event by DNA polymerase.

High throughput Sequencing:

The HTS analysis of DDR2 SELEX was performed as described in chapter 2. Since the random window of the library used for this SELEX was 40 nt long, sequences between 37-42 nucleotides were analysed. It was observed that the diversity of the pool after performing 14 rounds of selection had not decreased promisingly i.e. 91.3 % in the 14th round as described in table 5.2.

SELEX	Total sequences	Unique sequence	Diversity
Round 0	4237948	4220712	99,6 %
Round 1	2124522	2105756	99,1 %
Round 2	1700523	1648217	96,9 %
Round 3	1743768	1721184	98,7 %
Round 4	1756855	1737607	98,9 %
Round 5	1766688	1748941	99,0 %
Round 6	3269073	3254788	99,6 %
Round 7	3558194	3538779	99,4 %
Round 8	2622835	2593860	98,9 %
Round 9	3975317	3911863	98,4 %
Round 10	837761	825240	98,5 %
Round 11	667668	656871	98,3 %
Round 12	850664	834867	98,1 %
Round 13	680680	641899	94,3 %
Round 14	510826	466544	91,3 %

Table 5.2: Diversity of rounds in SELEX against DDR2. The rate of decrease in the diversity is too slow. After 14 rounds of selection only 9 percent diversity has decreased.

Only few candidates showed increase in the frequency during the SELEX. Based on the NGS evolution profile, 4 sequences were selected named as D2.1, D2.2, D2.3 and D2.4 as shown in Table 5.3.

Cndts	Sequences	R5	R6	R7	R8	R9	R10	R11	R12	R13	R14
D2.2	GCCATCCCGTCAGTCTCAGTCACTCATTGGTGTCTCG	0	0.31	1.41	35.8	23.7	48.9	85.4	74.1	42.6	62.6
D2.3	TATCACCCCGTCAAGTCAGTCAAGGTTGTTGTGTCTGTGCG	0	0	0	2.29	1.76	9.55	13.5	7.05	10.3	19.6
D2.4	GTCCTGTCTGTCTGTATGTCCCATCTGTTGCGTCCACCG	0	0	0	0	3.27	7.16	12	12.9	13.2	19.6
D2.1	TCCACATTACCTTCTTTGCATCCTTCATGTTGCGTCTCG	0	0	0	0	1.76	3.58	3	0	2.94	19.6

Table 5.3: NGS analysis of SELEX against DDR2. The NGS data analysis of the four highest abundant sequences. The sequences are given with their reads per million from R5 to R14. Sequence D2.2 and D2.3 evolved from cell SELEX rounds share three motifs of 7 bases together while D2.4 and D2.1 shares small motifs together.

All the selected sequences were 39 or 40 nt long. On alignment of these sequences with reference to the most abundant sequence D2.2, we identified conserved motifs that occurred in combination with each other for all sequences as described in figure 5.1.

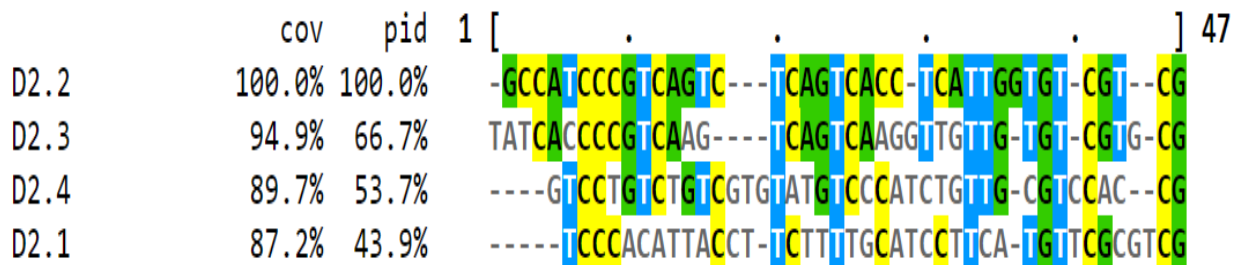


Figure 5.1: Alignment of selected sequences from DDR2 SELEX. Sequences were aligned by using ClustalW. The alignment of sequences are given with cov % (percentage of positions covered by motif) and PID (percentage identity) with reference to D2.2 sequence. Different conserved motifs identified in all sequences are indicated in the background colours.

Sequences D2.2 and D2.3 were the highly represented sequences which also share high homology between them. Interestingly, D2.2 and D2.3 were evolved during R6 and R8 respectively which were cell SELEX rounds. As D2.2 was evolved in R6 (first cell SELEX round), the evolution was higher in R8 (second cell SELEX round) as compared to R7 (filtration SELEX round). In later rounds which were based on selection against histidine tagged recombinant DDR2, the evolution of these candidates were not increased as shown in table 5.3.

Slot Blot Assay of DDR2 candidates:

Four candidates (D2.1, D2.2, D2.3 and D2.4) were analysed by Dot blot Assay (slot format) based on filter retention method as described in chapter 2. For this assay, 5nM of FAM labeled candidates were used against 50nM of DDR2. We observed an increase in fluorescence intensity in the slots subjected to D2.2 and D2.3 with DDR2, while there was no signal detected for D2.1 and D2.4 (Data not shown due to high background signal issues). Based on these results, we decided to perform new selection against DDR2 expressed on HUVEC cells with the doped library of D2.2 and D2.3. The discussion has been given in chapter 6 for this perspective.

Conclusion:

In this chapter, we have used Cross-Over SELEX targeting HUVEC cells expressing DDR2 and recombinant purified DDR2. After performing 14 rounds, the SELEX was analyzed by High throughput sequencing. Although the diversity of the pool was not decreased promisingly, 4 sequences were selected based on NGS evaluation. Two sequences D2.2 and D2.3 emerged from cell SELEX rounds were presented as most abundant sequences with an RPM of less than 100. As these sequences share high homology between them, we aim to perform a Cell SELEX with the doped libraries of these two sequences to generate better variants targeting DDR2 in its native conformation.

Chapter-6: Thesis Prospects and Summary

Research perspectives of aptamer selected against DDR1:

Although we have successfully selected an aptamer DS_3.1 against DDR1 which has been validated by Dot blot assay. This aptamer needs to be further characterized by different biophysical experiments. Stoltenburg et al. have demonstrated that the binding affinity of aptamer can vary based on the type of biophysical analysis method ²⁴⁵. DeRosa and colleagues have further emphasized on characterization of aptamer binding with several approaches, since they have demonstrated that some biophysical experiments failed to characterize the aptamer due to difference in nature of the target ²⁶⁹.

a) Biophysical characterization of DS_3.1 and DS_3.1t1 by Surface Plasmon Resonance (SPR):

Surface Plasmon Resonance has been extensively used in the study of aptamer binding kinetics ¹²¹. SPR allows for a highly sensitive real time analysis of molecule interactions ²⁷⁰. It allows label-free detection of interactions between targets immobilized at a solid–liquid interface and partners in solution injected in various tracks of the chip ²⁷¹. SPR is a well suited biophysical characterization method to determine the kinetic parameters, the equilibrium constant and the stoichiometry of a reaction.

In order to characterize the binding of DS_3.1 and DS_3.1t1, we aim to perform an SPR analysis. For this purpose the biotinylated aptamer will be immobilized on streptavidin coated CM5 sensor chip BIACORE. One problem associated to the immobilization of aptamer is the structural conformational changes associated to the fixation which can disturb the binding, especially if the primer is involved in binding. This problem can be solved in two ways. (i) 5'prime biotinylated aptamers are synthesized with a spacer 18 to be immobilized on the chip without any structural impairment. (ii) Aptamers are synthesized with additional 18-20 bases at 5'prime end which will be a complementary sequence to the biotinylated anchor immobilized on the streptavidin coated CM5 chip, but the risk associated with this method is an impairment of structural folding due to the anchor.

b) Determination of Kd of DS_3.1 and DS_3.1t1 by Isothermal Titration

Calorimetry (ITC):

Isothermal titration calorimetry (ITC) is an example of thermodynamic related techniques applicable for characterising the affinity between aptamer and its target ²⁷². ITC relies on the fact that formation of the aptamer-protein complex is an exothermic process which releases heat. Unlike other techniques, ITC provides a detailed thermodynamic picture of the molecular interaction, i.e. binding constant (Ka), reaction stoichiometry (n), enthalpy change (ΔH), entropy change (ΔS), and Gibbs free energy change (ΔG) which makes this method sensitive and suitable for the analysis of binding affinity by thermodynamic characterization ²⁷³. Since ITC is a label free technique and it works by directly measuring the binding equilibrium of a ligand with its binding partner in solution, it can better characterize the binding affinity due to its sensitivity. The limitations associated with ITC is that it requires high concentrations of ligand or target for measurement and larger total amounts of material than most other methods.

Determining the concentrations appropriate for an ITC experiment depends on the relationship between the protein and the ligand, as the amounts of each need to be adjusted for the magnitude of heat and the expected binding constant ²⁷⁴. These values should fit into a theoretical c-window in order to analyse the data. The C value is described by the equation

$$C = n \times Ka \times [M]$$

Where n is the stoichiometry of the reaction, Ka is the binding constant and [M] is the aptamer concentration. The optimal C value should be between 10 and 100, and can be adjusted by varying the concentration of the aptamer. The concentrations of the aptamer and target proteins used in ITC depends on the binding constant of the aptamer. For an optimal C value above 10, the concentration of the ligand in the syringe must be 20X more than the concentration in the sample cell.

In vivo imaging of melanoma cells using nanoparticles conjugated DS_3.1:

MRI is a highly resolution imaging technique widely used in clinical research. As discussed earlier in chapter 1 that aptamer conjugated with nano-particles have been successfully used for targeting tumor sites without any in vivo toxicity ^{229 275}. Since silica has good biocompatibility as is accepted as “Generally Recognized As Safe” GRAS, silica based nanoparticles have been used in imaging, drug delivery and therapy ²⁷⁶. Furthermore silica nanoparticles encapsulating

fluorescent dye known as Cornell dots have been approved by FDA as human melanoma targeting imaging probe in Phase 1 clinical trial ²⁷⁷.

As our main objective is to identify aptamers as an in vivo imaging agent, we aim to perform an MRI of melanoma tumor in xenograft model using aptamer DS_3.1 conjugated with silica nanoparticles. For this purpose, we aim to use dually fluorescent silica nanoparticles (DF-SiO₂ NPs) of 19nm covalently covered with a PEG ²⁷⁸. In an investigation of biodistribution in mice, it has been demonstrated that the fluorescent silica nanoparticle accumulation increases due to enhanced permeability and retention effect caused by PEG, thus make them a valuable label for in vivo imaging studies.

Research Perspectives for selection of DNA aptamers against DDR2:

For the successful selection of an aptamer against the DDR2 extracellular domain receptor, we are currently performing SELEX in two different ways as a perspective. The 1st perspective is using the doped library of the evolved candidates from the previous selection (chapter 5) and perform Cell SELEX ¹⁶⁹. 2nd perspective is to perform a Functional SELEX based on particle display ¹⁶⁶.

DOPED SELEX against Extracellular domain of DDR2:

As discussed earlier that doped SELEX has been demonstrated as a useful tool to optimize aptamer selection against the specific target ¹⁷¹. In Chapter 3, we also have demonstrated that doped SELEX can generate better variants of already selected aptamer with high affinity. Based on these results we decided to perform a doped SELEX against the extracellular domain of DDR2 target receptor.

Doped Library:

Based on the HTS analysis of the previous DDR2 SELEX, 4 candidates were selected. After performing an analysis by in vitro fluorescence assay aptamers D2.2 and D2.3 were selected as described earlier in Chapter 5. D2.2 and D2.3 are the sequences evolved from cell SELEX rounds and share high similarity between them due to presence of 3 same motifs of 7 bases each as shown below in Figure 6.1. We are therefore highly interested in performing Cell SELEX based on the doped library of D2.2 and D2.3.

D2.2 Random Window= GCCAT**CCCGTCA**GTC**TCAGTCA**CCTCATTG**GTGTCGT**CG

D2.3 Random Window= TATCAC**CCCGTCA**AG**TCAGTCA**AGGTTGTT**GTGTCGT**GCG

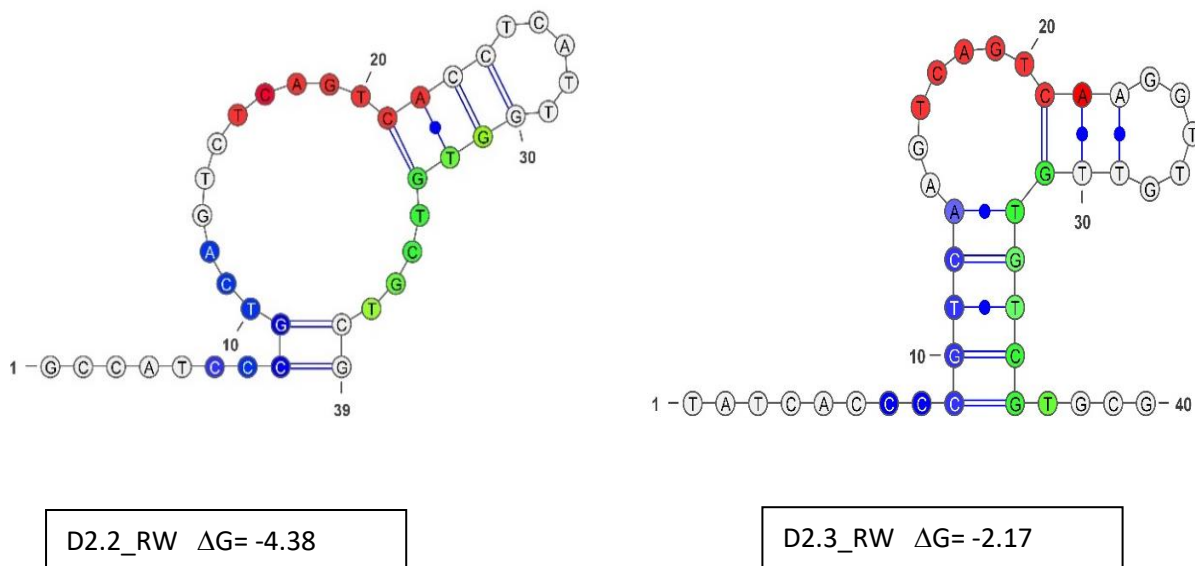


Figure 6.1: mfold predicted structure of D2.2 and D2.3 random window. D2.2 and D2.3 share three motifs (given in blue, red and green) which are involved in stem and loop formation.

For this purpose, we have recently synthesized two separate doped libraries of D2.2 and D2.3 by doping 5% of other three bases along with 85% of the original base position present in the library. The percentage of original sequence present in the doped library will be 0.2%. Although SELEX is a bet but here we are interested in performing a cell SELEX driven by D2.2 and D2.3 by doping, which can possibly generate better variants.

Aptabeacon approach as a Functional SELEX against DDR2:

In Functional SELEX, the affinity of sequences in a library is quantitatively measured individually by Fluorescent Activated Cell Sorting (FACS) in a high-throughput manner²⁷⁹. For this purpose, oligonucleotide library up to 100 million (10^8) sequences can be sorted out by FACS. Functional SELEX has been discussed in Chapter 1.

Functional SELEX has high advantages, as it provides a more efficient screening method by selecting aptamers in few rounds compared to the conventional SELEX method where the rate of decrease in diversity is very slow. It may be assumed that in conventional SELEX methods, protein targets potentially display many aptatopes with different binding affinity

SELEX Procedure:

As discussed earlier that the diversity of the starting library should be up to 10^8 sequences to perform functional SELEX. One way of decreasing the diversity of the library is to perform few rounds of conventional SELEX and then switch to functional SELEX. Soh and colleagues have reported an aptamer selection by functional SELEX in which the library was first subjected to “pre-enrichment” reducing the diversity to a scale that can be used as particle displaying aptamers generated through emulsion PCR for FACS analysis ¹⁷⁵.

With the perspective to select an aptamer against DDR2, we have recently performed 4 rounds of Magnetic Beads SELEX as shown in Table 6.1. For this purpose, we used a mixture of 30 ssDNA libraries of 30 nucleotide random window with same forward and reverse primers for amplification. The random window of all these libraries contains bases 1T and 29V (V = A, G, C). For each library the position of the thymine in the random window is changed as shown in figure 6.2. Indeed for conventional SELEX rounds, there is no need of labeling the aptabeacon library with fluorophore and quencher.

Rounds	ssDNA (pmoles)	Counter Selection	Selection	Washing PBS-Mg 1X
		DDR-1 (pmoles)	DDR-2 (pmoles)	
1	2000	10	10	5*100 μ L (1 min) 3*100 μ L (10 min)
2	175	10	10	5*100 μ L (1 min) 3*100 μ L (10 min)
3	100	05	2.5	5*100 μ L (1 min) 3*100 μ L (10 min)
4	50	02	1	5*200 μ L (1 min) 3*100 μ L (20 min)

Table 6.1: Selection conditions applied conventional-SELEX rounds against DDR2. Conditions of conventional SELEX rounds performed in order to decrease the diversity for functional SELEX.

With the aim to decrease the diversity, earlier 4 rounds of selection were performed with high stringency. As mentioned in Table 6.1, the concentration of ssDNA and DDR2 was decreased and the washing was performed with higher volume with time up to 20 minutes to discard sequences of non-interest. The agarose gel results of the first 4 rounds after PCR have been shown in figure 6.3.

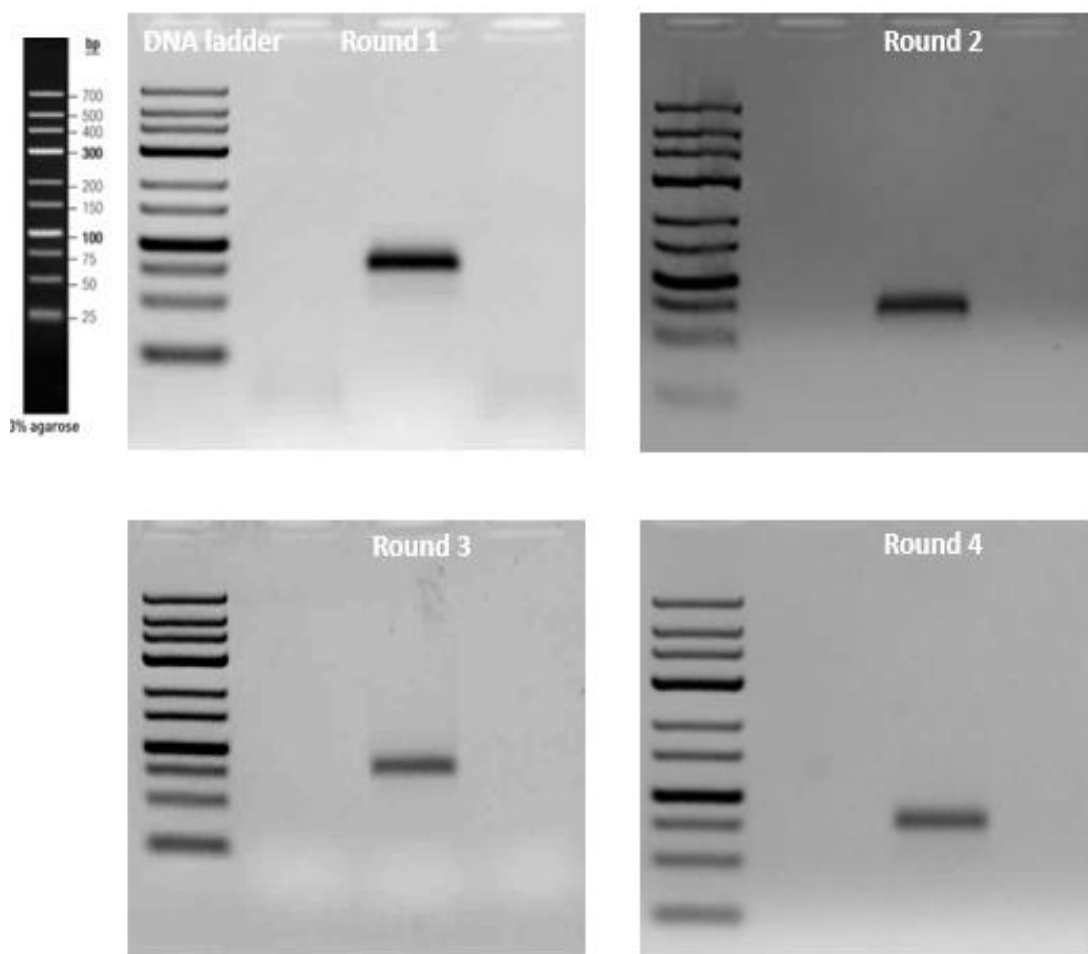


Figure 6.3: Agarose gel images of amplified rounds in conventional SELEX against DDR2. 3% agarose gel result of the first 4 rounds of DDR2 SELEX as magnetic beads SELEX. Library (72bp) can be seen with 0.5 μ g of DNA ladder in each gel. PCR was performed with Taq polymerases for each round. After PCR 4 μ L of amplified volume was loaded with loading buffer. The intensity of the band correspond to the PCR amplification has decreased as the SELEX proceeded.

The fifth round will be functional SELEX round. Scheme of functional SELEX with aptabeacon library is described in figure 6.4.

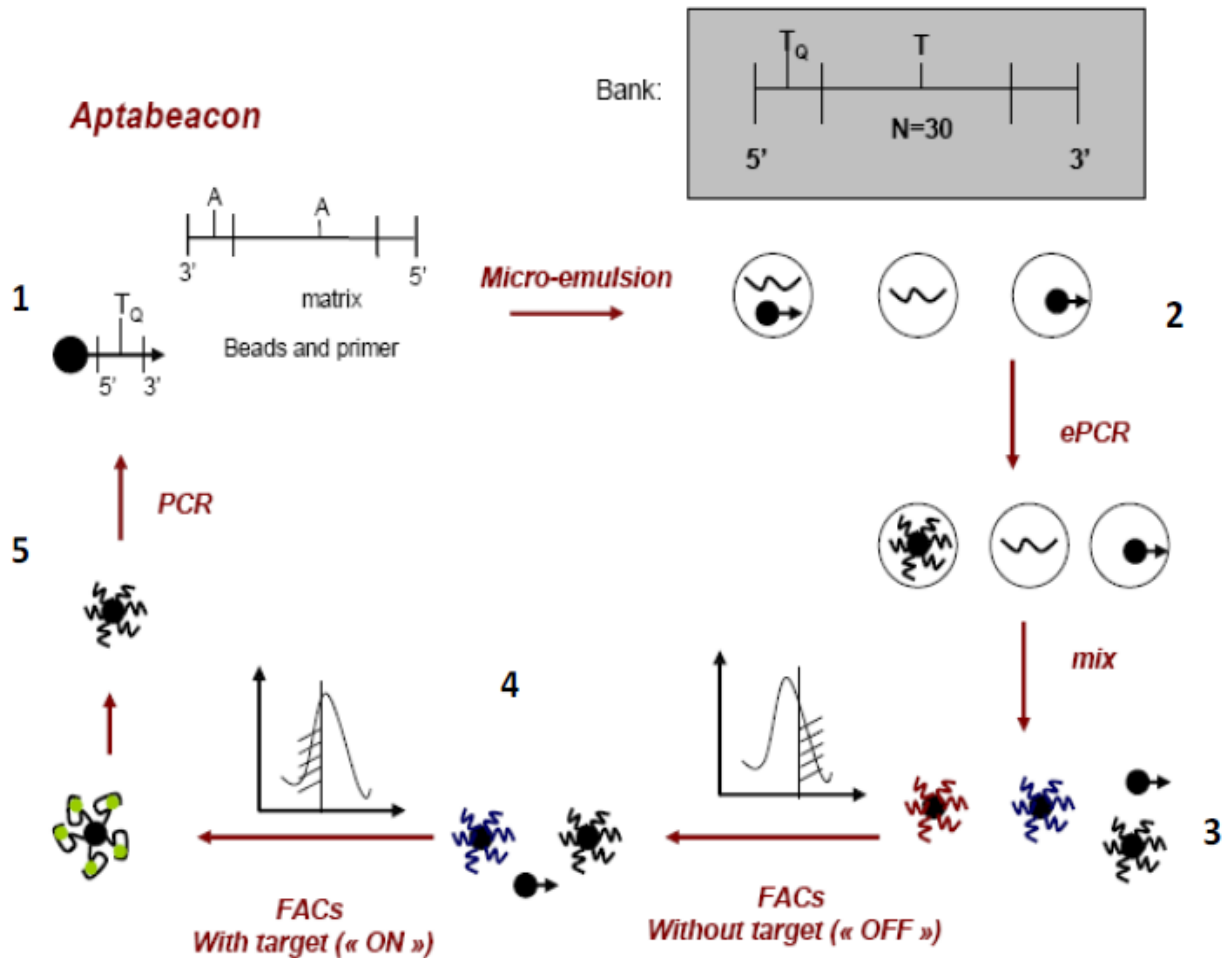


Figure 6.4: Scheme of Aptabeacon selection by Particle Display method. The scheme shows the principle of the generation of an aptabeacon and the basic underlying working steps to generate this kind of new beacons. **1** Beads are functionalized with the primer bearing a quencher Q. **2** PCR reaction in emulsion allows the amplification of the sequences and the incorporation of a homogeneous sequence population on the beads surface. **3** Breaking of the emulsion and recovering of the beads. **4** Two rounds of FACS selection elucidate the beads that show a switch depending on the presence of the ligand. **5** A PCR reaction amplifies the selected sequences and prepares the new matrix for the next round of selection and amplification.

Click SELEX against HMMP14:

SELEXs with modified bases have been discussed already in chapter 1. Here in this chapter, we will discuss only about Click-SELEX with indole to select an aptamer against HMMP14 receptor. As discussed earlier that hydrophobic aromatic side chains have the most profound influence on the success rate of SELEX. Indole is not only an aromatic but also can form another H-Bond with the target, thus increases the range of epitopes that are available for binding. Vaught has demonstrated that benzyl and indole modified nucleobases enabled successful aptamer selection whereas non-modified DNA failed to generate aptamers targeting TNRSF9²⁸². The Click-SELEX strategy was first described by Mayer and colleagues in 2015, selecting successfully an aptamer with high affinity ($K_d = 18.4$ nM) against Cycle 3 GFP using 5-ethynyl-2'-deoxyuridine triphosphate in the SELEX library instead of Thymine²³⁵. This dUTP present in the library was further derivatized with the addition of Indole by using copper(I)-catalyzed alkyne-azide cycloaddition (CuAAC) or click chemistry^{174 283}. All these results shows that SELEX with modified DNA libraries can make it more versatile and flexible to generate high affinity aptamers. Click-SELEX further makes it easy to apply due to the compatibility of Indole bearing triphosphate for enzymatic processes during SELEX thus providing an easy way to generate libraries¹⁷².

SELEX Libraries:

In order to select an aptamer against HMMP14 and to compare the SELEX, we are currently performing two SELEXs in parallel i.e. SELEX with and without Indole bearing click libraries. The random window of this library contains equal distribution of bases theoretically.

'5-CACGACGCAAGGGACACAGG-N42-CAGCACGACACCGCAGAGGCA-3'

N= dA:dG:dC:EdU = 1:1:1:1.

For Click-SELEX, the EdU in the library is further modified by adding an Indole molecule using Click reaction as shown in Figure 6.5 reported by Mayer and colleagues²³⁵. The detail about the reaction step has been discussed in chapter 2.

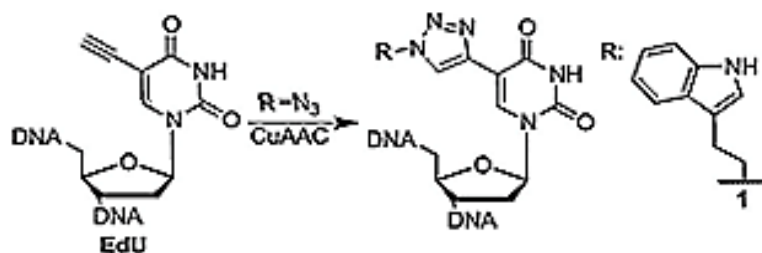


Figure 6.5: CuAAC functionalization of EdU-containing DNA molecules with Indole azide.

Comparison of Click and Non-Click SELEX Libraries by HTS Sequencing:

Before starting the SELEX, we first performed a high throughput sequencing of the libraries to analyze the compositions of bases in the random window after PCR amplification. For this purpose the samples were prepared for NGS as suggested by the sequencing platform (described in Chapter 2). For the NGS amplification of the Click-SELEX library, we first clicked the library with indole (Figure 6.5) according to the procedure discussed in Chapter 2 and later performed NGS with the clicked Library. Furthermore, dNTPs (dA, dG, dC) and EdU instead of dT were used for PCR amplification of both libraries. After sequencing, the base composition in the libraries were analyzed as shown in figure 6.6.

The NGS results shows that in non-modified library the composition of bases in the sequences are nearly in the range of 23%-24% for Adenine and Cytosine, and 27%-28% for Guanine and Thymine (Figure 6.6-A), while in modified SELEX library the percentage of EdU is less as compared to other bases (Figure 6.6-B). It is due to the lower yield of EdU, as the chemical synthesis is based on 3' to 5' that's results in less incorporation of EdU due to lower rate of reaction as compared to other natural bases. This issue can be simply overcome by increasing the percentage of EdU during chemical synthesis as Azema et al. has successfully demonstrated that rate of incorporation of different bases can be balanced through concentration modulation²⁸⁴.

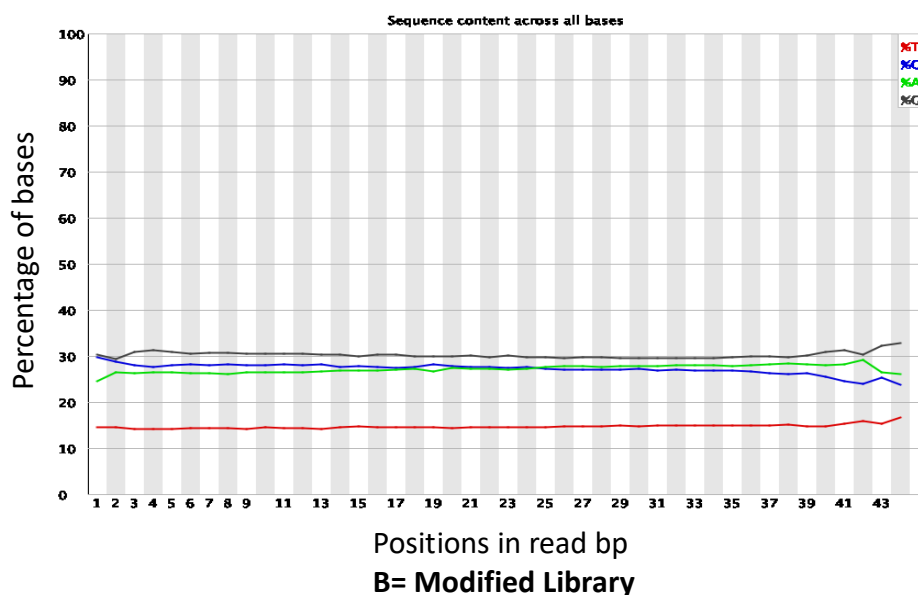
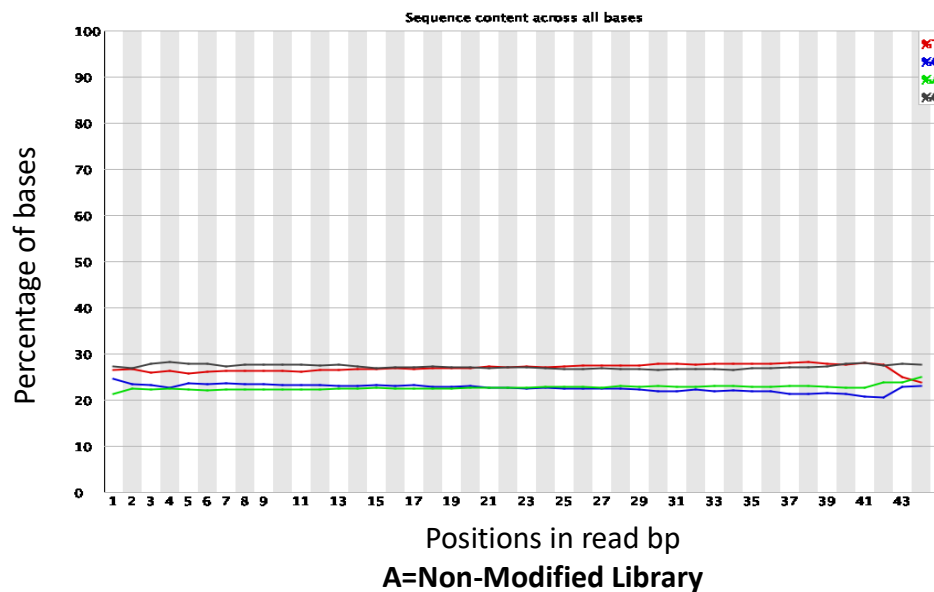


Figure 6.6: Analysis of base compositions in Click and Non-Click SELEX libraries by NGS.

It is quite evident that EdU is present in the modified library which is enough to perform Click-SELEX by addition of Indole through Click chemistry. As far as the diversity is concerned, the number of EdU bases (15%) present in the library is enough to induce diversity and to drive the SELEX successfully in generating high affinity aptamers.

SELEX with Click-Library:

We have performed 5 rounds of selection against HMMP14 receptor using Click-SELEX Library. For this purpose we used Magnetic based SELEX²⁴⁵ and Filtration SELEX¹²⁹. The detail about the SELEX procedures has given in chapter 2, while the selection protocol for Click-SELEX is given in table 6.2.

SELEX Rounds		Click-SELEX						
		Library ssDNA pmoles	CS-1 Ni /NC 5 uL	CS-2 GST-H pmoles	CS-3 HMMP2 pmoles	Selection HMMP14 pmoles	Ratio HMMP14: ssDNA	Washing PBS-Mg 1X
1	Magnetic Beads SELEX	700	5 uL	100	17.5	17.5	1:40	5*100 μ L
2	Magnetic Beads SELEX	300	5 uL	None	7.5	7.5	1:40	8*100 μ L
3	Magnetic Beads SELEX	300	5 uL	None	7.5	7.5	1:40	8*100 μ L
4	Filtration SELEX	300	NC	100	7.5	7.5	1:40	10* 1 mL
5	Filtration SELEX	100	NC	100	2.5	2.5	1:40	10* 1 mL

Table 6.2: Selection conditions applied for Click SELEX against HMMP14.

In each round of Click-SELEX, the EdU present in the library was modified with an azide-bearing Indole by CuAAC. After incubation with HMMP14 in the selection step, the bound sequences were eluted and amplified by PCR with EdU triphosphate instead of thymidine. This step removes the modification in the elongating strand and reintroduces the alkyne moiety. The azide bearing indole was then reintroduced by click chemistry (CuAAC) and the obtained library is subjected to the next selection cycle. The only limitation associated with Click-SELEX is the yield of the clicked library. We have observed that a large amount of library is required to have an efficient Click reaction to obtain enough clicked library for future rounds.

SELEX with Non-Click library:

SELEX with the EdU bearing library (without any modification by Click reaction) was also performed in order to compare the two SELEXs. We performed 5 rounds of SELEXs with Magnetic beads based SELEX and Filtration SELEX, in the same manner as Click SELEX. The ratio (1:40) of library and the target concentration was kept same to provide same competition level in the mixture between the ligand and the target for both SELEXs. Except the starting library where we initiated the non-modified SELEX with 2nmoles (for Click-SELEX, it was 700 pmoles as the yield was low). Moreover the washing volume was also kept similar as Click-SELEX (Table 6.3).

SELEX Rounds		Non Click-SELEX						
		Library ssDNA pmoles	CS-1 Ni /NC	CS-2 GST-H pmoles	CS-3 HMMP2 pmoles	Selection HMMP14 pmoles	Ratio HMMP14: ssDNA	Washing PBS-Mg 1X
1	Magnetic Beads SELEX	2000	5 μ L	None	10	10	1:200	5*100 μ L
2	Magnetic Beads SELEX	300	5 μ L	None	7.5	7.5	1:40	8*100 μ L
3	Magnetic Beads SELEX	300	5 μ L	None	7.5	7.5	1:40	8*100 μ L
4	Filtration SELEX	300	NC	100	7.5	7.5	1:40	10* 1 mL
5	Filtration SELEX	100	NC	100	2.5	2.5	1:40	10* 1 mL

Table 6.3: Selection conditions applied for Non-Click SELEX against HMMP14.

HTS Sequencing of Click-SELEX and Non-Click SELEX:

After performing 5 rounds of selection, we performed the high throughput sequencing for all rounds of both SELEX. Sequences with window range within 39-45 nucleotides were recovered while the shorter and longer sequences were discarded from the data. There was no

evidence of evolution observed in both SELEXs after performing 5 rounds in both SELEX. The diversity of the pool was still above 99 percent for each round (data not shown).

We believe that 5 rounds of selection are not enough to select a high affinity aptamer with a large library of 10^{15} sequences. Tolle et al, in their method paper for CLICK-SELEX has mentioned that 15 rounds of selection were required to select an aptamer of 18nM Kd ¹⁷³. Moreover, they have also demonstrated that the Click-SELEX started evolving from Round 6, as the starting library had a diversity of more than 10^{15} sequences.

Indeed, we are interested in selecting an aptamer which is dependant on indole moiety for its affinity as described by Tolle et al ²³⁵. Thus we want to sort the click SELEX and non-click SELEX to select interesting sequences after performing more rounds.

SUMMARY:

Aptamers are single stranded oligonucleotides with high affinity and specificity against target molecule. Since the discovery of aptamers, it has been largely translated into clinical practice. Due to the superiority of aptamers on traditional peptide or protein based ligands in terms of affinity, selectivity, chemical versatility and safety, they are extremely useful in in-vivo imaging of cancer cells. The aim of molecular imaging is to enable the precise visualization of specific markers of a pathological process, in a non-invasive manner, and thus to facilitate the subsequent establishment of appropriate treatments. Discoidin Domain Receptors (DDR) and Matrix metalloproteinases-14 (MMP-14) have been proposed as markers of tumor proliferation and invasion in melanoma. This thesis focuses on the selection of DNA aptamers against these biomarkers of melanoma, considering various aspects related to their selection from large pools of randomized ssDNA libraries.

The main focus was on selection of DNA aptamers based on alternative supports for candidates sorting with massive parallel sequencing. In **Chapter 3**, we have demonstrated the selection of DNA aptamer DS_3.1 against DDR1 which binds to its target with a K_d of 33 nM. Therefore, this developed DNA aptamer can be exploited as a promising imaging module for non-invasive cancer diagnosis. For this purpose we aim to perform an MRI imaging in xenograft model by conjugating the aptamer with silica nanoparticles. In **Chapter 4** we focused on the selection of DNA aptamer against receptor HMM14 which is highly involved in metastatic melanoma. Unfortunately after iterative rounds of SELEX without counter selection step, the selection was driven against the co-receptor histidine tag rather than HMM14 with the evolution of high affinity parasitic sequences. With the aim to select an aptamer against HMMP14, we are performing a click SELEX with indole modification on EdU which has been described to improve the versatility of aptamer. **Chapter 5** is based on the selection of an aptamer against DDR2 by cross-over SELEX. In this chapter we focused on targeting the receptor in recombinant form as well as expressing on cells. Beside low reduction in diversity, few sequences were evolved after iterative rounds of selection. Two sequences D2.2 and D2.3 evolved from cell SELEX rounds are selected based on their structural characterization. We aim to perform a cell SELEX from the doped libraries of these two sequences. Functional SELEX has been applied to select high affinity aptamers. We therefore aim to also perform functional SELEX against DDR2 by using aptabeacon library, where sequences of interest can be easily sorted by using FACS. This sorting will be based on the structural switch dependent fluorescence of the sequences on binding with target as these sequences will contain fluorescein

fluorophore on the single thymine in the random window while quencher dabcyI on the thymine in the 5' flanked region. Our final goal is to use all these aptamers as theranostic agents in melanoma cancer.

References:

1. Ernfors P. Cellular origin and developmental mechanisms during the formation of skin melanocytes. *Exp Cell Res.* 2010;316(8):1397-1407. doi:10.1016/j.yexcr.2010.02.042
2. Arnold M, Kvaskoff M, Thuret A, Guénel P, Bray F, Soerjomataram I. Cutaneous melanoma in France in 2015 attributable to solar ultraviolet radiation and the use of sunbeds. *J Eur Acad Dermatology Venereol.* 2018;32(10):1681-1686. doi:10.1111/jdv.15022
3. Damsky WE, Rosenbaum LE, Bosenberg M. Decoding melanoma metastasis. *Cancers (Basel).* 2011;3(1):126-163. doi:10.3390/cancers3010126
4. Warycha MA, Berman RS, Osman I. Meta-Analysis of Sentinel Lymph Node Positivity in Thin Melanoma (≤ 1 mm). *Cancer.* 2009;115(4):869-879. doi:10.1002/cncr.24044
5. Nguyen DX, Massagué J. Genetic determinants of cancer metastasis. *Nat Rev Genet.* 2007;8(5):341-352. doi:10.1038/nrg2101
6. Naylor S. Biomarkers: Current perspectives and future prospects. *Expert Rev Mol Diagn.* 2003;3(5):525-529. doi:10.1586/14737159.3.5.525
7. Perera FP, Weinstein IB. Molecular epidemiology: Recent advances and future directions. *Carcinogenesis.* 2000;21(3):517-524. doi:10.1093/carcin/21.3.517
8. Schulte P, Perera F. *Molecular Epidemiology: Principles and Practices.*; 1993. doi:10.5935/0004-2749.20150030
9. González-González M, Montero JAA, Fernandez LMG, et al. Genomics and proteomics approaches for biomarker discovery in sporadic colorectal cancer with metastasis. *Cancer Genomics and Proteomics.* 2013;10(1):19-26.
10. Orton D, Doucette A. Proteomic Workflows for Biomarker Identification Using Mass Spectrometry — Technical and Statistical Considerations during Initial Discovery. *Proteomes.* 2013;1(2):109-127. doi:10.3390/proteomes1020109
11. Hudler P, Kocevar N, Komel R. Proteomic Approaches in Biomarker Discovery: New Perspectives in Cancer Diagnostics. *Sci World J.* 2014;2014:1-18.

doi:10.1155/2014/260348

12. Sun Y, Wang L, Guo SC, Wu XB, Xu XH. High-throughput sequencing to identify miRNA biomarkers in colorectal cancer patients. *Oncol Lett.* 2014;8(2):711-713. doi:10.3892/ol.2014.2215
13. Karagiannis P, Fittall M, Karagiannis SN. Evaluating biomarkers in melanoma. *Front Oncol.* 2015;4(January):1-11. doi:10.3389/fonc.2014.00383
14. Carlson J, Slominski A, Linette G, Mihm Jr M, Ross J. Biomarkers in melanoma: Staging, prognosis and detection of early metastases. *Expert Rev Mol Diagn.* 2003;3(3):303-330. doi:10.1586/14737159.3.3.303
15. Paul MK, Mukhopadhyay AK. Tyrosine kinase – Role and significance in Cancer. *Int J Med Sci.* 2004;1(283):101-115. doi:10.7150/ijms.1.101
16. Robinson DR, Wu YM, Lin SF. The protein tyrosine kinase family of the human genome. *Oncogene.* 2000;19(49):5548-5557. doi:10.1038/sj.onc.1203957
17. Hubbard, Stevan R et Till JH. Protein tyrosine kinase structures and functions. *AnnuRevBiochem.* 2000;69:373-398. doi:10.1146/annurev.biochem.69.1.373
18. Johnson JD, Edman JC, Rutter WJ. A receptor tyrosine kinase found in breast carcinoma cells has an extracellular discoidin I-like domain. *Proc Natl Acad Sci U S A.* 1993;90(12):5677-5681. doi:10.1073/pnas.90.12.5677
19. Vogel W, Gish GD, Alves F, Pawson T. The Discoidin Domain Receptor Tyrosine Kinases Are Activated by Collagen. *Mol Cell.* 1997;1:13-23. doi:10.1016/S1097-2765(00)80003-9
20. Shrivastava A, Radziejewski C, Campbell E, et al. An Orphan Receptor Tyrosine Kinase Family Whose Members Serve as Nonintegrin Collagen Receptors. *Mol Cell.* 1997;1:25-34. doi:10.1016/S1097-2765(00)80004-0
21. Poole S, Firtelt RA, Rowekamp W, Germany W. Sequence and Expression of the Discoidin I Gene Family in Dictyostelium discoideum. *J Mol Biol.* 1981:273-289. doi:10.1016/0022-2836(81)90278-3
22. Johnson JD, Edmant JC, Rutter WJ. A receptor tyrosine kinase found in breast

- carcinoma cells has an extracellular discoidin I-like domain. 1993;90(June):5677-5681.
23. Vogel WF, Abdulhussein R, Ford CE. Sensing extracellular matrix: An update on discoidin domain receptor function. *Cell Signal*. 2006;18(8):1108-1116. doi:10.1016/j.cellsig.2006.02.012
 24. Leitinger B. Transmembrane Collagen Receptors. *Annu Rev Cell Dev Biol*. 2011;27(1):265-290. doi:10.1146/annurev-cellbio-092910-154013
 25. Edelhoff S, Lai C. Mapping of the Receptor Protein- Tyrosine Kinase 10 to Human Chromosome 1q21-q23 and Mouse Chromosome 1H1-5 by Fluorescence in Situ Hybridization. *Genomics*. 1995;4(10):337-339. doi:10.1016/0888-7543(95)80158-i
 26. Alves F, Saupe S, Ledwon M, Schaub F, Hiddemann W, Vogel WF. Identification of two novel, kinase-deficient variants of discoidin domain receptor 1: differential expression in human colon cancer cell lines. *FASEB J*. 2001;15(7):1321-1323. doi:10.1096/fj.00-0626fje
 27. Curat CA, Eck M, Dervillez X, Vogel WF. Mapping of Epitopes in Discoidin Domain Receptor 1 Critical for Collagen Binding. *J Biol Chem*. 2001;276(49):45952-45958. doi:10.1074/jbc.M104360200
 28. Carafoli F, Mayer MC, Shiraishi K, Pecheva MA, Chan LY, Nan R. Article Structure of the Discoidin Domain Receptor 1 Extracellular Region Bound to an Inhibitory Fab Fragment Reveals Features Important for Signaling. *Struct Des*. 2012;20(4):688-697. doi:10.1016/j.str.2012.02.011
 29. Ichikawa O, Osawa M, Nishida N, Goshima N, Nomura N, Shimada I. Structural basis of the collagen-binding mode of discoidin domain receptor 2. *EMBO J*. 2007;26(18):4168-4176. doi:10.1038/sj.emboj.7601833
 30. Xu H, Abe T, Liu JKH, Zalivina I, Hohenester E, Leitinger B. Normal Activation of Discoidin Domain Receptor 1 Mutants with Disulfide Cross-links , Insertions , or Deletions in the Extracellular Juxtamembrane Region. *J Biol Chem*. 2014;289(19):13565-13574. doi:10.1074/jbc.M113.536144
 31. Carafoli F, Bihan D, Stathopoulos S, et al. Crystallographic Insight into Collagen Recognition by Discoidin Domain Receptor 2. *Structure*. 2009;17(12):1573-1581.

- doi:10.1016/j.str.2009.10.012
32. Myllyharju J, Kivirikko KI. Collagens , modifying enzymes and their mutations in humans , flies and worms. *TRENDS Genet.* 2004;20(1):33-43.
doi:10.1016/j.tig.2003.11.004
 33. Egeblad M, Rasch MG, Weaver VM. Dynamic interplay between the collagen scaffold and tumor evolution. *Curr Opin Cell Biol.* 2010;22(5):697-706.
doi:10.1016/j.ceb.2010.08.015
 34. Leitinger B. Molecular analysis of collagen binding by the human discoidin domain receptors, DDR1 and DDR2. Identification of collagen binding sites in DDR2. *J Biol Chem.* 2003;278(19):16761-16769. doi:10.1074/jbc.M301370200
 35. Leitinger B, Kwan APL. The discoidin domain receptor DDR2 is a receptor for type X collagen. *Matrix Biol.* 2006;25:355-364. doi:10.1016/j.matbio.2006.05.006
 36. Leitinger B. Molecular Analysis of Collagen Binding by the Human Discoidin Domain Receptors , DDR1 and DDR2. *J Biol Chem.* 2003;278(19):16761-16769.
doi:10.1074/jbc.M301370200
 37. Xu H, Raynal N, Stathopoulos S, Myllyharju J, Farndale RW, Leitinger B. Collagen binding specificity of the discoidin domain receptors : Binding sites on collagens II and III and molecular determinants for collagen IV recognition by DDR1. *Matrix Biol.* 2011;30(1):16-26. doi:10.1016/j.matbio.2010.10.004
 38. Finger C, Escher C, Schneider D. The Single Transmembrane Domains of Human Receptor Tyrosine Kinases Encode Self-Interactions. *Sci Signal.* 2014;2(September 2009). doi:10.1126/scisignal.2000547
 39. Mihai C, Chotani M, Elton TS, Agarwal G. Mapping of DDR1 Distribution and Oligomerization on the Cell Surface by FRET Microscopy. *J Mol Biol.* 2009;385(2):432-445. doi:10.1016/j.jmb.2008.10.067
 40. Thomas PH, Ganesan TS, Radcliffe J, Hospital JR. Functional analysis of discoidin domain receptor 1: effect of adhesion on DDR1 phosphorylation. *FASEB J.* 2001.
doi:10.1096/fj.01-0414fje
 41. Lu KK, Trcka D, Bendeck MP. Collagen stimulates discoidin domain receptor 1-

- mediated migration of smooth muscle cells through Src. *Cardiovasc Pathol*. 2011;20(2):71-76. doi:10.1016/j.carpath.2009.12.006
42. Ikeda K, Wang LH, Torres R, et al. Discoidin domain receptor 2 interacts with Src and Shc following its activation by type I collagen. *J Biol Chem*. 2002;277(21):19206-19212. doi:10.1074/jbc.M201078200
 43. Yang K, Kim JH, Kim HJ, Park IS, Kim IY, Yang BS. Tyrosine 740 phosphorylation of discoidin domain receptor 2 by Src stimulates intramolecular autophosphorylation and Shc signaling complex formation. *J Biol Chem*. 2005;280(47):39058-39066. doi:10.1074/jbc.M506921200
 44. Azreq M-A El, Kadiri M, Boisvert M, Pagé N, Tessier PA, Aoudjit F. Discoidin domain receptor 1 promotes Th17 cell migration by activating the RhoA/ROCK/MAPK/ERK signaling pathway. *Oncotarget*. 2016;7(29). doi:10.18632/oncotarget.10455
 45. Ongusaha PP, Kim J il, Fang L, et al. p53 induction and activation of DDR1 kinase counteract p53-mediated apoptosis and influence p53 regulation through a positive feedback loop. *EMBO J*. 2003;22(6):1289-1301. doi:10.1093/emboj/cdg129
 46. Poudel B, Lee YM, Kim DK. DDR2 inhibition reduces migration and invasion of murine metastatic melanoma cells by suppressing MMP2/9 expression through ERK/NF- κ B pathway. *Acta Biochim Biophys Sin (Shanghai)*. 2015;47(4):292-298. doi:10.1093/abbs/gmv005
 47. Xu H, Bihan D, Chang F, Leitinger B. Discoidin Domain Receptors Promote α 1b1- and α 2b1- Integrin Mediated Cell Adhesion to Collagen by Enhancing Integrin Activation. *PLoS One*. 2012;7(12):1-12. doi:10.1371/journal.pone.0052209
 48. Iwai LK, Chang F, Huang PH. Phosphoproteomic analysis identifies insulin enhancement of discoidin domain receptor 2 phosphorylation. *Cell Adhes Migr*. 2013;7(2):161-164. doi:10.4161/cam.22572
 49. Valiathan RR, Marco M, Leitinger B, Kleer CG, Fridman R. Discoidin domain receptor tyrosine kinases: New players in cancer progression. *Cancer Metastasis Rev*. 2012;31(1-2):295-321. doi:10.1007/s10555-012-9346-z

50. Das S, Ongusaha PP, Yang YS, Park JM, Aaronson SA, Lee SW. Discoidin domain receptor 1 receptor tyrosine kinase induces cyclooxygenase-2 and promotes chemoresistance through nuclear factor- κ B pathway activation. *Cancer Res.* 2006;66(16):8123-8130. doi:10.1158/0008-5472.CAN-06-1215
51. Kim HG, Hwang SY, Aaronson SA, Mandinova A, Lee SW. DDR1 receptor tyrosine kinase promotes prosurvival pathway through Notch1 activation. *J Biol Chem.* 2011;286(20):17672-17681. doi:10.1074/jbc.M111.236612
52. Shintani Y, Fukumoto Y, Chaika N, Svoboda R, Wheelock MJ, Johnson KR. Collagen I-mediated up-regulation of N-cadherin requires cooperative signals from integrins and discoidin domain receptor. *J Cell Biol.* 2008;180(6):1277-1289. doi:10.1083/jcb.200708137
53. Poudel B, Lee YM, Kim DK. DDR2 inhibition reduces migration and invasion of murine metastatic melanoma cells by suppressing MMP2/9 expression through ERK/NF- κ B pathway. *Acta Biochim Biophys Sin (Shanghai).* 2015;47(4):292-298. doi:10.1093/abbs/gmv005
54. Hammerman PS, Sos ML, Ramos AH, et al. Mutations in the DDR2 kinase gene identify a novel therapeutic target in squamous cell lung cancer. *Cancer Discov.* 2011;1(1):78-89. doi:10.1158/2159-8274.CD-11-0005
55. Ram R, Lorente G, Nikolich K, Urfer R, Foehr E, Nagavarapu U. Discoidin domain receptor-1a (DDR1a) promotes glioma cell invasion and adhesion in association with matrix metalloproteinase-2. *J Neurooncol.* 2006;76(3):239-248. doi:10.1007/s11060-005-6874-1
56. Quan J, Yahata T, Adachi S, Yoshihara K, Tanaka K. Identification of receptor tyrosine kinase, discoidin domain receptor 1 (DDR1), as a potential biomarker for serous ovarian cancer. *Int J Mol Sci.* 2011;12(2):971-982. doi:10.3390/ijms12020971
57. Shen Q, Cicinnati VR, Zhang X, et al. Role of microRNA-199a-5p and discoidin domain receptor 1 in human hepatocellular carcinoma invasion. *Mol Cancer.* 2010;9:1-12. doi:10.1186/1476-4598-9-227
58. Chiaretti S, Li X, Gentleman R, et al. Gene expression profiles of B-lineage adult acute lymphocytic leukemia reveal genetic patterns that identify lineage derivation and

- distinct mechanisms of transformation. *Clin Cancer Res.* 2005;11(20):7209-7219.
doi:10.1158/1078-0432.CCR-04-2165
59. Hanahan D, Weinberg RA. Hallmarks of cancer: the next generation. *Cell.* 2011;144(5):646-674. doi:10.1016/j.cell.2011.02.013
 60. Henriët E, Sala M, Abou Hammoud A, et al. Multitasking discoidin domain receptors are involved in several and specific hallmarks of cancer. *Cell Adhes Migr.* 2018;12(4):363-377. doi:10.1080/19336918.2018.1465156
 61. Juin A, Di Martino J, Leitinger B, et al. Discoidin domain receptor 1 controls linear invadosome formation via a Cdc42-Tuba pathway. *J Cell Biol.* 2014;207(4):517-533. doi:10.1083/jcb.201404079
 62. Wang C-Z, Yeh Y-C, Tang M-J. DDR1/E-cadherin complex regulates the activation of DDR1 and cell spreading. *Am J Physiol Physiol.* 2009;297(2):C419-C429. doi:10.1152/ajpcell.00101.2009
 63. Siddiqui K, Kim GW, Lee DH, et al. Actinomycin D Identified as an Inhibitor of Discoidin Domain Receptor 2 Interaction with Collagen through an Insect Cell Based Screening of a Drug Compound Library. *Biol Pharm Bull.* 2009;32(1):136-141. doi:10.1248/bpb.32.136
 64. Rix U, Hantschel O, Dürnberger G, et al. nilotinib , and dasatinib reveal Chemical proteomic profiles of the BCR-ABL inhibitors imatinib , nilotinib , and dasatinib reveal novel kinase and nonkinase targets. *Neoplasia.* 2012;110(12):4055-4063. doi:10.1182/blood-2007-07-102061
 65. Canning P, Tan L, Chu K, Lee SW, Gray NS, Bullock AN. Structural mechanisms determining inhibition of the collagen receptor DDR1 by selective and multi-targeted type II kinase inhibitors. *J Mol Biol.* 2014;426(13):2457-2470. doi:10.1016/j.jmb.2014.04.014
 66. Kryza D, Debordeaux F, Azéma L, et al. Ex Vivo and In Vivo Imaging and Biodistribution of Aptamers Targeting the Human Matrix MetalloProtease-9 in Melanomas. *PLoS One.* 2016;11(2):e0149387. doi:10.1371/journal.pone.0149387
 67. Camorani S, Crescenzi E, Colecchia D, et al. Aptamer targeting EGFRvIII mutant

- hampers its constitutive autophosphorylation and affects migration, invasion and proliferation of glioblastoma cells. *Oncotarget*. 2015;5. doi:10.18632/oncotarget.6066
68. Timpl R, Brown JC. Supramolecular assembly of basement membranes. *Bioessays*. 1995;18(2):123-132. doi:10.1002/bies.950180208
 69. Egeblad M, Werb Z. New functions for the matrix metalloproteinases in cancer progression. *Nat Rev Cancer*. 2002;2(3):161-174. doi:10.1038/nrc745
 70. Streuli C. ECM remodeling and differentiation. *Curr Opin Cell Biol*. 1999;11:634-640. doi:10.1016/s0955-0674(99)00026-5
 71. Tchetverikov I, Lohmander LS, Verzijl N, et al. MMP protein and activity levels in synovial fluid from patients with joint injury, inflammatory arthritis, and osteoarthritis. *Ann Rheum Dis*. 2005;64(5):694-698. doi:10.1136/ard.2004.022434
 72. Gross J, Lapiere CM. Collagenolytic Activity in Amphibian Tissues: a Tissue Culture Assay. *Proc Natl Acad Sci*. 1962;48(6):1014-1022. doi:10.1073/pnas.48.6.1014
 73. Löffek S, Schilling O, Franzke CW. Series “matrix metalloproteinases in lung health and disease” edited by J. Müller-Quernheim and O. Eickelberg number 1 in this series: Biological role of matrix metalloproteinases: A critical balance. *Eur Respir J*. 2011;38(1):191-208. doi:10.1183/09031936.00146510
 74. Chantrain C, DeClerck YA. Les métalloprotéases matricielles et leurs inhibiteurs synthétiques dans la progression tumorale. *Medecine/Sciences*. 2002;18(5):565-575. doi:10.1051/medsci/2002185565
 75. Bode W, Fernandez-Catalan C, Tschesche H, Grams F, Nagase H, Maskos K. Structural properties of matrix metalloproteinases. *Cell Mol Life Sci*. 1999;55(4):639-652. doi:10.1007/s000180050320
 76. Massova I, Kotra LP, Mobashery S, Fridman R. Matrix metalloproteinases: Structures, evolution, and diversification. *FASEB J*. 1998;12(12):1075-1095. doi:10.1096/fasebj.12.12.1075
 77. Murphy G, J.P DA. The Matrix metalloproteinases and their inhibitors. *AmJRespirCell MolBiol*. 1992;7:120-125. doi:10.1165/ajrcmb/7.2.120

78. Ferrantini M, Belardelli F. Gene therapy of cancer with interferon: Lessons from tumor models and perspectives for clinical applications. *Semin Cancer Biol.* 2000;10(2):145-157. doi:10.1006/scbi.2000.0333
79. Stöcker W, Grams F, Reinemer P, et al. The metzincins — Topological and sequential relations between the astacins, adamalysins, serralyins, and matrixins (collagenases) define a super family of zinc-peptidases. *Protein Sci.* 1995;4(5):823-840. doi:10.1002/pro.5560040502
80. Galazka G, Windsor LJ, Birkedal-Hansen H, Engler JA. APMA (4-aminophenylmercuric acetate) activation of stromelysin-1 involves protein interactions in addition to those with cysteine-75 in the propeptide. *Biochemistry.* 1996;35(34):11221-11227. doi:10.1021/bi960618e
81. Springman EB, Angleton EL, Birkedal-Hansen H, Van Wart HE. Multiple modes of activation of latent human fibroblast collagenase: Evidence for the role of a Cys73 active-site zinc complex in latency and a “cysteine switch” mechanism for activation. *Proc Natl Acad Sci U S A.* 1990;87(1):364-368. doi:10.1073/pnas.87.1.364
82. Pei D, Weiss SJ. Furin-dependent intracellular activation of the human stromelysin-3 zymogen. *Nature.* 1995;375(6528):244-247. doi:10.1038/375244a0
83. Kang T, Pei D, Nagase H. Activation of membrane-type matrix metalloproteinase 3 zymogen by the proprotein convertase furin in the trans-Golgi network. *Cancer Res.* 2002;62(3):675-681.
84. Moore WGI, Bodden MK, Windsor LJ, Decarlo A, Engler JA. Matrix Metalloproteinases : A Review *. *Crit Rev Oral Biol Med.* 1993;4(2):197-250. doi:10.1177/10454411930040020401
85. Ninomiya-tsuji J, Kishimoto K, Hiyama A. The kinase TAK1 can activate the NIK-I κ B as well as the MAP kinase cascade in the IL-1 signalling pathway. *Nature.* 1999;398(March 1999):252-256. doi:10.1038/18465
86. Han Y, Tuan T, Wu H, Hughes M, Garner WL. TNF- α stimulates activation of pro-MMP2 in human skin through NF- κ B mediated induction of MT1-MMP. *J Cell Sci.* 2000;114:131-139.

87. Lafleur MA, Handsley MM, Knäuper V, Murphy G, Edwards DR. Endothelial tubulogenesis within fibrin gels specifically requires the activity of membrane-type-matrix metalloproteinases (MT-MMPs). *J Cell Sci.* 2002;115:3427-3428.
88. Okada A, Bellocq J, Rouyert N, et al. Membrane-type matrix metalloproteinase (MT-MMP) gene is expressed in stromal cells of human colon , breast , and head and neck carcinomas. *proc Natl Acad Sci.* 1995;92(March):2730-2734.
doi:10.1073/pnas.92.7.2730
89. Gen L, Beatriz GG, Gonzalo P, Arroyo AG. MT1-MMP : Universal or particular player in angiogenesis ? *Cancer Metastasis Rev.* 2006;25:77-86. doi:10.1007/s10555-006-7891-z
90. Coussensq LM. Matrix metalloproteinases and the development of cancer. *Chem Biol.* 1996;3:895-904. doi:10.1016/s1074-5521(96)90178-7
91. Nakada M, Yamada A, Takino T, et al. Suppression of Membrane-type 1 Matrix Metalloproteinase (MMP) -mediated MMP- 2 Activation and Tumor Invasion by Testican 3 and Its Splicing Variant Gene Product, N-Tes1. *Cancer Res.* 2001;61:8896-8902.
92. D'Ortho MP, Will H, Atkinson S, et al. Membrane-type matrix metalloproteinases 1 and 2 exhibit broad-spectrum proteolytic capacities comparable to many matrix metalloproteinases. *Eur J Biochem.* 1997;250(3):751-757. doi:10.1111/j.1432-1033.1997.00751.x
93. Bu FH, Hughes CE, Margerie D, et al. Membrane type 1 matrix metalloproteinase (MT1-MMP) cleaves the recombinant aggrecan substrate rAgg1mut at the 'aggrecanase' and the MMP sites. . Characterization of MT1-MMP catabolic activities on the interglobular domain of aggrecan. *Biochem J.* 1998;165:159-165.
doi:10.1042/bj3330159
94. Baramova EN, Bajou K, Remacle A, et al. Involvement of PA / plasmin system in the processing of pro-MMP-9 and in the second step of pro-MMP-2 activation. *FEBS Lett.* 1997;405(2):157-162. doi:10.1016/S0014-5793(97)00175-0
95. Dollery CM, Libby P. Atherosclerosis and proteinase activation. *Cardiovasc Res.* 2006;69(3):625-635. doi:10.1016/j.cardiores.2005.11.003

96. Tuerk C, Gold L. Systematic evolution of ligands by exponential enrichment: RNA ligands to bacteriophage T4 DNA polymerase. *Science*. 1990;249(4968):505-510. doi:10.1126/science.2200121
97. AD E, JW S. In vitro selection of RNA molecules that bind specific ligands. *Nature*. 1990;346(6287):818-822. doi:10.1038/346183a0
98. Da Rocha Gomes S, Miguel J, Azéma L, et al. ^{99m}Tc-MAG3-aptamer for imaging human tumors associated with high level of matrix metalloprotease-9. *Bioconjug Chem*. 2012;23(11):2192-2200. doi:10.1021/bc300146c
99. Sett A, Borthakur BB, Bora U. Selection of DNA aptamers for extra cellular domain of human epidermal growth factor receptor 2 to detect HER2 positive carcinomas. *Clin Transl Oncol*. 2017;19(8):976-988. doi:10.1007/s12094-017-1629-y
100. Damase TR, Miura TA, Parent CE, Allen PB. Application of the Open qPCR Instrument for the in Vitro Selection of DNA Aptamers against Epidermal Growth Factor Receptor and Drosophila C Virus. *ACS Comb Sci*. 2018;20(2):45-54. doi:10.1021/acscombsci.7b00138
101. Percze K, Szakács Z, Scholz É, et al. Aptamers for respiratory syncytial virus detection. *Sci Rep*. 2017;7(February):1-11. doi:10.1038/srep42794
102. Kim YS, Song MY, Jurng J, Kim BC. Isolation and characterization of DNA aptamers against Escherichia coli using a bacterial cell-systematic evolution of ligands by exponential enrichment approach. *Anal Biochem*. 2013;436(1):22-28. doi:10.1016/j.ab.2013.01.014
103. Wang L, Wang R, Wei H, Li Y. Selection of aptamers against pathogenic bacteria and their diagnostics application. *World J Microbiol Biotechnol*. 2018;34(10):0. doi:10.1007/s11274-018-2528-2
104. Duan N, Wu S, Chen X, et al. Selection and characterization of aptamers against Salmonella Typhimurium using whole-bacterium SELEX. *J Agric Food Chem*. 2013;61:3229-3234. doi:10.1021/jf400767d
105. Rangel AE, Chen Z, Ayele TM, Heemstra JM. In vitro selection of an XNA aptamer capable of small-molecule recognition. *Nucleic Acids Res*. 2018;46(16):8057-8068.

doi:10.1093/nar/gky667

106. Takeuchi Y, Endo M, Suzuki Y, et al. Single-molecule observations of RNA-RNA kissing interactions in a DNA nanostructure. *Biomater Sci.* 2016;4(1):130-135.
doi:10.1039/c5bm00274e
107. Hicke BJ, Marion C, Chang YF, et al. Tenascin-C Aptamers Are Generated Using Tumor Cells and Purified Protein. *J Biol Chem.* 2001;276(52):48644-48654.
doi:10.1074/jbc.M104651200
108. Sefah K, Shangguan D, Xiong X, O'Donoghue MB, Tan W. Development of DNA aptamers using cell-selex. *Nat Protoc.* 2010;5(6):1169-1185.
doi:10.1038/nprot.2010.66
109. Civit L, Theodorou I, Frey F, et al. Targeting hormone refractory prostate cancer by in vivo selected DNA libraries in an orthotopic xenograft mouse model. *Sci Rep.* 2019;9(1):1-16. doi:10.1038/s41598-019-41460-2
110. Tuerk C, Gold L. Systematic evolution of ligands by exponential enrichment: Chemi-SELEX. *Science (80-)*. 1990;249(August):505-510.
<http://www.google.com/patents/US6300074>.
111. Musheev MU, Krylov SN. Selection of aptamers by systematic evolution of ligands by exponential enrichment: Addressing the polymerase chain reaction issue. *Anal Chim Acta.* 2006;564(1):91-96. doi:10.1016/j.aca.2005.09.069
112. Stoltenburg R, Reinemann C, Strehlitz B. SELEX-A (r)evolutionary method to generate high-affinity nucleic acid ligands. *Biomol Eng.* 2007;24(4):381-403.
doi:10.1016/j.bioeng.2007.06.001
113. Alshaer W, Hillaireau H, Vergnaud J, Ismail S, Fattal E. Functionalizing Liposomes with anti-CD44 Aptamer for Selective Targeting of Cancer Cells. *Bioconjug Chem.* November 2014. doi:10.1021/bc5004313
114. Boomer RM, Lewis SD, Healy JM, Kurz M, Wilson C, McCauley TG. Conjugation to Polyethylene Glycol Polymer Promotes Aptamer Biodistribution to Healthy and Inflamed Tissues. *Oligonucleotides.* 2005;15(3):183-195. doi:10.1089/oli.2005.15.183
115. Ni S, Yao H, Wang L, et al. Chemical modifications of nucleic acid aptamers for

- therapeutic purposes. *Int J Mol Sci.* 2017;18(8). doi:10.3390/ijms18081683
116. de Smidt PC, Doan T Le, Falco S de, Berkel TJC va. Association of antisense oligonucleotides with lipoproteins prolongs the plasma half-life and modifies the tissue distribution. *Nucleic Acids Res.* 2007;19(17):4695-4700. doi:10.1093/nar/19.17.4695
 117. Noeske J, Buck J, Wöhnert J, Schwalbe H. Non-Protein Coding RNAs. 2009;13:229-230. doi:10.1007/978-3-540-70840-7
 118. Rentmeister A, Mayer G, Kuhn N, Famulok M. Conformational changes in the expression domain of the Escherichia coli thiM riboswitch. *Nucleic Acids Res.* 2007;35(11):3713-3722. doi:10.1093/nar/gkm300
 119. Sun H, Zhu X, Lu PY, Rosato RR, Tan W, Zu Y. Oligonucleotide aptamers: New tools for targeted cancer therapy. *Mol Ther - Nucleic Acids.* 2014;3(April). doi:10.1038/mtna.2014.32
 120. Westhof E, Patel DJ. Nucleic acids from self-assembly to induced-fit recognition. Editorial overview. *Curr Opin Struct Biol.* 1997;7(3):305-309. doi:10.1016/S0959-440X(97)80044-9
 121. Stoltenburg R, Strehlitz B. Refining the results of a classical SELEX experiment by expanding the sequence data set of an aptamer pool selected for protein A. *Int J Mol Sci.* 2018;19(2). doi:10.3390/ijms19020642
 122. Quang NN, Bouvier C, Henriques A, Lelandais B, Ducongé F. Time-lapse imaging of molecular evolution by high-throughput sequencing. *Nucleic Acids Res.* 2018;46(15):7480-7494. doi:10.1093/nar/gky583
 123. Bruno JG. In vitro selection of DNA to chloroaromatics using magnetic microbead-based affinity separation and fluorescence detection. *Biochem Biophys Res Commun.* 1997;234(1):117-120. doi:10.1006/bbrc.1997.6517
 124. Murphy MB. An improved method for the in vitro evolution of aptamers and applications in protein detection and purification. *Nucleic Acids Res.* 2003;31(18):110e - 110. doi:10.1093/nar/gng110
 125. Stoltenburg R, Reinemann C, Strehlitz B. FluMag-SELEX as an advantageous method for DNA aptamer selection. *Anal Bioanal Chem.* 2005;383(1):83-91.

doi:10.1007/s00216-005-3388-9

126. Wu X, Chen J, Wu M, Zhao JX. Aptamers: Active targeting ligands for cancer diagnosis and therapy. *Theranostics*. 2015;5(4):322-344. doi:10.7150/thno.10257
127. Atzberger P, Gerdon AE, Xiao Y, et al. Micromagnetic selection of aptamers in microfluidic channels. *Proc Natl Acad Sci*. 2009;106(9):2989-2994. doi:10.1073/pnas.0813135106
128. Pristoupil T., Kramlova.M. Microchromatographic separation of ribonucleic acids from proteins on nitrocellulose membranes. *J Chromatog*. 1968;32:769-770. doi:10.1016/s0021-9673(01)80565-3
129. Challa S, Tzipori S, Sheoran A. Selective Evolution of Ligands by Exponential Enrichment to Identify RNA Aptamers against Shiga Toxins. *J Nucleic Acids*. 2014;2014:1-8. doi:10.1155/2014/214929
130. Song KM, Lee S, Ban C. Aptamers and their biological applications. *Sensors*. 2012;12(1):612-631. doi:10.3390/s120100612
131. Ohuchi S. Cell-SELEX Technology. *Biores Open Access*. 2012;1(6):265-272. doi:10.1089/biores.2012.0253
132. Blank M, Weinschenk T, Priemer M, Schluesener H. Systematic Evolution of a DNA Aptamer Binding to Rat Brain. 2001;276(19):16464-16468. doi:10.1074/jbc.M100347200
133. Ara MN, Hyodo M, Ohga N, Hida K, Harashima H. Development of a Novel DNA Aptamer Ligand Targeting to Primary Cultured Tumor Endothelial Cells by a Cell-Based SELEX Method. *PLoS One*. 2012;7(12). doi:10.1371/journal.pone.0050174
134. Jiménez E, Sefah K, López-Colón D, et al. Generation of Lung Adenocarcinoma DNA Aptamers for Cancer Studies. *PLoS One*. 2012;7(10):1-7. doi:10.1371/journal.pone.0046222
135. Kunii T, Ogura SI, Mie M, Kobatake E. Selection of DNA aptamers recognizing small cell lung cancer using living cell-SELEX. *Analyst*. 2011;136(7):1310-1312. doi:10.1039/c0an00962h

136. Thiel WH, Bair T, Peek AS, et al. Rapid Identification of Cell-Specific , Internalizing RNA Aptamers with Bioinformatics Analyses of a Cell-Based Aptamer Selection. 2012;7(9). doi:10.1371/journal.pone.0043836
137. Mayer G, Ahmed ML, Dolf A, Endl E, Knolle PA, Famulok M. Fluorescence-activated cell sorting for aptamer SELEX with cell mixtures. 2010;5(12):1993-2004. doi:10.1038/nprot.2010.163
138. Moon J, Kim G, Lee S, Park S. Identification of Salmonella Typhimurium-specific DNA aptamers developed using whole-cell SELEX and FACS analysis. *J Microbiol Methods*. 2013;95(2):162-166. doi:10.1016/j.mimet.2013.08.005
139. Berkhout B, Klaver B. In vivo selection of randomly mutated retroviral genomes. 1993;21(22):5020-5024.
140. Bel N Van, Das AT, Berkhout B. In Vivo SELEX of Single-Stranded Domains in the HIV-1 Leader RNA. 2014;88(4):1870-1880. doi:10.1128/JVI.02942-13
141. Mi J, Liu Y, Rabbani ZN, et al. In vivo selection of tumor-targeting RNA motifs. *Nat Chem Biol*. 2010;6(1):22-24. doi:10.1038/nchembio.277
142. Mi J, Ray P, Liu J, et al. In Vivo Selection Against Human Colorectal Cancer Xenografts Identifies an Aptamer That Targets RNA Helicase Protein DHX9. *Mol Ther - Nucleic Acids*. 2016;5(April):e315. doi:10.1038/mtna.2016.27
143. Chen L, He W, Jiang H, et al. In vivo SELEX of bone targeting aptamer in prostate cancer bone metastasis model. *Int J Nanomedicine*. 2019;14:149-159. doi:10.2147/IJN.S188003
144. Wang H, Zhang Y, Yang H, et al. In Vivo SELEX of an Inhibitory NSCLC-Specific RNA Aptamer from PEGylated RNA Library. *Mol Ther Nucleic Acid*. 2018;10(March):187-198. doi:10.1016/j.omtn.2017.12.003
145. Cheng C, Chen YH, Lennox KA, Behlke MA, Davidson BL. In vivo SELEX for identification of brain-penetrating aptamers. *Mol Ther - Nucleic Acids*. 2013;2(January):e67. doi:10.1038/mtna.2012.59
146. Mendonsa SD, Bowser MT. In Vitro Evolution of Functional DNA Using Capillary Electrophoresis. *J Am Chem Soc*. 2004;126(1):20-21. doi:10.1021/ja037832s

147. Bowser MT, K. MR. Isolating Aptamers Using Capillary Electrophoresis–SELEX (CE–SELEX). *Methods Mol Biol.* 2009;535:v-vi. doi:10.1007/978-1-59745-557-2
148. Dembowski SK, Bowser MT. CE-SELEX : Rapid Aptamer Selection Using Capillary Electrophoresis. *AB Sciex.* 2016:1-10. [https://sciex.com/Documents/tech notes/ce-selex-rapid-aptamer-selection.pdf](https://sciex.com/Documents/tech%20notes/ce-selex-rapid-aptamer-selection.pdf).
149. Mallikaratchy P, Stahelin R V, Cao Z, Cho W, Tan W. Selection of DNA ligands for protein kinase C- δ . *Chem Commun.* 2006;(30):3229-3231. doi:10.1039/b604778e
150. Tang J, Xie J, Shao N, Yan Y. The DNA aptamers that specifically recognize ricin toxin are selected by two in vitro selection methods. *Electrophoresis.* 2006;27(7):1303-1311. doi:10.1002/elps.200500489
151. Berezovski M V., Musheev MU, Drabovich AP, Jitkova J V., Krylov SN. Non-SELEX: Selection of aptamers without intermediate amplification of candidate oligonucleotides. *Nat Protoc.* 2006;1(3):1359-1369. doi:10.1038/nprot.2006.200
152. Lisi S, Fiore E, Scarano S, et al. Non-SELEX isolation of DNA aptamers for the homogeneous-phase fluorescence anisotropy sensing of tau Proteins. *Anal Chim Acta.* 2018;1038:173-181. doi:10.1016/j.aca.2018.07.029
153. Jing M, Bowser MT. Isolation of DNA aptamers using micro free flow electrophoresis. *Lab Chip.* 2011;11(21):3703-3709. doi:10.1039/c1lc20461k
154. Hybarger G, Bynum J, Williams RF, Valdes JJ, Chambers JP. A microfluidic SELEX prototype. *Anal Bioanal Chem.* 2006;384(1):191-198. doi:10.1007/s00216-005-0089-3
155. Ryckelynck M, Baudrey S, Rick C, et al. Using droplet-based microfluidics to improve the catalytic properties of RNA under multiple-turnover conditions. *Rna.* 2015;21(3):458-469. doi:10.1261/rna.048033.114
156. Trachman RJ, Abdolahzadeh A, Andreoni A, et al. Crystal Structures of the Mango-II RNA Aptamer Reveal Heterogeneous Fluorophore Binding and Guide Engineering of Variants with Improved Selectivity and Brightness. *Biochemistry.* 2018;57(26):3544-3548. doi:10.1021/acs.biochem.8b00399
157. Autour A, Jeng SCY, Cawte AD, et al. Fluorogenic RNA Mango aptamers for imaging small non-coding RNAs in mammalian cells. *Nat Commun.* 2018;9(1).

doi:10.1038/s41467-018-02993-8

158. Nutiu R, Li Y. In vitro selection of structure-switching signaling aptamers. *Angew Chemie - Int Ed*. 2005;44(7):1061-1065. doi:10.1002/anie.200461848
159. Stoltenburg R, Nikolaus N, Strehlitz B. Capture-SELEX: Selection of DNA aptamers for aminoglycoside antibiotics. *J Anal Methods Chem*. 2012;1(1). doi:10.1155/2012/415697
160. Paniel N, Istamboulié G, Triki A, Lozano C, Barthelmebs L, Noguier T. Selection of DNA aptamers against penicillin G using Capture-SELEX for the development of an impedimetric sensor. *Talanta*. 2017;162(July 2016):232-240. doi:10.1016/j.talanta.2016.09.058
161. Spiga FM, Maietta P, Guiducci C. More DNA-aptamers for small drugs: A capture-SELEX coupled with surface plasmon resonance and high-throughput sequencing. *ACS Comb Sci*. 2015;17(5):326-333. doi:10.1021/acscombsci.5b00023
162. Lauridsen LH, Doessing HB, Long KS, Nielsen AT. A capture-SELEX strategy for multiplexed selection of RNA aptamers against small molecules. *Methods Mol Biol*. 2018;1671:291-306. doi:10.1007/978-1-4939-7295-1_18
163. Boussebayle A, Groher F, Suess B. RNA-based Capture-SELEX for the selection of small molecule-binding aptamers. *Methods*. 2019;161(March):10-15. doi:10.1016/j.ymeth.2019.04.004
164. Boussebayle A, Torka D, Ollivaud S, et al. Next-level riboswitch development—implementation of Capture-SELEX facilitates identification of a new synthetic riboswitch. *Nucleic Acids Res*. 2019;47(9):4883-4895. doi:10.1093/nar/gkz216
165. Boder ET, Wittrup KD. Yeast surface display for screening combinatorial polypeptide libraries. *Nat Biotechnol*. 1997;15:553-557. doi:10.1038/nbt0697-553
166. Wang J, Gong Q, Maheshwari N, Eisenstein M, Arcila ML, Soh HT. Particle Display: A Quantitative Screening Method for Generating High-Affinity Aptamers**. *Angew Chem Int Ed Engl*. 2014;53(19):4796-4801. doi:10.1002/anie.201xxxxxx
167. Luo Z, He L, Wang J, Fang X, Zhang L. Developing a combined strategy for monitoring the progress of aptamer selection. *Analyst*. 2017;142(17):3136-3139.

doi:10.1039/c7an01131h

168. Diehl F, Li M, He Y, Kinzler KW, Vogelstein B, Dressman D. BEAMing: Single-molecule PCR on microparticles in water-in-oil emulsions. *Nat Methods*. 2006;3(7):551-559. doi:10.1038/nmeth898
169. Autour A, Westhof E, Ryckelynck M. ISpinach: A fluorogenic RNA aptamer optimized for in vitro applications. *Nucleic Acids Res*. 2016;44(6):2491-2500. doi:10.1093/nar/gkw083
170. Gold L, Ayers D, Bertino J, et al. Aptamer-based multiplexed proteomic technology for biomarker discovery. *PLoS One*. 2010;5(12). doi:10.1371/journal.pone.0015004
171. Kimoto M, Yamashige R, Matsunaga K, Yokoyama S, Hirao I. Generation of high-affinity DNA aptamers using an expanded genetic alphabet. *Nat Biotechnol*. 2013;(September 2012):1-6. doi:10.1038/nbt.2556
172. Kornreich-Leshem H, Jäger S, Thum O, Rasched G, Famulok M, Engeser M. A Versatile Toolbox for Variable DNA Functionalization at High Density. *J Am Chem Soc*. 2005;127(43):15071-15082. doi:10.1021/ja051725b
173. Pfeiffer F, Tolle F, Rosenthal M, Brändle GM, Ewers J, Mayer G. Identification and characterization of nucleobase-modified aptamers by click-SELEX. *Nat Protoc*. 2018;13(5):1153-1180. doi:10.1038/nprot.2018.023
174. El-Sagheer AH, Brown T. Click chemistry with DNA. *Chem Soc Rev*. 2010;39(4):1388-1405. doi:10.1039/b901971p
175. Gordon CKL, Wu D, Feagin TA, et al. Click-PD: A Quantitative Method for Base-Modified Aptamer Discovery. *bioRxiv*. 2019:626572. doi:10.1101/626572
176. Sefah K, Yang Z, Bradley KM, et al. In vitro selection with artificial expanded genetic information systems. *Proc Natl Acad Sci*. 2014;111(4):1449-1454. doi:10.1073/pnas.1311778111
177. Hollenstein M, Hipolito CJ, Lam CH, Perrin DM. Toward the combinatorial selection of chemically modified DNAzyme RNase a mimics active against all-RNA substrates. *ACS Comb Sci*. 2013;15(4):174-182. doi:10.1021/co3001378

178. Hollenstein M, Hipolito CJ, Lam CH, Perrin DM. A self-cleaving DNA enzyme modified with amines, guanidines and imidazoles operates independently of divalent metal cations (M²⁺). *Nucleic Acids Res.* 2009;37(5):1638-1649.
doi:10.1093/nar/gkn1070
179. Cho M, Xiao Y, Nie J, et al. Quantitative selection of DNA aptamers through microfluidic selection and high-throughput sequencing. *Proc Natl Acad Sci.* 2010;107(35):15373-15378. doi:10.1073/pnas.1009331107
180. Berezhnoy A, Stewart CA, Mcnamara JO, et al. Isolation and optimization of murine IL-10 receptor blocking oligonucleotide aptamers using high-throughput sequencing. *Mol Ther.* 2012;20(6):1242-1250. doi:10.1038/mt.2012.18
181. Quang NN, Perret G, Ducongé F. Applications of high-throughput sequencing for in vitro selection and characterization of aptamers. *Pharmaceuticals.* 2016;9(4):1-15.
doi:10.3390/ph9040076
182. Alam KK, Chang JL, Burke DH. FASTAptamer: A bioinformatic toolkit for high-throughput sequence analysis of combinatorial selections. *Mol Ther - Nucleic Acids.* 2015;4(3):e230. doi:10.1038/mtna.2015.4
183. Kinghorn AB, Fraser LA, Lang S, Shiu SCC, Tanner JA. Aptamer bioinformatics. *Int J Mol Sci.* 2017;18(12). doi:10.3390/ijms18122516
184. Kubiczek D, Bodenberger N, Rosenau F. Aptamers as promising agents in diagnostic and therapeutic applications. *Antimicrob Res Nov bioknowledge Educ programs.* 2017;6:368-378. <http://www.formatex.info/microbiology6/book/368-378.pdf>.
185. Usselman CWNSSJRB. 乳鼠心肌提取 HHS Public Access. *Physiol Behav.* 2017;176(3):139-148. doi:10.1016/j.physbeh.2017.03.040
186. Ruckman J, Green LS, Beeson J, et al. 2'-Fluoropyrimidine RNA-based Aptamers to the 165-Amino Acid Form of Vascular Endothelial Growth Factor (VEGF 165). *J Biol Chem.* 1998;273(32):20556-20567. doi:10.1074/jbc.273.32.20556
187. Sadiq MA, Hanout M, Sarwar S, et al. Platelet derived growth factor inhibitors: A potential therapeutic approach for ocular neovascularization. *Saudi J Ophthalmol.* 2015;29(4):287-291. doi:10.1016/j.sjopt.2015.05.005

188. Green LS, Jellinek D, Jenison R, Östman A, Heldin CH, Janjic N. Inhibitory DNA ligands to platelet-derived growth factor B-chain. *Biochemistry*. 1996;35(45):14413-14424. doi:10.1021/bi961544+
189. Biesecker G, Dihel L, Enney K, Bendele RA. Derivation of RNA aptamer inhibitors of human complement C5. In: *Immunopharmacology*. Vol 42. ; 1999:219-230. doi:10.1016/S0162-3109(99)00020-X
190. Menne J, Eulberg D, Beyer D, et al. C-C motif-ligand 2 inhibition with emapticap pegol (NOX-E36) in type 2 diabetic patients with albuminuria. *Nephrol Dial Transpl*. 2017;(April 2016):307-315. doi:10.1093/ndt/gfv459
191. Wlotzka B, Leva S, Eschgfäller B, et al. In vivo properties of an anti-GnRH Spiegelmer: An example of an oligonucleotide-based therapeutic substance class. *Proc Natl Acad Sci U S A*. 2002;99(13):8898-8902. doi:10.1073/pnas.132067399
192. Leva S, Lichte A, Burmeister J, et al. GnRH binding RNA and DNA Spiegelmers: A novel approach toward GnRH antagonism. *Chem Biol*. 2002;9(3):351-359. doi:10.1016/S1074-5521(02)00111-4
193. Vater A, Klussmann S. Turning mirror-image oligonucleotides into drugs: The evolution of Spiegelmer® therapeutics. *Drug Discov Today*. 2015;20(1):147-155. doi:10.1016/j.drudis.2014.09.004
194. Oberthu D, Achenbach J, Gabdulkhakov A, et al. Crystal structure of a mirror-image L-RNA aptamer (Spiegelmer) in complex with the natural L-protein target CCL2. *Nat Commun*. 2015:1-11. doi:10.1038/ncomms7923
195. Schwoebel F, Van Eijk LT, Zboralski D, et al. The effects of the anti-hepcidin Spiegelmer NOX-H94 on inflammation-induced anemia in cynomolgus monkeys. *Blood*. 2013;121(12):2311-2315. doi:10.1182/blood-2012-09-456756
196. Bates PJ, Laber DA, Miller DM, Thomas SD, Trent JO. Discovery and Development of the G-rich Oligonucleotide AS1411 as a novel treatment for cancer. *Exp Mol Pathol*. 2010;86(3):151-164. doi:10.1016/j.yexmp.2009.01.004.Discovery
197. Hoellenriegel J, Zboralski D, Maasch C, et al. The Spiegelmer NOX-A12, a novel CXCL12 inhibitor, interferes with chronic lymphocytic leukemia cell motility and

- causes chemosensitization. *Blood*. 2014;123(7):1032-1039. doi:10.1182/blood-2013-03-493924
198. Toole, Bock C. Selection of single-stranded DNA molecules that bind and inhibit human thrombin. *Nature*. 1992;355(November):564-566. doi:10.1038/355564a0
199. Troisi R, Napolitano V, Spiridonova V, Krauss IR, Sica F. Several structural motifs cooperate in determining the highly effective anti-thrombin activity of NU172 aptamer. *Nucleic Acids Res*. 2018;46(22):12177-12185. doi:10.1093/nar/gky990
200. Diener JL, Daniel Lagassé HA, Duerschmied D, et al. Inhibition of von Willebrand factor-mediated platelet activation and thrombosis by the anti-von Willebrand factor A1-domain aptamer ARC1779. *J Thromb Haemost*. 2009;7(7):1155-1162. doi:10.1111/j.1538-7836.2009.03459.x
201. Rusconi CP, Roberts JD, Pitoc GA, et al. Antidote-mediated control of an anticoagulant aptamer in vivo. *Nat Biotechnol*. 2004;22(11):1423-1428. doi:10.1038/nbt1023
202. Cohen MG, Purdy DA, Rossi JS, et al. First clinical application of an actively reversible direct factor IXa inhibitor as an anticoagulation strategy in patients undergoing percutaneous coronary intervention. *Circulation*. 2010;122(6):614-622. doi:10.1161/CIRCULATIONAHA.109.927756
203. Kong HY, Byun J. Nucleic acid aptamers: New methods for selection, stabilization, and application in biomedical science. *Biomol Ther*. 2013;21(6):423-434. doi:10.4062/biomolther.2013.085
204. Jayasena SD. Aptamers: An emerging class of molecules that rival antibodies in diagnostics. *Clin Chem*. 1999;45(9):1628-1650.
205. Drolet, McDermott, Romig. An enzyme-linked oligonucleotide assay. *Nat Biotechnol*. 1996;14:1021-1025. doi:10.1038/nbt0896-1021
206. Vivekananda J, Kiel JL. Anti-Francisella tularensis DNA aptamers detect tularemia antigen from different subspecies by Aptamer-Linked Immobilized Sorbent Assay. *Lab Invest*. 2006;86(6):610-618. doi:10.1038/labinvest.3700417
207. O'Sullivan CK. Aptasensors - The future of biosensing? *Fresenius J Anal Chem*.

- 2002;372(1):44-48. doi:10.1007/s00216-001-1189-3
208. Song S, Wang L, Li J, Zhao J, Fan C. Aptamer-based biosensor. *Trends Anal Chem.* 2008;27(4). doi:10.1016/j.trac.2007.12.004
209. Radi A. Electrochemical Aptamer-Based Biosensors: Recent Advances and Perspectives. *Int J Electrochem.* 2011;2011:1-17. doi:10.4061/2011/863196
210. Stojanovic MN, de Prada P, Landry DW. Aptamer-based folding fluorescent sensor for cocaine. *J Am Chem Soc.* 2001;123(21):4928-4931. doi:10.1021/ja0038171
211. Liu J, Lu Y. Fast colorimetric sensing of adenosine and cocaine based on a general sensor design involving aptamers and nanoparticles. *Angew Chemie - Int Ed.* 2005;45(1):90-94. doi:10.1002/anie.200502589
212. Cella LN, Sanchez P, Zhong W, Myung N V, Chen W, Mulchandani A. <Nano-aptasensor-for-Protective-Antigen-Toxin-of-Anthrax_2010_Analytical-Chemistry.pdf>. *AnalChem.* 2010;82(5):2042-2047. doi:10.1021/ac902791q
213. Rohloff JC, Gelinis AD, Jarvis TC, et al. Nucleic acid ligands with protein-like side chains: Modified aptamers and their use as diagnostic and therapeutic agents. *Mol Ther - Nucleic Acids.* 2014;3(July):e201. doi:10.1038/mtna.2014.49
214. Lollo B, Steele F, Gold L. Beyond antibodies: New affinity reagents to unlock the proteome. *Proteomics.* 2014;14(6):638-644. doi:10.1002/pmic.201300187
215. Candia J, Cheung F, Kotliarov Y, et al. Assessment of Variability in the SOMAscan Assay. *Sci Rep.* 2017;7(1):1-13. doi:10.1038/s41598-017-14755-5
216. Russell TM, Green LS, Rice T, et al. Potential of high-affinity, slow off-rate modified aptamer reagents for Mycobacterium tuberculosis proteins as tools for infection models and diagnostic applications. *J Clin Microbiol.* 2017;55(10):3072-3088. doi:10.1128/JCM.00469-17
217. Sattlecker M, Kiddle SJ, Newhouse S, et al. Alzheimer's disease biomarker discovery using SOMAscan multiplexed protein technology. *Alzheimer's Dement.* 2014;10(6):724-734. doi:10.1016/j.jalz.2013.09.016
218. De Groote MA, Nahid P, Jarlsberg L, et al. Elucidating Novel Serum Biomarkers

- Associated with Pulmonary Tuberculosis Treatment. *PLoS One*. 2013;8(4).
doi:10.1371/journal.pone.0061002
219. Hathout Y, Brody E, Clemens PR, et al. Large-scale serum protein biomarker discovery in Duchenne muscular dystrophy. *Proc Natl Acad Sci U S A*. 2015;112(23):7153-7158. doi:10.1073/pnas.1507719112
220. Di Narzo AF, Telesco SE, Brodmerkel C, et al. High-Throughput Characterization of Blood Serum Proteomics of IBD Patients with Respect to Aging and Genetic Factors. *PLoS Genet*. 2017;13(1):1-18. doi:10.1371/journal.pgen.1006565
221. Mehan MR, Ayers D, Thirstrup D, et al. Protein signature of lung cancer tissues. *PLoS One*. 2012;7(4). doi:10.1371/journal.pone.0035157
222. Chu TC, Shieh F, Lavery LA, et al. Labeling tumor cells with fluorescent nanocrystal-aptamer bioconjugates. *Biosens Bioelectron*. 2006;21(10):1859-1866. doi:10.1016/j.bios.2005.12.015
223. Bagalkot V, Zhang L, Levy-Nissenbaum E, et al. Quantum Dot–Aptamer Conjugates for Synchronous Cancer Imaging, Therapy, and Sensing of Drug Delivery Based on Bi-Fluorescence Resonance Energy Transfer. *Nano Lett*. 2007;7(10):3065-3070. doi:10.1021/nl071546n
224. Pieve C Da, Perkins AC, Missailidis S. Anti-MUC1 aptamers: radiolabelling with ^{99m}Tc and biodistribution in MCF-7 tumour-bearing mice. *Nucl Med Biol*. 2009;36(6):703-710. doi:10.1016/j.nucmedbio.2009.04.004
225. Charlton J, Kirschenheuter GP, Smith D. Highly potent irreversible inhibitors of neutrophil elastase generated by selection from a randomized DNA-valine phosphonate library. *Biochemistry*. 1997;36(10):3018-3026. doi:10.1021/bi962669h
226. Bless NM, Smith D, Charlton J, et al. Protective effects of an aptamer inhibitor of neutrophil elastase in lung inflammatory injury. *Curr Biol*. 1997;7(11):877-880. doi:10.1016/S0960-9822(06)00376-9
227. Charlton J, Sennello J, Smith D. In vivo imaging of inflammation using an aptamer inhibitor of human neutrophil elastase. *Chem Biol*. 1997;4(11):809-816. <https://www.ncbi.nlm.nih.gov/pubmed/9384527>.

228. Jacobson O, Yan X, Niu G, et al. PET imaging of tenascin-C with a radiolabeled single-stranded DNA aptamer. *J Nucl Med.* 2015;56(4):616-621. doi:10.2967/jnumed.114.149484
229. Hu H, Dai A, Sun J, et al. Aptamer-conjugated Mn₃O₄@SiO₂ core-shell nanoprobe for targeted magnetic resonance imaging. *Nanoscale.* 2013;5(21):10447-10454. doi:10.1039/c3nr03490a
230. Dimitrova N, Zamudio JR, Jong RM, et al. Public Access NIH Public Access. *PLoS One.* 2017;32(7):736-740. doi:10.1371/journal.pone.0178059
231. McEntee K, Weinstock GM, Lehman IR. recA protein-catalyzed strand assimilation: stimulation by Escherichia coli single-stranded DNA-binding protein. *Proc Natl Acad Sci.* 1980;77(2):857-861. doi:10.1073/pnas.77.2.857
232. Javadi A, Shamaei M, Ziazi LM, et al. Qualification study of two genomic DNA extraction methods in different clinical samples. *Tanaffos.* 2014;13(4):41-47.
233. Tan SC, Yiap BC. DNA, RNA, and Protein Extraction: The Past and The Present. *J Biomed Biotechnol.* 2009;2009:1-10. doi:10.1155/2009/574398
234. Zhang S, Bu X, Zhao H, et al. A host deficiency of discoidin domain receptor 2 (DDR2) inhibits both tumour angiogenesis and metastasis. *J Pathol.* 2014;232(4):436-448. doi:10.1002/path.4311
235. Tolle F, Brändle GM, Matzner D, Mayer G. Ein universeller Zugang zu Nucleobasen-modifizierten Aptameren. *Angew Chemie.* 2015;127(37):11121-11125. doi:10.1002/ange.201503652
236. Beaucage SL, Iyer RP. Advances in the Synthesis of Oligonucleotides by the Phosphoramidite Approach. *Tetrahedron.* 1992;48(12):2223-2311. doi:10.1016/S0040-4020(01)88752-4
237. Tolle F, Wilke J, Wengel J, Mayer G. By-product formation in repetitive PCR amplification of DNA libraries during SELEX. *PLoS One.* 2014;9(12):1-12. doi:10.1371/journal.pone.0114693
238. Liang C, Li D, Zhang G, et al. Comparison of the methods for generating single-stranded DNA in SELEX. *Analyst.* 2015;140(10):3439-3444. doi:10.1039/c5an00244c

239. Williams KP, Bartel DP. PCR product with strands of unequal length. *Nucleic Acids Res.* 1995;23(20):4220-4221. doi:10.1093/nar/23.20.4220
240. Avci-Adali M, Paul A, Wilhelm N, Ziemer G, Wendel HP. Upgrading SELEX technology by using lambda exonuclease digestion for single-stranded DNA generation. *Molecules.* 2010;15(1):1-11. doi:10.3390/molecules15010001
241. Higuchi RG, Ochman H. Production of single-stranded DNA templates by exonuclease digestion following the polymerase chain reaction. *Nucleic Acids Res.* 1989;17:5865-. doi:10.1093/nar/17.14.5865
242. Chory J, Pollard JD. Separation of Small DNA Fragments by Conventional Gel Electrophoresis. *Curr Protoc Mol Biol.* 2004:1-8. doi:10.1002/0471142727.mb0207s47
243. Martin M. Cutadapt removes adapter sequences from high-throughput sequencing reads. *EMBnet.journal.*:1-3. doi:10.14806/ej.17.1.200
244. Zuker M. Mfold web server for nucleic acid folding and hybridization prediction. *Nucleic Acids Res.* 2003;31(13):3406-3415. doi:10.1093/nar/gkg595
245. Stoltenburg R, Schubert T, Strehlitz B. In vitro selection and interaction studies of a DNA aptamer targeting Protein A. *PLoS One.* 2015;10(7). doi:10.1371/journal.pone.0134403
246. Henriët E, Sala M, Abou Hammoud A, et al. Multitasking discoidin domain receptors are involved in several and specific hallmarks of cancer. *Cell Adhes Migr.* 2018;12(4):363-377. doi:10.1080/19336918.2018.1465156
247. Rammal H, Saby C, Magnien K, et al. Discoidin domain receptors: Potential actors and targets in cancer. *Front Pharmacol.* 2016;7(MAR). doi:10.3389/fphar.2016.00055
248. Fu HL, Valiathan RR, Arkwright R, et al. Discoidin domain receptors: Unique receptor tyrosine kinases in collagen-mediated signaling. *J Biol Chem.* 2013;288(11):7430-7437. doi:10.1074/jbc.R112.444158
249. Brannon-Peppas L, Blanchette JO. Nanoparticle and targeted systems for cancer therapy. *Adv Drug Deliv Rev.* 2012;64(SUPPL.):206-212. doi:10.1016/j.addr.2012.09.033

250. Cheng L, Lopez-Beltran A, Massari F, MacLennan GT, Montironi R. Molecular testing for BRAF mutations to inform melanoma treatment decisions: A move toward precision medicine. *Mod Pathol*. 2018;31(1):24-38. doi:10.1038/modpathol.2017.104
251. Rahul S. Desikan, MD, PhD1, Andrew J. Schork, MS2, Yunpeng Wang, PhD3, 5, Aree Witoelar, PhD5, Manu Sharma, PhD6, 7, Linda K. McEvoy, PhD1, Dominic Holland, PhD3, James B. Brewer, MD, PhD1, 3, Chi-Hua Chen, PhD1, 4, Wesley K. Thompson, PhD4 DH. Safety and efficacy of vemurafenib in BRAFV600E and BRAFV600K mutation-positive melanoma (BRIM-3): extended follow-up of a phase 3, randomised, open-label study. *Lancet oncol*. 2015;15:323-332. doi:10.1016/S1470-2045(14)70012-9.
252. Li K, Xiu CL, Gao LM, et al. Screening of specific nucleic acid aptamers binding tumor markers in the serum of the lung cancer patients and identification of their activities. *Tumor Biol*. 2017;39(7):1-7. doi:10.1177/1010428317717123
253. Robertson DL, Joyce GF. Selection in vitro of an RNA enzyme that specifically cleaves single-stranded DNA. *Nature*. 1990;344(0028-0836 (Print)):467-468. doi:10.1038/344467a0
254. Shaw J pyng, Kent K, Bird J, Fishback J, Froehler B. Modified deoxyoligonucleotides stable to exonuclease degradation in serum. *Nucleic Acids Res*. 1991;19(4):747-750. doi:10.1093/nar/19.4.747
255. Konitsiotis AD, Raynal N, Bihan D, Hohenester E, Farndale RW, Leitinger B. Characterization of high affinity binding motifs for the discoidin domain receptor DDR2 in collagen. *J Biol Chem*. 2008;283(11):6861-6868. doi:10.1074/jbc.M709290200
256. Carafoli F, Hohenester E. Collagen recognition and transmembrane signalling by discoidin domain receptors. *Biochim Biophys Acta - Proteins Proteomics*. 2013;1834(10):2187-2194. doi:10.1016/j.bbapap.2012.10.014
257. Tsuji S, Tanaka T, Hirabayashi N, et al. RNA aptamer binding to polyhistidine-tag. *Biochem Biophys Res Commun*. 2009;386(1):227-231. doi:10.1016/j.bbrc.2009.06.014
258. Suh SH, Dwivedi HP, Jaykus LA. Development and evaluation of aptamer magnetic capture assay in conjunction with real-time PCR for detection of *Campylobacter jejuni*.

- LWT - Food Sci Technol.* 2014;56(2):256-260. doi:10.1016/j.lwt.2013.12.012
259. Bartel DP, Zapp ML, Green MR, Szostak JW. HIV-1 rev regulation involves recognition of non-Watson-Crick base pairs in viral RNA. *Cell.* 1991;67(3):529-536. doi:10.1016/0092-8674(91)90527-6
260. Beaudry AA, Joyce GF. Directed evolution of an RNA enzyme. *Science (80-).* 1992;257(5070):635-641. doi:10.1126/science.1496376
261. Cibiel A, Quang NN, Gombert K, Thézé B, Garofalakis A, Ducongé F. From ugly duckling to swan: Unexpected identification from cell-SELEX of an anti-annexin A2 aptamer targeting tumors. *PLoS One.* 2014;9(1):1-11. doi:10.1371/journal.pone.0087002
262. McInerney P, Adams P, Hadi MZ. Error Rate Comparison during Polymerase Chain Reaction by DNA Polymerase. *Mol Biol Int.* 2014;2014:1-8. doi:10.1155/2014/287430
263. Forloni M, Liu AY, Wajapeyee N. Random mutagenesis using error-prone DNA polymerases. *Cold Spring Harb Protoc.* 2018;2018(3):220-230. doi:10.1101/pdb.prot097741
264. Autour A, Westhof E, Ryckelynck M. ISpinach: A fluorogenic RNA aptamer optimized for in vitro applications. *Nucleic Acids Res.* 2016;44(6):2491-2500. doi:10.1093/nar/gkw083
265. Neves MAD, Slavkovic S, Churcher ZR, Johnson PE. Salt-mediated two-site ligand binding by the cocaine-binding aptamer. *Nucleic Acids Res.* 2017;45(3):1041-1048. doi:10.1093/nar/gkw1294
266. Agarwal G, Mihai C, Iscru DF. Interaction of Discoidin Domain Receptor 1 with Collagen type 1. *J Mol Biol.* 2007;367(2):443-455. doi:10.1016/j.jmb.2006.12.073
267. Pan W, Clawson GA. The shorter the better: Reducing fixed primer regions of oligonucleotide libraries for aptamer selection. *Molecules.* 2009;14(4):1353-1369. doi:10.3390/molecules14041353
268. Thiel WH, Bair T, Wyatt Thiel K, et al. Nucleotide Bias Observed with a Short SELEX RNA Aptamer Library. *Nucleic Acid Ther.* 2011;21(4):253-263. doi:10.1089/nat.2011.0288

269. McKeague M, De Girolamo A, Valenzano S, et al. Comprehensive Analytical Comparison of Strategies Used for Small Molecule Aptamer Evaluation. *Anal Chem.* 2015;87(17):8608-8612. doi:10.1021/acs.analchem.5b02102
270. Dausse E, Barré A, Aimé A, et al. Aptamer selection by direct microfluidic recovery and surface plasmon resonance evaluation. *Biosens Bioelectron.* 2016;80:418-425. doi:10.1016/j.bios.2016.02.003
271. Goodchild J. Therapeutic oligonucleotides. *Methods Mol Biol.* 2011;764(3):1-15. doi:10.1007/978-1-61779-188-8_1
272. Potty ASR, Kourentzi K, Fang H, et al. Biophysical characterization of DNA aptamer interactions with vascular endothelial growth factor. *Biopolymers.* 2009;91(2):145-156. doi:10.1002/bip.21097
273. Slavkovic S, Johnson PE. Isothermal titration calorimetry studies of aptamer-small molecule interactions: practicalities and pitfalls. *J Aptamers.* 2018;2:45-51.
274. Wiseman T, Williston S, Brandts JF, Lin Lung-Nan. Rapid Measurement of Binding Constants and Heats of Binding using ITC. *Anal Biochem.* 1989;137:131-137. doi:10.1016/0003-2697(89)90213-3
275. Lim EK, Kim B, Choi Y, et al. Aptamer-conjugated magnetic nanoparticles enable efficient targeted detection of integrin $\alpha v \beta 3$ via magnetic resonance imaging. *J Biomed Mater Res - Part A.* 2014;102(1):49-59. doi:10.1002/jbm.a.34678
276. Lee J, Lee N, Kim H, Kim J. Uniform Mesoporous Dye-Doped Silica Nanoparticles Decorated with Multiple Magnetite Nanocrystals for Simultaneous Enhanced Magnetic Resonance Imaging, Fluorescence Imaging, and Drug Delivery. *J Am Chem Soc.* 2010;132:552-557. doi:10.1021/ja905793q
277. Aldave GJ. Efecto de la temperatura y tiempo de tostado en los caracteres sensoriales y en las propiedades químicas de granos de cacao (*Theobroma cacao L.*) procedente de Uchiza , San Martín – Perú para la obtención de NIBS. 2016;121(7):112. doi:10.1172/JCI45600.2768
278. Adumeau L, Genevois C, Roudier L, Schatz C, Couillaud F, Mornet S. Impact of surface grafting density of PEG macromolecules on dually fluorescent silica

- nanoparticles used for the in vivo imaging of subcutaneous tumors. *Biochim Biophys Acta - Gen Subj*. 2017;1861(6):1587-1596. doi:10.1016/j.bbagen.2017.01.036
279. Wang J, Gong Q, Maheshwari N, et al. Particle display: A quantitative screening method for generating high-affinity aptamers. *Angew Chemie - Int Ed*. 2014;53(19):4796-4801. doi:10.1002/anie.201309334
280. Sanzani SM, Reverberi M, Fanelli C, Ippolito A. Detection of ochratoxin a using molecular beacons and real-time PCR thermal cyclers. *Toxins (Basel)*. 2015;7(3):812-820. doi:10.3390/toxins7030812
281. Alvarado-González M, Gallo M, Lopez-Albarran P, Flores-Holguín N, Glossman-Mitnik D. DFT study of the interaction between the conjugated fluorescein and dabcyf system, using fluorescence quenching method. *J Mol Model*. 2012;18(9):4113-4120. doi:10.1007/s00894-012-1413-4
282. Eaton BE. Expanding the Chemistry of DNA for in Vitro Selection. *J Am Chem Soc*. 2010;132(30):4141-4151. doi:10.1021/ja908035g
283. Pfeiffer F, Rosenthal M, Siegl J, Ewers J, Mayer G. Customised nucleic acid libraries for enhanced aptamer selection and performance. *Curr Opin Biotechnol*. 2017;48:111-118. doi:10.1016/j.copbio.2017.03.026
284. Azéma L, Bathany K, Rayner B. 2'-O-Appended polyamines that increase triple-helix-forming oligonucleotide affinity are selected by dynamic combinatorial chemistry. *ChemBioChem*. 2010;11(18):2513-2516. doi:10.1002/cbic.201000538